ERDC/CHL TR-17-8

Coastal and Hydraulics Laboratory

US Army Corps of Engineers®
Engineer Research and Development Center

ERDC
INNOVATIVE SOLUTIONS for a safer, better world

Sediment and Hydraulic Measurements with Computed Bed Load on the Missouri River, Sioux City to Hermann, 2014

David Abraham, Marielys Ramos-Villanueva, Thad Pratt, Naveen Ganesh, David May, William Butler, Tate McAlpin, Keaton Jones, John Shelley, and Daniel Pridal

May 2017

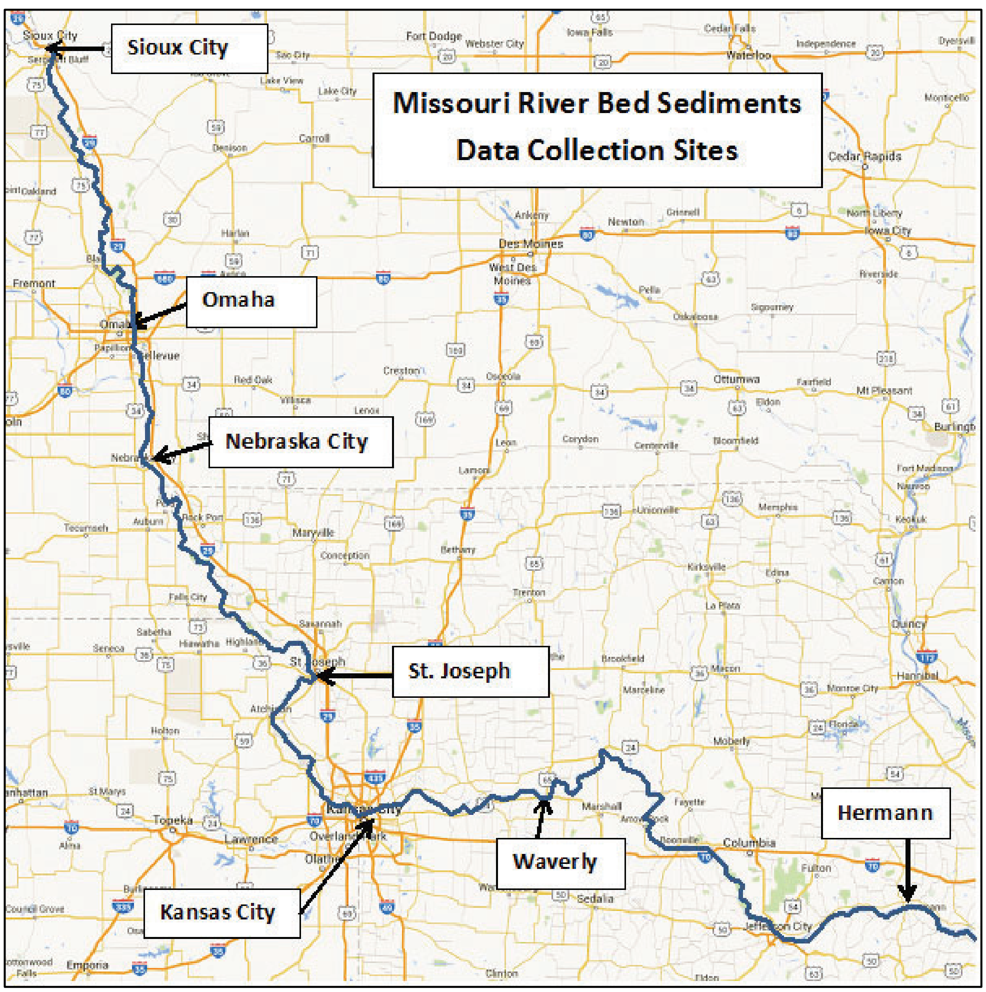

ERDC/CHL TR-17-8
May 2017

Sediment and Hydraulic Measurements with Computed Bed Load on the Missouri River, Sioux City to Hermann, 2014

David Abraham, Marielys Ramos-Villanueva,
Thad Pratt, Naveen Ganesh, David May, William Butler,
Tate McAlpin, and Keaton Jones

Coastal and Hydraulics Laboratory
U.S. Army Engineer Research and Development Center
3909 Halls Ferry Road
Vicksburg, MS 39180-6199

John Shelley

U.S. Army Corps of Engineers, Kansas City District
601 E 12th St.
Kansas City, MO 64106

Daniel Pridal

U.S. Army Corps of Engineers, Omaha District
1616 Capitol Ave., Ste. 9000
Omaha, NE 68102

Final report

Prepared for U.S. Army Corps of Engineers, Kansas City District
601 E 12th St.
Kansas City, MO 64106

U.S. Army Corps of Engineers, Omaha District
1616 Capitol Ave., Ste. 9000
Omaha, NE 68102

Under Work Unit HC2022

Abstract

This work was performed to assist the U.S. Army Corps of Engineers, Omaha and Kansas City Districts, in quantifying sediment bed load and suspended load at several sites on the Missouri River for the purpose of defining sediment-discharge rating curves and for possible parameterization of bed-load transport equations. Seven sites were selected, and all sites were surveyed three times, separated by at least 4 weeks (or 20% flow difference) between surveys. Multi-beam, acoustic Doppler current profiler, suspended sediment, and bed material samples were collected for each site visit. As requested by the Districts, all units are in English units. In addition to quantifying all the intended data types listed above, bed-load transport values were computed for all sites and all trips using the Integrated Section Surface Difference Over Time version 2 (ISSDOTv2) method and compared with the Meyer-Peter Mueller and Einstein bed-load transport functions. The study provides a complete sediment picture (bed load, suspended bed-material load, and wash load) over a 630-mile reach of a large sand bed river, with seven sites representing increasingly larger flows along the river length. The data set will be very useful for additional studies.

Contents

Figures and Tables

Figures

Tables

Unit Conversion Factors

Multiply	By	To Obtain
feet	0.3048	meters
miles (U.S. statute)	1,609.347	meters
square feet	0.09290304	square meters
tons (2,000 pounds, mass)	907.1847	kilograms

Preface

This study was conducted for the U.S. Army Corps of Engineers (USACE), Kansas City and Omaha Districts, which provided funding.

The work was performed by the USACE, Engineer Research and Development Center, Coastal and Hydraulics Laboratory (USACE-ERDC-CHL), during the time period of March 2014 to December 2015. At the time of publication, Mr. Keith Flowers was Chief of the River Engineering Branch (CEERD-HFR), and Dr. Cary Talbot was Chief of the Flood and Storm Protection Division (CEERD-HF). Mr. Jeffrey R. Eckstein was Deputy Director of CHL, and Mr. José E. Sánchez was the Director.

COL Bryan S. Green was the Commander of the ERDC, and the Director was Dr. David W. Pittman.

1 Introduction

1.1 Background

Advances in technology, equipment, and methodologies have greatly increased the quantity, quality, and types of data that can be obtained for the study of natural phenomenon. The study of riverine sedimentation is no exception. All the typical parameters such as water depth, velocity, and slope, as well as bathymetry, can now be measured with greater accuracy and more detail than in previous years. Additionally, new methodologies have been developed that allow the computation of bed-load transport in large sand bed rivers. This portion of the total sediment load was once called the “unmeasured” load. For example, see Einstein (1950) and Colby (1955). Since it is now measureable in more detail and accuracy than in the past, a more complete measurement of the total sediment load in a large sand bed river, like the Missouri River, is possible.

1.2 Objective

The main purpose of the data collection effort was to obtain the necessary data to quantify the amount and transport rate of suspended and bed-load sediments at several sites on the Missouri River for the purpose of defining sediment-discharge rating curves, determination of the total sediment load, and for parameterizing bed-load transport equations.

1.3 Approach

Hydraulic and sediment measurements were performed during each data collection date at seven different sites on the Missouri River, between Sioux City, IA, and Hermann, MO. The sites were selected in relatively straight sections of the river and at locations where the U.S. Geological Survey (USGS) operates river gaging stations. See Figure 1 for the location of the data collection sites along the Missouri River. Table 1 presents the river miles at the upstream and downstream ends of each site, and Table 2 presents the coordinates to locate the center of the transect data collection. The location of each site was chosen to be near a USGS gage station, and the locations of the gage stations are provided in Table 3, according to the USGS website.

Figure 1. Map locating the Missouri River data collections sites.

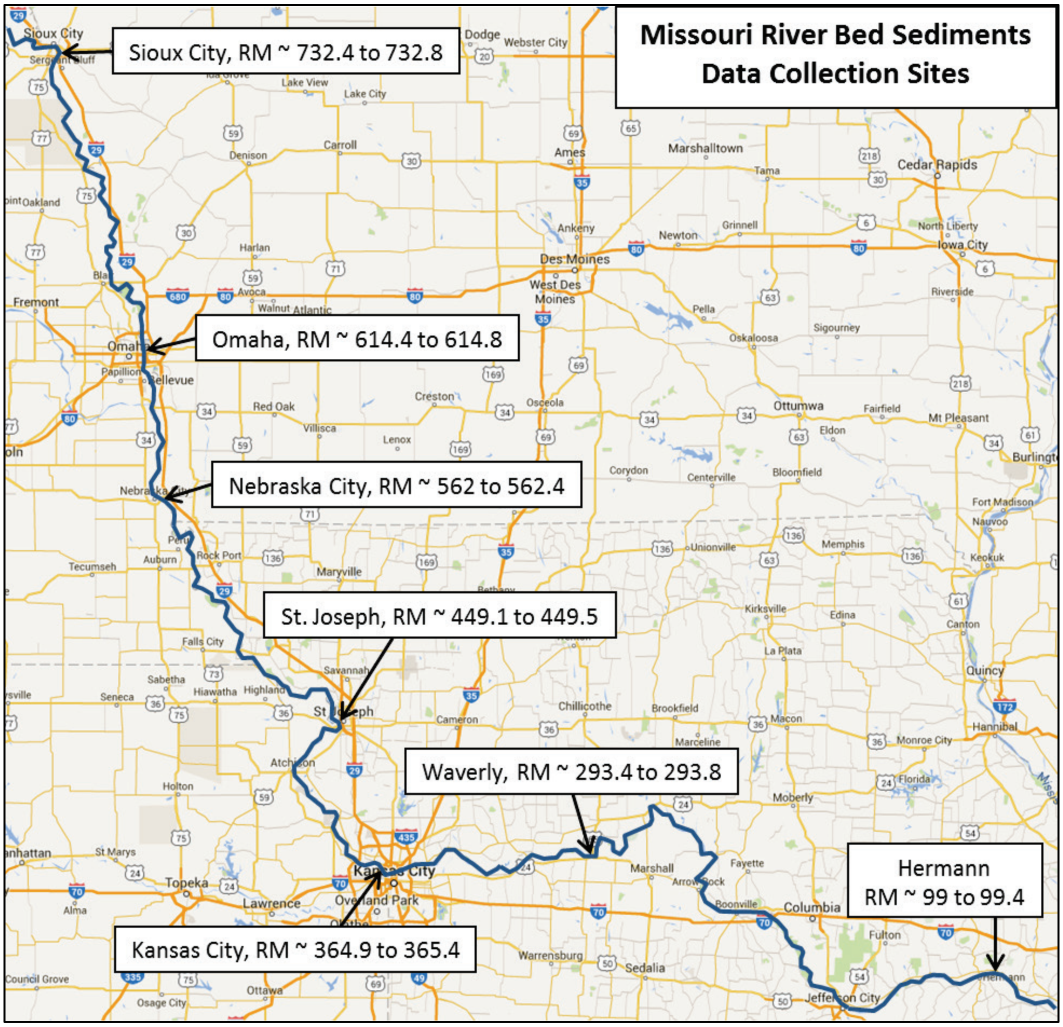

Table 1. River miles of the upstream and downstream ends of the Missouri River data collection sites.

Site	Multi-Beam Data	
	Upstream End (River Miles)	Downstream End (River Miles)
Sioux City	732.8	732.4
Omaha	614.8	614.4
Nebraska City	562.4	562
St. Joseph	449.5	449.1
Kansas City	365.4	364.9
Waverly	293.8	293.4
Hermann	99.4	99

Table 2. North American Datum of 1983 (NAD83) coordinates of the transect center for the data collection sites.

Site	Transect Center	
	NAD83 Latitude	NAD83 Longitude
Sioux City	42° 29' 16.98" N	96° 25' 9.63" W
Omaha	41° 14' 36.04" N	95° 54' 47.45" W
Nebraska City	40° 40' 19.0" N	95° 49' 59.76" W
St. Joseph	39° 46' 4.43" N	94° 51' 52.19" W
Kansas City	39° 07' 14.26" N	94° 34' 13.10" W
Waverly	39° 12' 53.61" N	93° 31' 8.80" W
Hermann	38° 42' 18.07" N	91° 27' 46.20" W

Table 3. NAD83 coordinates of the USGS gage stations near the data collection sites.

Site	USGS Gage Location	
	NAD83 Latitude	NAD83 Longitude
Sioux City	42° 29' 09" N	96° 24' 49" W
Omaha	41° 15' 32" N	95° 55' 20" W
Nebraska City	40° 40' 55" N	95° 50' 48" W
St. Joseph	39° 45' 12" N	94° 51' 25" W
Kansas City	39° 06' 42" N	94° 35' 17" W
Waverly	39° 12'54" N	93° 30' 54" W
Hermann	38° 42' 35" N	91° 26' 19" W

The hydraulic measurements included acoustic Doppler current profiler (ADCP) flow and velocity, water surface elevation and slope, and temperature measurements. The collection of sediment data included multi-beam surveys, bed and suspended material sampling and testing, and bed-load transport calculations. These measurements and procedures used to obtain the field data are described in the following chapter.

2 Collected Data Types

ADCP flow and velocity – The velocity and discharge for each data collection date were measured using an ADCP. The measurements were made bank-to-bank moving across the channel, inside the surveyed area, in both directions left-to-right and right-to-left. A total of four flow measurements were taken, two before the multi-beam data collection (left-to-right and right-to-left) and two after it was performed (left-to-right and right-to-left).

The ADCP also provides real-time vertical profiles of instantaneous velocities, from which velocity profiles across a section can be created. The water depth and cross-section shape can also be observed in these profiles.

Water surface elevations and slopes – Water surface elevation measurements were taken upstream and downstream of the multi-beam survey area at each site, for all three data collection dates. Water surface slope was calculated, using the following equation:

$$\left(\frac{z_{upstream} - z_{downstream}}{L}\right) \tag{1}$$

where $z_{upstream}$ and $z_{downstream}$ are the upstream and downstream water surface elevations, respectively, and L is the distance between the two measurement locations, both in units of feet.

Water temperature – Water temperature was measured in degrees Fahrenheit during each data collection visit at each of the seven sites.

Multi-beam surveys – The multi-beam surveys conducted for this study followed the standard protocol developed for the computation of bed load using the Integrated-Section Surface Difference Over Time version 2 (ISSDOTv2) method (see description below). This protocol will be able to be found in an upcoming ERDC technical report[1]. The initial multi-beam survey performed at each of the seven sites included the full extent of the

---

[1] McAlpin, T., D. Abraham, D. May, T. Waller, W. Butler, T. Pratt, and A. Jackson. In preparation. The Integrated Section Surface Difference Over Time (ISSDOTv2) method and numerical code. ERDC/CHL Technical Report. Vicksburg, MS: U.S. Army Engineer Research and Development Center.

channel from bank to bank if possible, depending on boat accessibility and safety. For the subsequent surveys, the covered area was limited to the extent considered to be the active sand transport portion of the channel. This is the portion of a cross section of a river reach not impeded by dikes, piers, weirs, dams, or other types of structures. At least four but as many as eight repetitions of each swath were made.

Bed material samples – Bed material samples were collected on a transect during each multi-beam survey period, using a BM-54 sampler. Sediment sample stations were positioned equidistant from each other along the cross section at each site. The location of the data collection stations was consistent for all dates and was recorded in the field via a global positioning system (GPS) using NAD83. The coordinates are also provided at this study using the Universal Transverse Mercator (UTM) Grid System. The collected samples were tested for gradation and bulk density at the U.S. Army Engineer Research and Development Center, Vicksburg, MS.

Suspended sediment samples – Duplicated suspended sediment samples were obtained using a P-6 iso-kinetic sampler. During this process, samples at different depths in a column were taken at the same sampling stations mentioned earlier for bed material. The duplicate samples were taken to provide particle size analysis and total suspended material flux computation by size class, at each site and for each data collection date.

As described above for the velocity measurements, ADCP echo intensity was recorded to measure the intensity of the acoustic backscatter from particles. The suspended sediment concentration data were used to calibrate the ADCP acoustic backscatter and to develop suspended sediment concentration profiles across the channel, two before the multi-beam data collection and two after it was performed.

Bed load transport computations – The ISSDOTv2 method was used for computing the bed load, which in this study is defined as the portion of the bed-material load (BML) moving in sand waves, or bed forms. This is in contrast to the suspended, which as the name implies, moves while suspended in the water column. This method uses difference plots of time-sequenced, three-dimensional bathymetric data in its computational procedure. The data were obtained in the multi-beam surveys mentioned above. In this method, scour volumes determined from the difference plots are related to the average transport in a sand wave as in Abraham et al. (2011). In this study, the method was applied to each bathymetric swath location for which several repetitions were made (temporally sequential) and a transport value computed for that portion of the river section. This was done for the multiple swaths that were made at each site, and the values for each swath were summed to provide the total bed-load transport at that site.

Bed-load transport values were also computed for each swath of each site using two bed-load transport functions. The selected functions were those of Meyer-Peter and Muller (1948) and Einstein (1950). The ISSDOTv2 and transport function bed-load computational results are reported in each site's section of this document.

All of the above-described data types were collected at seven different sites on the Missouri River, between Sioux City, IA, and Hermann, MO. They are presented in the following sub-sections according to site, from upstream to downstream starting with Sioux City, IA, and ending with Hermann, MO.

3 Site 1: Sioux City, Iowa

ADCP flow and velocity measurements, water surface elevation and slope measurements, and water temperature measurements, along with multi-beam surveys, bed and suspended material sampling and testing, and bed load calculations, were performed during each data collection date at Sioux City, IA. The measurement area is shown in Figure 2 as the green polygon. The red line indicates the cross section where ADCP measurements were taken and suspended and bed material samples were collected. The bank-to-bank width of the river at this location is estimated to fluctuate between 530 and 635 feet (ft); the length of the study area was approximately 2,000 ft. The approximate location of the USGS gage station near the data collection site is also shown as the blue pin. This location might not be accurate in the figure. Coordinates for the gage site as given in the USGS web site are listed in Table 3. The data collection dates for Sioux City were April 30, 2014; June 5, 2014; and June 20, 2014.

Figure 2. Sioux City, IA, data collection site.

3.1 Acoustic Doppler current profiler (ADCP) flow and velocity

The velocity and discharge for each data collection date and site were measured using an ADCP. Table 4 presents the cross-section average flow (cubic feet per second [ft^3/s]), area (square feet [ft^2]), and average velocity (feet per second [ft/s]) for each date, calculated from the measured data. See Appendix I-a for the measured data. (Inquiries for data listed in any appendix should be directed to District personnel at the Omaha or Kansas City District offices.)

Table 4. Total flow, area, and average velocity on the given dates at Sioux City, IA.

Date	Total Flow, Q (ft^3/s)	Total Area, A (ft^2)	Velocity Q/A (ft/s)
April 30, 2014	28,691	7,730	3.71
June 5, 2014	32,642	8,720	3.74
June 20, 2014	78,082	15,294	5.11

Real-time vertical profiles of instantaneous velocities are also obtained from the ADCP measurements. Figure 3 to Figure 5 present the velocity magnitude, before the multi-beam measurements, from left to right. In the figures, the velocity magnitude is quantified by the range of colors shown on the right side of each figure, where the higher velocities are denoted by red and the lower velocities by blue. The velocity profiles for after the multi-beam measurements are available at Appendix I-a.

Figure 3. Velocity magnitude at Sioux City, IA – April 30, 2014, 15:15:00.

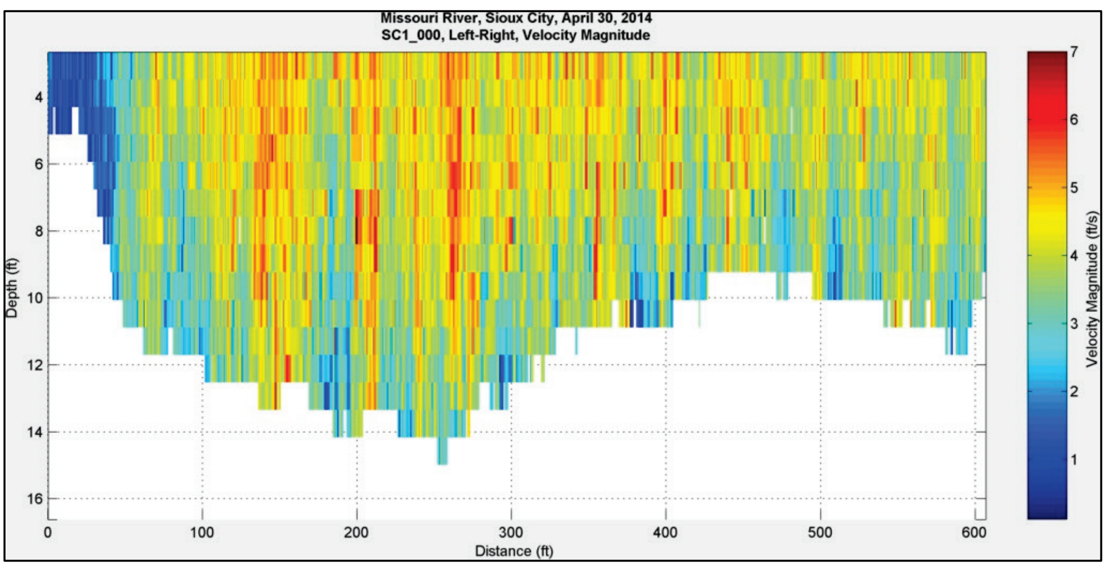

Figure 4. Velocity magnitude at Sioux City, IA – June 5, 2014, 15:51:45.

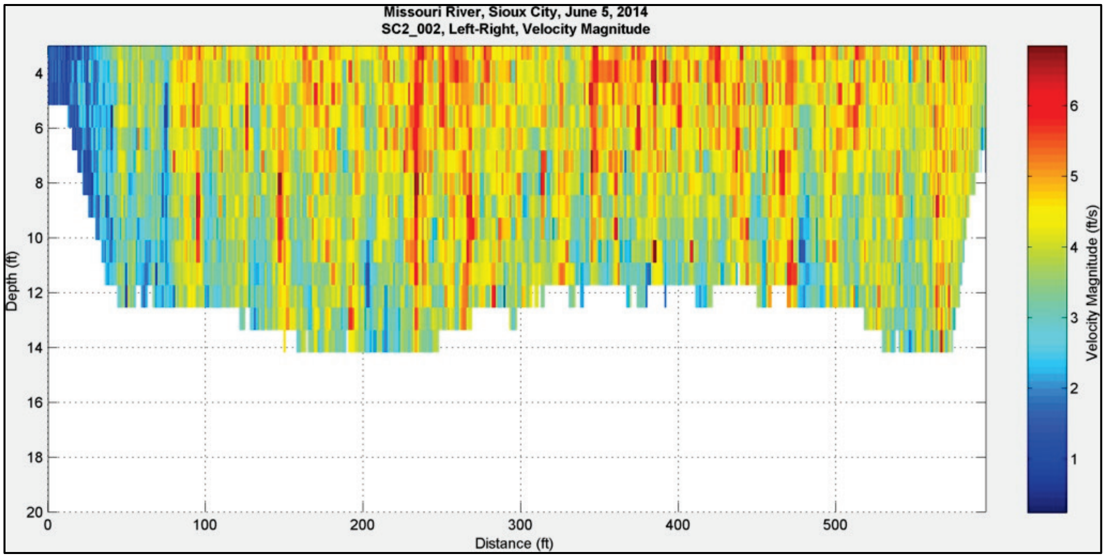

Figure 5. Velocity magnitude at Sioux City, IA – June 20, 2014, 16:11:59.

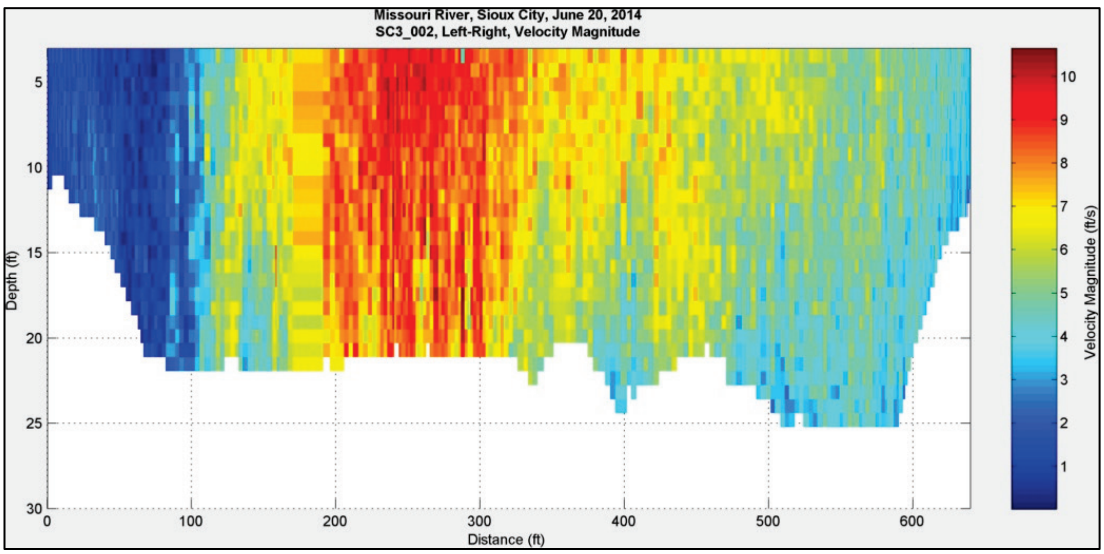

3.2 Water surface elevation and slope

Water surface elevation measurements were taken upstream and downstream of the multi-beam survey area. Figure 6 shows the upstream elevations, at distance zero, connected to the downstream elevations, at a distance of 2,000 ft, for each data collection date. Table 5 presents the slope values for the Sioux City, IA, location for the three dates. The measured data are available in Appendix I-b.

Figure 6. Water surface elevation at Sioux City, IA. – from upstream to downstream.

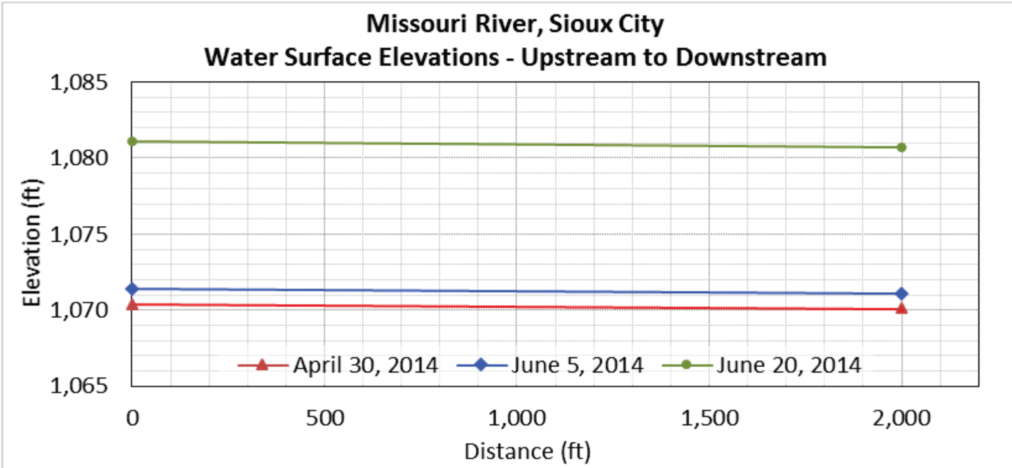

Table 5. Water surface slopes at Sioux City, IA.

Date	Water Surface Slope (%)
April 30, 2014	0.00015
June 5, 2014	0.00015
June 20, 2014	0.00020

3.3 Water temperature

Table 6 presents the average temperature for each date (see Appendix I-c for the measured values).

Table 6. Water temperature at Sioux City, IA.

Date	Temperature (F)
April 30, 2014	49.7
June 5, 2014	70.5
June 20, 2014	74.1

3.4 Multi-beam surveys

The initial multi-beam survey performed at Sioux City, IA, included the full extent of the channel from bank to bank, as shown in Figure 7, where the dark blue areas are deeper and the red areas are shallower. This survey is used to determine the location of the sand waves throughout the study area and to then decide where to run the ISSDOTv2 swaths according to the location of the active sand transport portion of the channel. The selected area with swath lines and numbers displayed in red is shown in Figure 8. This shows the actual area that was used for the ISSDOTv2 bed-load computations. The length of the multi-beam swaths is approximately 2,000 ft for all three data collection dates.

Figure 7. Multi-beam survey extent at Sioux City, IA – April 30, 2014.

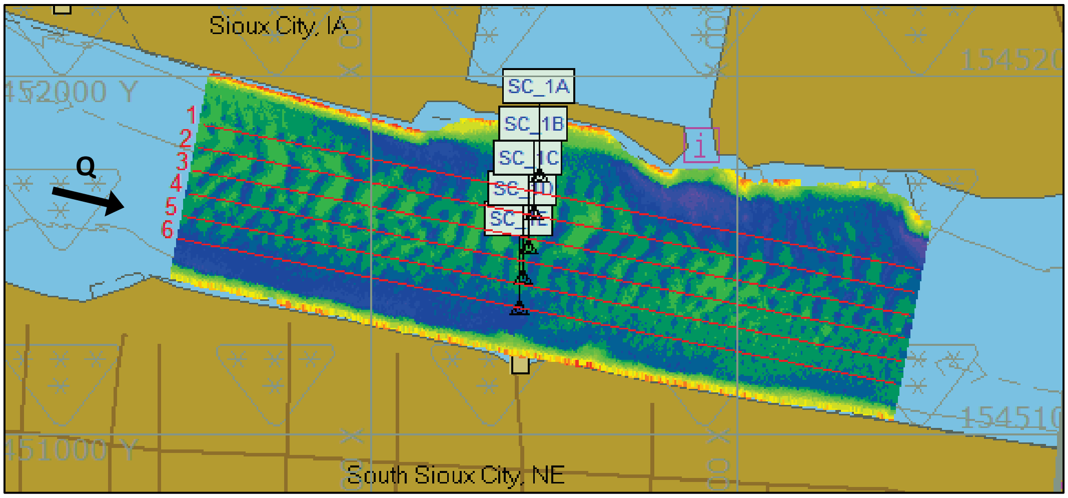

Figure 8. Multi-beam survey extent at Sioux City, IA – June 5 and June 20, 2014.

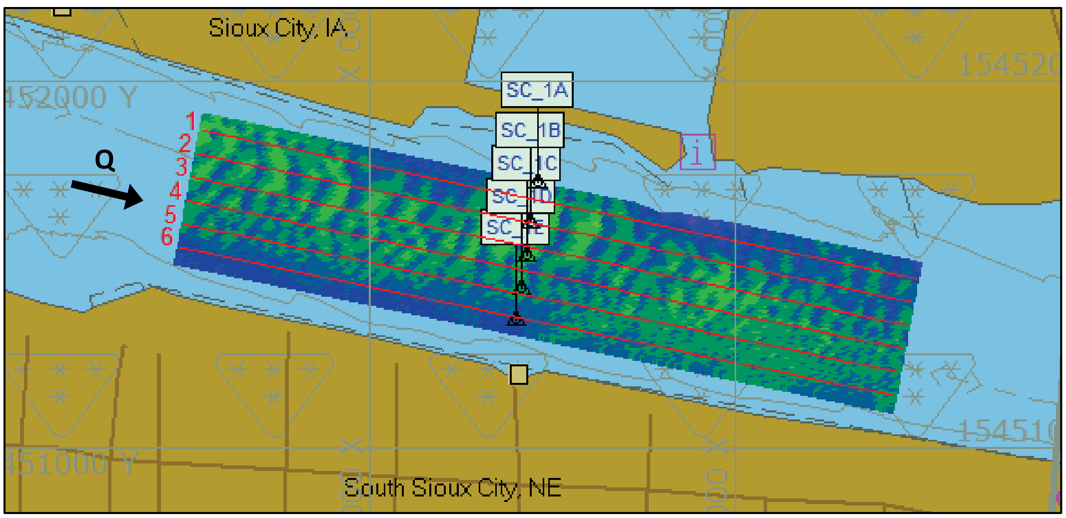

3.5 Bed material samples

Five sediment sample stations were positioned equidistant from each other along the cross section, as presented on Figure 9, which is the same location at which the suspended sediment samples and the ADCP velocity data were obtained. The first station, Station A, was positioned on the left descending bank, and the last station, Station E, on the right descending bank. Table 7 provides the locations of sample stations according to the NAD83. See Appendix I-d for the coordinates using the UTM Grid System.

The grain size distribution for the five bed material samples of the first collection date, April 30, 2014, is provided in Figure 10. Figure 11 and Figure 12 present the same information for the second and third collected samples, respectively. The measured data are available in Appendix I-e.

Table 7. Sediment sample stations NAD83 coordinates at Sioux City, IA.

Station	NAD83 Latitude	NAD83 Longitude
SC A	42° 29' 18.9645" N	96° 25' 9.3372" W
SC B	42° 29' 17.9120" N	96° 25' 9.4914" W
SC C	42° 29' 16.9778" N	96° 25' 9.6256" W
SC D	42° 29' 16.1013" N	96° 25' 9.7897" W
SC E	42° 29' 15.2757" N	96° 25' 9.8902" W

Figure 9. Sediment sample stations at the Missouri River – Sioux City, IA.

Figure 10. Bed material grain size distribution for Sioux City, IA – April 30, 2014.

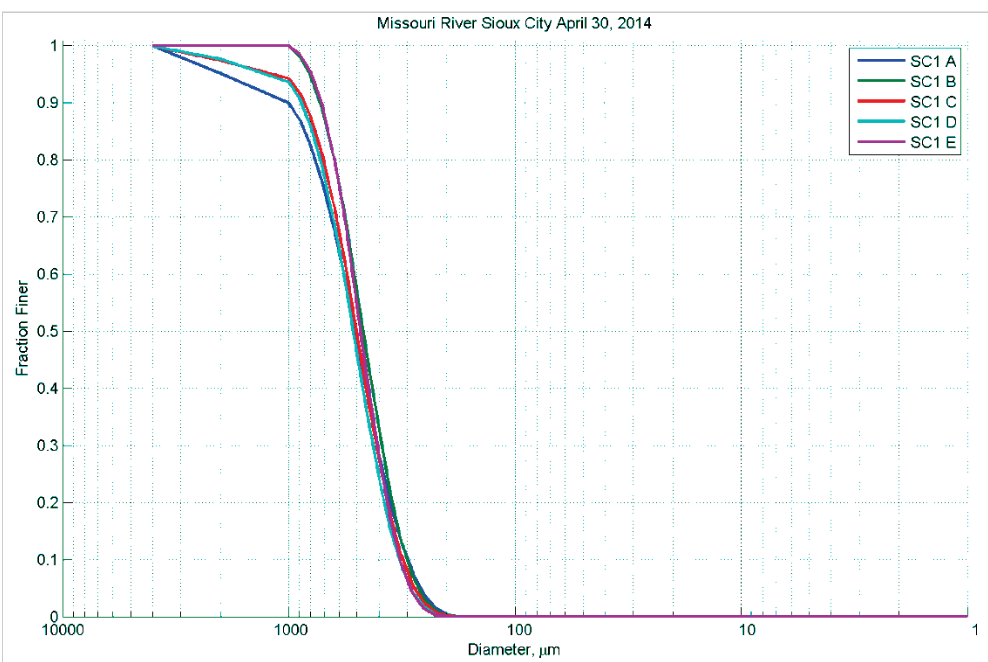

Figure 11. Bed material grain size distribution for Sioux City, IA – June 5, 2014.

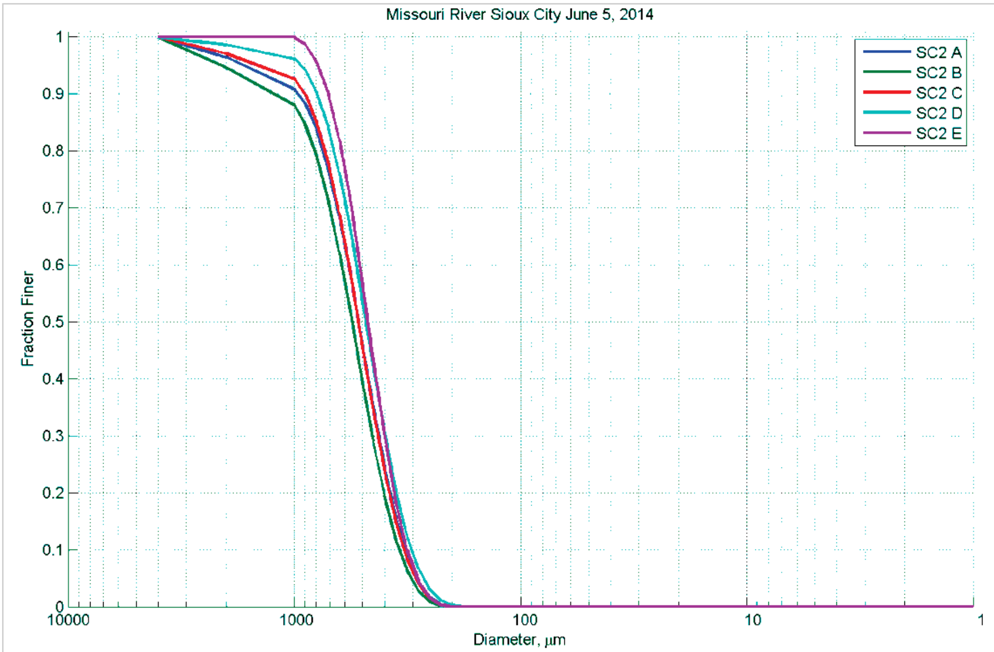

Figure 12. Bed material grain size distribution for Sioux City, IA – June 20, 2014.

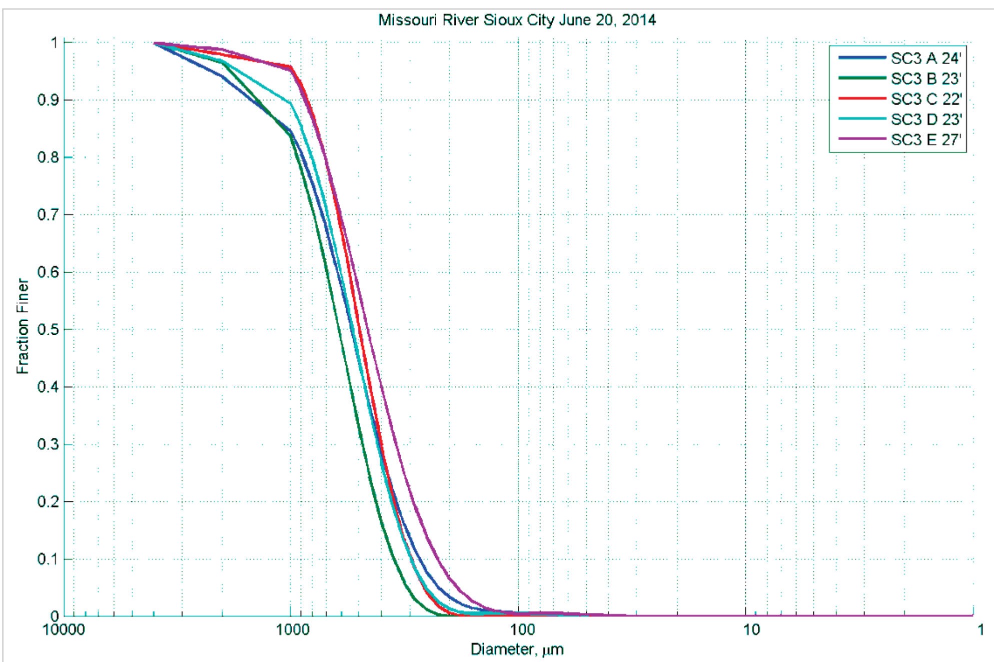

3.6 Suspended sediment

During this process, samples at different depths in a column were taken at the five stations shown in Figure 9, for each data collection date. Duplicate samples were taken to provide both particle size analysis and total suspended material flux computation by size class. For the particle size analysis, plots were created presenting the particle size distribution at different depths for each station. The measured data are available in Appendix I-f.

Particle size distribution for the first data collection date, April 30, 2014, is shown in Figure 13 to Figure 17. It is organized starting from the station closer to the left descending bank, Station A, to the station closer to the right descending bank, Station E.

Particle size distribution for the second data collection date, June 5, 2014, is shown in Figure 18 to Figure 22.

Particle size distribution for the third data collection date, June 20, 2014, is shown in Figure 23 to Figure 27.

Figure 13. Particle size distribution at different depths (feet) in Station A – April 30, 2014.

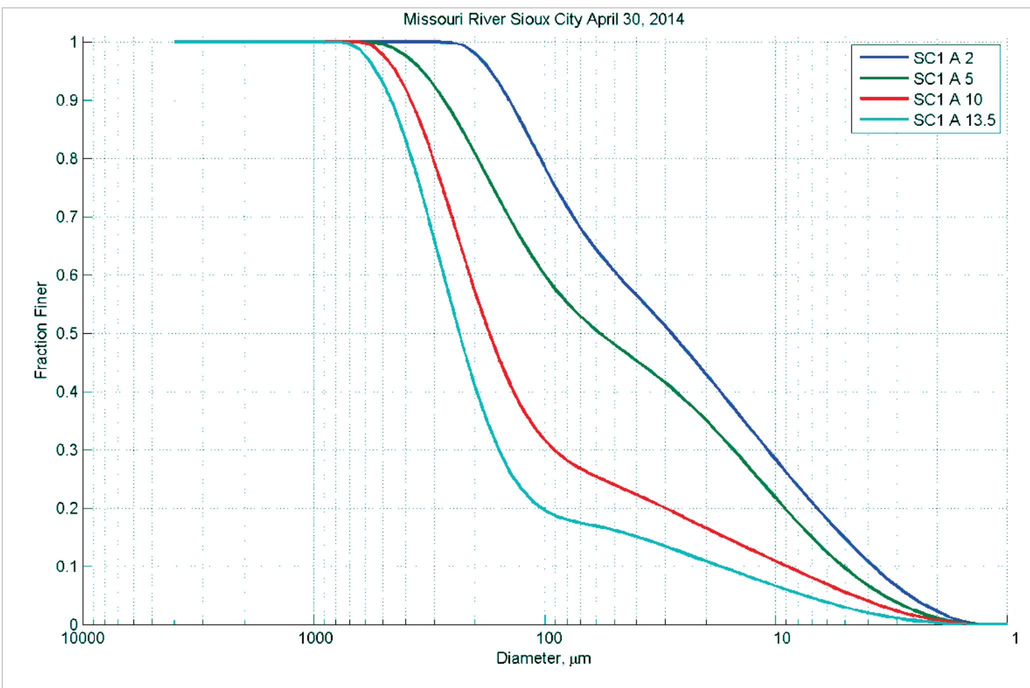

Figure 14. Particle size distribution at different depths (feet) in Station B – April 30, 2014.

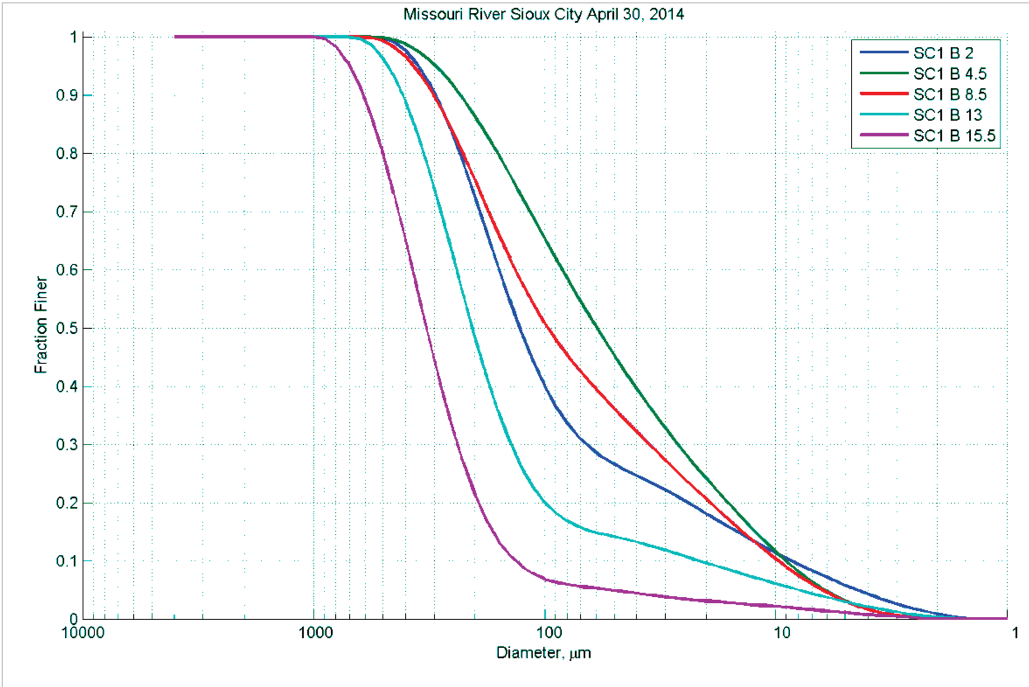

Figure 15. Particle size distribution at different depths (feet) in Station C – April 30, 2014.

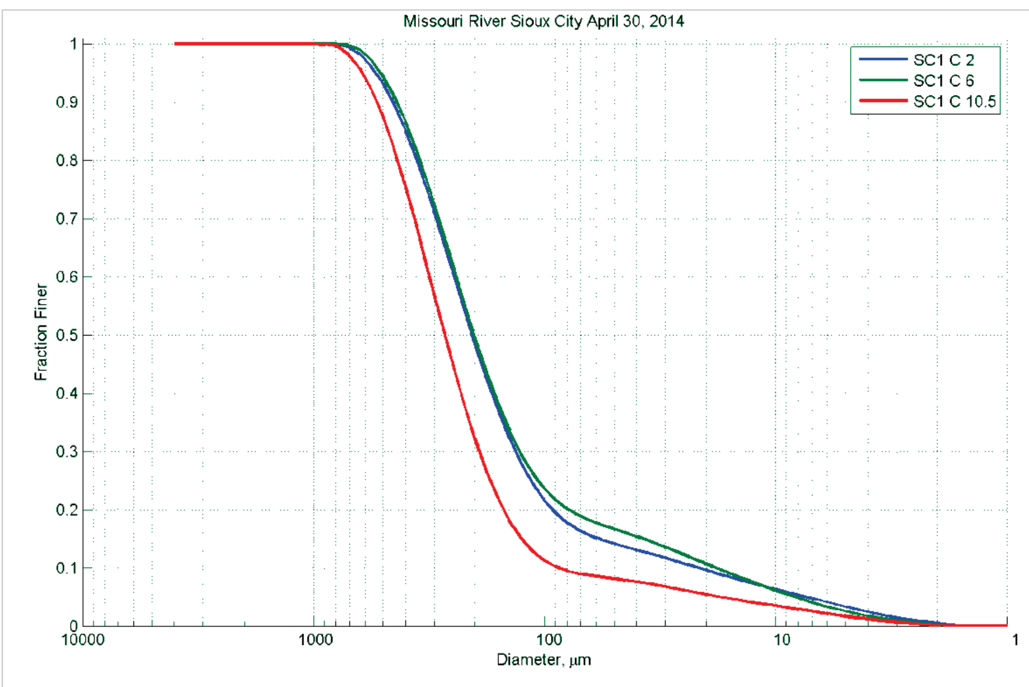

Figure 16. Particle size distribution at different depths (feet) in Station D – April 30, 2014.

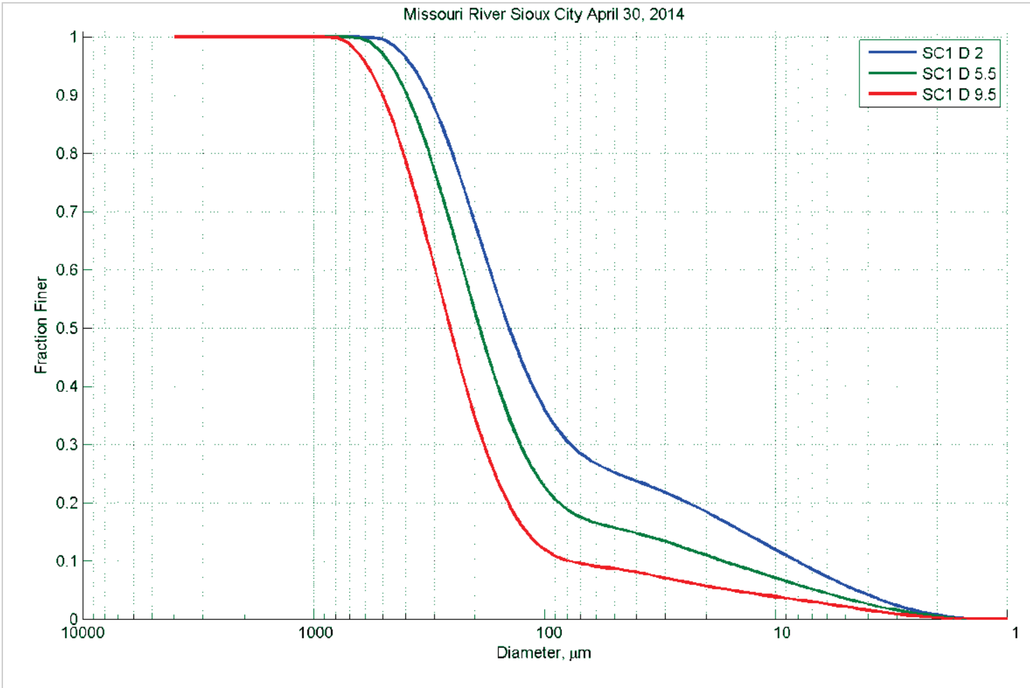

Figure 17. Particle size distribution at different depths (feet) in Station E – April 30, 2014.

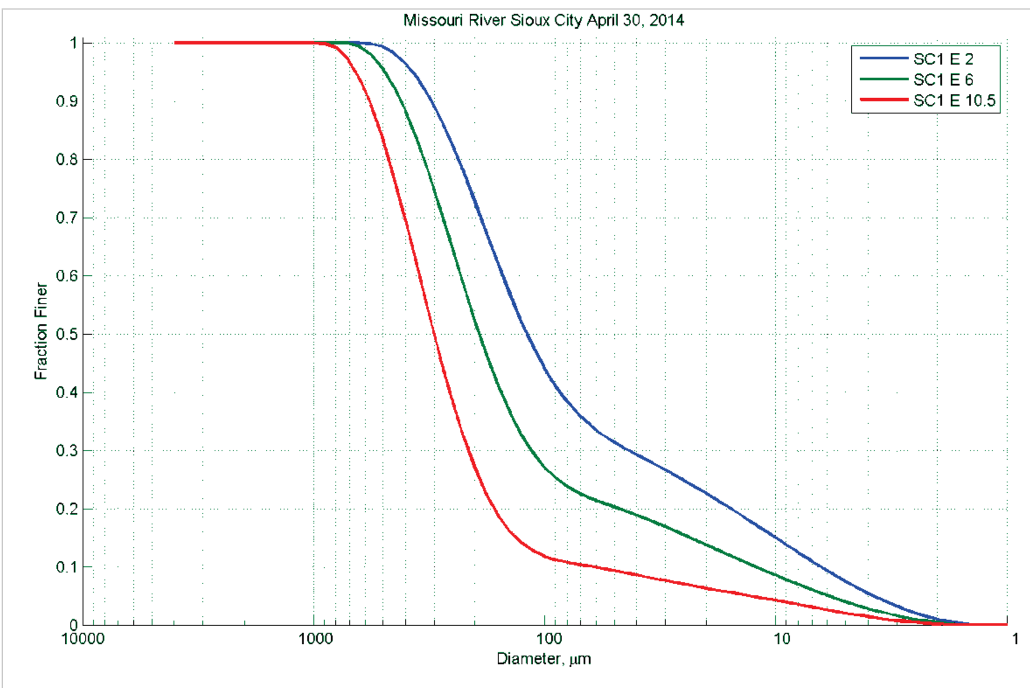

Figure 18. Particle size distribution at different depths (feet) in Station A – June 5, 2014.

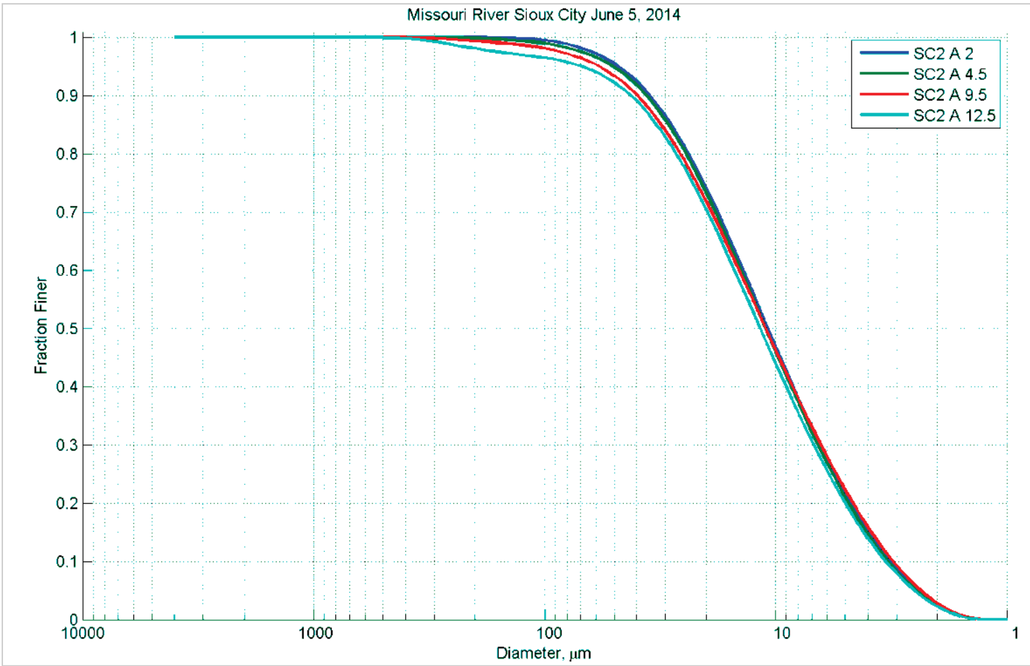

Figure 19. Particle size distribution at different depths (feet) in Station B – June 5, 2014.

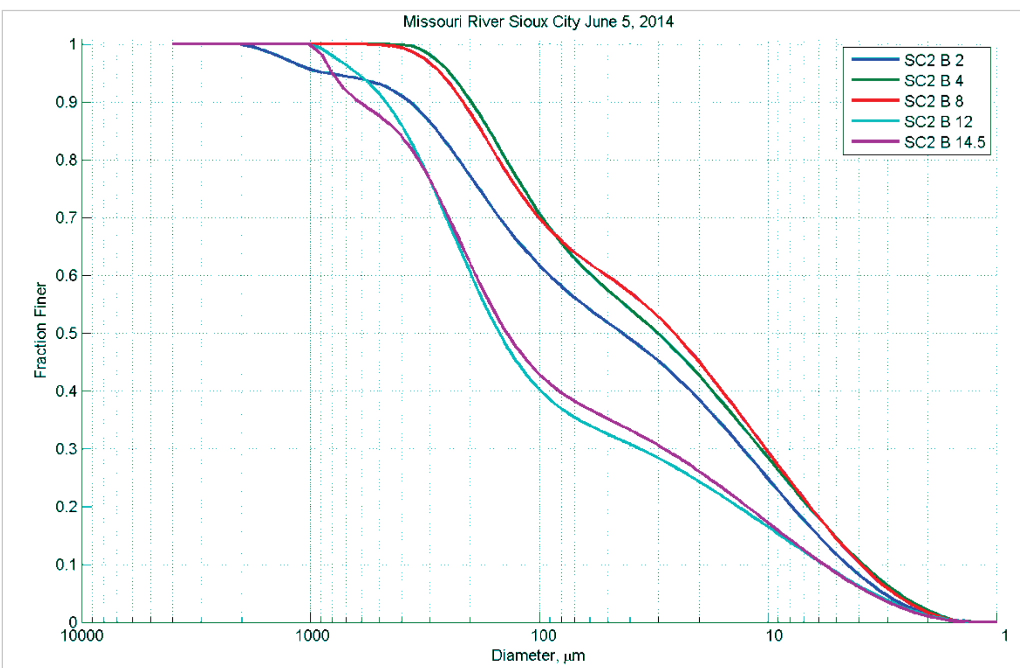

Figure 20. Particle size distribution at different depths (feet) in Station C – June 5, 2014.

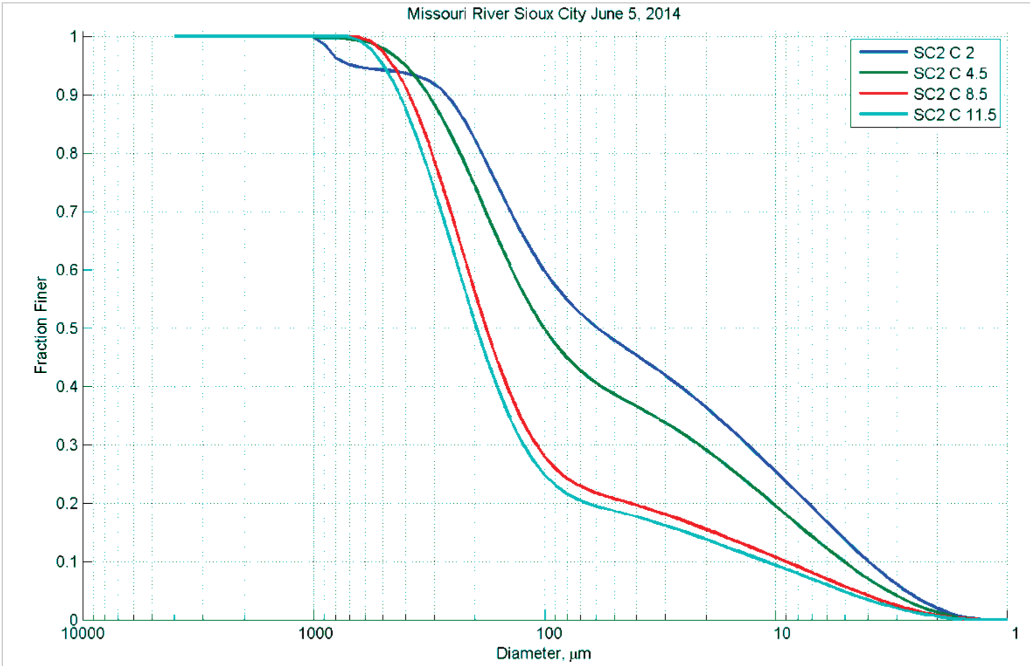

Figure 21. Particle size distribution at different depths (feet) in Station D – June 5, 2014.

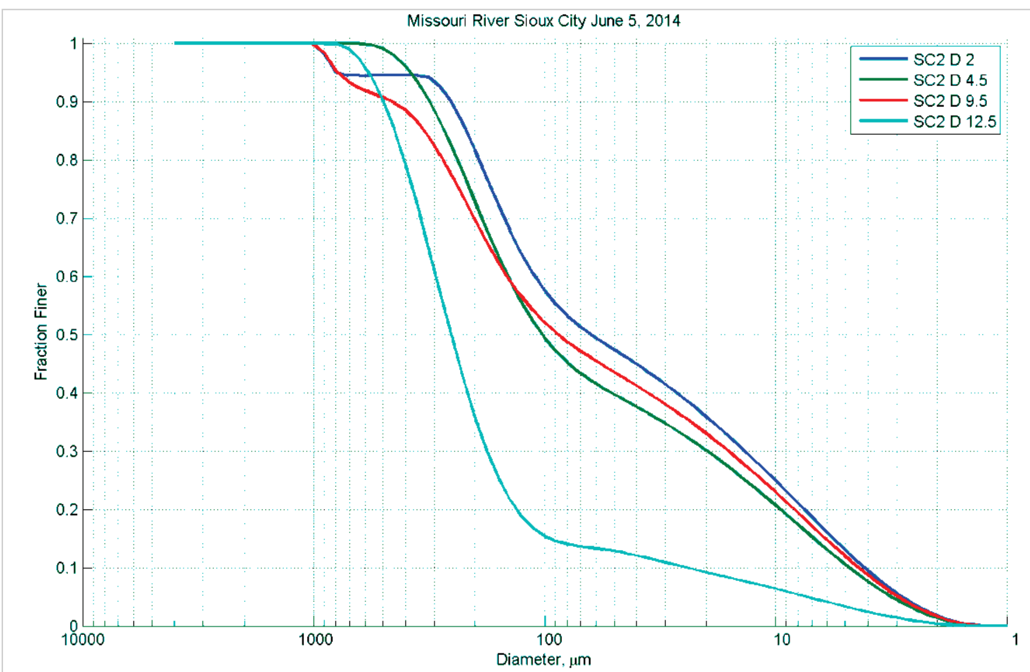

Figure 22. Particle size distribution at different depths (feet) in Station E – June 5, 2014.

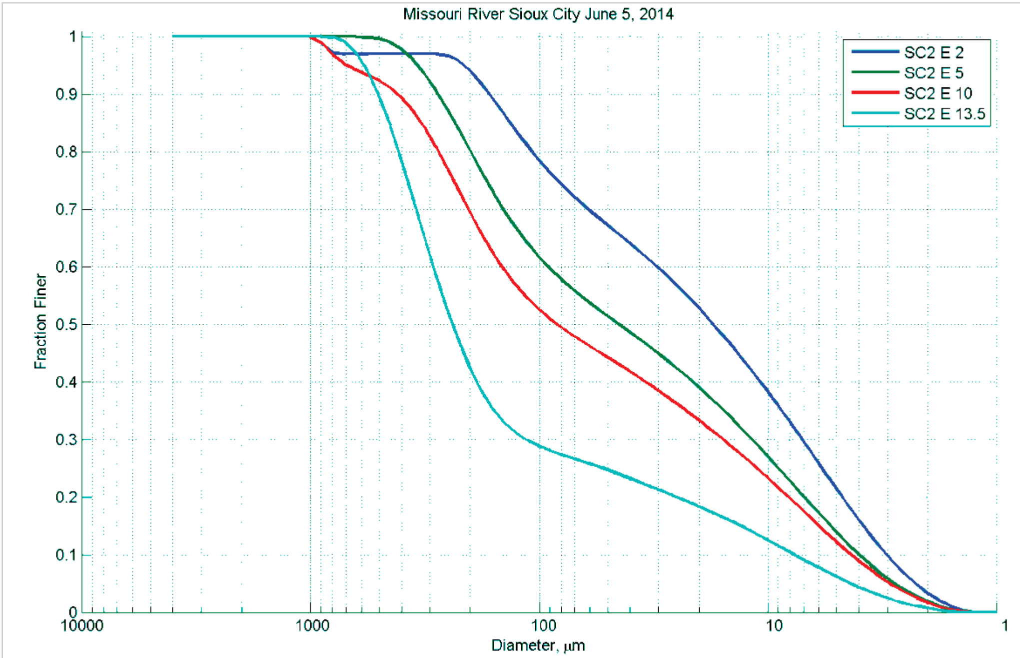

Figure 23. Particle size distribution at different depths (feet) in Station A – June 20, 2014.

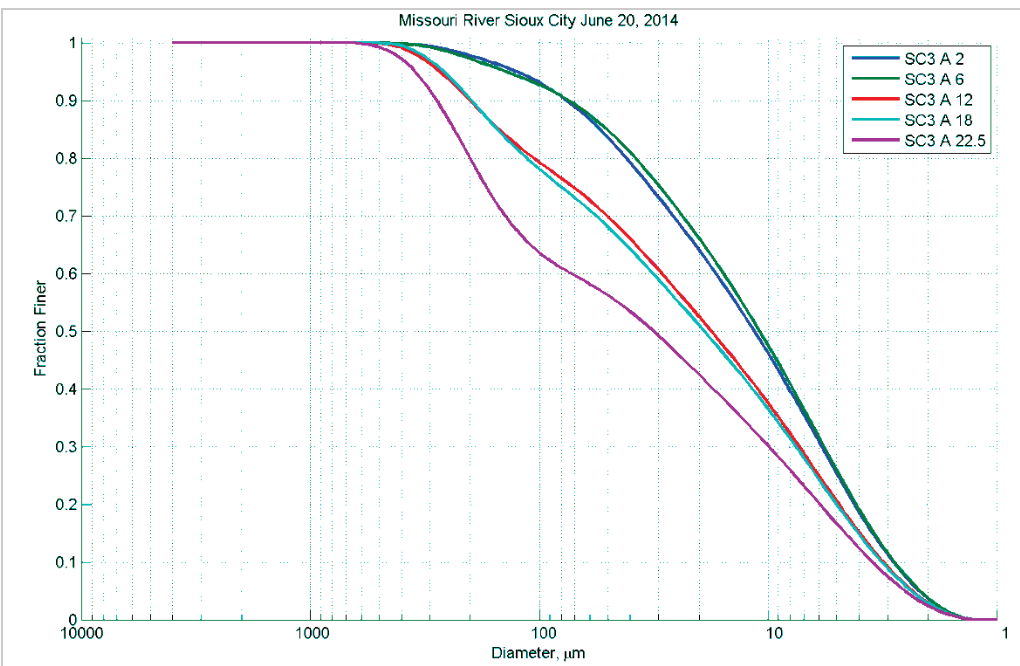

Figure 24. Particle size distribution at different depths (feet) in Station B – June 20, 2014.

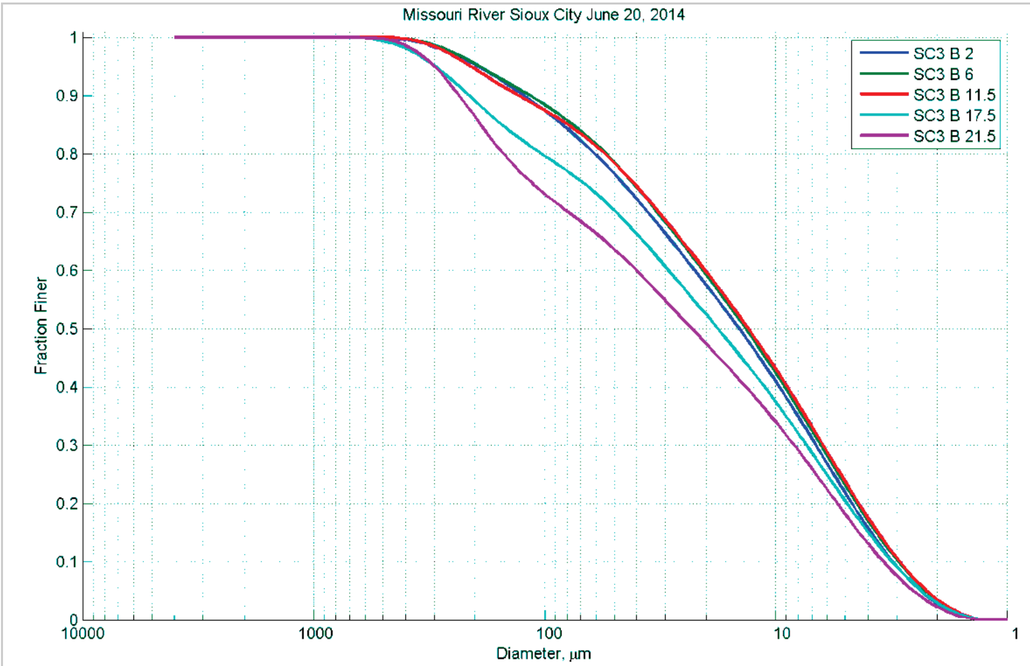

Figure 25. Particle size distribution at different depths (feet) in Station C – June 20, 2014.

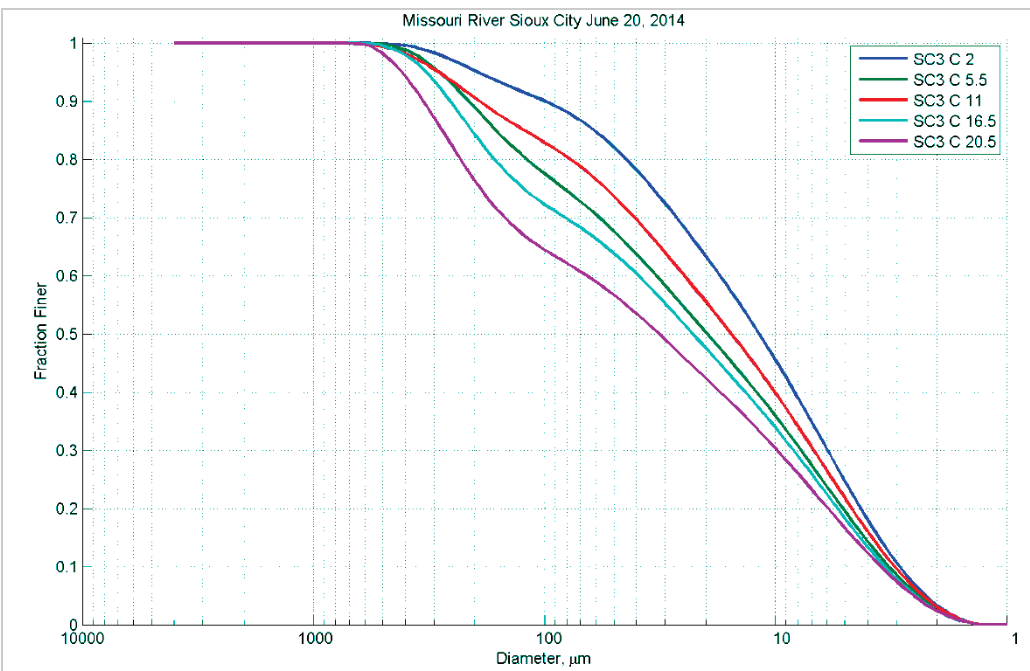

Figure 26. Particle size distribution at different depths (feet) in Station D – June 20, 2014.

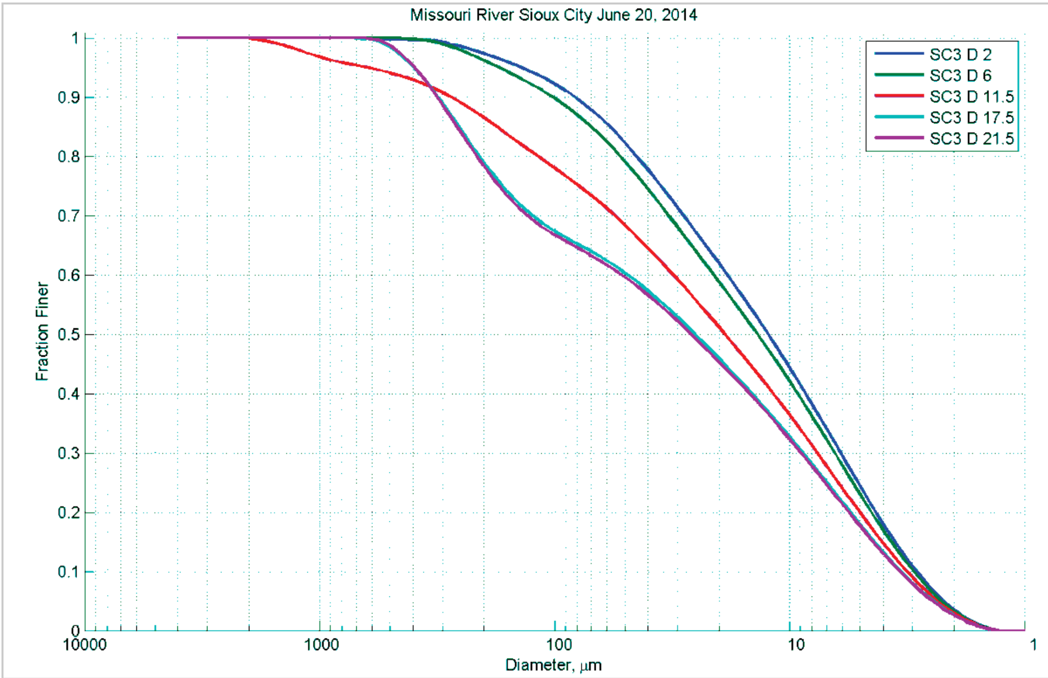

Figure 27. Particle size distribution at different depths (feet) in Station E – June 20, 2014.

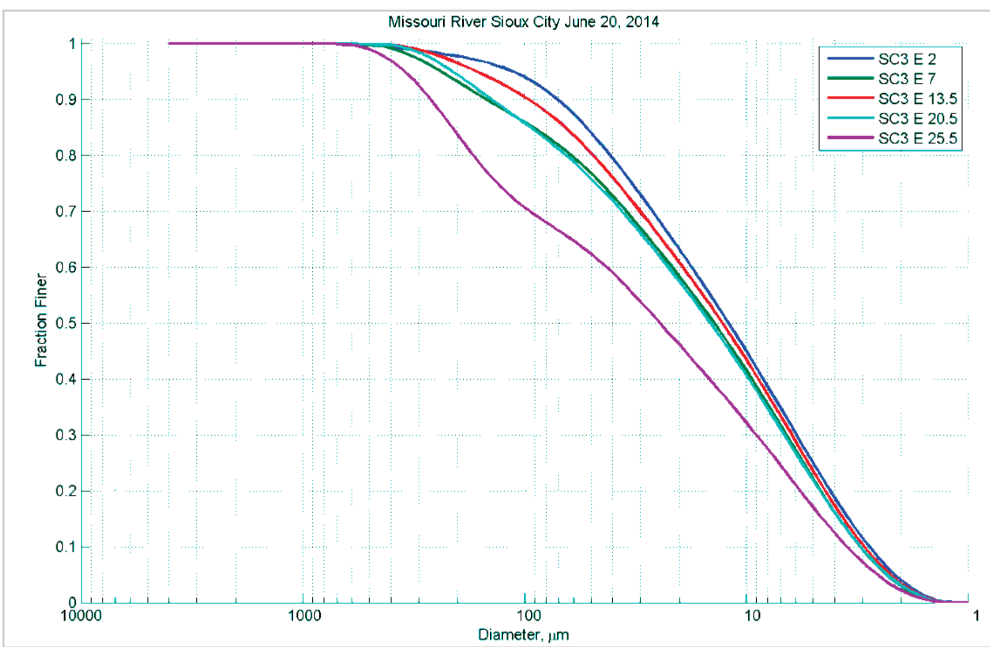

Suspended sediment concentration was also measured from the collected samples. Table 8 to Table 10 present the concentration values for each data collection date. Suspended sediment concentration profiles were created using the measured data, presented in Figure 28 to Figure 30. In Figure 29, the Station A data are significantly higher in concentration than the other stations and inverse in regards to depth vs. concentration. These data were checked and are the collected values. The samples were collected near the marina entrance and could have been affected by transient vessels and/or unusual flow conditions in that area. These data should be considered as anomalous. See Appendix I-f for more details about the measured data.

Table 8. Suspended sediment concentration at Sioux City, IA – April 30, 2014.

Station	Depth (ft)	Concentration (mg/L)*
SC 1A	2	44.8
SC 1A	5	51.9
SC 1A	10	125.5
SC 1A	13.5	240.0
Total depth	14.7	(Bottom)
SC 1B	2	78.9
SC 1B	5	114.7
SC 1B	8.5	129.2
SC 1B	13	213.9
SC 1B	15.5	306.5
Total depth	16.3	(Bottom)
SC 1C	2	103.7
SC 1C	6	152.6
SC 1C	10.5	355.3
Total depth	12.9	(Bottom)
SC 1D	2	75.3
SC 1D	5.5	143.1
SC 1D	9.5	244.1
Total depth	11.5	(Bottom)
SC 1E	2	49.7
SC 1E	6	133.6
SC 1E	10.5	300.6
Total depth	11.5	(Bottom)

*milligrams per liter

Table 9. Suspended sediment concentration at Sioux City, IA – June 5, 2014.

Station	Depth (ft)	Concentration (mg/L)
SC 2A	2	488.39
SC 2A	4.5	500.37
SC 2A	9.5	482.36
SC 2A	12.5	419.08
Total Depth	15.3	(Bottom)
SC 2B	2	66.11
SC 2B	4	98.47
SC 2B	8	112.69
SC 2B	12	161.44
SC 2B	14.5	202.78
Total depth	16.1	(Bottom)
SC 2C	2	73.55
SC 2C	4.5	102.48
SC 2C	8.5	114.61
SC 2C	11.5	159.84
Total depth	14.2	(Bottom)
SC 2D	2	74.80
SC 2D	4.5	97.89
SC 2D	9.5	116.61
SC 2D	12.5	174.92
Total depth	14.3	(Bottom)
SC 2E	2	69.69
SC 2E	5	68.67
SC 2E	10	81.52
SC 2E	13.5	136.87
Total depth	15.1	(Bottom)

Table 10. Suspended sediment concentration at Sioux City, IA – June 20, 2014.

Station	Depth (ft)	Concentration (mg/L)
SC 3A	2	1,711.11
SC 3A	6	1,886.77
SC 3A	12	1,870.00
SC 3A	18	2,390.10
SC 3A	22.5	2,380.53
Total depth	25.5	(Bottom)
SC 3B	2	1,396.62
SC 3B	6	1,987.69
SC 3B	11.5	1,823.71
SC 3B	17.5	1,867.83
SC 3B	21.5	2,213.94
Total depth	25.9	(Bottom)
SC 3C	2	903.88
SC 3C	5.5	1,505.00
SC 3C	11	2,013.26
SC 3C	16.5	1,674.47
SC 3C	20.5	1,568.85
Total depth	23	(Bottom)
SC 3D	2	987.27
SC 3D	6	1,246.32
SC 3D	11.5	1,566.14
SC 3D	17.5	1,104.44
SC 3D	21.5	1,733.17
Total depth	24	(Bottom)
SC 3E	2	867.60
SC 3E	7	957.57
SC 3E	13.5	1118.42
SC 3E	20.5	1382.73
SC 3E	25.5	1532.86
Total depth	26.7	(Bottom)

Figure 28. Suspended sediment concentration at Sioux City, IA – April 30, 2014.

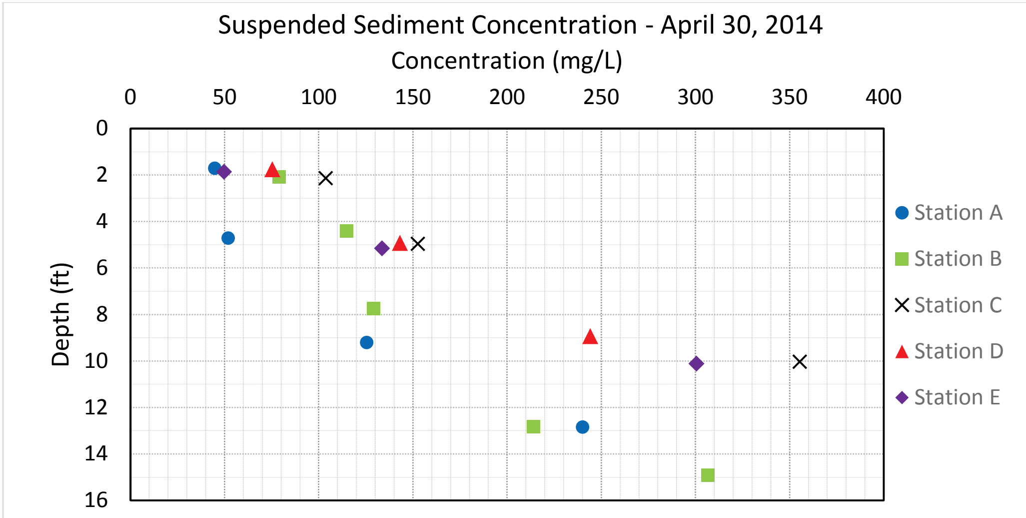

Figure 29. Suspended sediment concentration at Sioux City, IA – June 5, 2014.

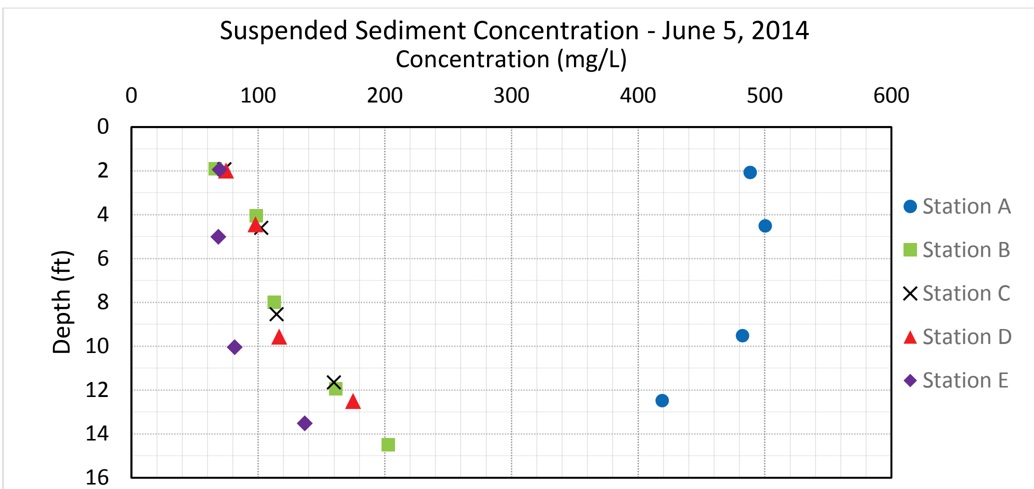

Figure 30. Suspended sediment concentration at Sioux City, IA – June 20, 2014.

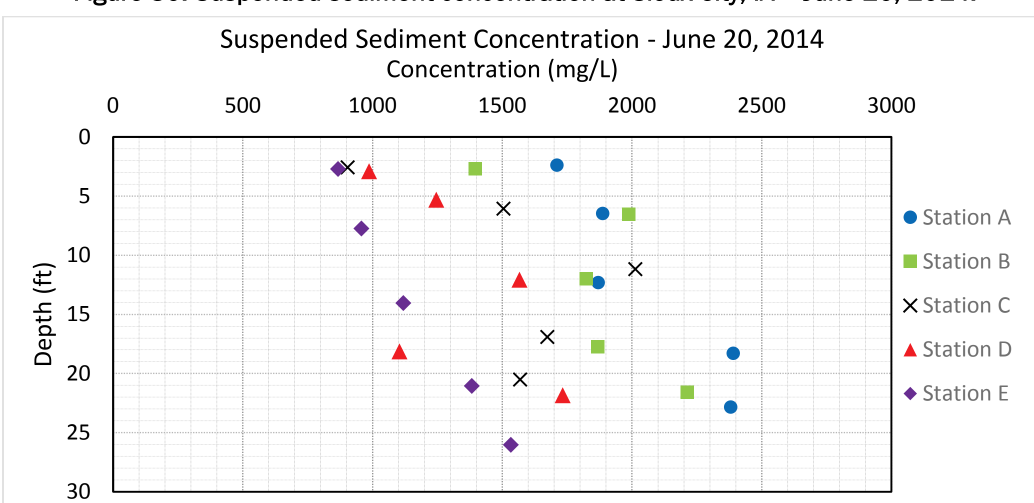

The suspended sediment concentration data were used to calibrate the ADCP acoustic backscatter and develop suspended sediment concentration profiles across the channel. Figure 31 to Figure 33 show the suspended sediment concentration profiles for the first left-to-right ADCP pass for each data collection date. For the other profiles, see Appendix I-g.

Figure 31. Suspended sediment concentration profile at Sioux City, IA – April 30, 2014.

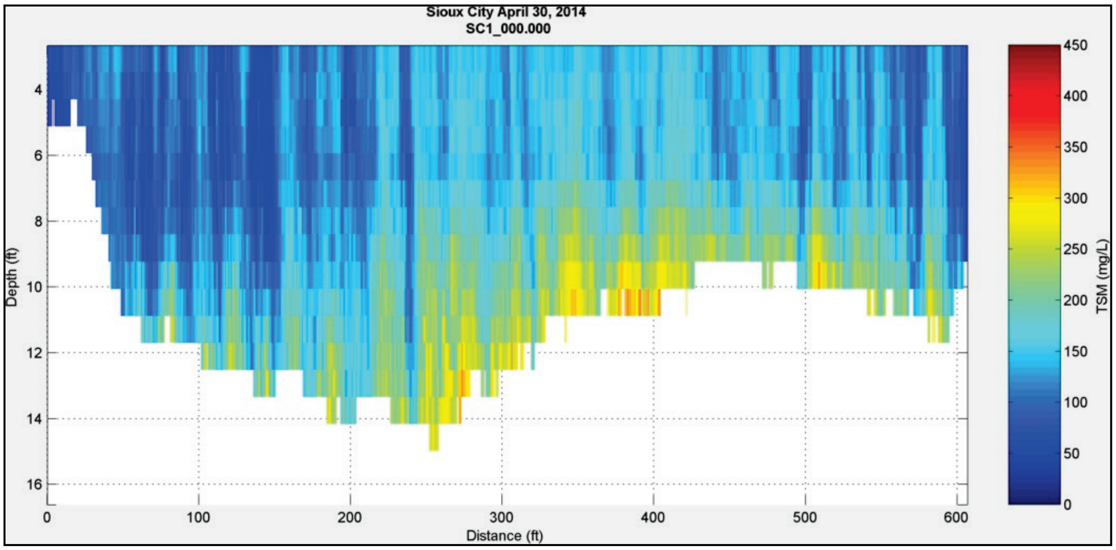

Figure 32. Suspended sediment concentration profile at Sioux City, IA – June 5, 2014.

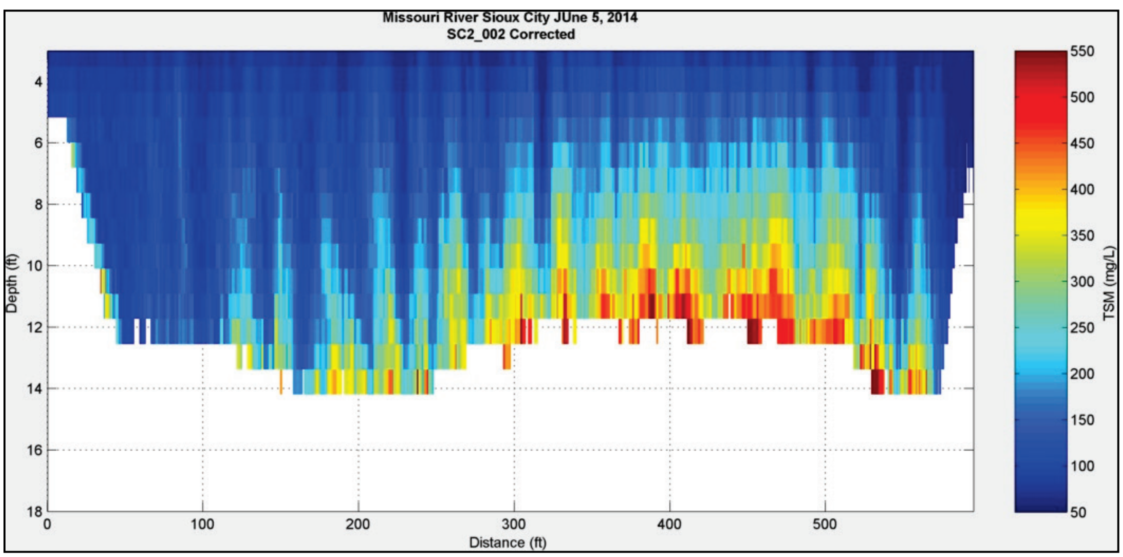

Figure 33. Suspended sediment concentration profile at Sioux City, IA – June 20, 2014.

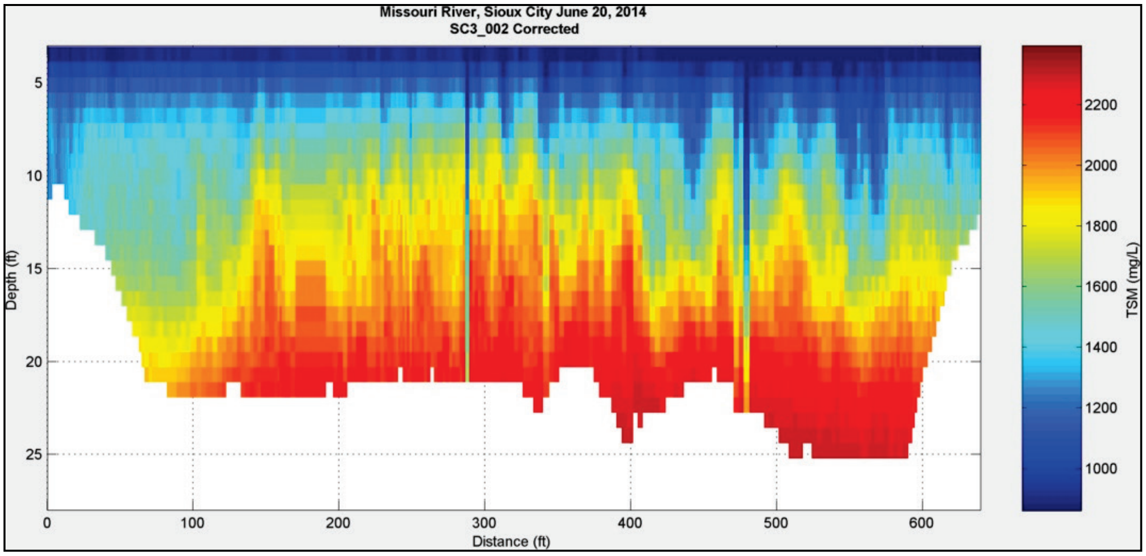

The suspended sediment concentration cross-section profiles obtained from the ADCP measurements were combined with the flow discharges, also obtained from the ADCP, to obtain the suspended sediment transport load, in tons per day. The method used for this study is explained in Heath et al. (2015, 13–14). The suspended sediment load can be divided classifying the suspended material by size and soil type. Table 11 presents the suspended sediment transport load, according to both classifications, for the first data collection date April 30, 2014. Table 12 and Table 13 present the same information for the second and third data collection dates, respectively. In all three tables, the categories under the Soil Type Classification were determined as follows: Clay Flux groups the size fractions 0.0001 to 0.0004 millimeters (mm), Silt Flux 0.0004 to 0.0625 mm, and Sand Flux 0.0625 to 2.00 mm.

Table 11. Suspended sediment load distributed by grain size and soil type – April 30, 2014.

Classification System	Category	Sediment Flux (tons/day)
Total load		15,845.70
Sediment size classification	0.001 – 0.004 mm	407.95
	0.004 – 0.008 mm	632.98
	0.008 – 0.016 mm	807.35
	0.016 – 0.031 mm	811.51
	0.031 – 0.063 mm	830.66
	0.063 – 0.125 mm	1,562.16
	0.125 – 0.250 mm	3,900.03
	0.250 – 0.500 mm	3,956.77
	0.500 – 1.00 mm	918.00
	1.00 – 2.00 mm	0.99
Soil type classification	Clay	408
	Silt	3,082.50
	Sand	10,337.95

Table 12. Suspended sediment load distributed by grain size and soil type – June 5, 2014.

Classification System	Category	Sediment Flux (tons/day)
Total load		15,845.70
Sediment size classification	0.001 – 0.004 mm	1,340.46
	0.004 – 0.008 mm	1,887.16
	0.008 – 0.016 mm	2,119.48
	0.016 – 0.031 mm	1,742.61
	0.031 – 0.063 mm	1,268.42
	0.063 – 0.125 mm	1,465.43
	0.125 – 0.250 mm	2,933.36
	0.250 – 0.500 mm	2,319.29
	0.500 – 1.00 mm	701.29
	1.00 – 2.00 mm	68.21
Soil type classification	Clay	1,340.46
	Silt	7,017.67
	Sand	7,487.58

Table 13. Suspended sediment load distributed by grain size and soil type – June 20, 2014.

Classification System	Category	Sediment Flux (tons/day)
Total load	Total Sediment Flux	360,003.10
Sediment size classification	0.001 – 0.004 mm	51,750.36
	0.004 – 0.008 mm	63,260.20
	0.008 – 0.016 mm	59,620.44
	0.016 – 0.031 mm	49,821.68
	0.031 – 0.063 mm	45,177.77
	0.063 – 0.125 mm	30,158.72
	0.125 – 0.250 mm	33,893.45
	0.250 – 0.500 mm	23,650.56
	0.500 – 1.00 mm	2,203.45
	1.00 – 2.00 mm	466.47
Soil type classification	Clay	51,750.36
	Silt	217,880.09
	Sand	90,372.65

3.7 Bed load transport

The ISSDOTv2 method was used for computing the bed-load transport. Table 14 shows the values obtained for the bed load, as well as the other sediment quantities determined from the suspended sediment samples at the Sioux City site. It provides a breakdown of the various measured sediment transport components, based on sediment size classification.

Table 14. Bed-load transport values from Sioux City, IA.

Data Collection Date	30-Apr-14	5-Jun-14	20-Jun-14
Flow (cubic feet per second [cfs])	28,691	32,642	78,082
Bed load (tons/day)	1,722	1,251	10,850
Suspended BML (tons/day)	10,338	7,488	90,373
Total BML (tons/day)	12,060	8,739	101,223
Bed load Fraction (%)	14.3%	14.3%	10.7%
Wash load (tons/day)	3,490	8,358	269,630
Total load (tons/day)	15,550	17,097	370,853

In Table 14, *bed load* is defined as the bed material moving at the bottom of the river in bed-forms; *suspended BML* refers to the suspended material with grain size higher than 0.063 mm; *total BML* is the sum of bed load and suspended BML; *bed load fraction* is the percentage of the total bed

material moving as bed load; *wash load* is fine sediments that never settle in the bed, with grain size of 0.063 mm or less; and *total load* combines the quantity of total BML and wash load.

A bed-load rating curve was prepared for this site by plotting the bed-load transport in tons per day versus the river flowrate. This graph is shown in Figure 34. The first two points were obtained with very similar flows and therefore have nearly the same amount of bed-load transport. The third trip on June 20, 2014, was more than double the flow and shows a correspondingly much higher transport rate.

Figure 34. Bed-load rating curve for Missouri River at Sioux City, IA.

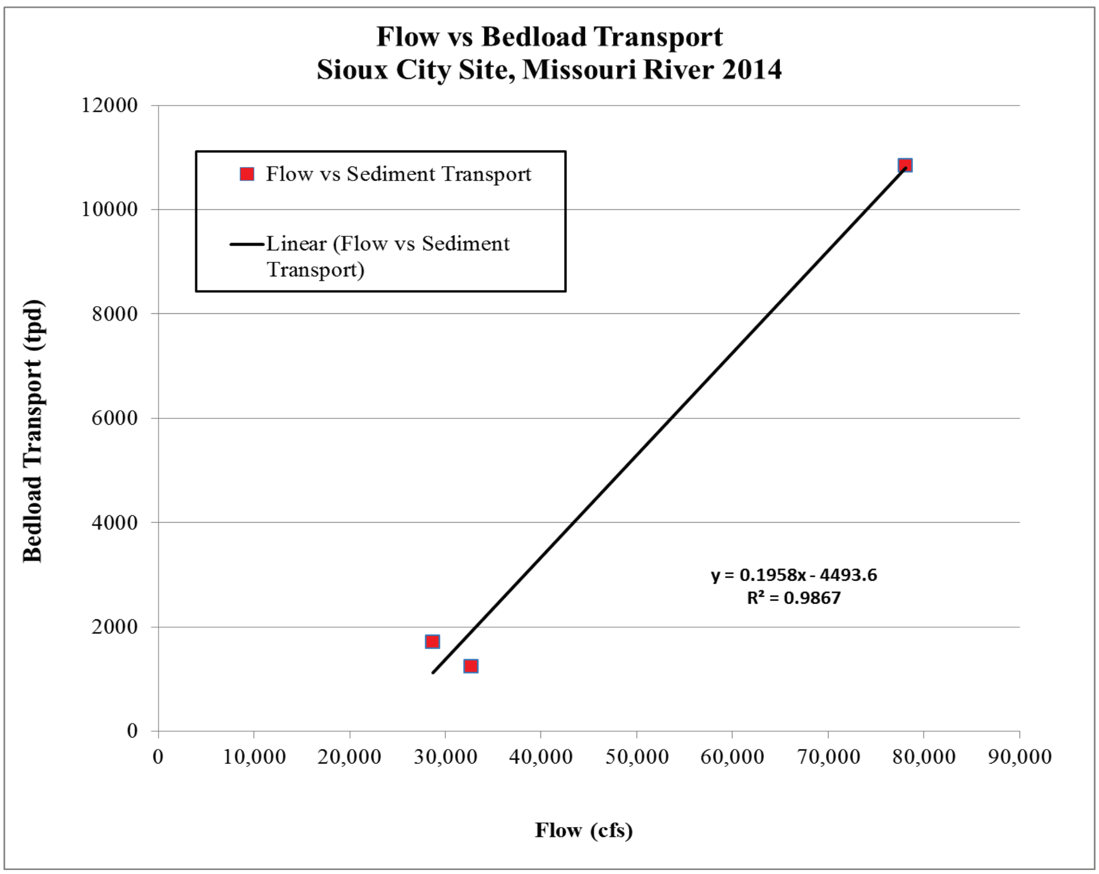

Bed-load transport values were also computed for this site using two analytic transport functions. One is the Meyer-Peter and Mueller formula (MPM), and the other is the Einstein formula. They were computed for each swath of bathymetric data. For instance, Figure 35 shows the bathymetry of this site with the six swath numbers (S1 to S6) labeled on it, indicating the lateral position where each swath was located. The hydraulic and sediment parameters obtained in the field data collection effort discussed before were extracted for each of these swaths.

Figure 35. Bathymetry for Missouri River at Sioux City, showing swath locations.

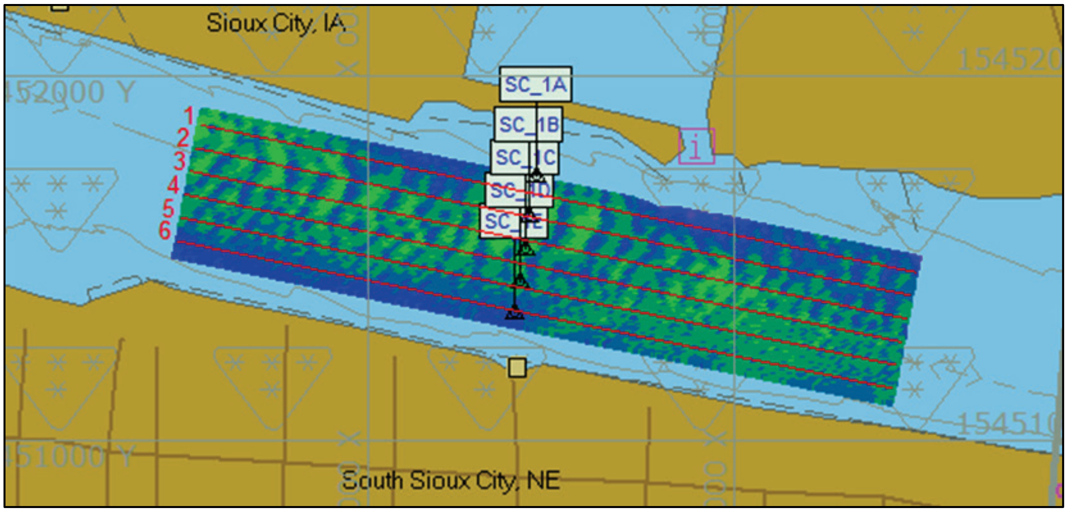

Flow, average velocity, and water depth were obtained from the ADCP data by a separate program written for that specific purpose. Water slope and water temperature were obtained from each appropriate data appendix. Bed sediment gradations used were selected based on their proximity to a given swath. The SAM Hydraulic Design Package for Channels[1] program was then used with these data to compute the bed-load values for each swath. This software package has provisions for entering hydraulic and sediment input parameters and can then compute bed-load transport values for several commonly used transport functions.

The results are plotted in Figure 36 to Figure 38 and show how the transport function values compare to the ISSDOTv2 measured values. They also show the lateral variability across the measured section from the left side to the right side of the channel. The red number in Figure 36 indicates an interpolated value.

[1] SAM Hydraulic Design Package for Channels. U.S. Army Engineer Research and Development Center, Coastal and Hydraulics Laboratory, Vicksburg, MS.

Figure 36. Bed-load transport at Sioux City, IA – April 30, 2014: ISSDOTv2 values compared to transport function computed values, where red indicates an interpolated value.

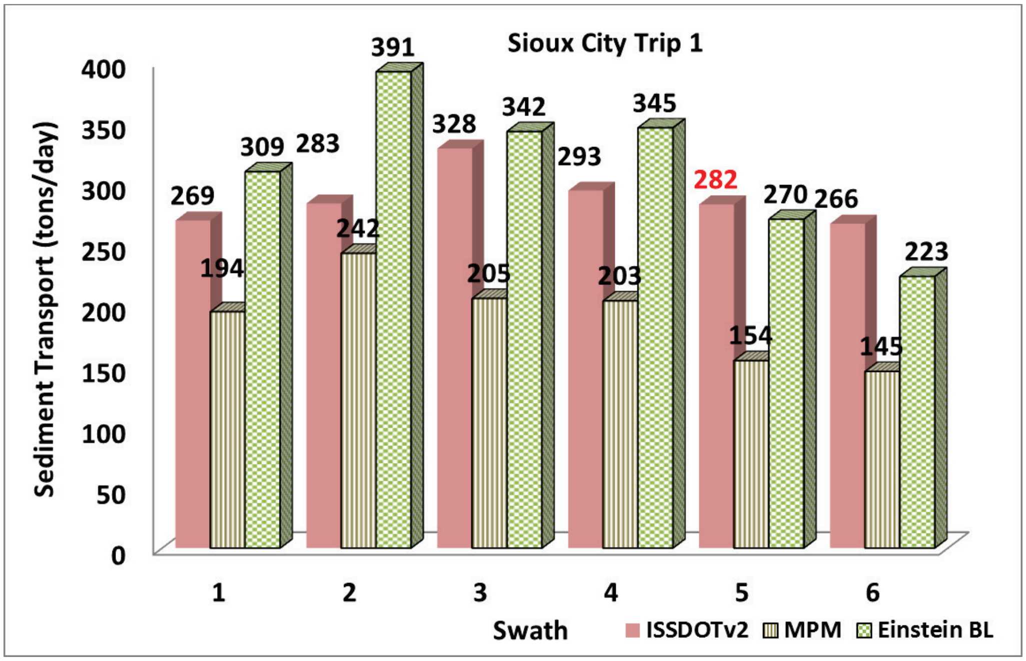

Figure 37. Bed-load transport at Sioux City, IA – June 5, 2014: ISSDOTv2 values compared to transport function computed values.

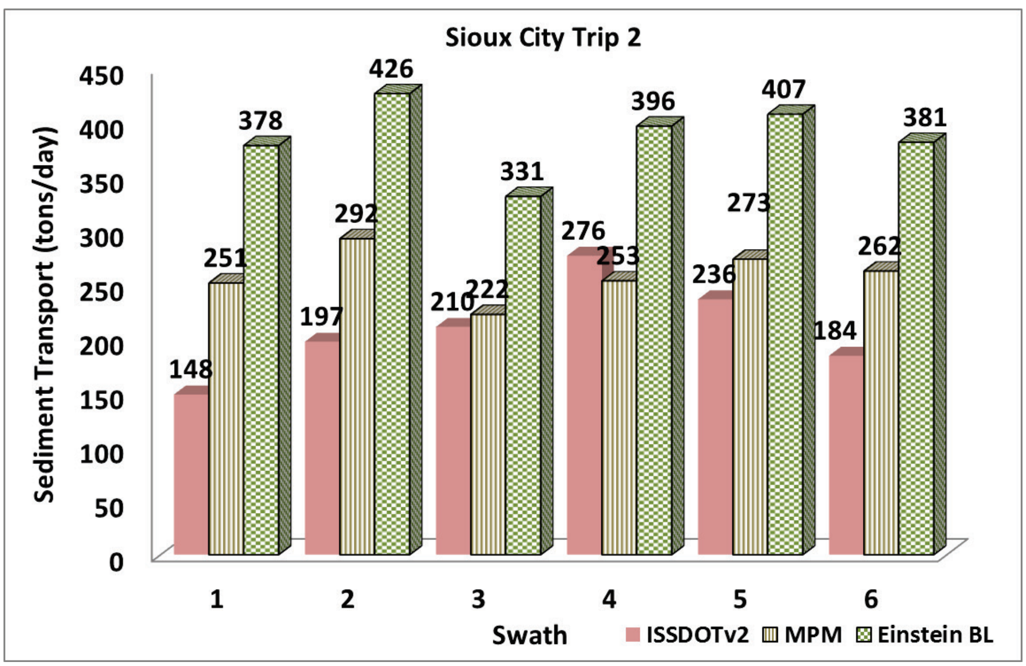

Figure 38. Bed-load transport at Sioux City, IA – June 20, 2014: ISSDOTv2 values compared to transport function computed values.

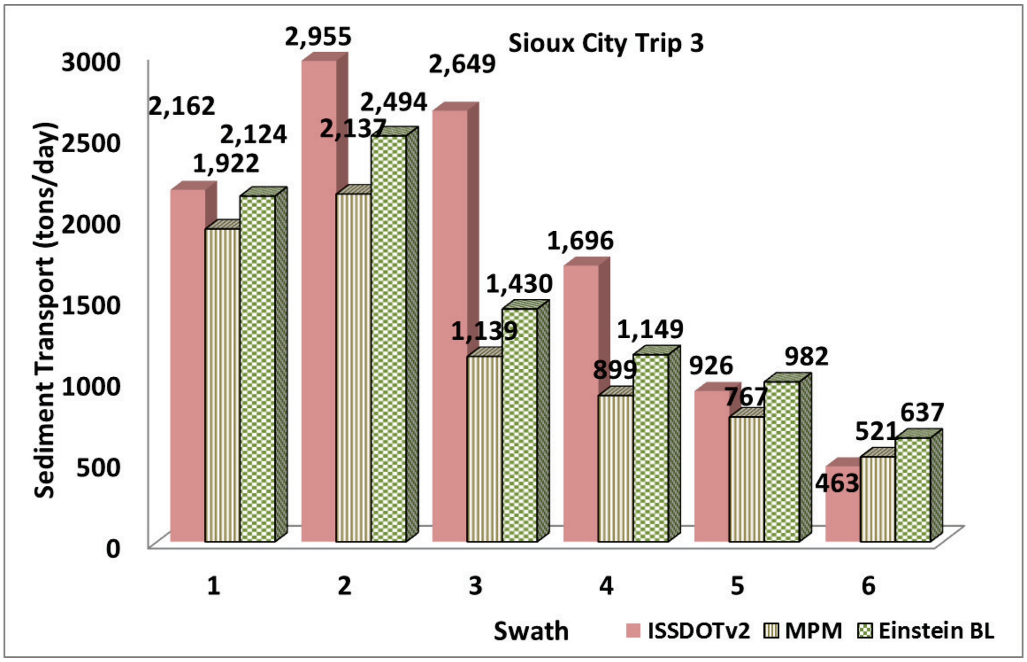

4 Site 2: Omaha, Nebraska

ADCP flow and velocity measurements, water surface elevation and slope measurements, and water temperature measurements, along with multi-beam surveys, bed and suspended material sampling and testing, and bed load calculations, were performed during each data collection date at Omaha, NE. The measuring area is shown on Figure 39 as the green polygon. The bank-to-bank width of the river at this location is estimated to fluctuate between 720 and 755 ft; the length of the study area was approximately 2,000 ft. The approximate location of the USGS gage station near the data collection site is also shown as the blue pin. This location might not be accurate in the figure. Coordinates for the gage site as given in the USGS web site are listed in Table 3. The red line indicates the cross section where ADCP measurements were taken and suspended and bed load material samples were collected. The data collection dates for this location were April 29, 2014; June 6, 2014; and June 21, 2014.

Figure 39. Omaha, NE, data collection site.

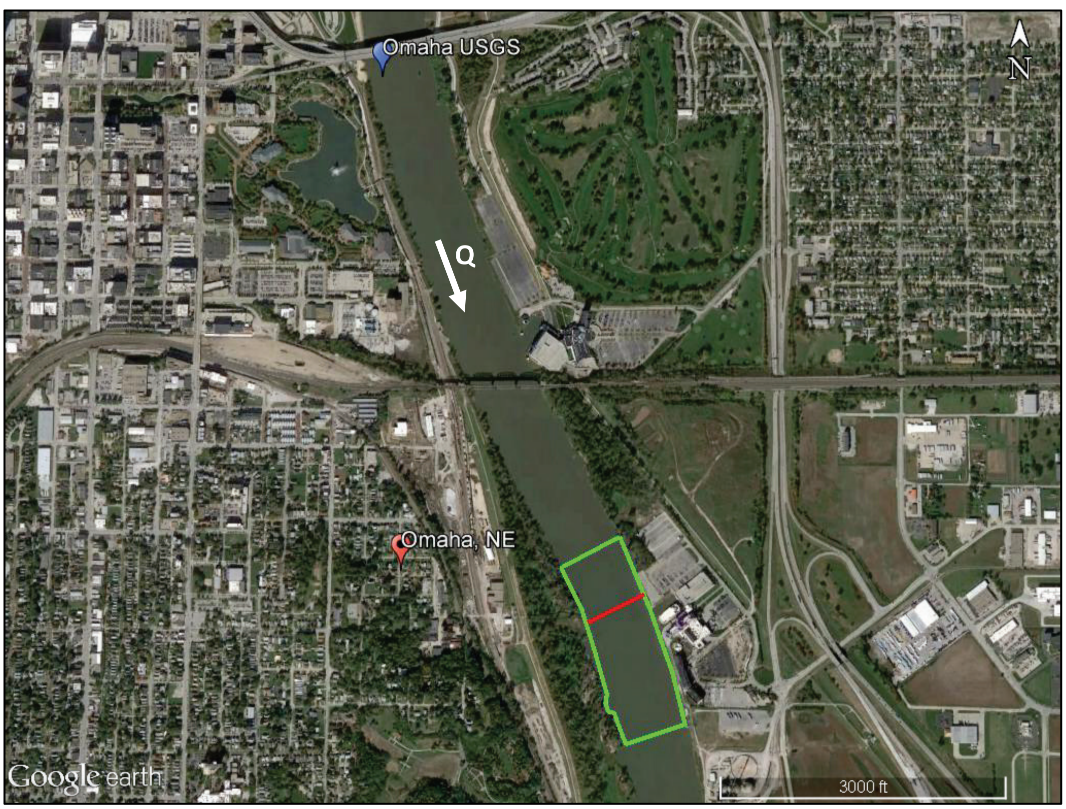

4.1 ADCP flow and velocity

The velocity and discharge on the given dates, and site, were measured using an ADCP. Table 15 presents the cross-section average flow (ft^3/s), area (ft^2), and average velocity (ft/s) for each date, calculated from the measured data. See Appendix II-a for the measured data.

Table 15. Total flow, area, and average velocity on the given dates at Omaha, NE.

Date	Total Flow, Q (ft^3/s)	Total Area, A (ft^2)	Velocity Q/A (ft/s)
April 29, 2014	29,496	8,439	3.50
June 6, 2014	38,826	10,467	3.71
June 21, 2014	93,688	17,622	5.32

Real-time vertical profiles of instantaneous velocities are also obtained from the ADCP measurements. Figure 40 to Figure 42 present the velocity magnitude, before the multi-beam measurements, from left to right. In the figures, the velocity magnitude is quantified by the range of colors shown on the right side of each figure, where the higher velocities are denoted by red and the lower velocities by blue. The velocity profiles for after the multi-beam measurements are available at Appendix II-a.

Figure 40. Velocity magnitude at Omaha, NE – April 29, 2014, 14:45:51.

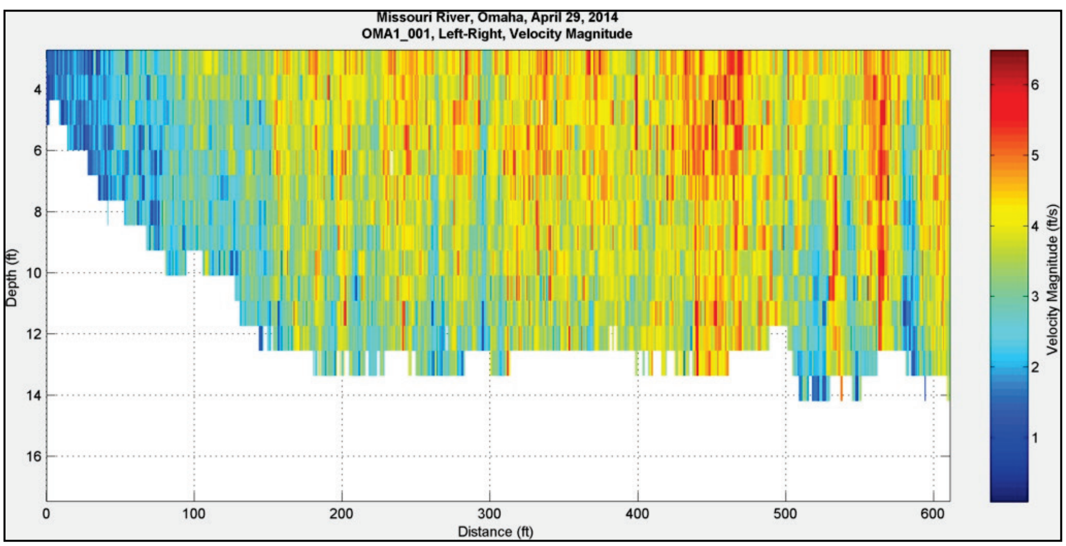

Figure 41. Velocity magnitude at Omaha, NE – June 6, 2014, 14:41:44.

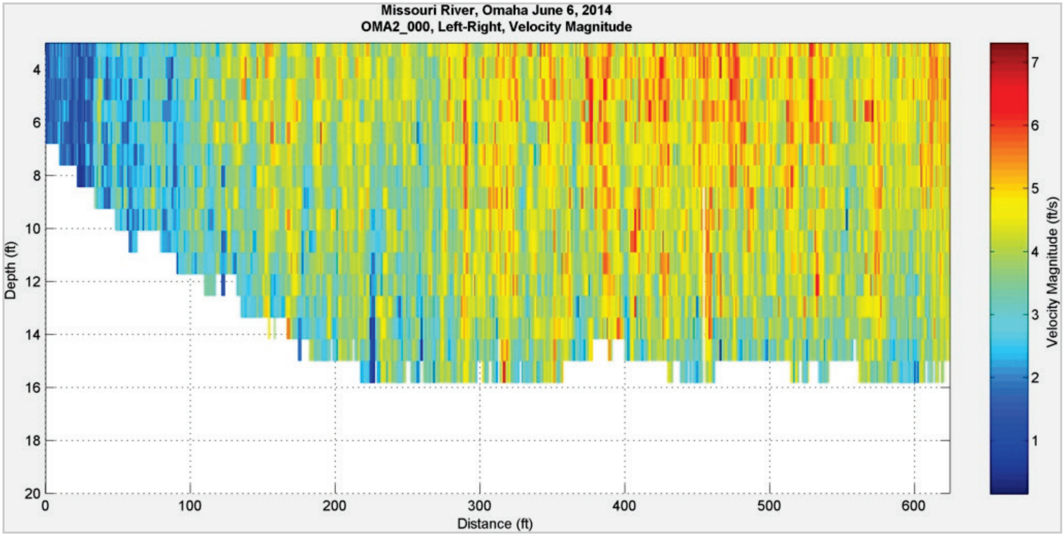

Figure 42. Velocity magnitude at Omaha, NE – June 21, 2014, 14:48:48.

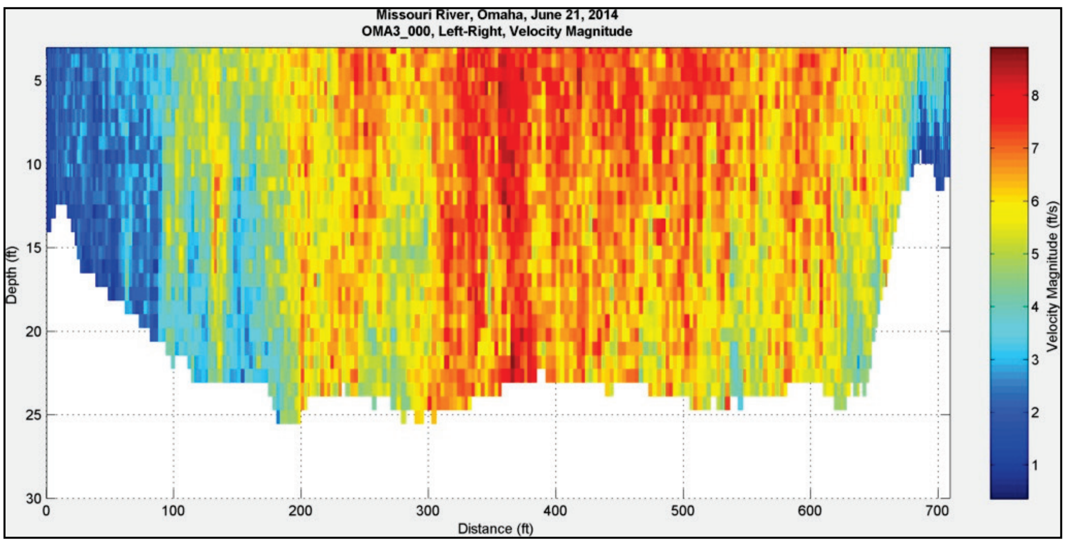

4.2 Water surface elevation and slope

Water surface elevation measurements were taken upstream and downstream of the multi-beam survey area. Figure 43 shows the upstream elevations, at distance zero, connected to the downstream elevations, at a distance of 2,000 ft, for each data collection date. Table 16 presents the slope values for the Omaha, NE, location for the three dates. The measured data are available at Appendix II-b.

Figure 43. Water surface elevation at Omaha, NE – from upstream to downstream.

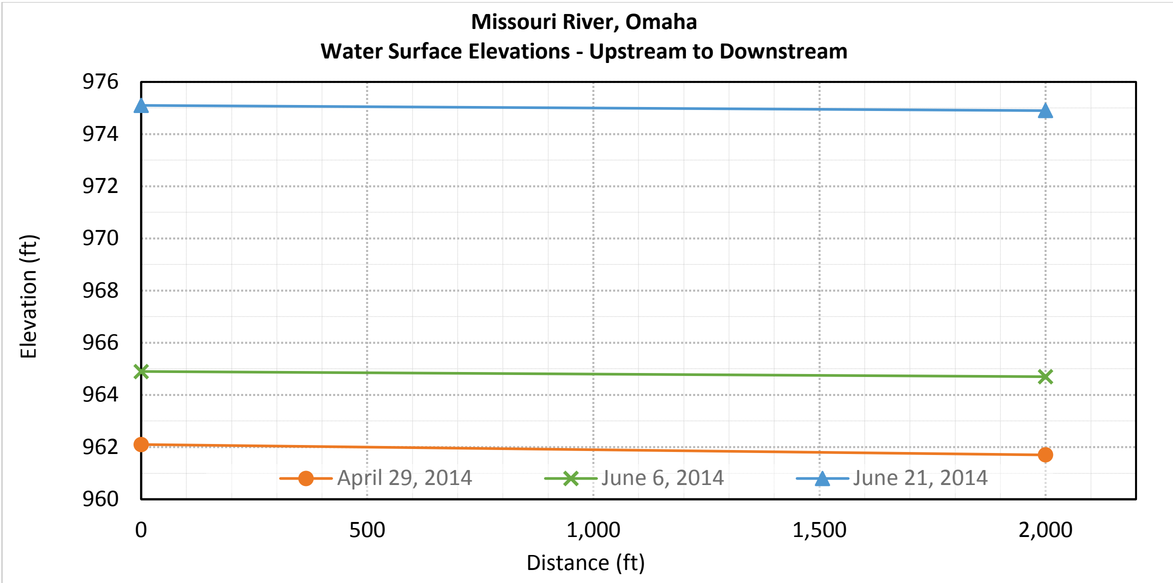

Table 16. Water surface slopes at Omaha, NE.

Date	Water Surface Slope (%)
April 29, 2014	0.00020
June 6, 2014	0.00010
June 21, 2014	0.00010

4.3 Water temperature

Table 17 presents the average temperature for each date (see Appendix II-c for the measured values).

Table 17. Water temperature at Omaha, NE.

Date	Temperature (F)
April 29, 2014	58.3
June 6, 2014	71.3
June 21, 2014	74.5

4.4 Multi-beam surveys

The initial multi-beam survey performed at Omaha, NE, included the full extent of the channel from bank to bank, as shown in Figure 44 where the dark blue areas are deeper and the red areas are shallower. This survey is used to determine the location of the sand waves throughout the study area and to then decide where to run the ISSDOTv2 swaths according to the location of the active sand transport portion of the channel. The selected area with swath lines and numbers displayed in red is shown in Figure 45. This shows the actual area that was used for the ISSDOTv2 bed-load computations. The length of the multi-beam swaths is approximately 2,000 ft for all three data collection dates.

Figure 44. Multi-beam survey extent at Omaha, NE – April 29, 2014.

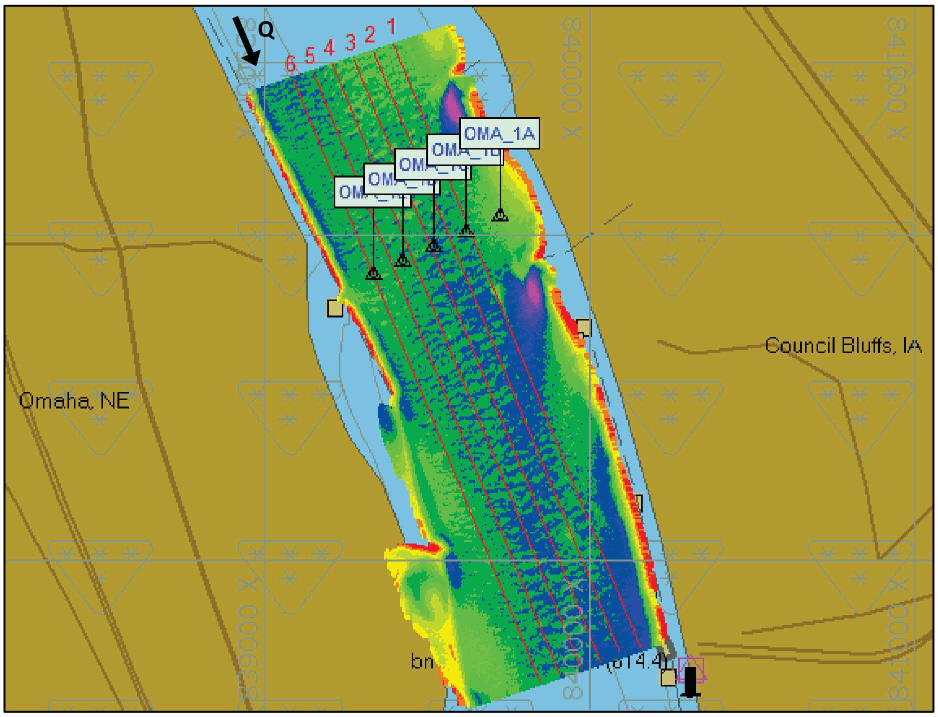

Figure 45. Multi-beam survey extent at Omaha, NE – June 6 and June 21, 2014.

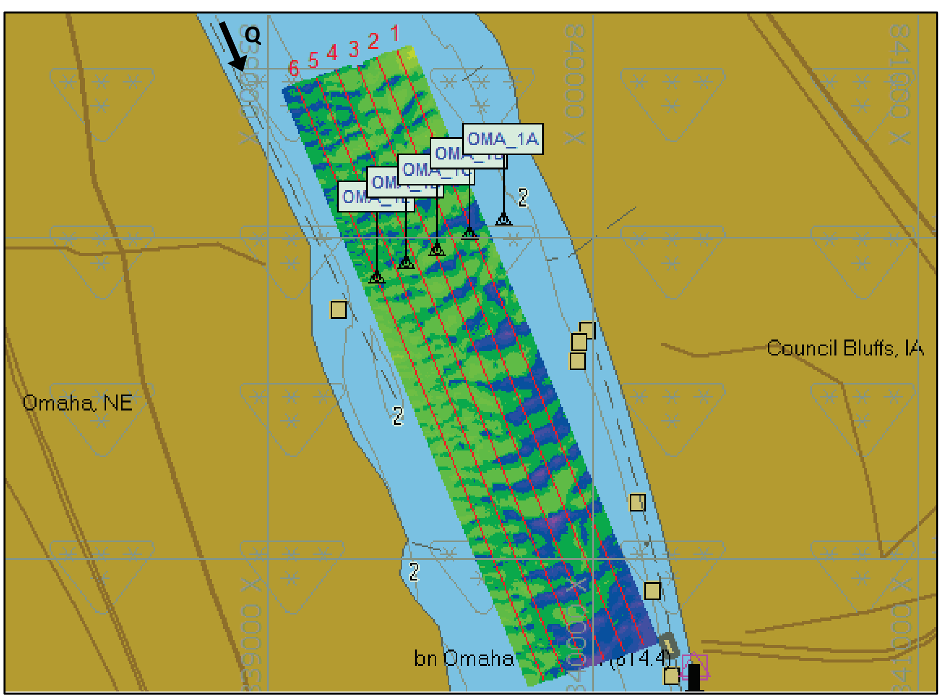

4.5 Bed material samples

Five sediment sample stations were positioned equidistant from each other along the cross section, as presented on Figure 46, which is the same location at which the suspended sediment samples and the ADCP velocity data were obtained. The first station, Station A, was positioned on the left descending bank, and the last station, Station E, on the right descending bank. Table 18 provides the locations of sample stations according to NAD83. See Appendix II-d for the coordinates using the UTM Grid System.

Figure 46. Sediment sample stations at the Missouri River – Omaha, NE.

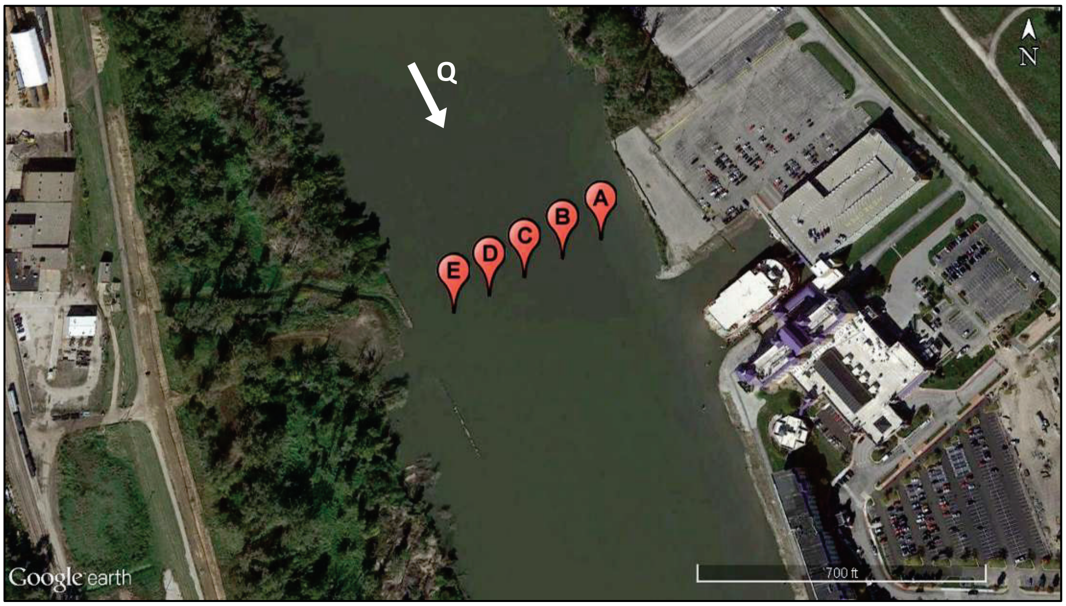

Table 18. Sediment sample stations NAD83 coordinates at Omaha, NE.

Station	NAD83 Latitude	NAD83 Longitude
OMA A	41° 14' 37.0369" N	95° 54' 44.8337" W
OMA B	41° 14' 36.5384" N	95° 54' 46.1476" W
OMA C	41° 14' 36.0356" N	95° 54' 47.4460" W
OMA D	41° 14' 35.5701" N	95° 54' 48.6376" W
OMA E	41° 14' 35.1244" N	95° 54' 49.8283" W

The grain size distribution for the five bed material samples of the first collection date, April 29, 2014, is provided at Figure 47. Figure 48 and Figure 49 present the gradation analysis for the second and third collected samples, respectively. The measured data are available in Appendix II-e.

Figure 47. Bed material grain size distribution for Omaha, NE – April 29, 2014.

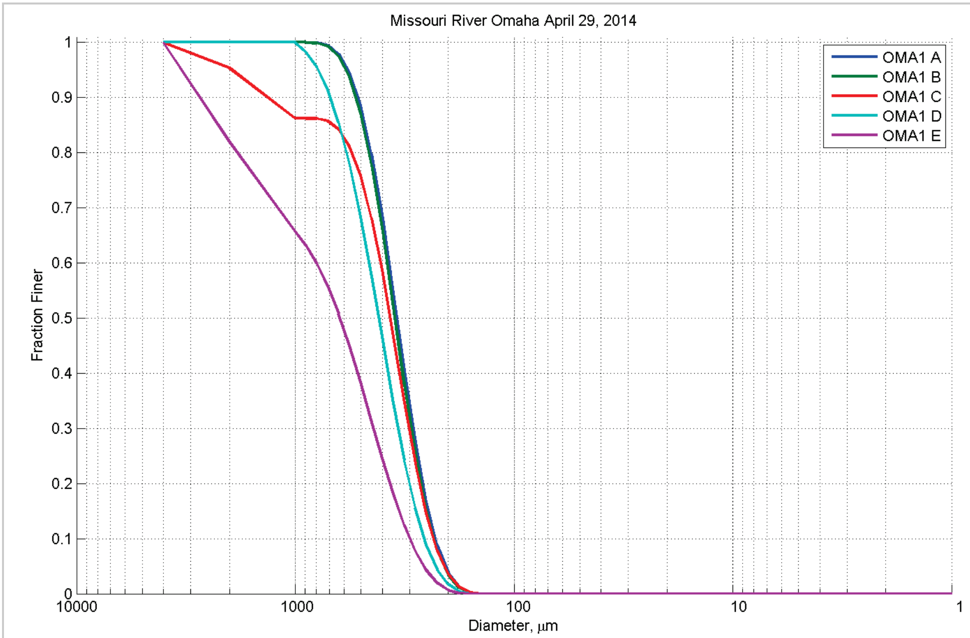

Figure 48. Bed material grain size distribution for Omaha, NE – June 6, 2014.

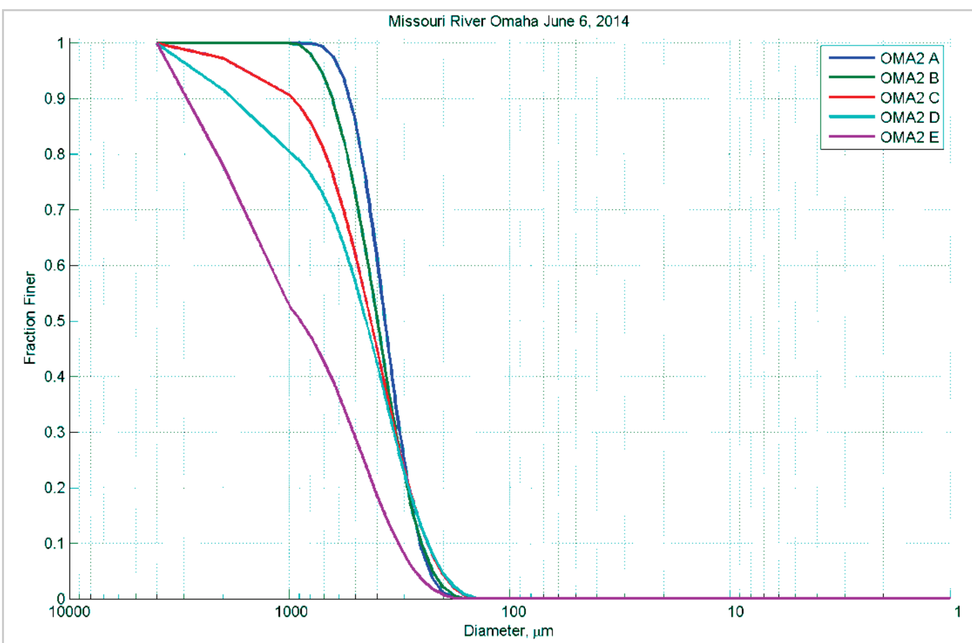

Figure 49. Bed material grain size distribution for Omaha, NE – June 21, 2014.

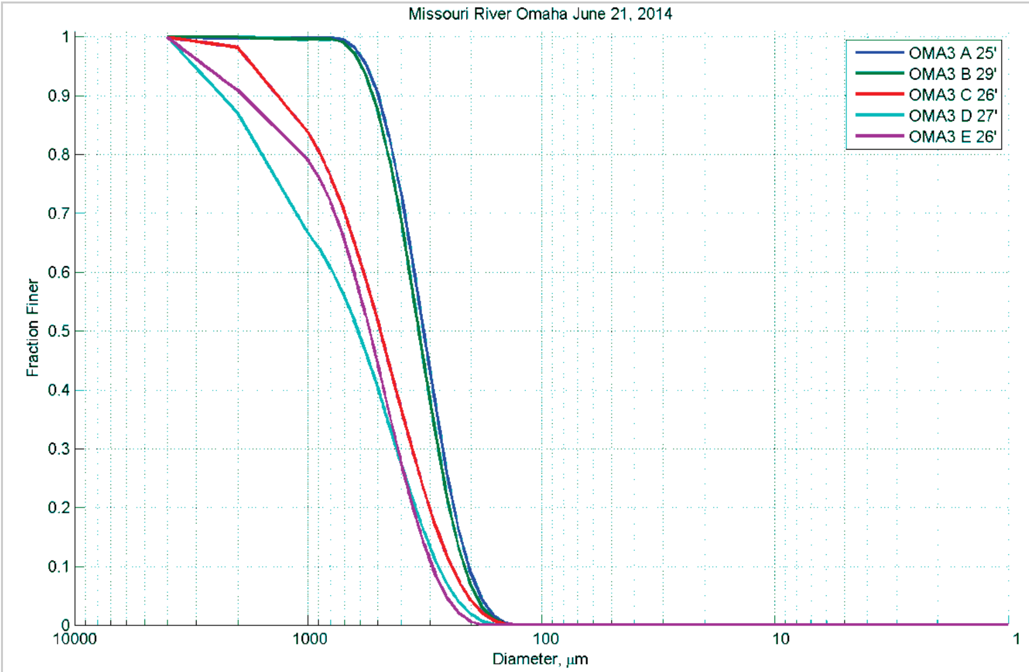

4.6 Suspended sediment

Suspended sediment samples at different depths in a column were taken at the five stations shown in Figure 46, for each data collection date. A particle size analysis was conducted for the samples of each station and date. The results are presented in this report as Figure 50 to Figure 64, and the measured data are available at Appendix II-e.

Particle size distribution for the first data collection date, April 29, 2014, is shown in Figure 50 to Figure 54. It is organized starting from the station closer to the left descending bank, Station A, to the station closer to the right descending bank, Station E.

Figure 50. Particle size distribution at different depths (feet) in Station A – April 29, 2014.

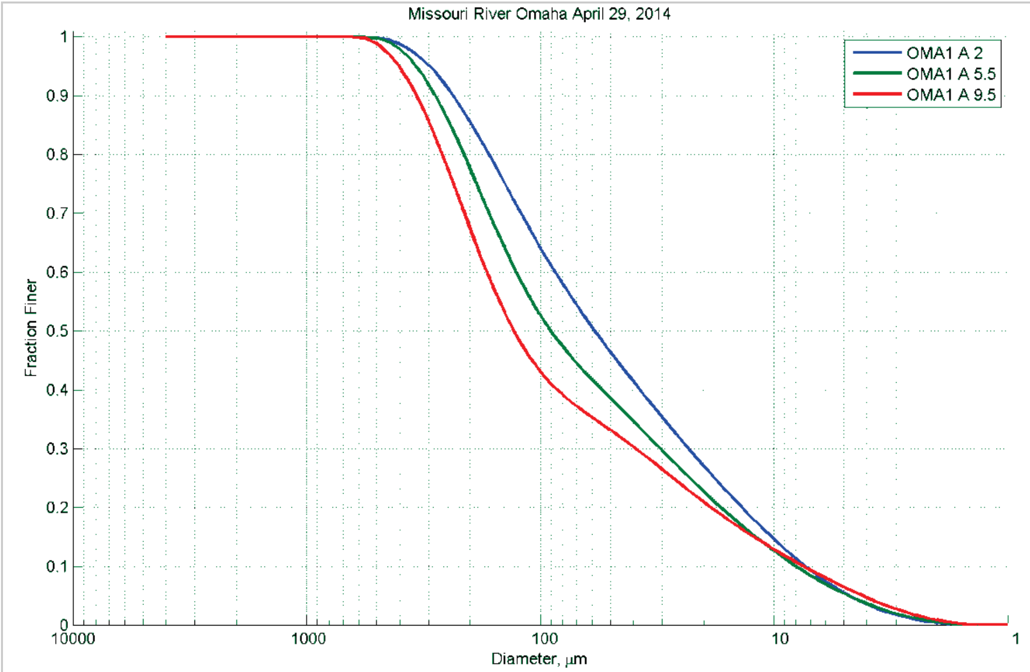

Figure 51. Particle size distribution at different depths (feet) in Station B – April 29, 2014.

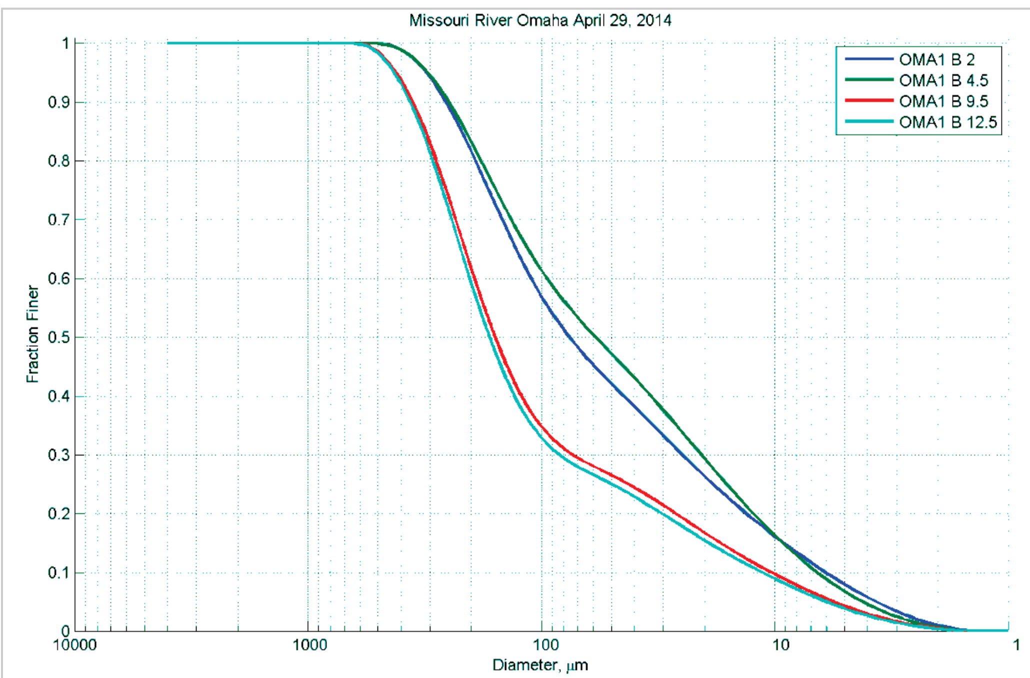

Figure 52. Particle size distribution at different depths (feet) in Station C – April 29, 2014.

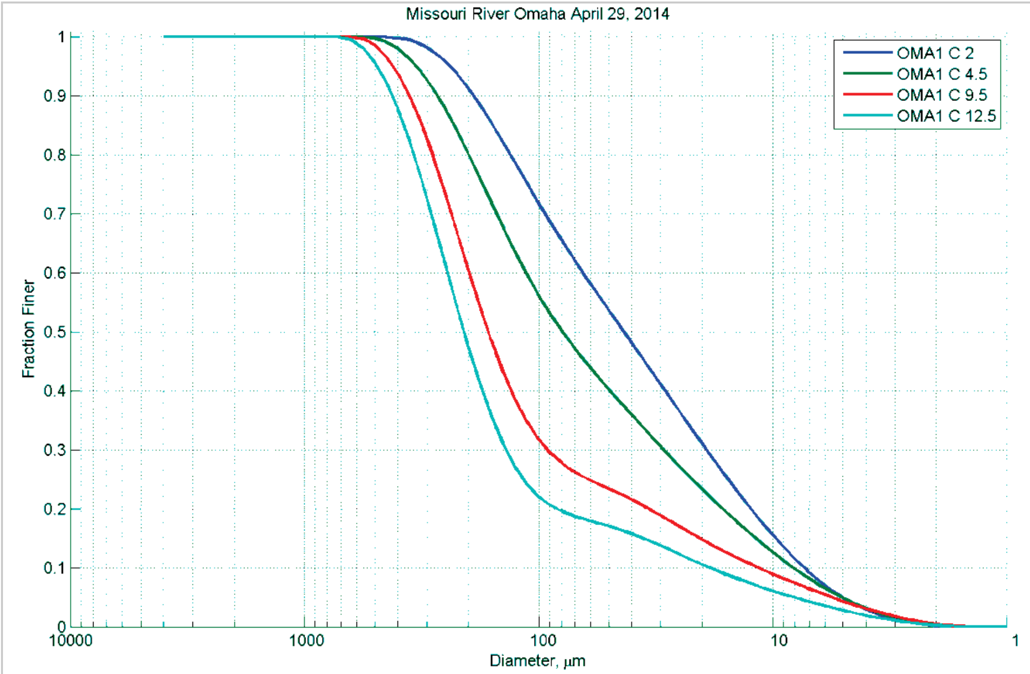

Figure 53. Particle size distribution at different depths (feet) in Station D – April 29, 2014.

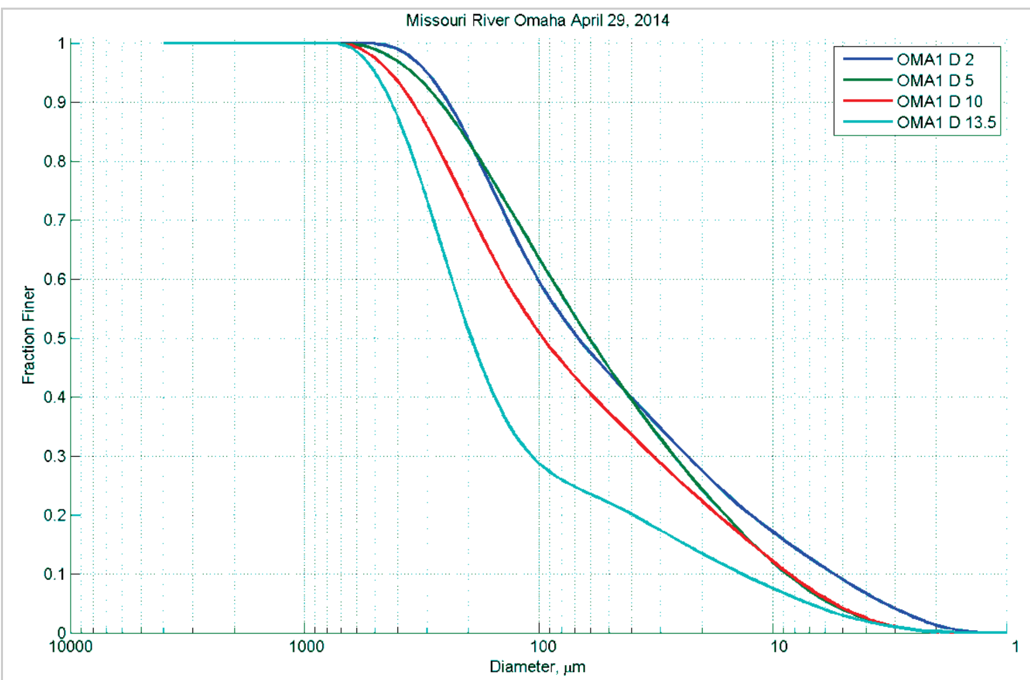

Figure 54. Particle size distribution at different depths (feet) in Station E – April 29, 2014.

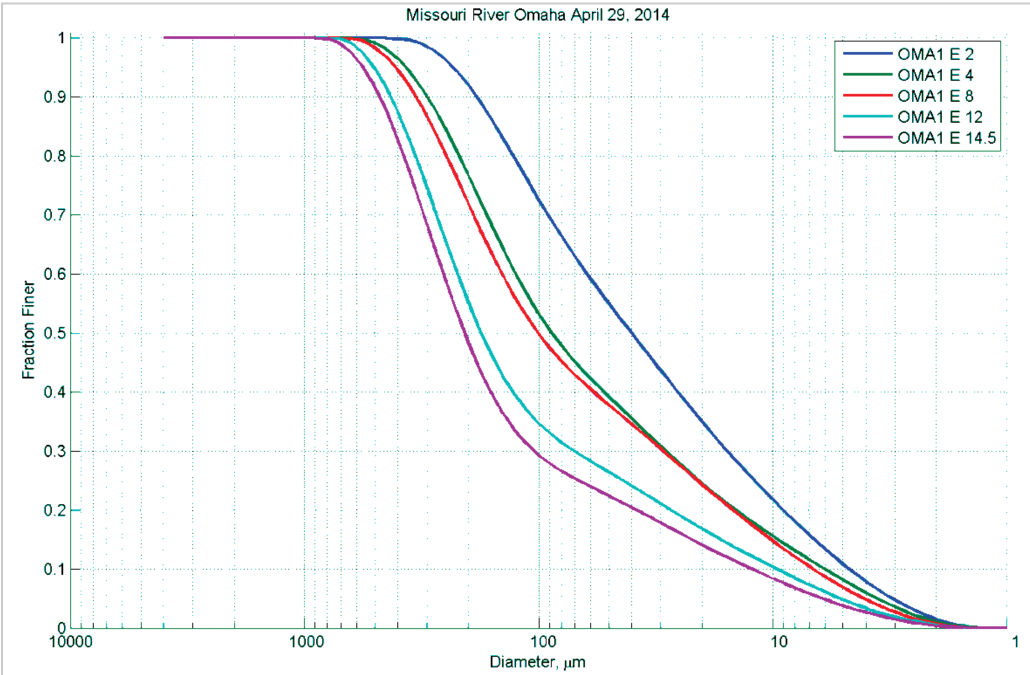

Particle size distribution for the second data collection date, June 6, 2014, are shown in Figure 55 to Figure 59.

Figure 55. Particle size distribution at different depths (feet) in Station A – June 6, 2014.

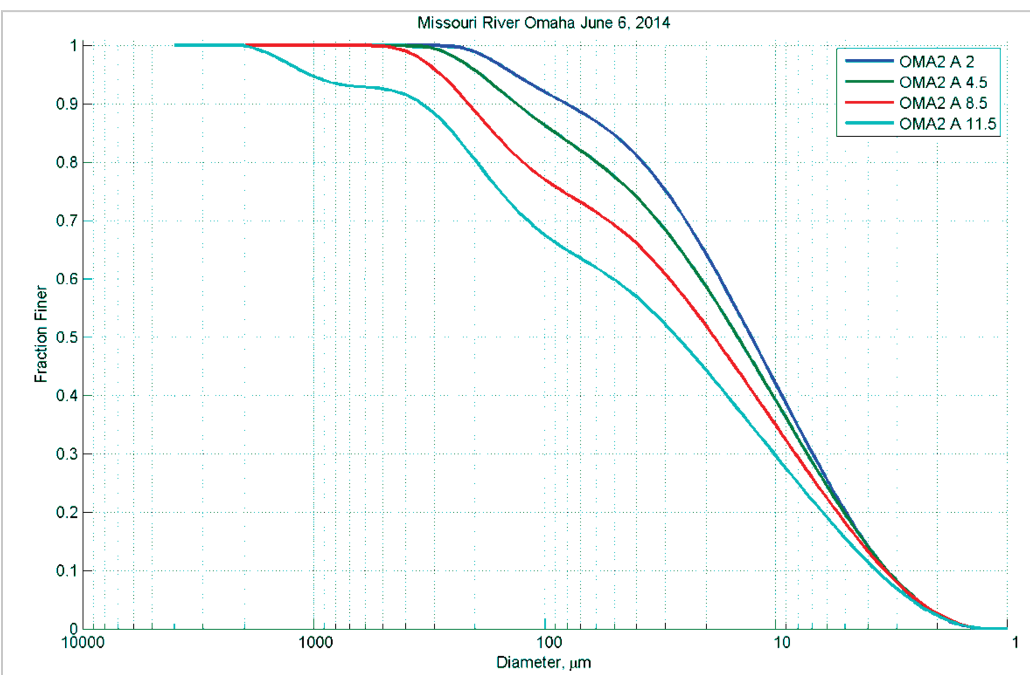

Figure 56. Particle size distribution at different depths (feet) in Station B – June 6, 2014.

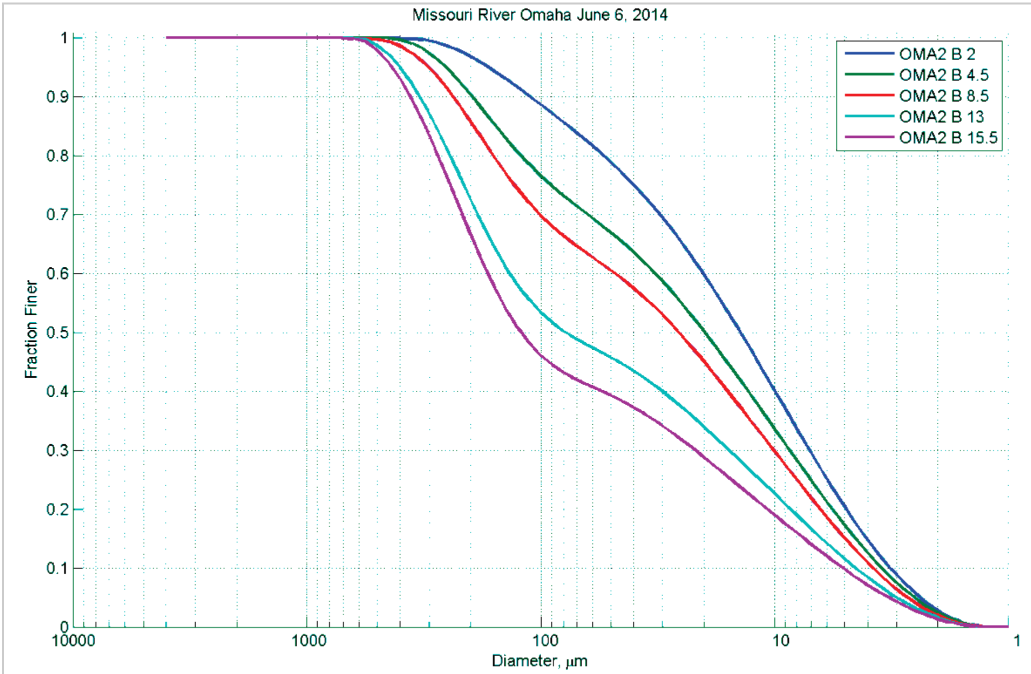

Figure 57. Particle size distribution at different depths (feet) in Station C – June 6, 2014.

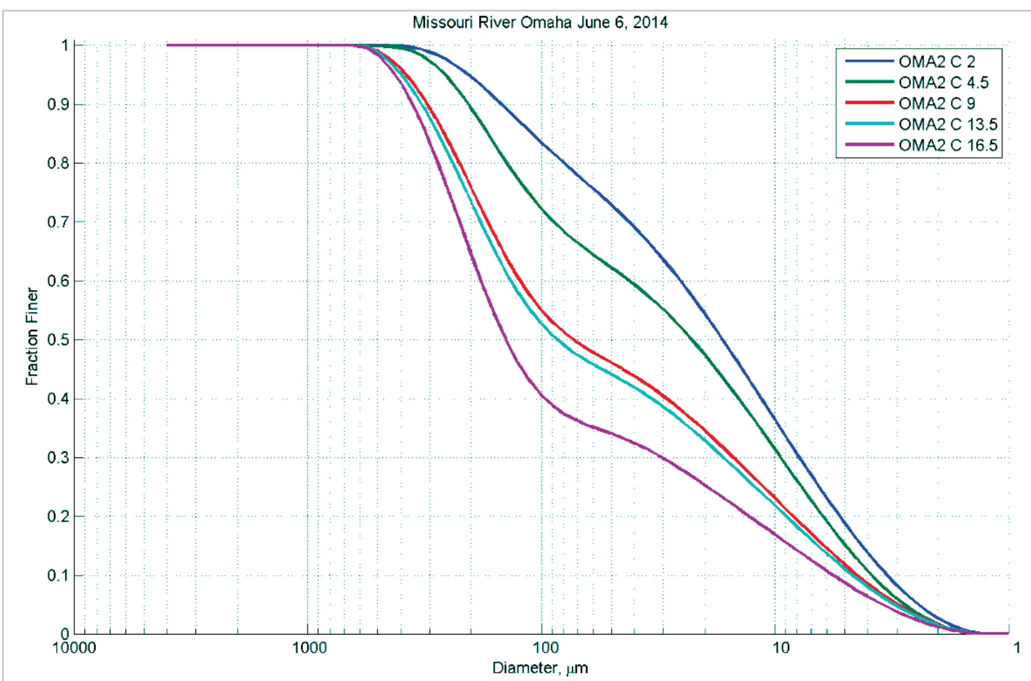

Figure 58. Particle size distribution at different depths (feet) in Station D – June 6, 2014.

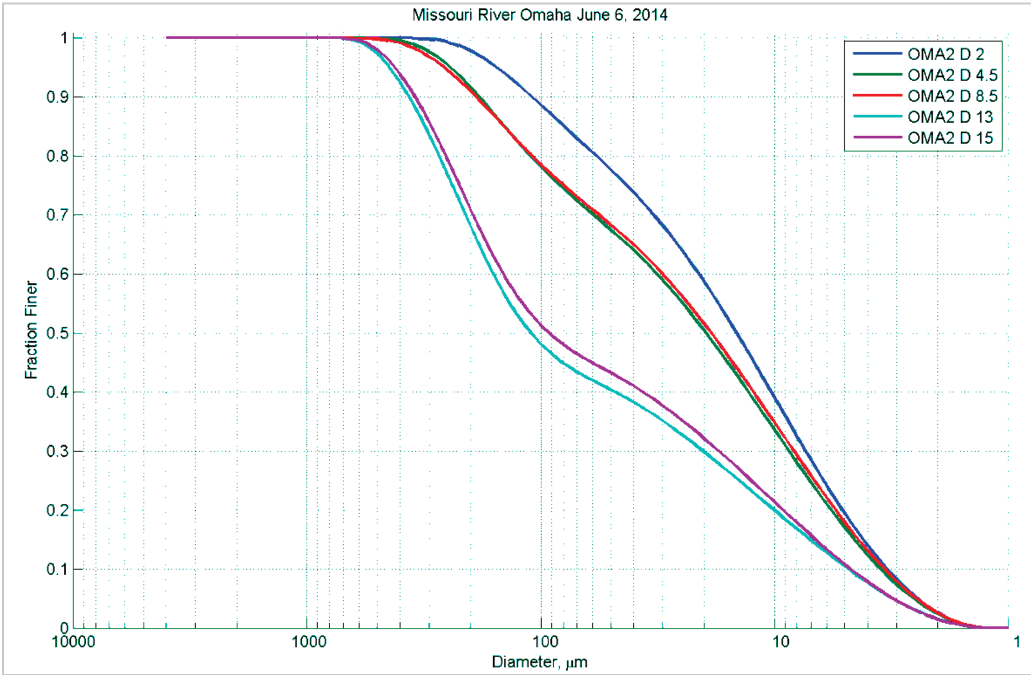

Figure 59. Particle size distribution at different depths (feet) in Station E – June 6, 2014.

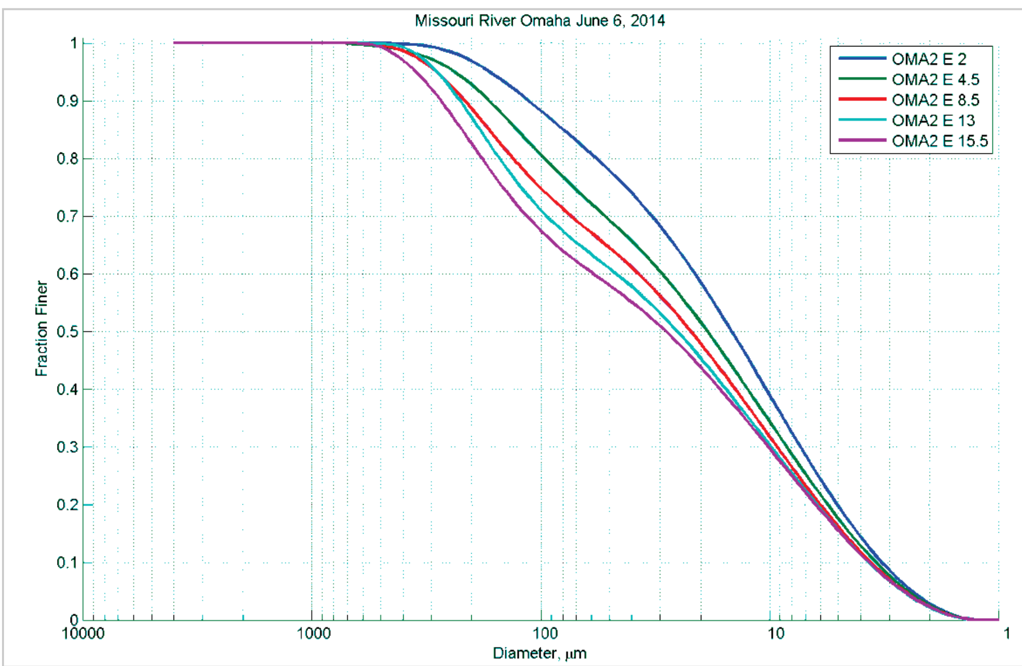

Particle size distribution for the third data collection date, June 21, 2014, is shown in Figure 60 to Figure 64.

Figure 60. Particle size distribution at different depths (feet) in Station A – June 21, 2014.

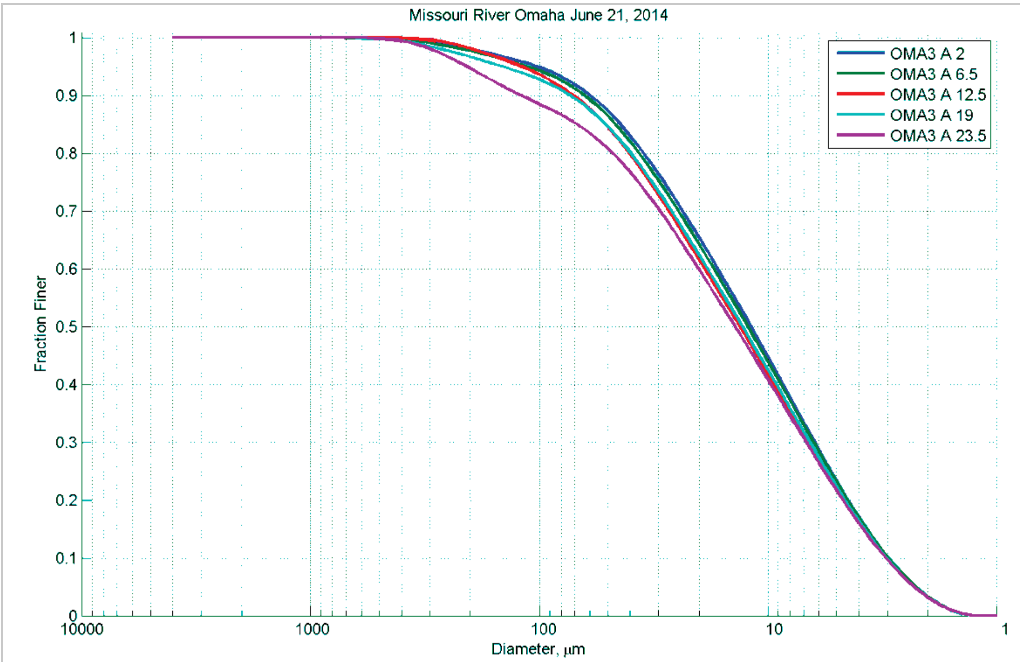

Figure 61. Particle size distribution at different depths (feet) in Station B – June 21, 2014.

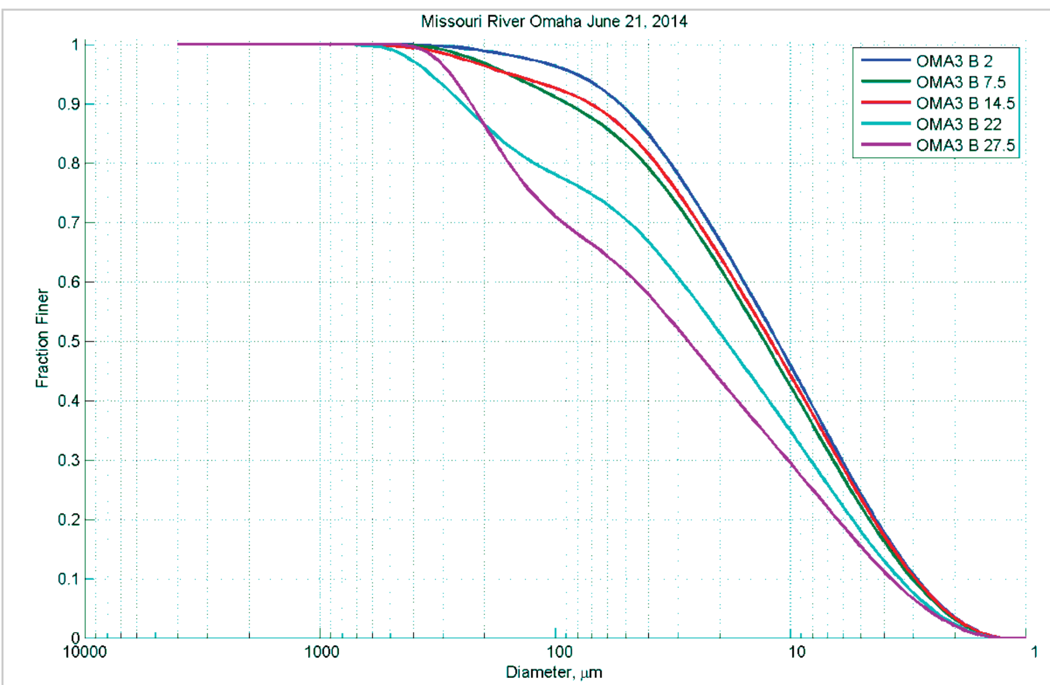

Figure 62. Particle size distribution at different depths (feet) in Station C – June 21, 2014.

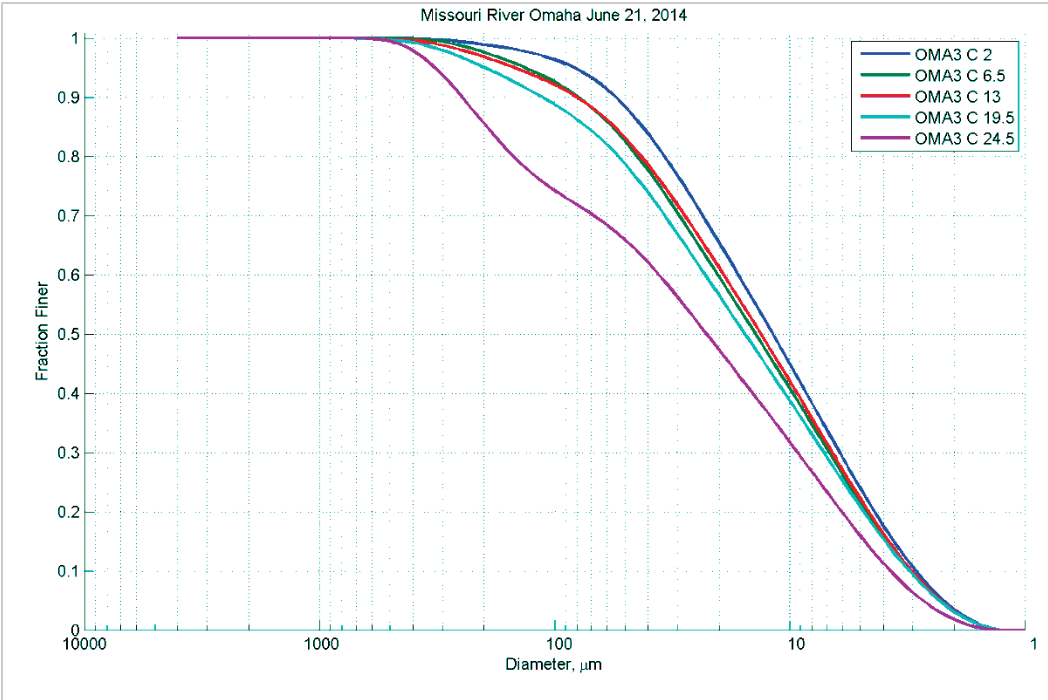

Figure 63. Particle size distribution at different depths (feet) in Station D – June 21, 2014.

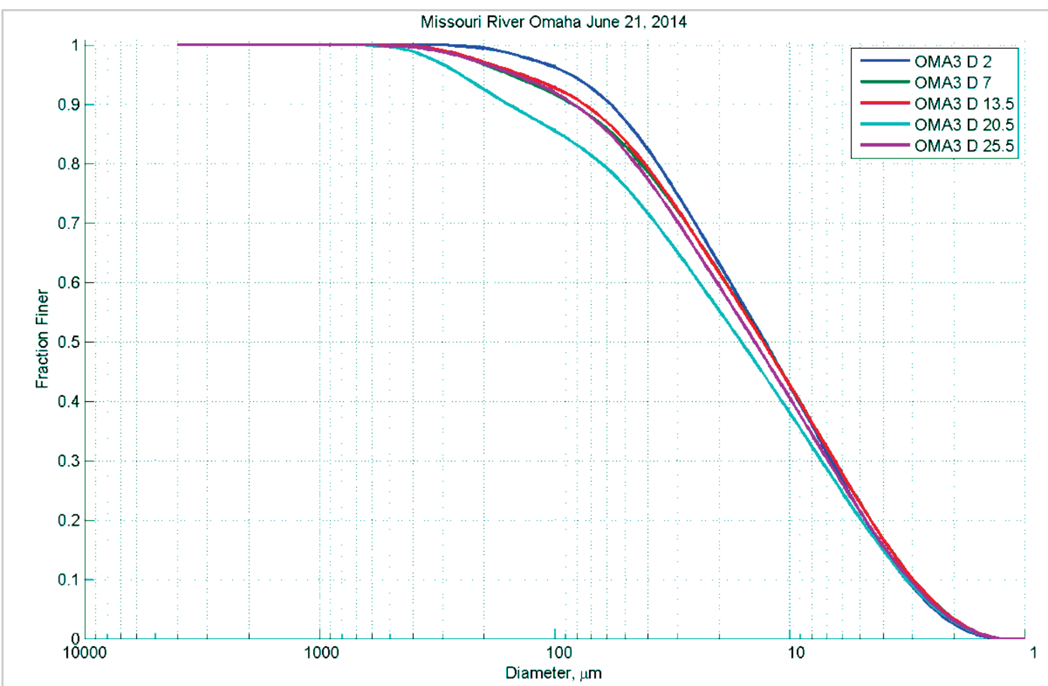

Figure 64. Particle size distribution at different depths (feet) in Station E – June 21, 2014.

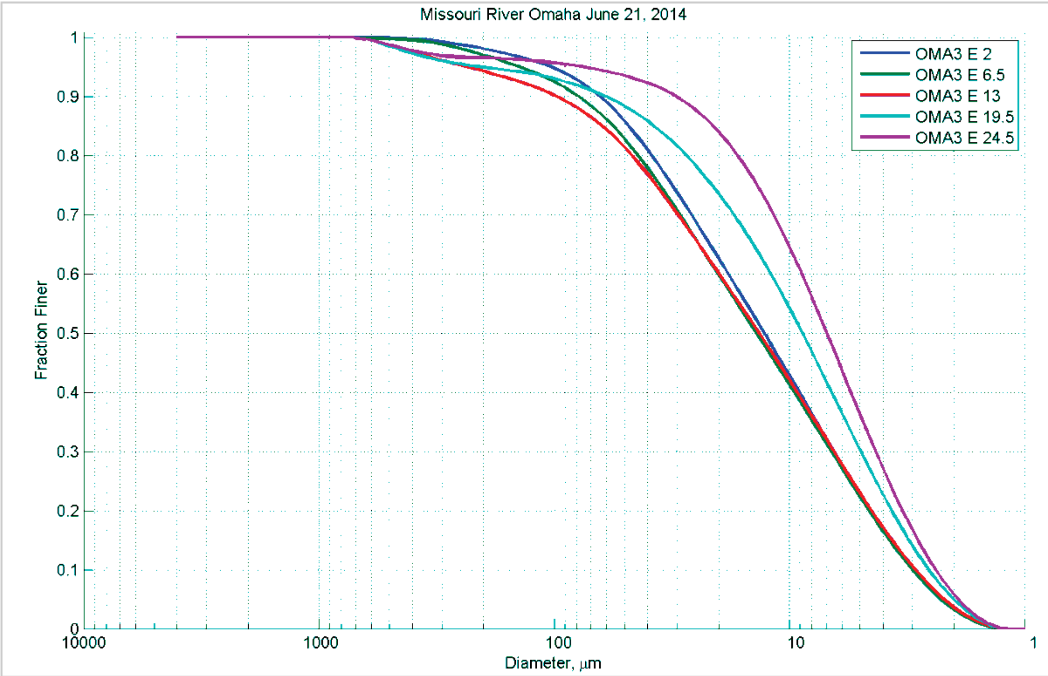

Suspended sediment concentration was also measured from the collected samples. Table 19 to Table 21 present the concentration values for each data collection date. Suspended sediment concentration profiles were created using the measured data, presented in Figure 65 to Figure 67. See Appendix II-f for more details about the measured data.

Table 19. Suspended sediment concentration at Omaha, NE – April 29, 2014.

Station	Depth (ft)	Concentration (mg/L)
OMA 1A	2	107.08
OMA 1A	5.5	106.57
OMA 1A	9.5	165.03
Total depth	11.9	(Bottom)
OMA 1B	2	107.52
OMA 1B	4.5	112.78
OMA 1B	9.5	205.07
OMA 1B	12.5	317.59
Total depth	15.4	(Bottom)
OMA 1C	2	164.32
OMA 1C	4.5	182.77
OMA 1C	9.5	258.48
OMA 1C	12.5	303.14
Total depth	15.1	(Bottom)
OMA 1D	2	121.27
OMA 1D	5	116.88
OMA 1D	10	180.60
OMA 1D	13.5	295.90
Total depth	15.5	(Bottom)
OMA 1E	2	103.56
OMA 1E	4	85.08
OMA 1E	8	148.44
OMA 1E	12	212.70
OMA 1E	14.5	345.00
Total depth	15.7	(Bottom)

Table 20. Suspended sediment concentration at Omaha, NE – June 6, 2014.

Station	Depth (ft)	Concentration (mg/L)
OMA 2A	2	235.71
OMA 2A	4.5	253.96
OMA 2A	8.5	271.77
OMA 2A	11.5	314.47
Total depth	15.1	(Bottom)
OMA 2B	2	237.95
OMA 2B	4.5	276.09
OMA 2B	8.5	292.17
OMA 2B	13	350.94
OMA 2B	15.5	488.00
Total depth	18.4	(Bottom)
OMA 2C	2	248.92
OMA 2C	4.5	283.02
OMA 2C	9	291.67
OMA 2C	13.5	455.78
OMA 2C	16.5	551.06
Total depth	18.9	(Bottom)
OMA 2D	2	221.72
OMA 2D	4.5	264.80
OMA 2D	8.5	276.18
OMA 2D	13	309.79
OMA 2D	15	409.36
Total depth	17.9	(Bottom)
OMA 2E	2	229.06
OMA 2E	4.5	247.97
OMA 2E	8.5	259.58
OMA 2E	13	292.12
OMA 2E	15.5	303.52
Total depth	17.9	(Bottom)

Table 21. Suspended sediment concentration at Omaha, NE – June 21, 2014.

Station	Depth (ft)	Concentration (mg/L)
OMA 3A	2	1,565.38
OMA 3A	6.5	1,511.51
OMA 3A	12.5	1,506.13
OMA 3A	19	1,771.94
OMA 3A	23.5	1,784.92
Total depth	26.4	(Bottom)
OMA 3B	2	1,411.51
OMA 3B	7.5	1,516.89
OMA 3B	14.5	1,523.21
OMA 3B	22	1,883.08
OMA 3B	27.5	2,227.48
Total depth	28.6	(Bottom)
OMA 3C	2	1,248.89
OMA 3C	6.5	1,426.51
OMA 3C	13	1,618.39
OMA 3C	19.5	1,610.87
OMA 3C	24.5	2,490.49
Total depth	26.4	(Bottom)
OMA 3D	2	1331.94
OMA 3D	7	1287.92
OMA 3D	13.5	1437.29
OMA 3D	20.5	1475.52
OMA 3D	25.5	1762.90
Total depth	27.2	(Bottom)
OMA 3E	2	1205.11
OMA 3E	6.5	1316.26
OMA 3E	13	1344.29
OMA 3E	19.5	1394.37
OMA 3E	24.5	1525.38
Total depth	26.9	(Bottom)

Figure 65. Suspended sediment concentration at Omaha, NE – April 29, 2014.

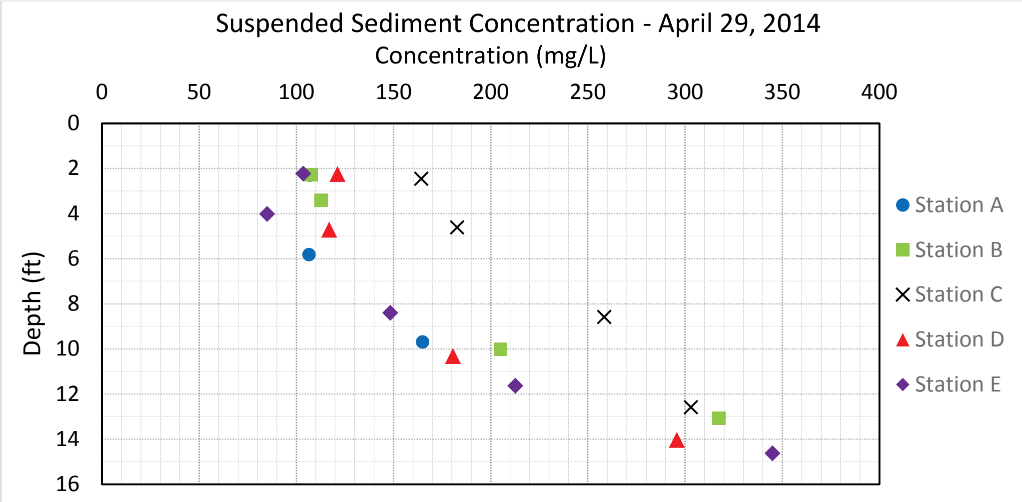

Figure 66. Suspended sediment concentration at Omaha, NE – June 6, 2014.

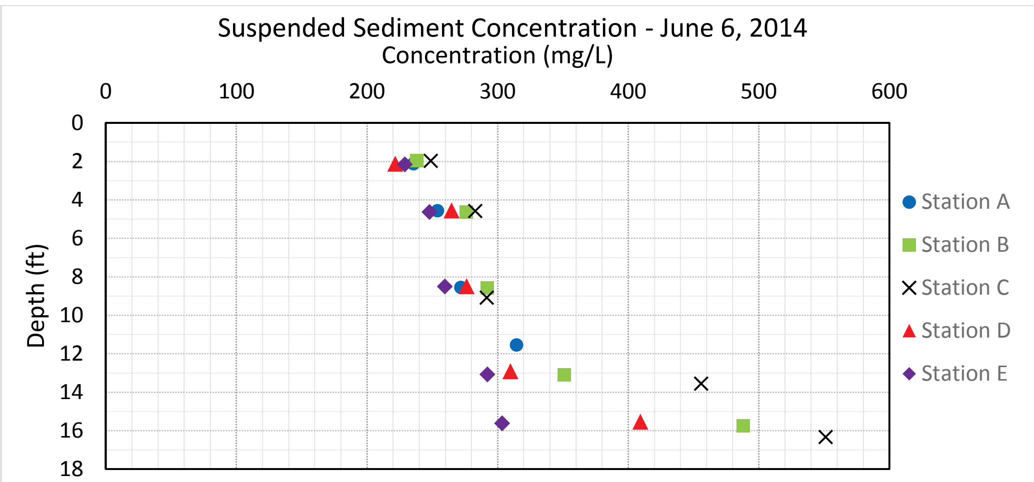

Figure 67. Suspended sediment concentration at Omaha, NE – June 21, 2014.

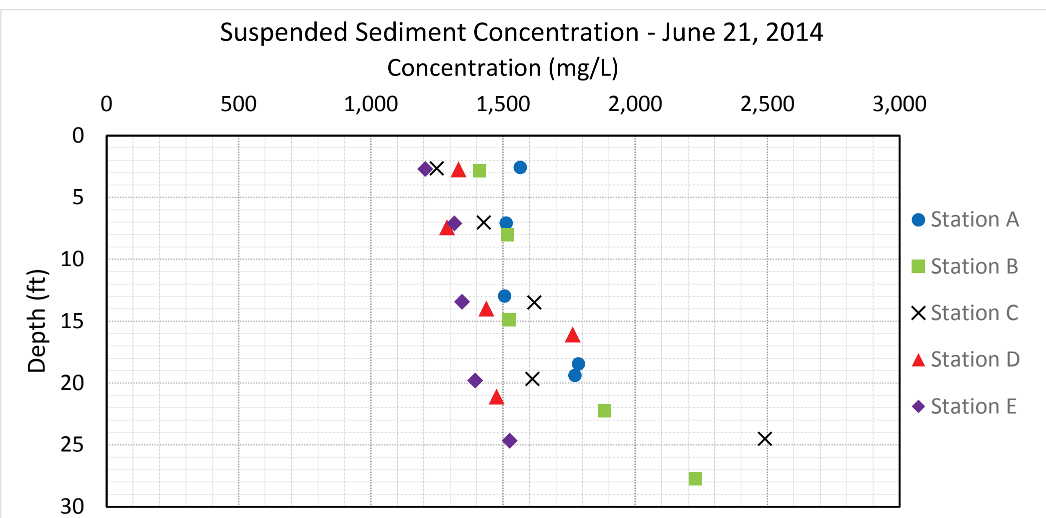

The suspended sediment concentration data were used to calibrate the ADCP acoustic backscatter and develop suspended sediment concentration profiles across the channel. Figure 68 to Figure 70 show the suspended sediment concentration profiles for the first left-to-right ADCP pass, for each data collection date. To see the other profiles, see Appendix II-f.

Figure 68. Suspended sediment concentration Profile at Omaha, NE - April 29, 2014.

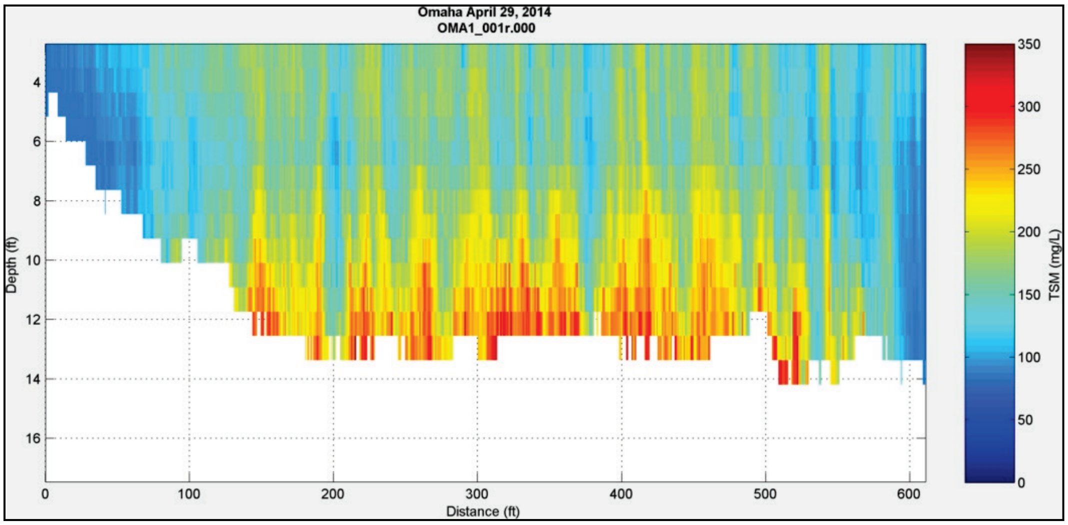

Figure 69. Suspended sediment concentration Profile at Omaha, NE – June 6, 2014.

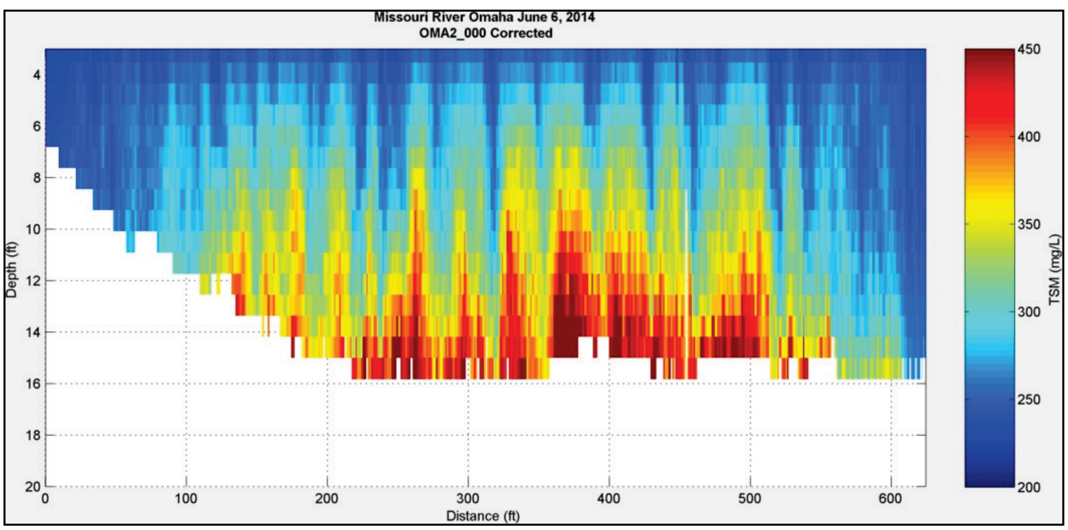

Figure 70. Suspended sediment concentration Profile at Omaha, NE – June 21, 2014.

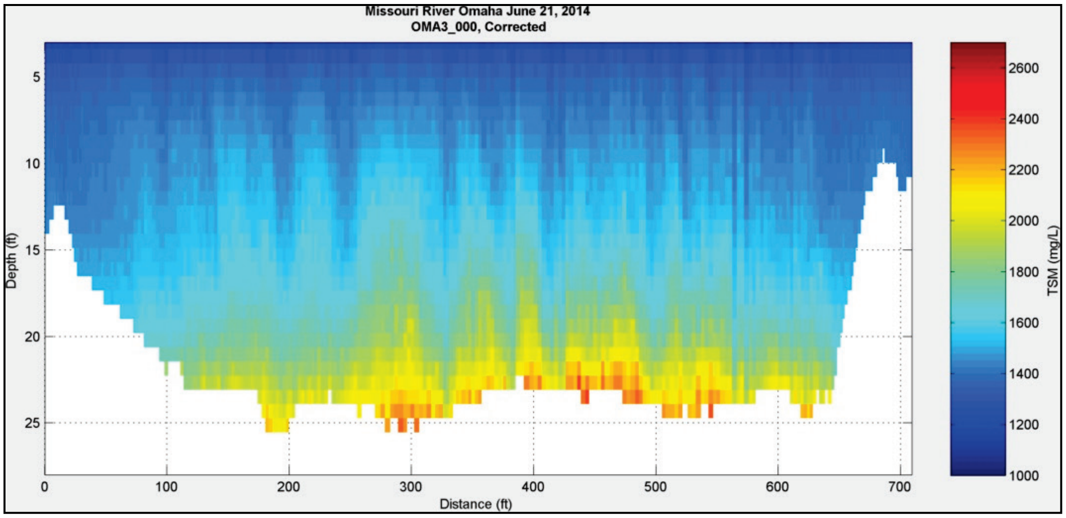

The suspended sediment concentration cross-section profiles obtained from the ADCP measurements were combined with the flow discharges, also obtained from the ADCP, to obtain the suspended sediment transport load, in tons per day. The method used for this study is explained in Heath et al. (2015, 13–14). The suspended sediment load can be divided classifying the suspended material by size and soil type. Table 22 presents the suspended sediment transport load, according to both classifications, for the first data collection date April 29, 2014. Table 23 and Table 24 present the same information for the second and third data collection dates, respectively. In all three tables, the categories under the Soil Type Classification were determined as follows: Clay Flux groups the size fractions 0.0001 to 0.0004 mm, Silt Flux 0.0004 to 0.0625 mm, and Sand Flux 0.0625 to 2.00 mm.

Table 22. Suspended sediment load distributed by grain size and soil type – April 29, 2014.

Classification System	Category	Sediment Flux (tons/day)
Total load		13,883.79
Sediment size classification	0.001 - 0.004 mm	488.25
	0.004 - 0.008 mm	839.92
	0.008 - 0.016 mm	1,182.80
	0.016 - 0.031 mm	1,363.06
	0.031 - 0.063 mm	1,520.50
	0.063 - 0.125 mm	1,972.93
	0.125 - 0.250 mm	3,503.74
	0.250 - 0.500 mm	2,677.33
	0.500 - 1.00 mm	335.27
	1.00 - 2.00 mm	0.00
Soil type classification	Clay	488.3
	Silt	4,906.28
	Sand	8,489.27

Table 23. Suspended sediment load distributed by grain size and soil type – June 6, 2014.

Classification System	Category	Sediment Flux (tons/day)
Total load		31,520.59
Sediment size classification	0.001 - 0.004 mm	3,269.77
	0.004 - 0.008 mm	4,412.89
	0.008 - 0.016 mm	4,917.92
	0.016 - 0.031 mm	4,200.27
	0.031 - 0.063 mm	3,199.73
	0.063 - 0.125 mm	3,143.43
	0.125 - 0.250 mm	4,909.65
	0.250 - 0.500 mm	3,102.26
	0.500 - 1.00 mm	293.88
	1.00 - 2.00 mm	70.80
Soil type classification	Clay	3,269.77
	Silt	16,730.81
	Sand	11,520.02

Table 24. Suspended sediment load distributed by grain size and soil type – June 21, 2014.

Classification System	Category	Sediment Flux (tons/day)
Total load		410,416.50
Sediment size classification	0.001 - 0.004 mm	62,529.68
	0.004 - 0.008 mm	78,764.12
	0.008 - 0.016 mm	80,518.52
	0.016 - 0.031 mm	70,044.47
	0.031 - 0.063 mm	57,251.97
	0.063 - 0.125 mm	27,914.35
	0.125 - 0.250 mm	20,152.93
	0.250 - 0.500 mm	11,965.28
	0.500 - 1.00 mm	1,275.17
	1.00 - 2.00 mm	0.00
Soil type classification	Clay	62,529.68
	Silt	286,579.08
	Sand	61,307.73

4.7 Bed load transport

The ISSDOTv2 method was used for computing the bed-load transport. Table 25 shows the values obtained for the bed load, as well as the other sediment quantities determined from the suspended sediment samples at the Omaha site. It provides a breakdown of the various measured sediment transport components.

Table 25. Bed-load transport values from Omaha, NE.

Data Collection Date	29-Apr-14	6-Jun-14	21-Jun-14
Flow (cfs)	29,496	38,826	93,688
Bed load (tons/day)	1,191	1,580	6,903
Suspended BML (tons/day)	8,489	11,520	61,308
Total BML (tons/day)	9,681	13,100	68,211
Bed load Fraction (%)	12.3%	12.1%	10.1%
Wash load (tons/day)	5,395	20,001	349,109
Total load	15,075	33,101	417,320

In Table 25, *bed load* is defined as the bed material moving at the bottom of the river in bed-forms; *suspended BML* refers to the suspended material with grain size higher than 0.063 mm; *total BML* is the sum of bed load and suspended BML; *bed load fraction* is the percentage of the total bed

material moving as bed load; *wash load* is fine sediments that never settle in the bed, with grain size of 0.063 mm or less; and *total load* combines the quantity of total BML and wash load.

A bed-load rating curve was prepared for this site by plotting the bed-load transport in tons per day versus the river flowrate. This graph is shown in Figure 71. The first two points (trips 1 and 2) were obtained at flows that were significantly lower than the flow of June 21, 2014, and therefore have correspondingly lower transport rates.

Figure 71. Bed-load rating curve Omaha, NE.

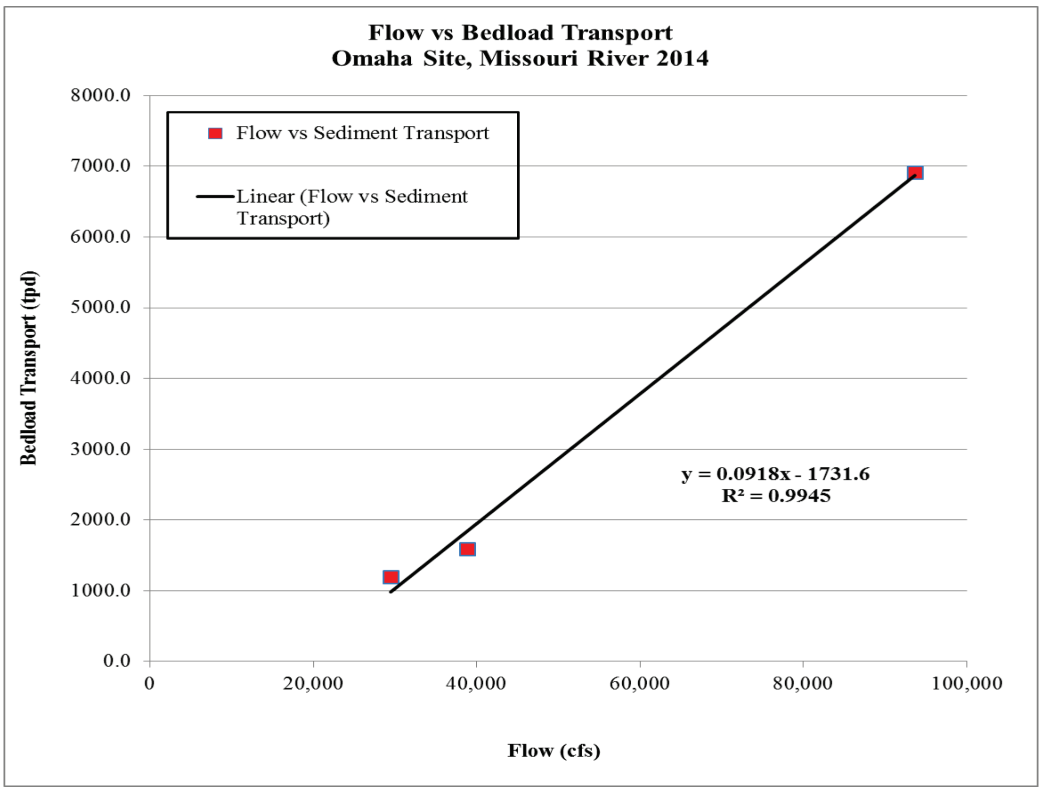

Bed-load transport values were also computed for this site using two analytic transport functions. One is the MPM formula, and the other is the Einstein formula. They were computed for each swath of bathymetric data. For instance, Figure 72 shows the bathymetry of this site with the six swath numbers (S1 to S6) labeled on it, indicating the lateral position where each swath was located. The hydraulic and sediment parameters obtained in the field data collection effort discussed before were extracted for each of these swaths.

Figure 72. Bathymetry for Missouri River at Omaha showing swath locations.

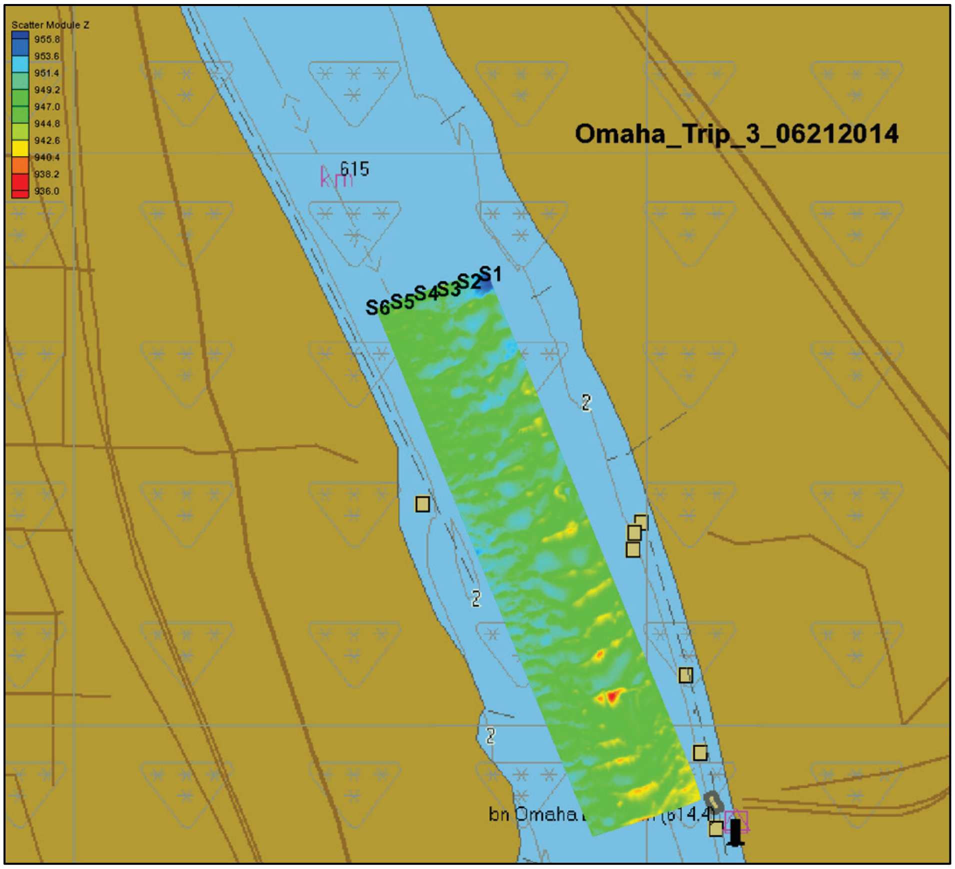

Flow, average velocity, and water depth were obtained from the ADCP data by a separate program written for that specific purpose. Water slope and water temperature were obtained from each appropriate data appendix. Bed sediment gradations used were selected based on their proximity to a given swath. The SAM Hydraulic Design Package for Channels program was then used with these data to compute the bed-load values for each individual swath. This software package has provisions for entering hydraulic and sediment input parameters and can then compute bed-load transport values for several commonly used transport functions.

The results are plotted in Figure 73 to Figure 75 and show how the transport function values compare to the ISSDOTv2 measured values. They also show the lateral variability across the measured section from the left side to the right side of the channel. The red number in Figure 75 indicates an interpolated value.

Figure 73. Bed-load transport at Omaha, NE – April 29, 2014: ISSDOTv2 values compared to transport function computed values.

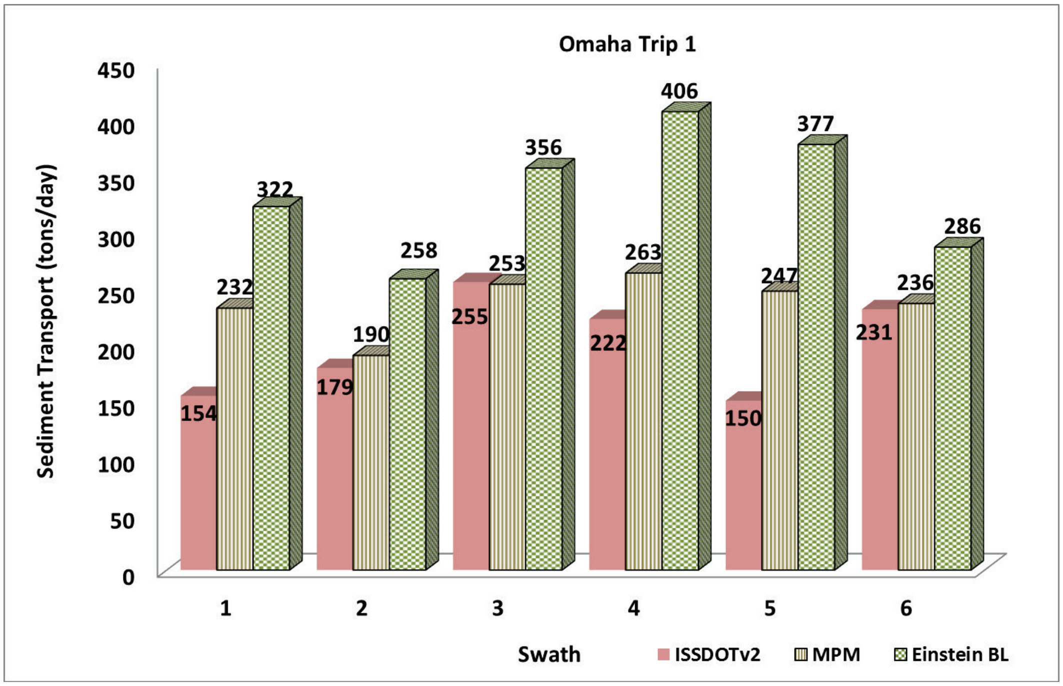

Figure 74. Bed-load transport at Omaha, NE – June 6, 2014: ISSDOTv2 values compared to transport function computed values.

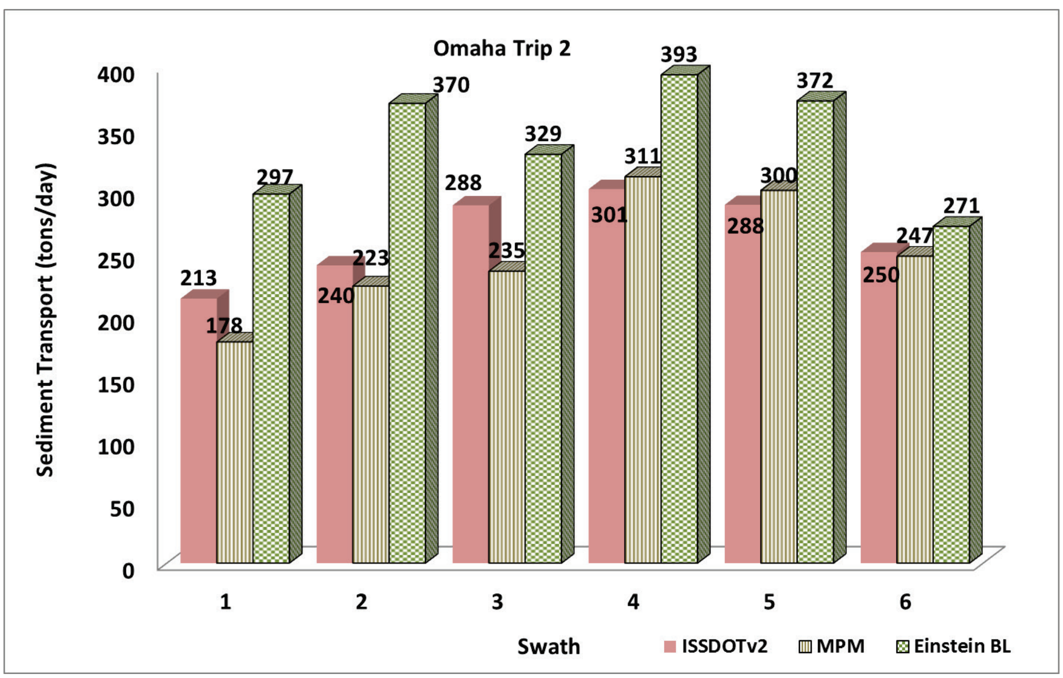

Figure 75. Bed-load transport at Omaha, NE– June 21, 2014: ISSDOTv2 values compared to transport function computed values, where red indicates an interpolated value.

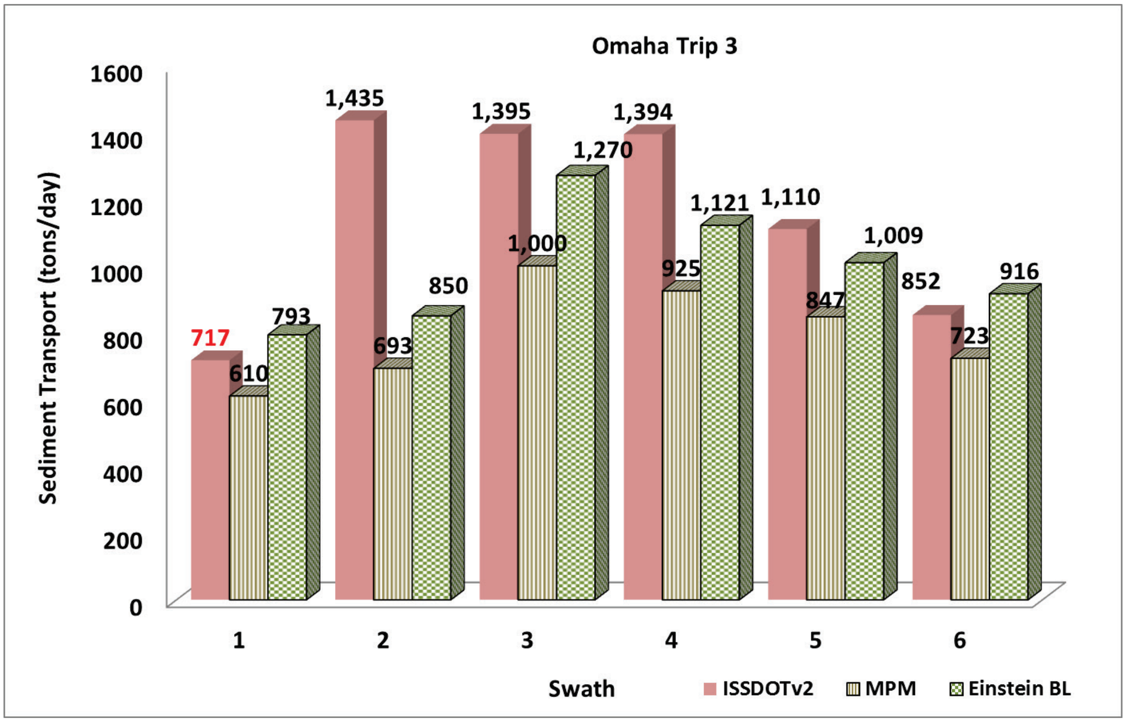

5 Site 3: Nebraska City, Nebraska

Multi-beam surveys, ADCP flow and velocity measurements, bed and suspended material sampling and testing, and water temperature, water surface elevation, and slope measurements were performed during each data collection date at Nebraska City, NE. The measuring area is shown on Figure 76 as the green polygon. The approximate location of the USGS gage station near the data collection site is also shown as the blue pin. This location might not be accurate in the figure. Coordinates for the gage site as given in the USGS web site are listed in Table 3. The red line indicates the cross section where ADCP measurements were taken and suspended and bed load material samples were collected. The bank-to-bank width of the river at this location is approximately 700 ft, and the length of the study area was approximately 2,000 ft. The data collection dates for this location were April 28, 2014; June 7, 2014; and June 22, 2014.

Figure 76. Nebraska City, NE, data collection site.

5.1 ADCP flow and velocity

The velocity and discharge for each data collection date, and site, were measured using an ADCP. Table 26 presents the cross-section average flow (ft^3/s), area (ft^2), and average velocity (ft/s) for each date, calculated from the measured data. See Appendix III-a for the measured data.

Table 26. Total flow, area, and average velocity on the given dates at Nebraska City, NE.

Date	Total Flow, Q (ft^3/s)	Total Area, A (ft^2)	Velocity Q/A (ft/s)
April 28, 2014	37,032	9,532	3.89
June 7, 2014	51,272	11,315	4.53
June 22, 2014	115,589	16,722	6.91

Real-time vertical profiles of instantaneous velocities are also obtained from the ADCP measurements. Figure 77 to Figure 79 present the velocity magnitude, before the multi-beam measurements, from left to right. In the figures, the velocity magnitude is quantified by the range of colors shown on the right side of each figure, where the higher velocities are denoted by red and the lower velocities by blue. The velocity profiles for after the multi-beam measurements are available at Appendix III-a.

Figure 77. Velocity Magnitude at Nebraska City, NE – April 28, 2014. 15:41:04.

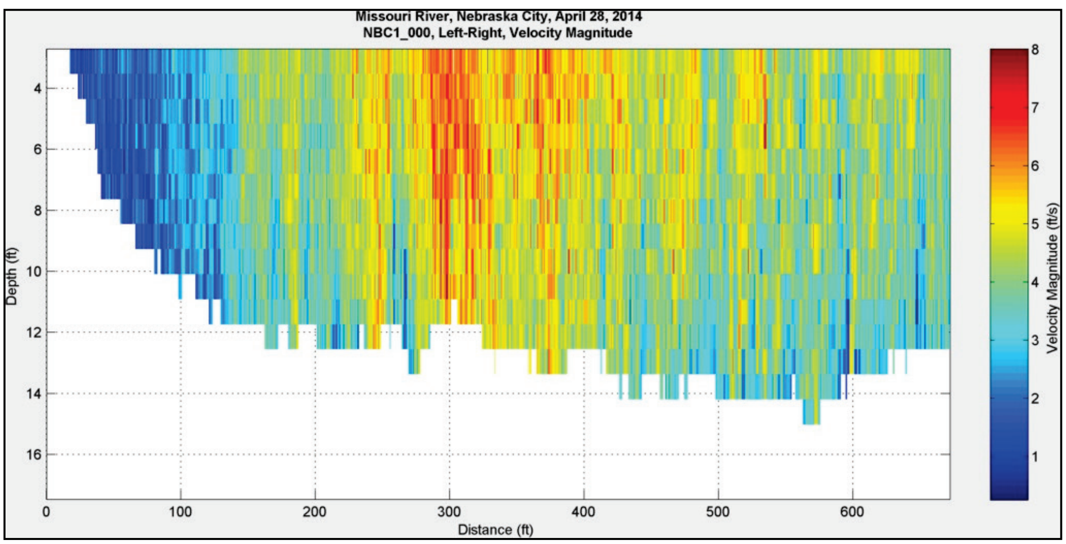

Figure 78. Velocity magnitude at Nebraska City, NE – June 7, 2014, 19:39:14.

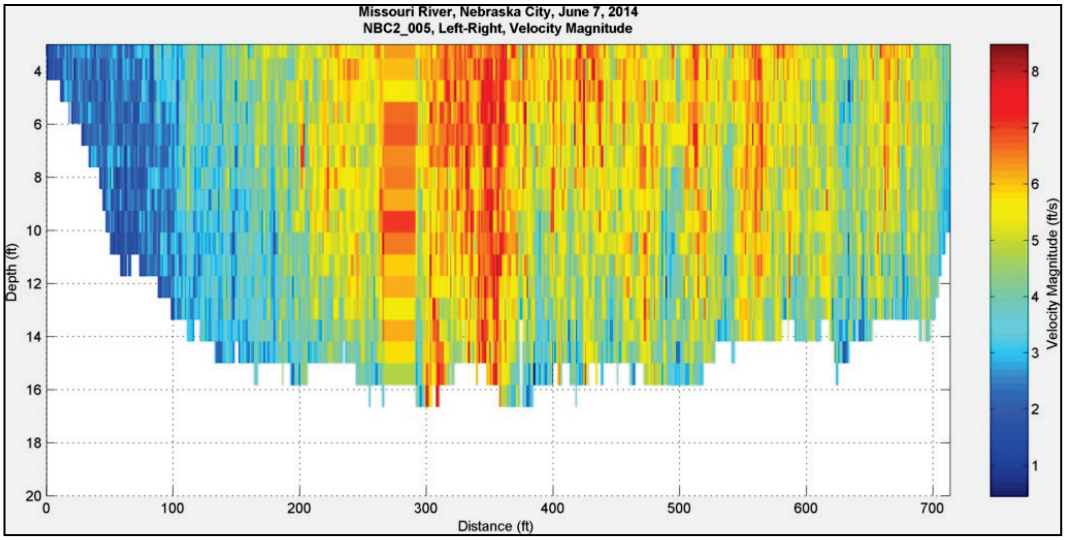

Figure 79. Velocity magnitude at Nebraska City, NE – June 22, 2014, 17:46:13.

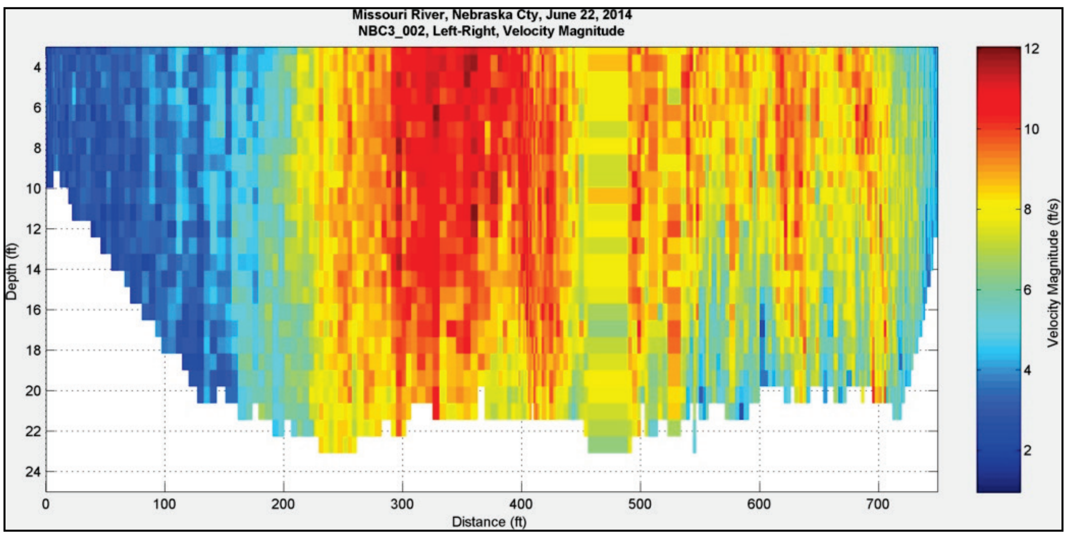

5.2 Water surface elevation and slope

Water surface elevation measurements were taken upstream and downstream of the multi-beam survey area. Figure 80 shows the upstream elevations, at distance zero, connected to the downstream elevations, at a distance of 2,000 ft, for each data collection date. Table 27 presents the slope values for the Nebraska City, NE, location for the three dates. The measured data are available at Appendix III-b.

Figure 80. Water surface elevation at Nebraska City, NE – From upstream to downstream.

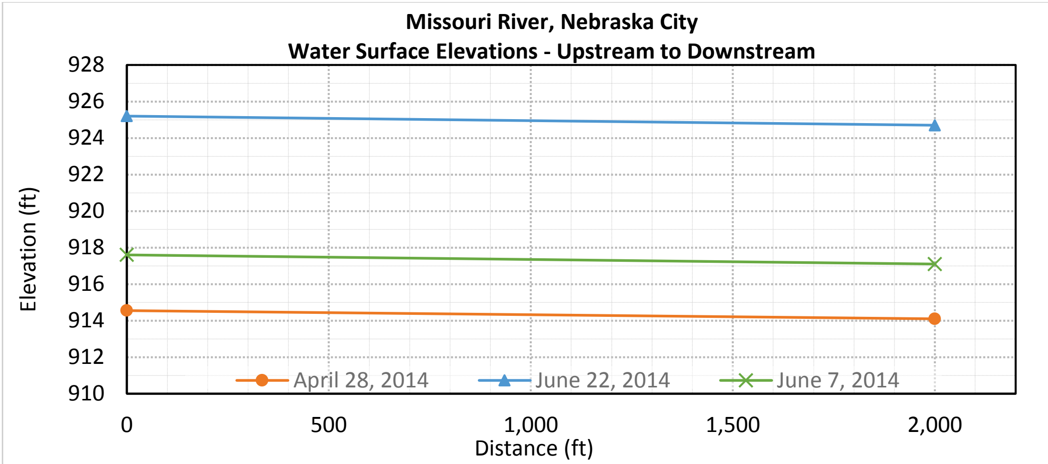

Table 27. Water surface slopes at Nebraska City, NE.

Date	Water Surface Slope (%)
April 28, 2014	0.00022
June 7, 2014	0.00025
June 22, 2014	0.00025

5.3 Water temperature

Table 28 presents the average temperature for each date (see Appendix III-g for the measured values).

Table 28. Water temperature at Nebraska City, NE.

Date	Temperature (F)
April 28, 2014	60.2
June 7, 2014	73.8
June 22, 2014	75.6

5.4 Multi-beam surveys

The initial multi-beam survey performed at Nebraska City, NE, included the full extent of the channel from bank to bank, as shown in Figure 81; where the dark blue areas are deeper and the red areas are shallower. This survey is used to determine the location of the sand waves throughout the study area and to then decide where to run the ISSDOTv2 swaths according to the location of the active sand transport portion of the channel. The selected area with swath lines and numbers displayed in red is shown in Figure 82. This shows the actual area that was used for the ISSDOTv2 bed-load computations. The length of the multi-beam swaths is approximately 2,000 ft for all three data collection dates.

Figure 81. Multi-beam survey extent at Nebraska City, NE – April 28, 2014.

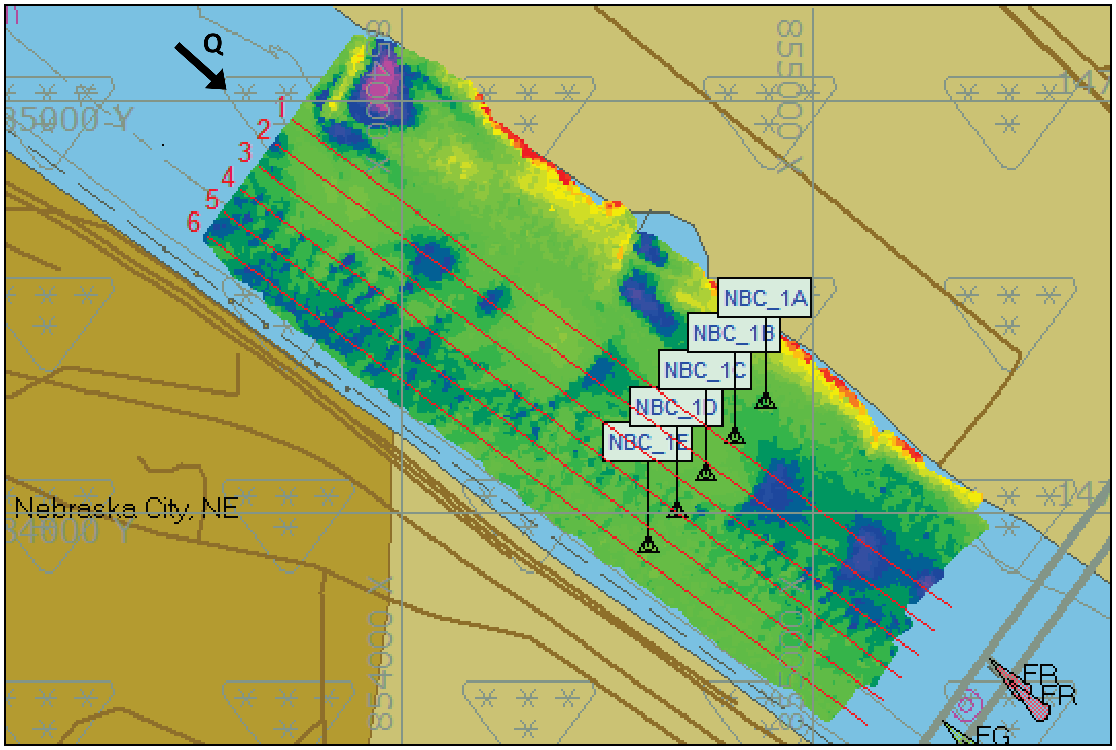

Figure 82. Multi-beam survey extent at Nebraska City, NE – June 7 and June 22, 2014.

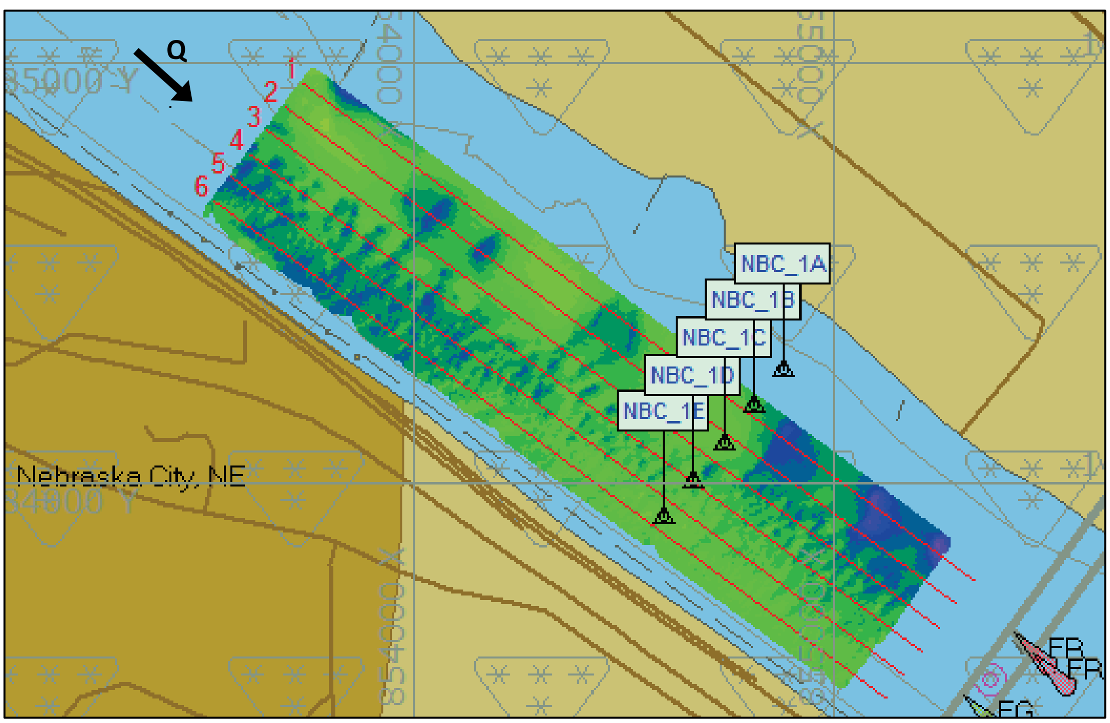

5.5 Bed material samples

Five sediment sample stations were positioned equidistant from each other along the cross section, as presented on Figure 83, which is the same location at which the suspended sediment samples and the ADCP velocity data were obtained. The first station, Station A, was positioned on the left descending bank, and the last station, Station E, on the right descending bank. Table 29 provides the locations of sample stations according to NAD83. See Appendix III-c for the coordinates using the Universal Transverse Mercator (UTM) Grid System.

Table 29. Sediment sample stations NAD83 Coordinates at Nebraska City, NE.

Station	NAD83 Latitude	NAD83 Longitude
NBC A	40° 40’ 20.7363” N	95° 49’ 57.9857” W
NBC B	40° 40’ 19.8715” N	95° 49’ 58.8868” W
NBC C	40° 40’ 19.0” N	95° 49’ 59.7596” W
NBC D	40° 40’ 18.0583” N	95° 50’ 0.6819” W
NBC E	40° 40’ 17.1925” N	95° 50’ 1.5209” W

Figure 83. Sediment sample stations at the Missouri River – Nebraska City, NE.

The grain size distribution for the five bed material samples of the first collection date, April 28, 2014, is provided at Figure 84. Figure 85 and Figure 86 present the gradation analysis for the second and third collected samples, respectively. The measured data are available in Appendix III-d.

Figure 84. Bed material grain size distribution for Nebraska City, NE – April 28, 2014.

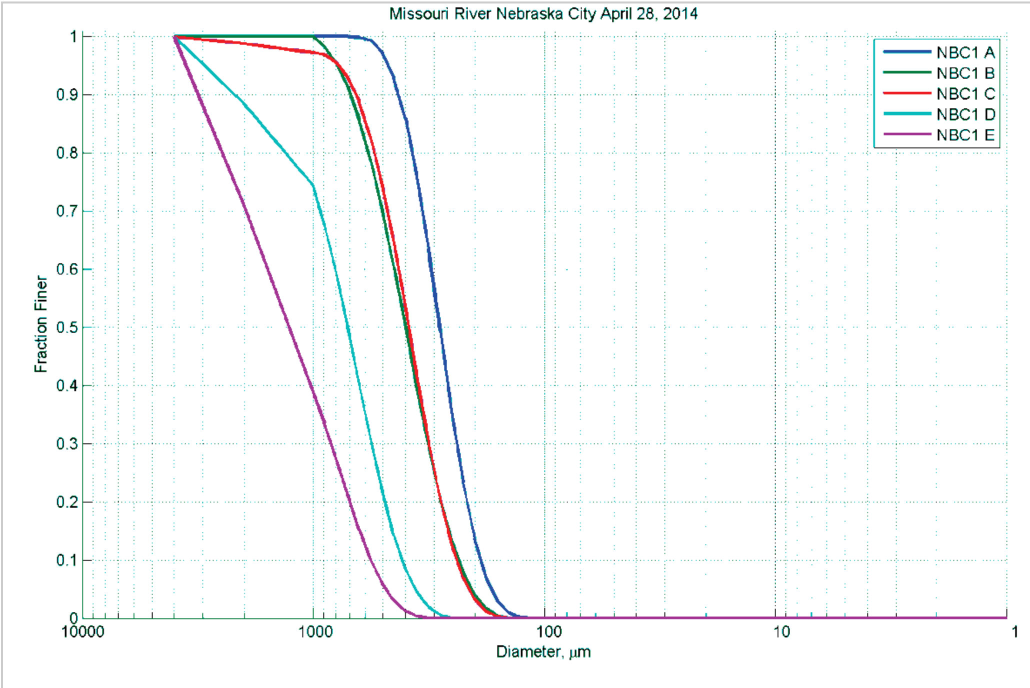

Figure 85. Bed material grain size distribution for Nebraska City, NE – June 7, 2014.

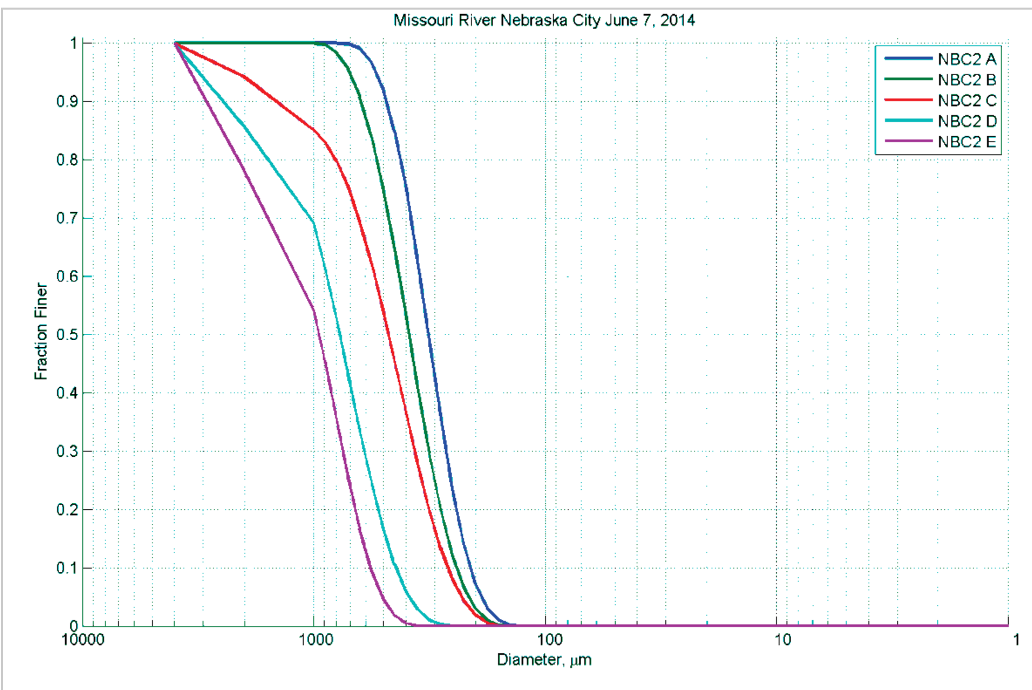

Figure 86. Bed material grain size distribution for Nebraska City, NE – June 22, 2014.

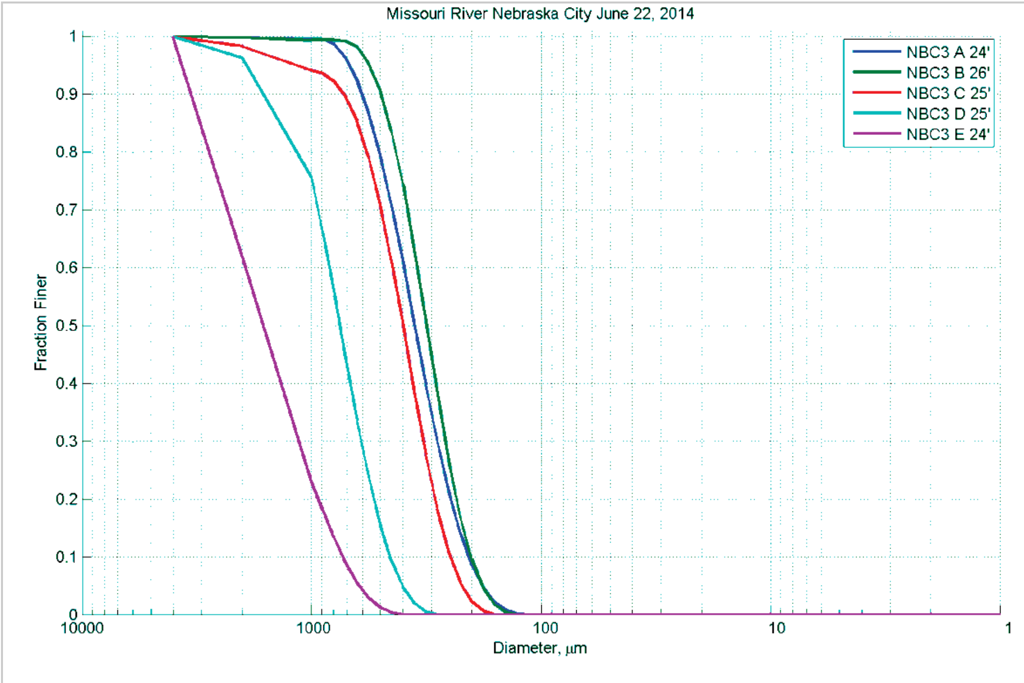

5.6 Suspended sediment

Suspended sediment samples at different depths in a column were taken at the five stations shown in Figure 83, for each data collection date. A particle size analysis was conducted for the samples of each station and date. The results are presented in this report as Figure 87 to Figure 101, and the measured data are available at Appendix III-e.

Particle size distribution for the first data collection date, April 28, 2014, is shown in Figure 87 to Figure 91. It is organized starting from the station closer to the left descending bank, Station A, to the station closer to the right descending bank, Station E.

Figure 87. Particle size distribution at different depths (feet) in Station A - April 28, 2014.

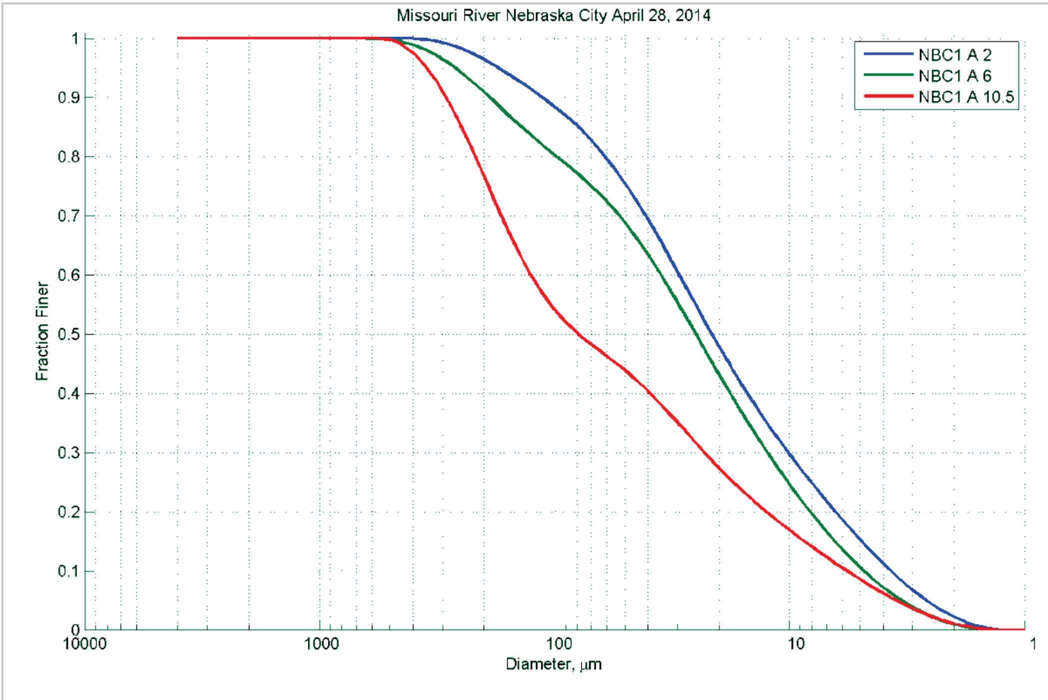

Figure 88. Particle size distribution at different depths (feet) in Station B - April 28, 2014.

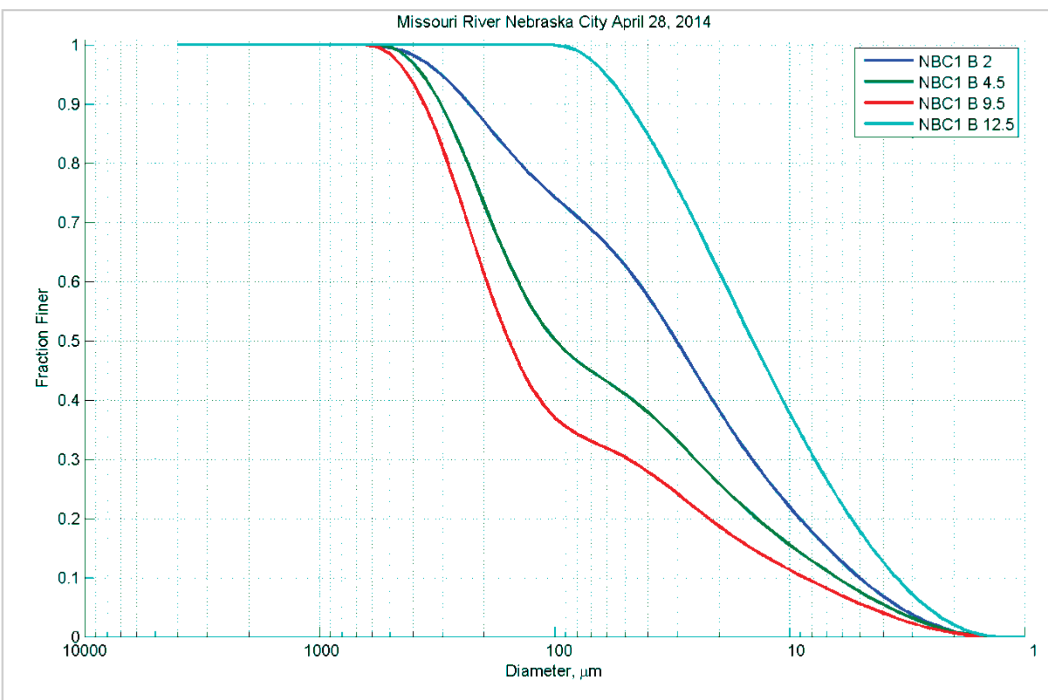

Figure 89. Particle size distribution at different depths (feet) in Station C - April 28, 2014.

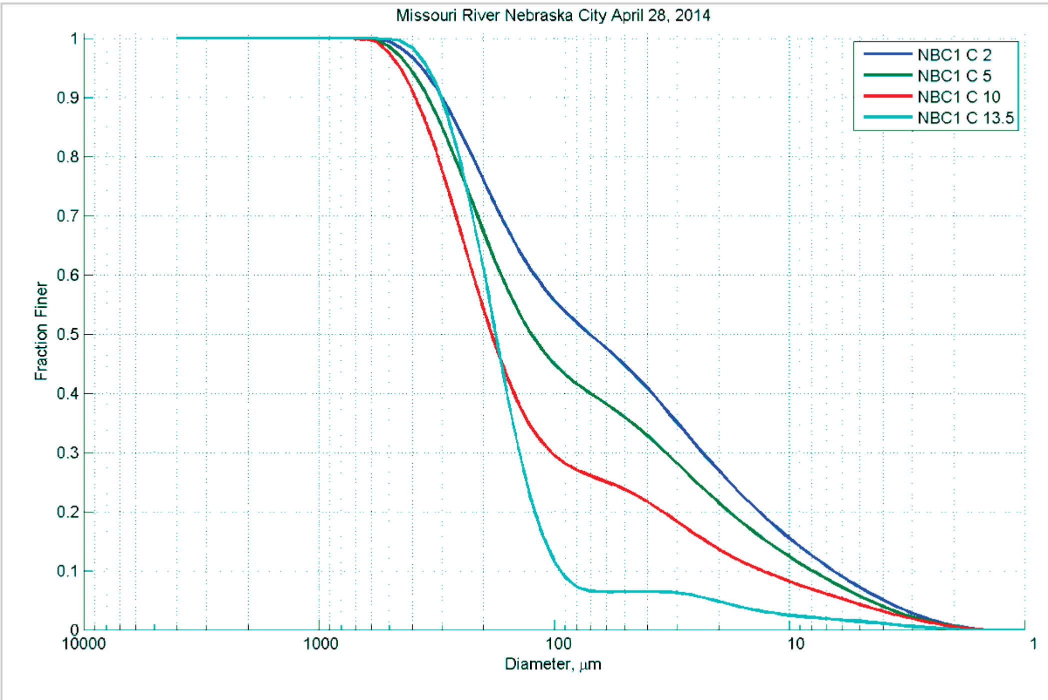

Figure 90. Particle size distribution at different depths (feet) in Station D - April 28, 2014.

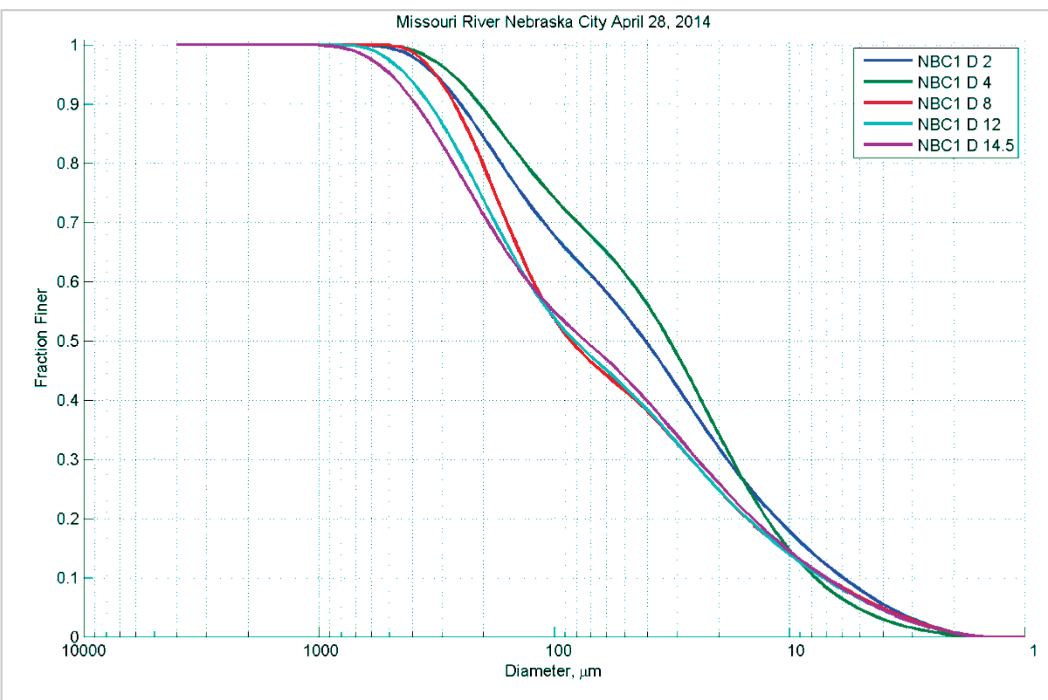

Figure 91. Particle size distribution at different depths (feet) in Station E - April 28, 2014.

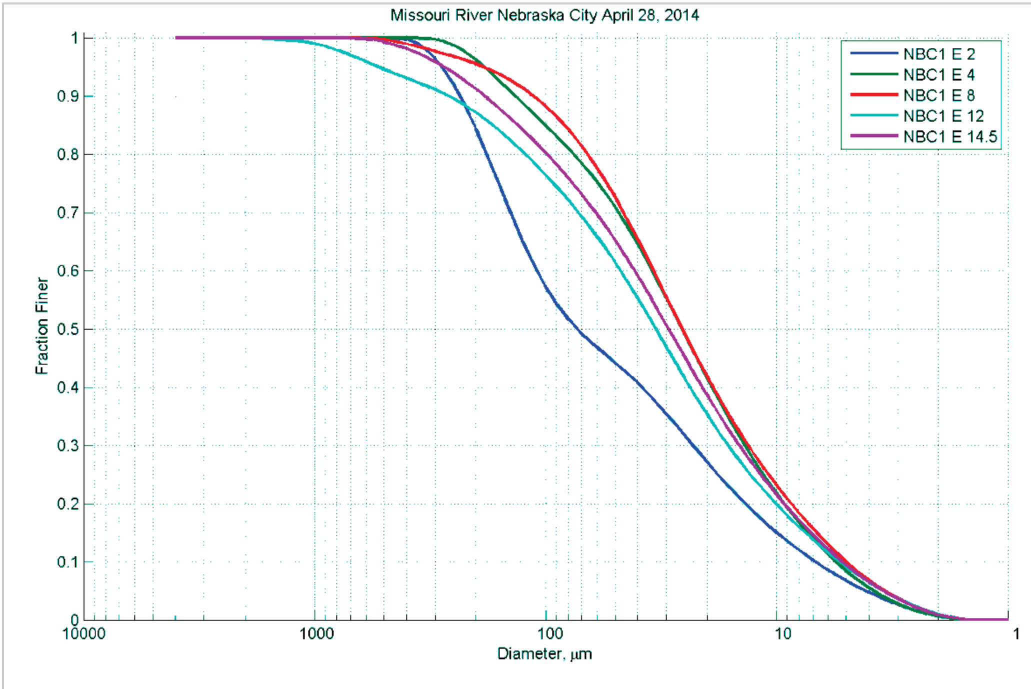

Particle size distribution for the second data collection date, June 7, 2014, is shown in Figure 92 to Figure 96.

Figure 92. Particle size distribution at different depths (feet) in Station A – June 7, 2014.

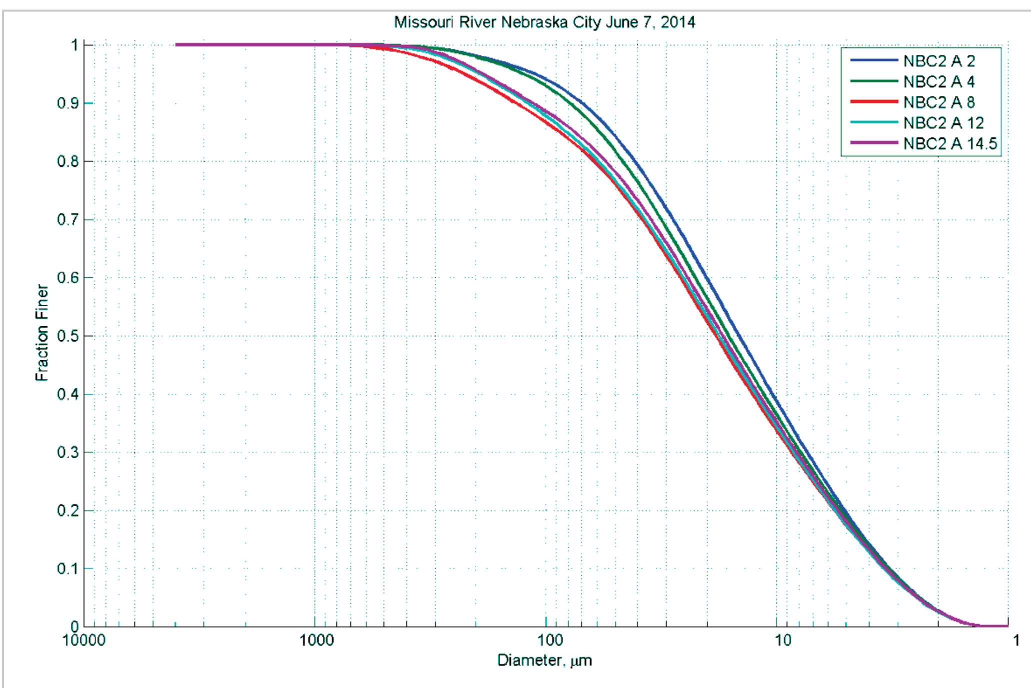

Figure 93. Particle size distribution at different depths (feet) in Station B – June 7, 2014.

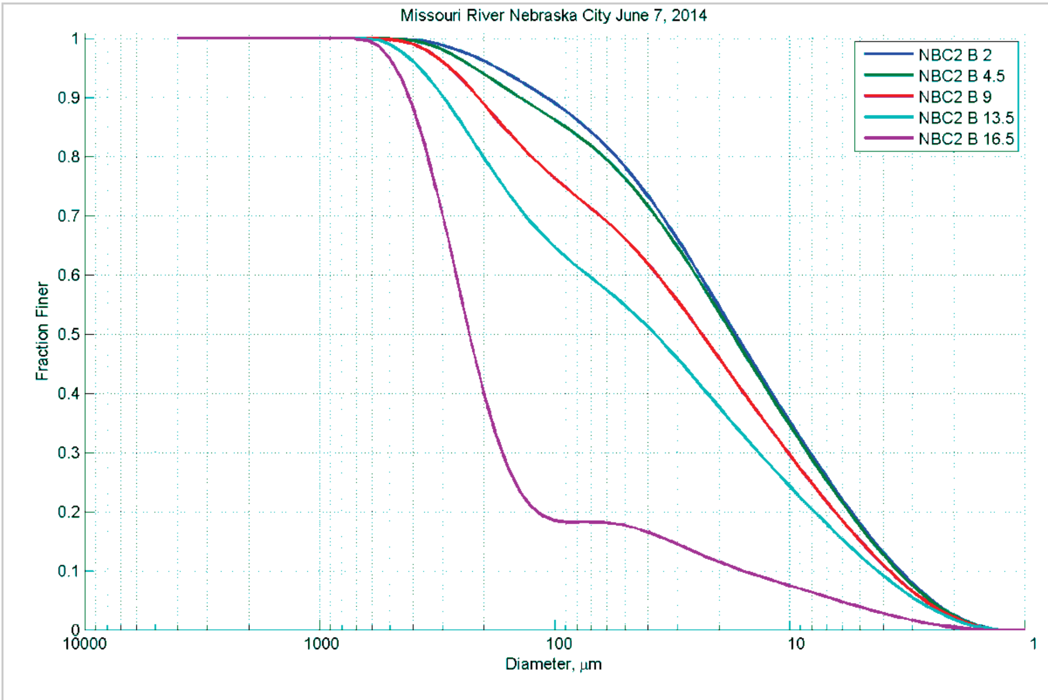

Figure 94. Particle size distribution at different depths (feet) in Station C – June 7, 2014.

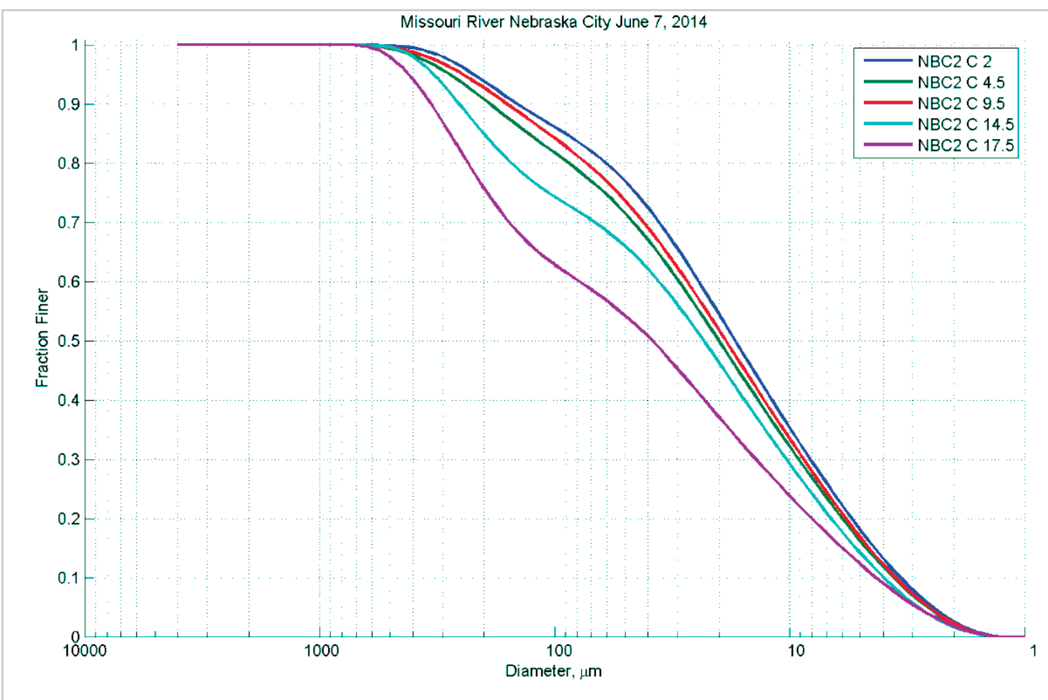

Figure 95. Particle size distribution at different depths (feet) in Station D – June 7, 2014.

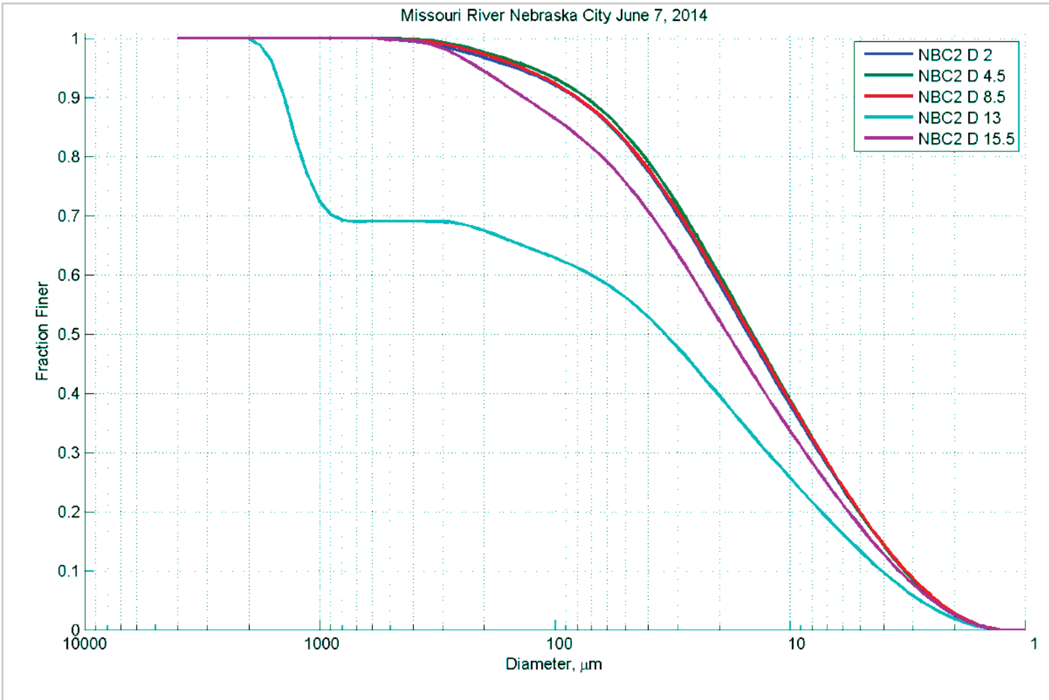

Figure 96. Particle size distribution at different depths (feet) in Station E – June 7, 2014.

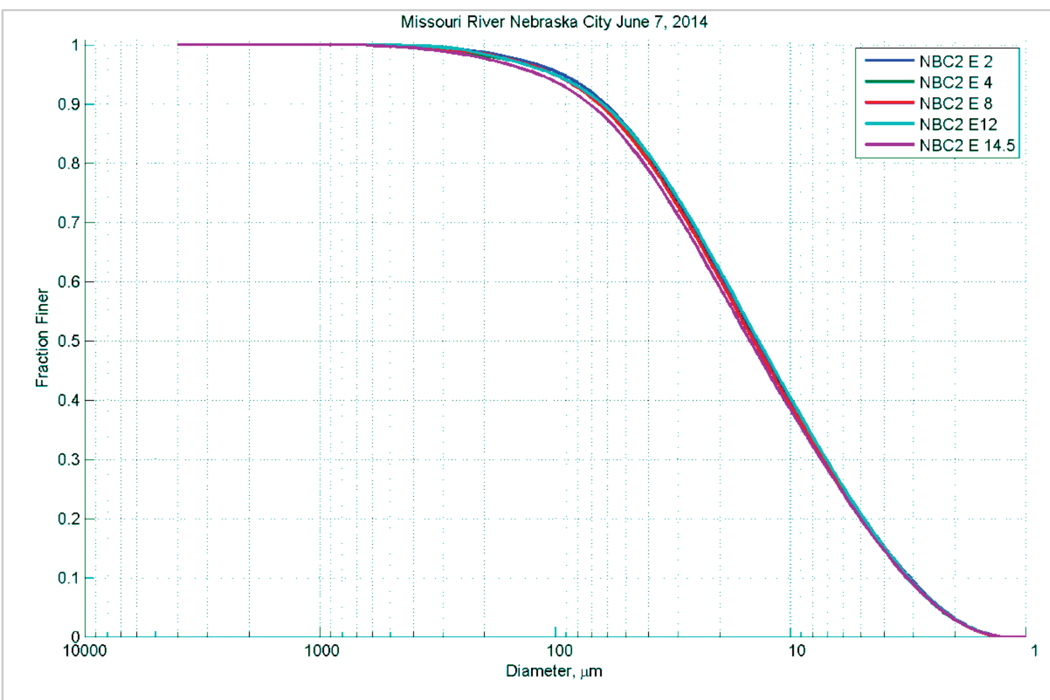

Particle size distribution for the third data collection date, June 22, 2014, is shown in Figure 97 to Figure 101.

Figure 97. Particle size distribution at different depths (feet) in Station A – June 22, 2014.

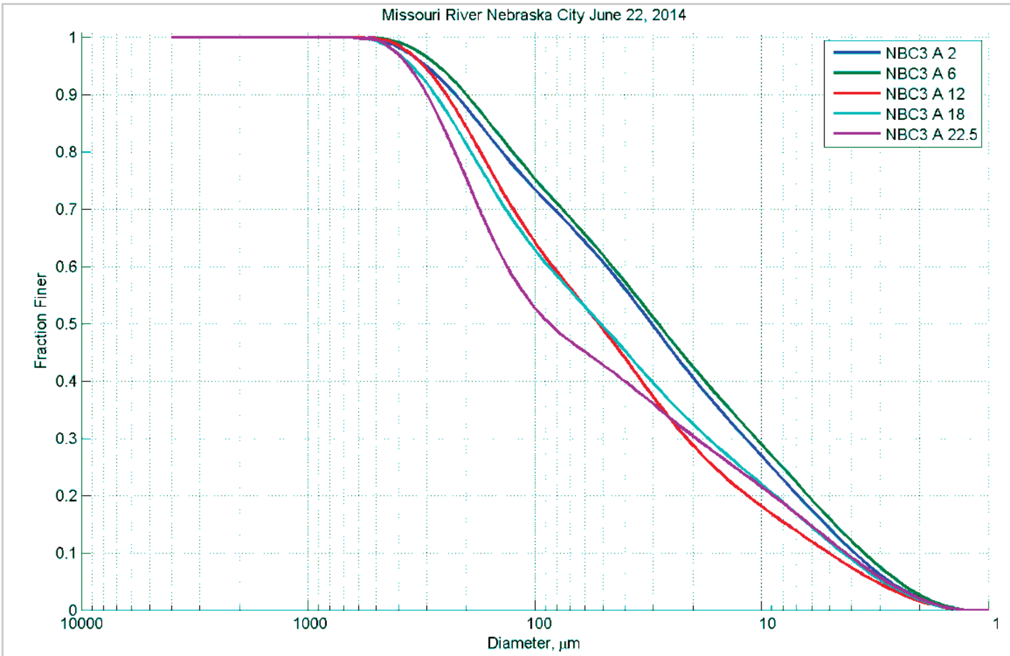

Figure 98. Particle size distribution at different depths (feet) in Station B – June 22, 2014.

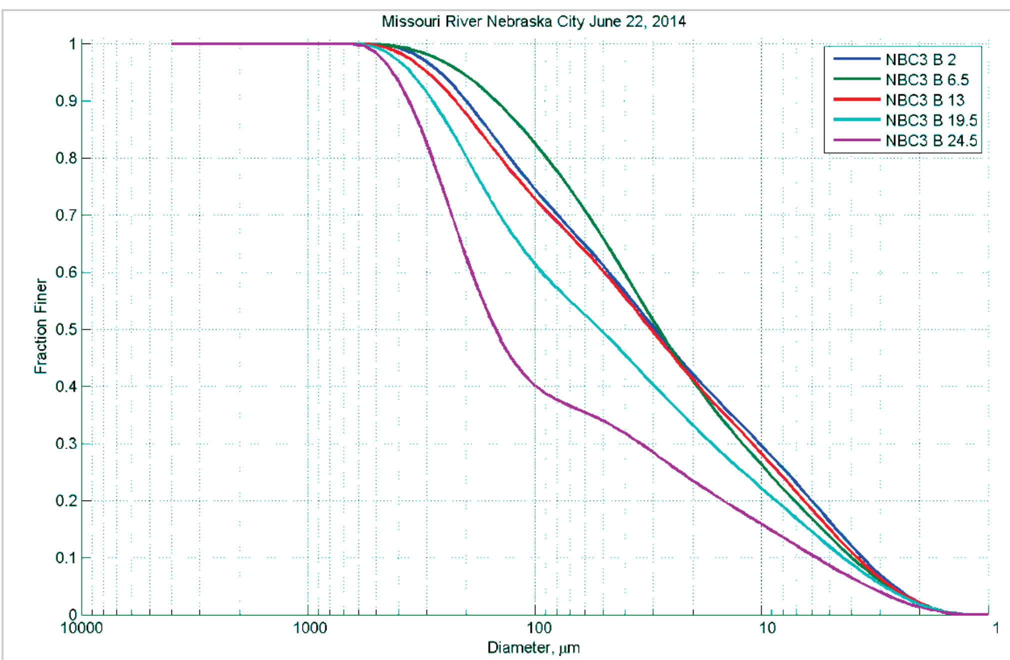

Figure 99. Particle size distribution at different depths (feet) in Station C – June 22, 2014.

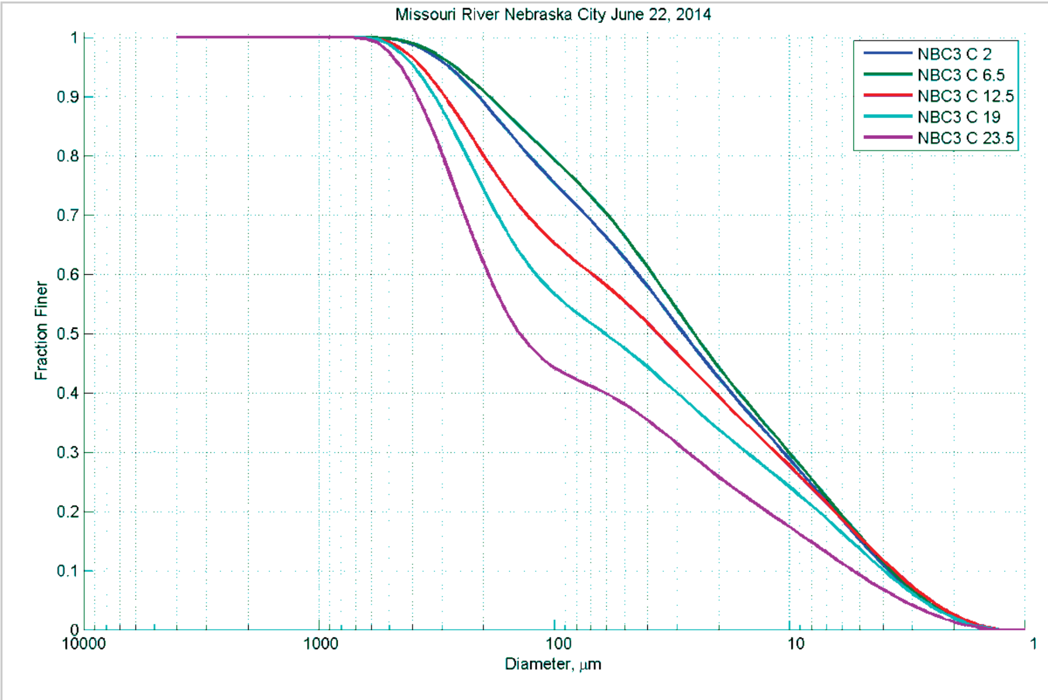

Figure 100. Particle size distribution at different depths (feet) in Station D – June 22, 2014.

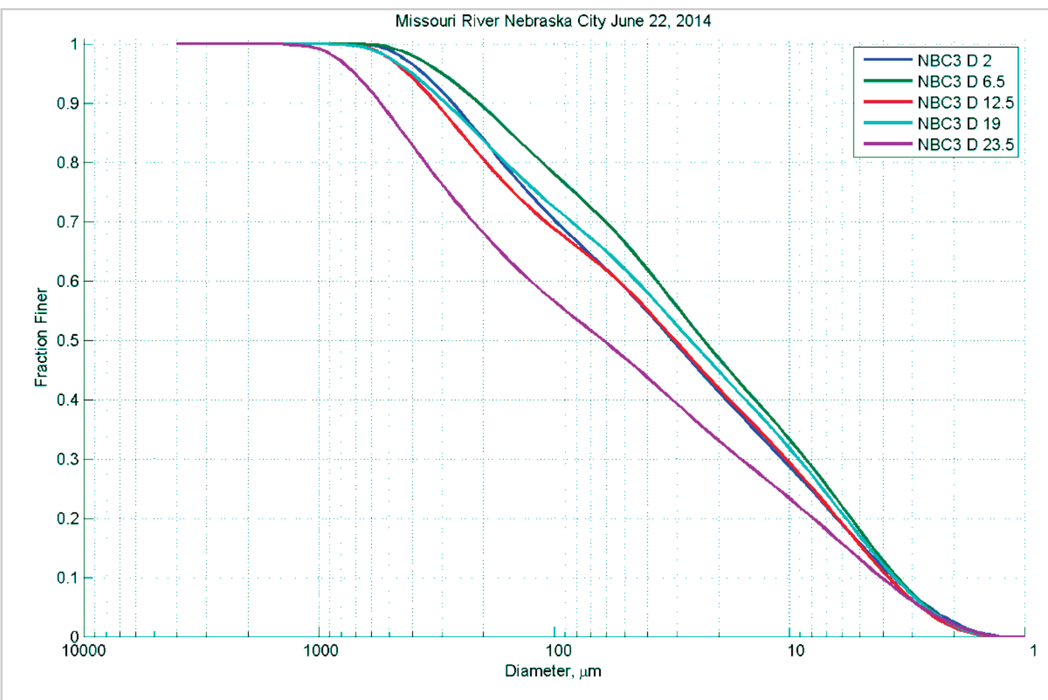

Figure 101. Particle size distribution at different depths (feet) in Station E – June 22, 2014.

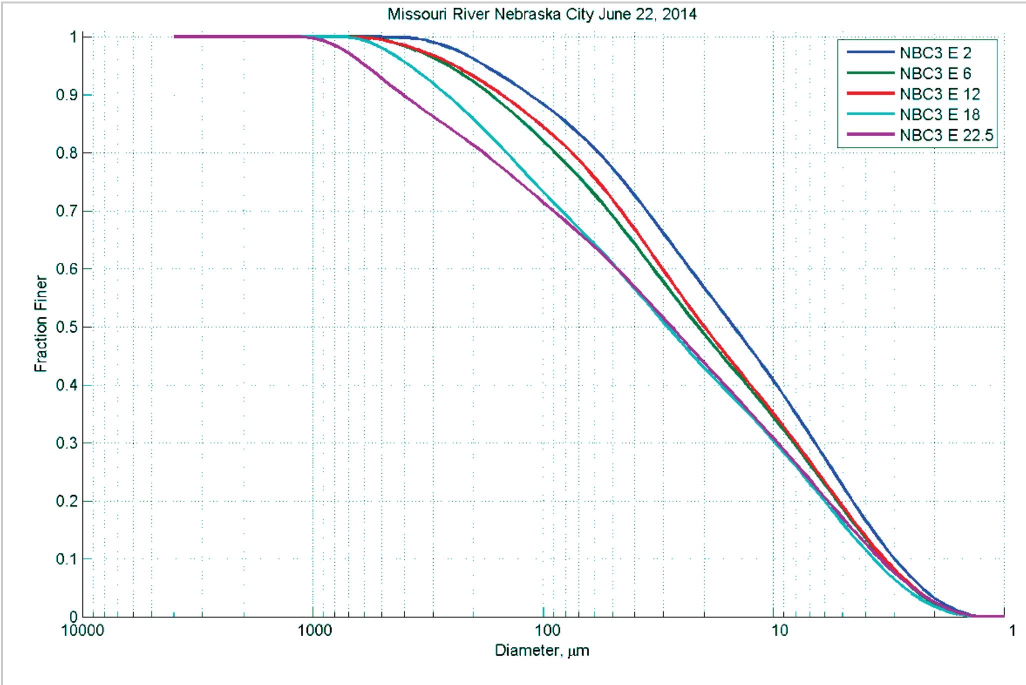

Suspended sediment concentration was also measured from the collected samples. Table 30 to Table 32 present the concentration values, for each data collection date. Suspended sediment concentration profiles were created using the measured data, presented in Figure 102 to Figure 104. See Appendix III-f for more details about the measured data.

Table 30. Suspended sediment concentration at Nebraska City, NE – April 28, 2014.

Station	Depth (ft)	Concentration (mg/L)
NBC 1A	2	133.61
NBC 1A	6	127.42
NBC 1A	10.5	184.44
Total depth	13.1	(Bottom)
NBC 1B	2	169.54
NBC 1B	4.5	209.41
NBC 1B	9.5	340.93
NBC 1B	12.5	496.79
Total depth	14.7	(Bottom)
NBC 1C	2	240.58
NBC 1C	5	231.08
NBC 1C	10	422.96
NBC 1C	13.5	684.78
Total depth	15.7	(Bottom)
NBC 1D	2	154.78
NBC 1D	4	155.97
NBC 1D	8	180.14
NBC 1D	12	201.11
NBC 1D	14.5	309.54
Total depth	15.9	(Bottom)
NBC 1E	2	149.19
NBC 1E	4	181.13
NBC 1E	8	128.55
NBC 1E	12	133.19
NBC 1E	14.5	162.64
Total depth	15.3	(Bottom)

Table 31. Suspended sediment concentration at Nebraska City, NE – June 7, 2014.

Station	Depth (ft)	Concentration (mg/L)
NBC 2A	2	511.69
NBC 2A	4	511.15
NBC 2A	8	557.67
NBC 2A	12	550.76
NBC 2A	14.5	746.62
Total depth	17	(Bottom)
NBC 2B	2	659.82
NBC 2B	4.5	624.85
NBC 2B	9	690.41
NBC 2B	13.5	927.53
NBC 2B	16.5	2667.71
Total depth	17.6	(Bottom)
NBC 2C	2	647.62
NBC 2C	4.5	780.31
NBC 2C	9.5	734.60
NBC 2C	14.5	1,018.80
NBC 2C	17.5	1,388.93
Total depth	18.8	(Bottom)
NBC 2D	2	582.02
NBC 2D	4.5	605.05
NBC 2D	8.5	629.35
NBC 2D	13	653.45
NBC 2D	15.5	694.53
Total depth	18.1	(Bottom)
NBC 2E	2	568.83
NBC 2E	4	569.03
NBC 2E	8	563.73
NBC 2E	12	595.28
NBC 2E	14.5	602.36
Total depth	16.9	(Bottom)

Table 32. Suspended sediment concentration at Nebraska City, NE – June 22, 2014.

Station	Depth (ft)	Concentration (mg/L)
NBC 3A	2	1,508.67
NBC 3A	6	1,407.44
NBC 3A	12	1,668.94
NBC 3A	18	1,868.57
NBC 3A	22.5	1,784.55
Total depth	24.9	(Bottom)
NBC 3B	2	1,804.19
NBC 3B	6.5	1,358.61
NBC 3B	13	1,745.65
NBC 3B	19.5	2,202.22
NBC 3B	24.5	2,344.92
Total depth	26.3	(Bottom)
NBC 3C	2	1,436.27
NBC 3C	6.5	1,587.44
NBC 3C	12.5	1,644.90
NBC 3C	19	1,905.85
NBC 3C	23.5	4,825.27
Total depth	24.7	(Bottom)
NBC 3D	2	1,379.58
NBC 3D	6.5	1,440.86
NBC 3D	12.5	1,568.73
NBC 3D	19	1,742.89
NBC 3D	23.5	1,625.71
Total depth	24.7	(Bottom)
NBC 3E	2	1,343.85
NBC 3E	6	1,378.77
NBC 3E	12	1,411.36
NBC 3E	18	1,496.07
NBC 3E	22.5	1,699.18
Total depth	23.2	(Bottom)

Figure 102. Suspended sediment concentration at Nebraska City, NE – April 28, 2014.

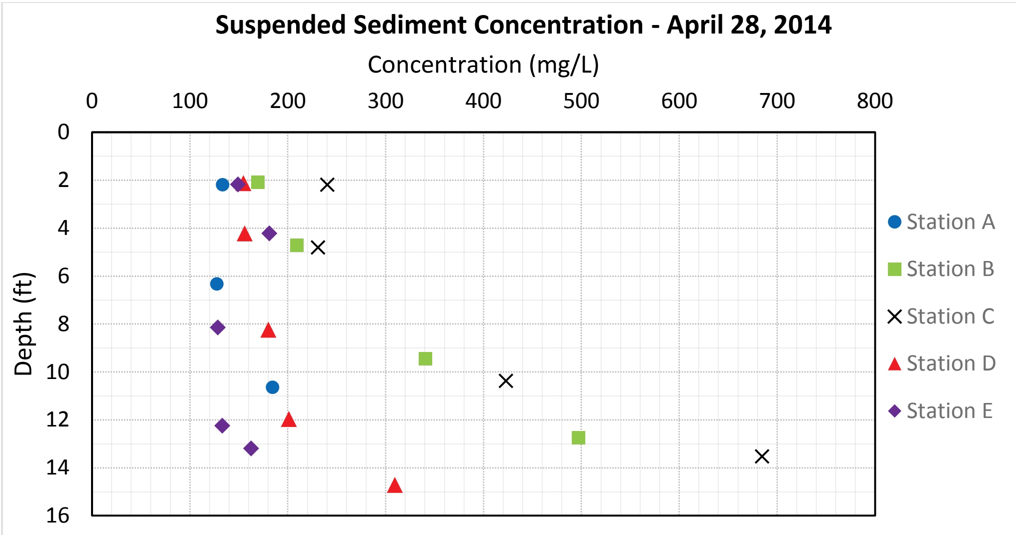

Figure 103. Suspended sediment Concentration at Nebraska City, NE – June 7, 2014.

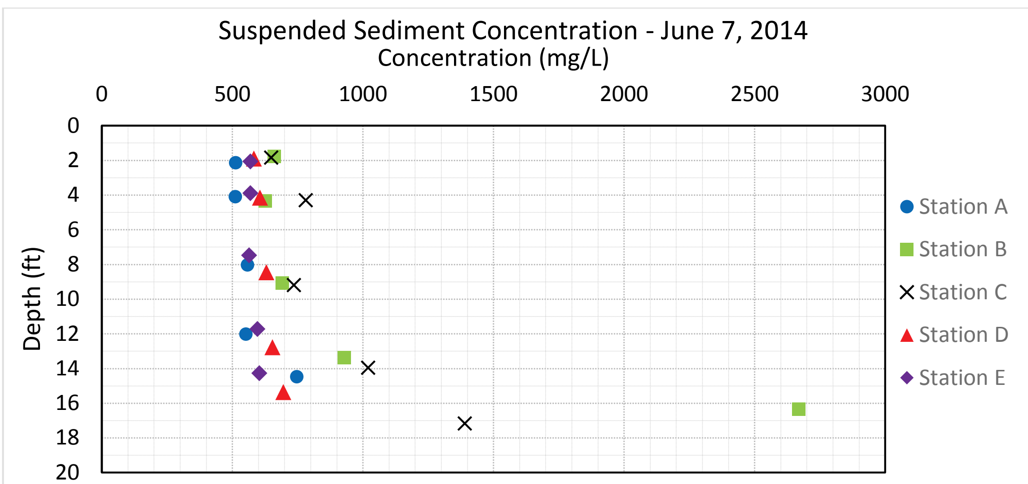

Figure 104. Suspended sediment concentration at Nebraska City, NE – June 22, 2014.

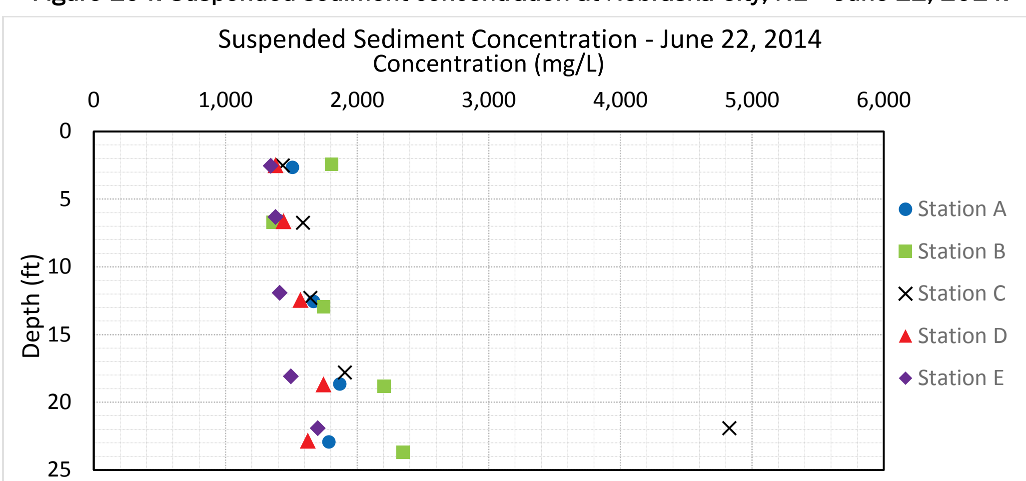

The suspended sediment concentration data were used to calibrate the ADCP acoustic backscatter and develop suspended sediment concentration profiles across the channel. Figure 105 to Figure 107 show the suspended sediment concentration profiles for the first left-to-right ADCP pass, for each data collection date. To see the other profiles, see Appendix III-f.

Figure 105. Suspended sediment concentration profile at Nebraska City, NE - April 28, 2014.

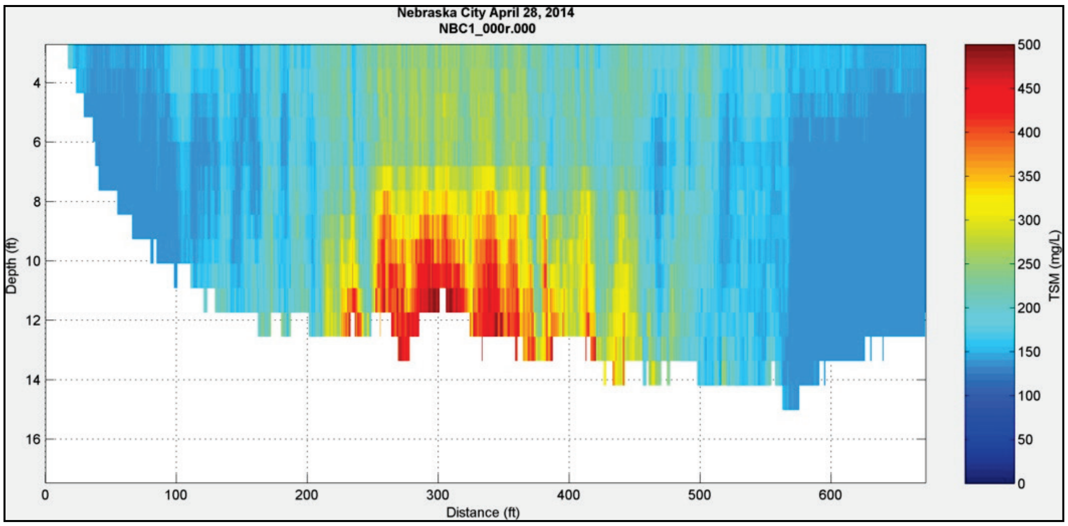

Figure 106. Suspended sediment concentration profile at Nebraska City, NE – June 7, 2014.

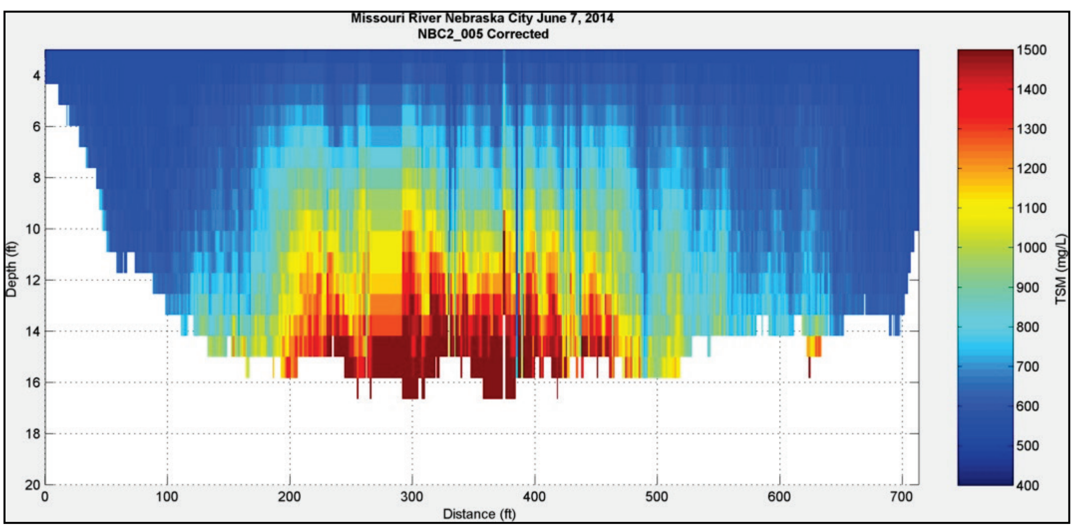

Figure 107. Suspended sediment concentration profile at Nebraska City, NE – June 22, 2014.

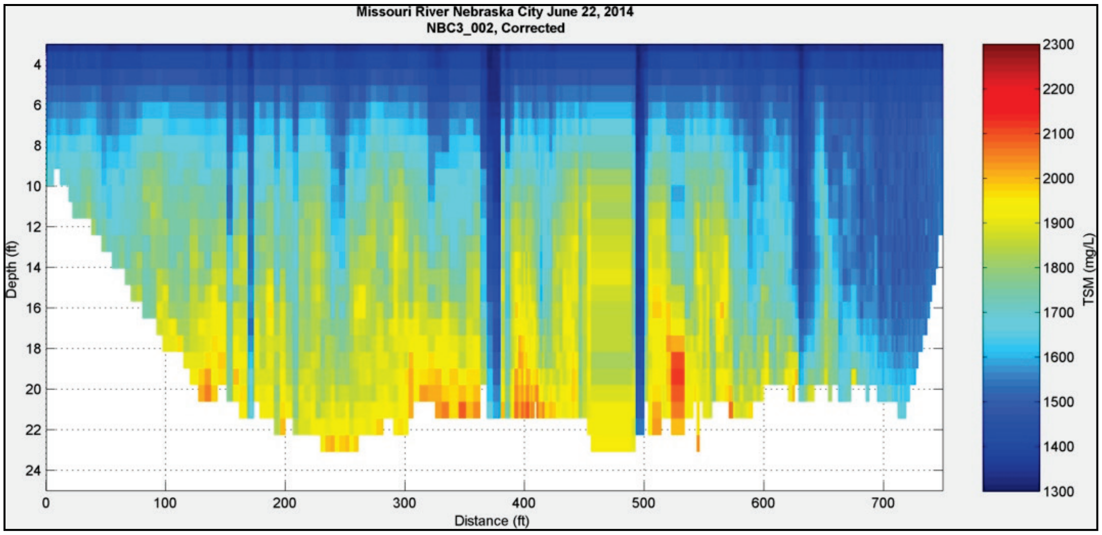

The suspended sediment concentration cross-section profiles obtained from the ADCP measurements were combined with the flow discharges, also obtained from the ADCP, to obtain the suspended sediment transport load, in tons per day. The method used for this study is explained in Heath et al. (2015, 13–14). The suspended sediment load can be divided classifying the suspended material by size and soil type. Table 33 presents the suspended sediment transport load, according to both classifications, for the first data collection date April 30, 2014. Table 34 and Table 35 present the same information for the second and third data collection dates, respectively. In all three tables, the categories under the Soil Type Classification were determined as follows: Clay Flux groups the size fractions 0.0001 to 0.0004 mm, Silt Flux 0.0004 to 0.0625 mm, and Sand Flux 0.0625 to 2.00 mm.

Table 33. Suspended sediment load distributed by grain size and soil type – April 28, 2014.

Classification System	Category	Sediment Flux (tons/day)
Total load		20,300.96
Sediment size classification	0.001 - 0.004 mm	991.80
	0.004 - 0.008 mm	1,594.67
	0.008 - 0.016 mm	2,311.38
	0.016 - 0.031 mm	2,949.23
	0.031 - 0.063 mm	2,869.79
	0.063 - 0.125 mm	2,450.64
	0.125 - 0.250 mm	4,163.31
	0.250 - 0.500 mm	2,675.81
	0.500 - 1.00 mm	282.38
	1.00 - 2.00 mm	11.94
Soil type Classification	Clay	991.80
	Silt	9,725.07
	Sand	9,584.08

Table 34. Suspended sediment load distributed by grain size and soil type – June 7, 2014.

Classification System	Category	Sediment Flux (tons/day)
Total load		115,220.52
Sediment size classification	0.001 - 0.004 mm	13,211.96
	0.004 - 0.008 mm	17,400.13
	0.008 - 0.016 mm	20,402.48
	0.016 - 0.031 mm	20,269.33
	0.031 - 0.063 mm	17,025.38
	0.063 - 0.125 mm	9,456.25
	0.125 - 0.250 mm	8,992.25
	0.250 - 0.500 mm	6,461.19
	0.500 - 1.00 mm	700.96
	1.00 - 2.00 mm	1,300.60
Soil type classification	Clay	13,211.96
	Silt	75,097.32
	Sand	26,911.25

Table 35. Suspended sediment load distributed by grain size and soil type – June 22, 2014.

Classification System	Category	Sediment Flux (tons/day)
Total load		517,935.62
Sediment size classification	0.001 - 0.004 mm	52,076.51
	0.004 - 0.008 mm	64,266.69
	0.008 - 0.016 mm	63,365.57
	0.016 - 0.031 mm	64,581.78
	0.031 - 0.063 mm	69,917.39
	0.063 - 0.125 mm	59,822.43
	0.125 - 0.250 mm	77,447.74
	0.250 - 0.500 mm	56,693.60
	0.500 - 1.00 mm	9,445.58
	1.00 - 2.00 mm	318.34
Soil type classification	Clay	52,076.51
	Silt	262,131.43
	Sand	203,727.69

5.7 Bed load transport

The ISSDOTv2 method was used for computing the bed-load transport. Table 36 shows the values obtained for the bed load, as well as the other sediment quantities determined from the suspended sediment samples at the Nebraska City site. It provides a breakdown of the various measured sediment transport components, based on sediment size classification.

Table 36. Bed-load transport values from Nebraska City, NE.

Data collection date	28-Apr-14	7-Jun-14	22-Jun-14
Flow (cfs)	37,032	51,272	115,589
Bed load (tons/day)	2,543	4,233	17,402
Suspended BML (tons/day)	9,584	26,911	203,728
Total BML (tons/day)	12,127	31,145	221,130
Bed load fraction (%)	21.0%	13.6%	7.9%
Wash load (tons/day)	10,717	88,309	314,208
Total load	22,844	119,454	535,338

In Table 36, *bed load* is defined as the bed material moving at the bottom of the river in bed-forms; *suspended BML* refers to the suspended material with grain size higher than 0.063 mm; *total BML* is the sum of bed load and suspended BML; *bed load fraction* is the percentage of the total bed

material moving as bed load; *wash load* is fine sediments that never settle in the bed, with grain size of 0.063 mm or less; and *total load* combines the quantity of total BML and wash load.

A bed-load rating curve was prepared for this site by plotting the bed-load transport in tons per day versus the river flowrate. This graph is shown in Figure 108. The R-squared value of 0.8901 shows a high correlation for a linear trend considering the range of flows. Also, note the decrease in Bed Load Fraction of Table 36 as flow increases. Two additional bed-load values were obtained at the Nebraska City site prior to the 2014 measurement effort, one in 2009 and one during the high-flow event of 2011. The latest version of the ISSDOTv2 code that was used in computing the 2014 bed-load values was also used to re-compute the 2009 and 2011 values. They were added to the rating curve as noted in the legend of Figure 108.

Figure 108. Bed-load rating curve for Nebraska City, NE.

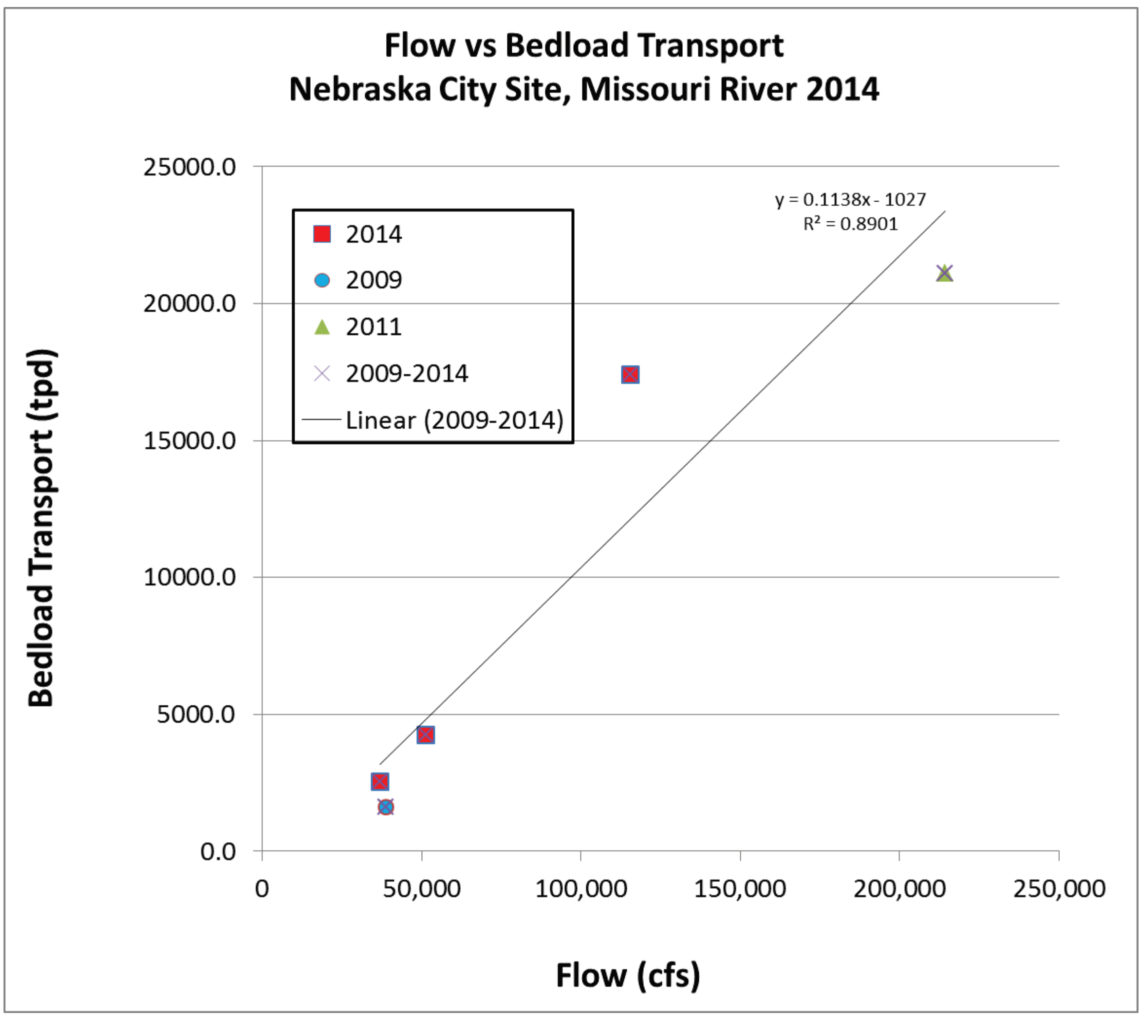

Bed-load transport values were also computed for this site using two analytic transport functions. One is the MPM formula, and the other is the Einstein formula. They were computed for each swath of bathymetric data. For instance, Figure 109 shows the bathymetry of this site with the six swath numbers (S1 to S6) labeled on it, indicating the lateral position where each swath was located. The hydraulic and sediment parameters obtained in the field data collection effort discussed before were extracted for each of these swaths.

Figure 109. Bathymetry for Nebraska City, NE, showing swath locations.

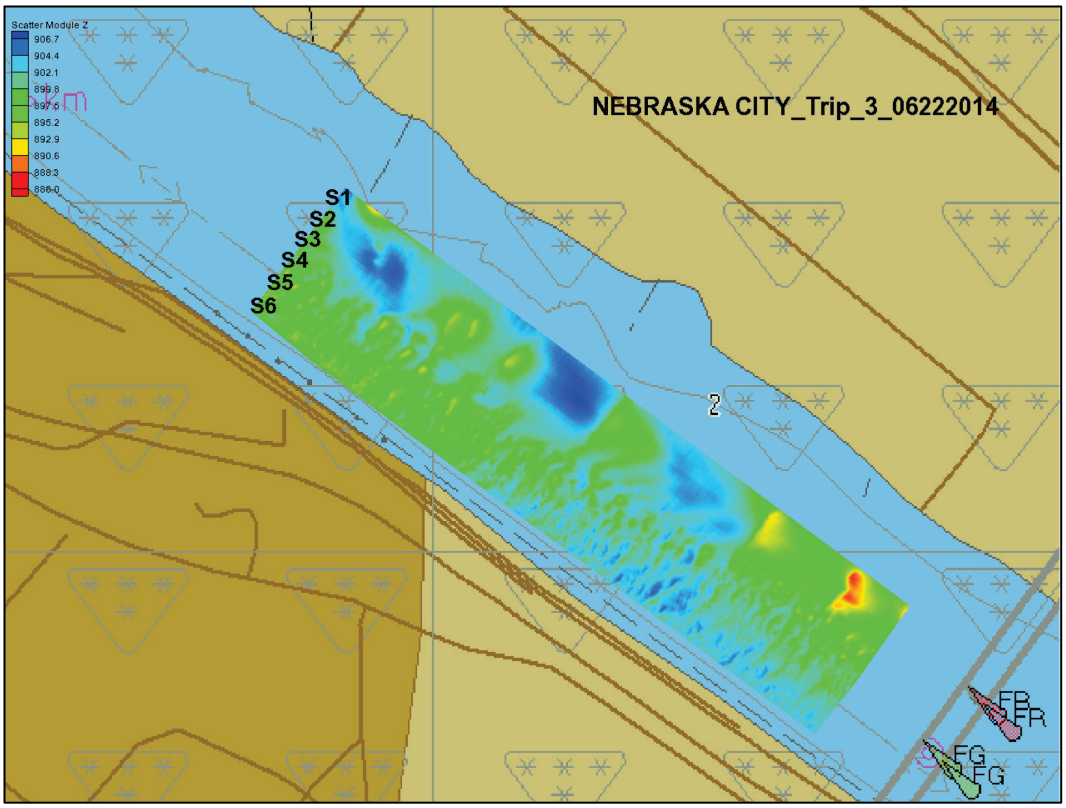

Flow, average velocity, and water depth were obtained from the ADCP data by a separate program written for that specific purpose. Water slope and water temperature were obtained from each appropriate data appendix. Bed sediment gradations used were selected based on their proximity to a given swath. The SAM Hydraulic Design Package for Channels program was then used with these data to compute the bed-load values for each swath. This software package has provisions for entering hydraulic and sediment input parameters and can then compute bed-load transport values for several commonly used transport functions.

The results are plotted in Figure 110 to Figure 112 and show how the transport function values compare to the ISSDOTv2 measured values. They also show the lateral variability across the measured section from the left side to the right side of the channel. The red numbers in Figure 110 and Figure 112 indicate an interpolated value.

Figure 110. Bed-load transport at Nebraska City, NE– April 28, 2014: ISSDOTv2 values compared to transport function computed values, where red indicates an interpolated value.

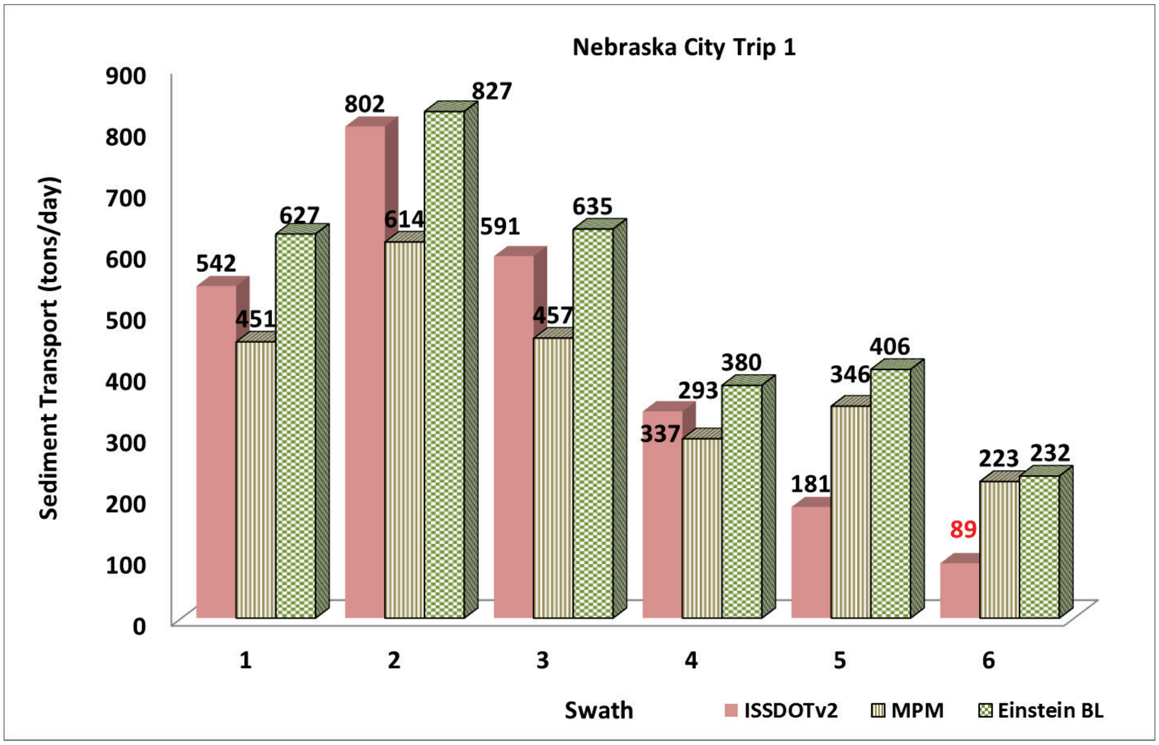

Figure 111. Bed-load transport at Nebraska City, NE– June 7, 2014: ISSDOTv2 values compared to transport function computed values.

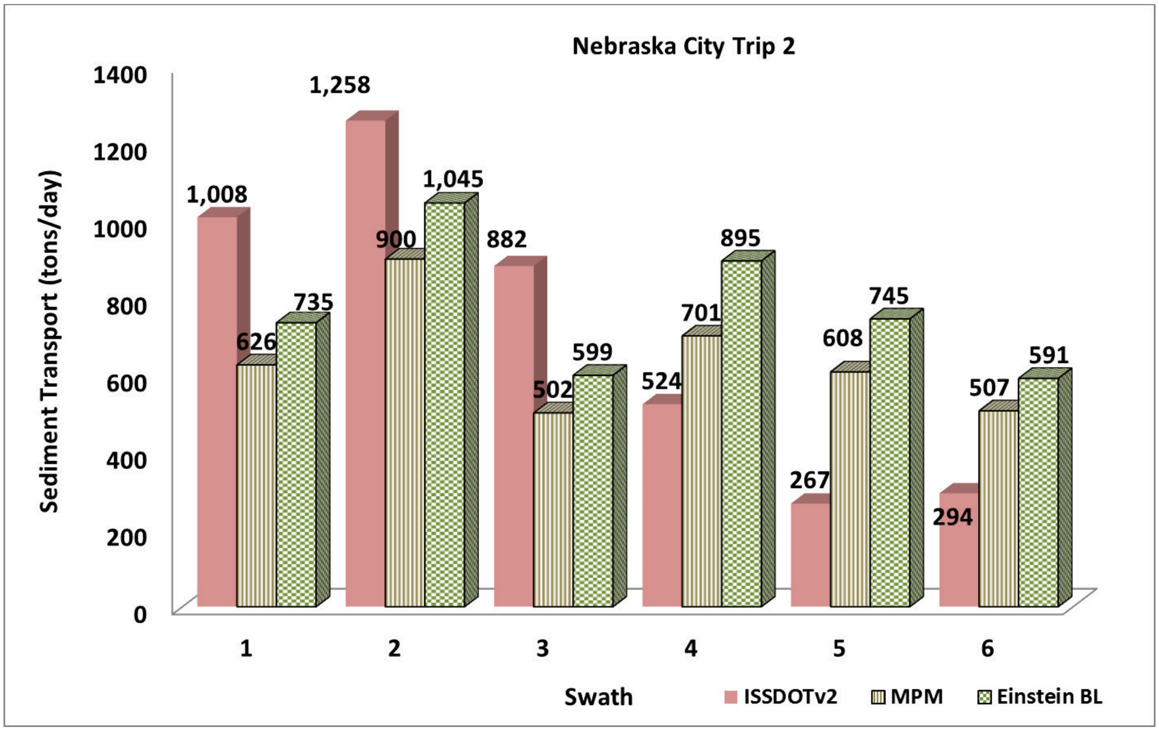

Figure 112. Bed-load transport at Nebraska City, NE– June 22, 2014: ISSDOTv2 values compared to transport function computed values, where red indicates an interpolated value.

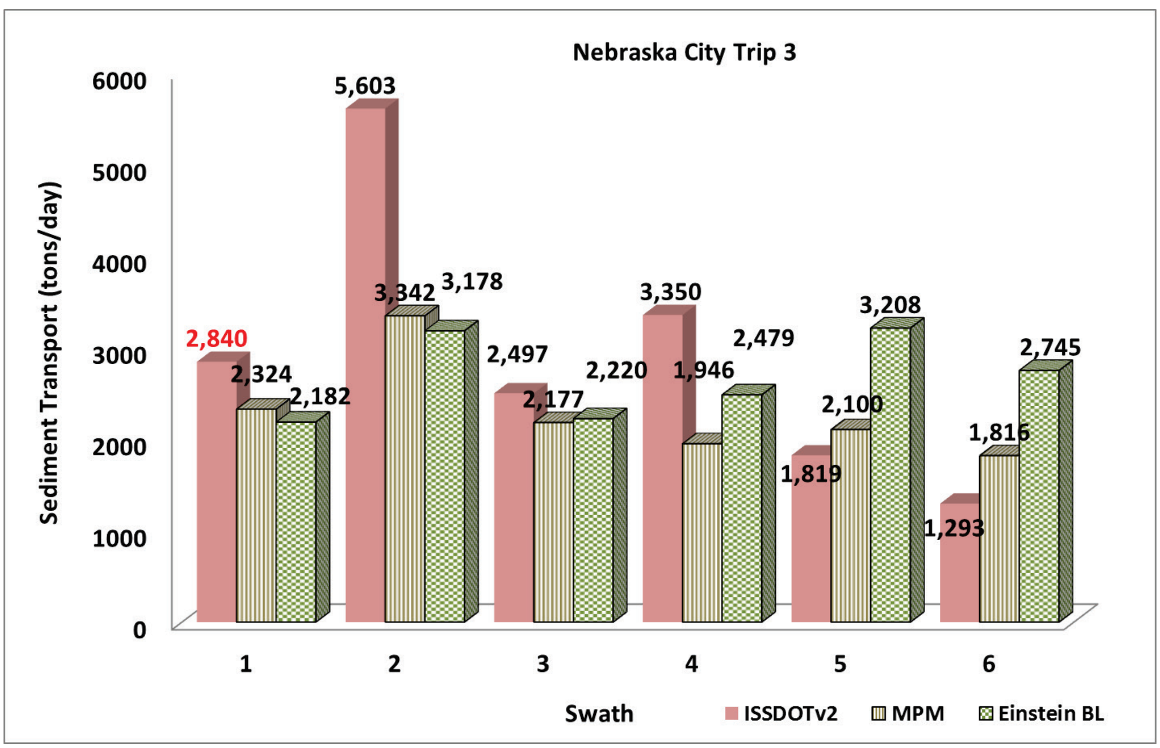

6 Site 4: Saint Joseph, Missouri

Multi-beam surveys, ADCP flow and velocity measurements, bed and suspended material sampling and testing, and water temperature, water surface elevation, and slope measurements were performed during each data collection date at St. Joseph, MO. The measuring area is shown on Figure 113 as the green polygon. The approximate location of the USGS gage station near the data collection site is also shown as the blue pin. This location might not be accurate in the figure. Coordinates for the gage site as given in the USGS web site are listed in Table 3. The red line indicates the cross section where ADCP measurements were conducted and suspended and bed load material samples were collected. The bank-to-bank width of the river at this location is approximately 820 ft; the length of the study area was approximately 1,500 ft. The data collection dates for St. Joseph were April 27, 2014; June 9, 2014; and June 24, 2014.

Figure 113. St. Joseph data collection site.

6.1 ADCP flow and velocity

The velocity and discharge for each data collection date, and site, were measured using an ADCP. Table 37 presents the cross-section average flow (ft^3/s), area (ft^2), and average velocity (ft/s) for each date, calculated from the measured data. See Appendix IV-a for the measured data.

Table 37. Total flow, area, and average velocity on the given dates at St. Joseph, MO.

Date	Total Flow, Q (ft^3/s)	Total Area, A (ft^2)	Velocity Q/A (ft/s)
April 27, 2014	36,857	10,921	3.38
June 8, 2014	97,663	20,158	4.85
June 24, 2014	113,735	21,961	5.18

Real-time vertical profiles of instantaneous velocities are also obtained from the ADCP measurements. Figure 114 to Figure 116 present the velocity magnitude, before the multi-beam measurements, from left to right. In the figures, the velocity magnitude is quantified by the range of colors shown on the right side of each figure where the higher velocities are denoted by red and the lower velocities by blue. The velocity profiles for after the multi-beam measurements are available at Appendix IV-a.

Figure 114. Velocity magnitude at St. Joseph, MO – April 27, 2014, 14:20:08.

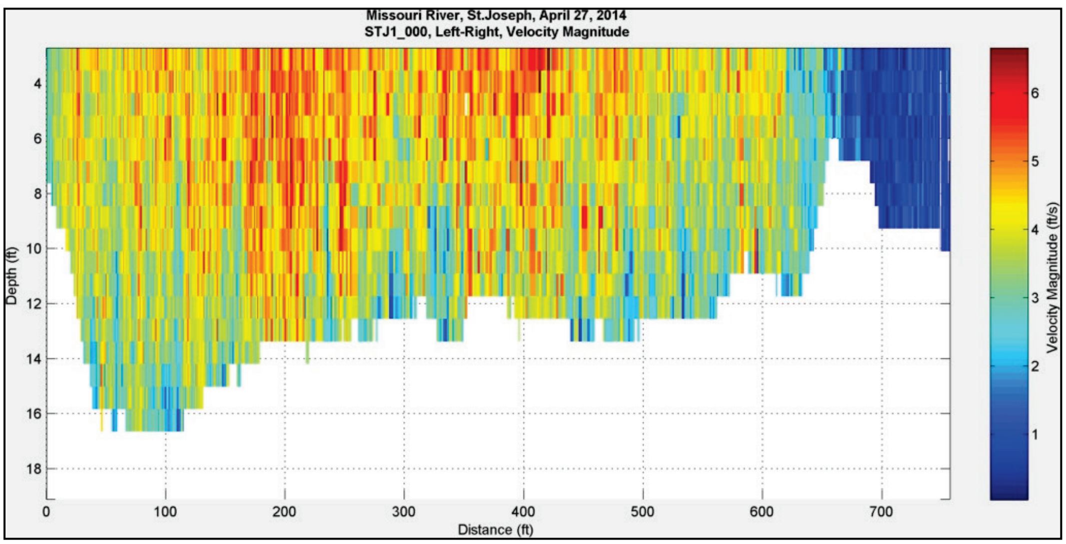

Figure 115. Velocity magnitude at St. Joseph, MO – June 8, 2014, 15:06:47.

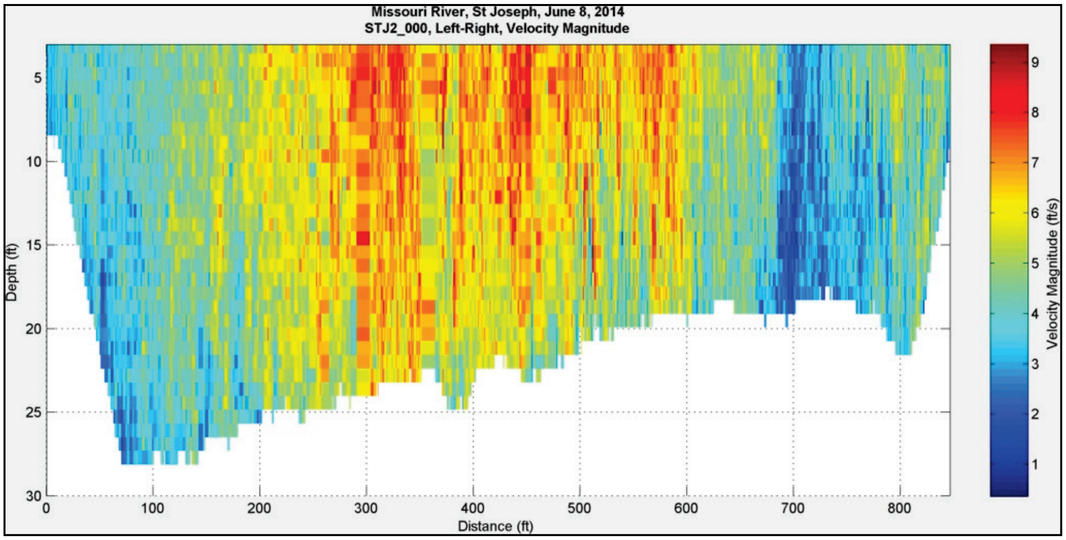

Figure 116. Velocity magnitude at St. Joseph, MO – June 24, 2014, 13:32:30.

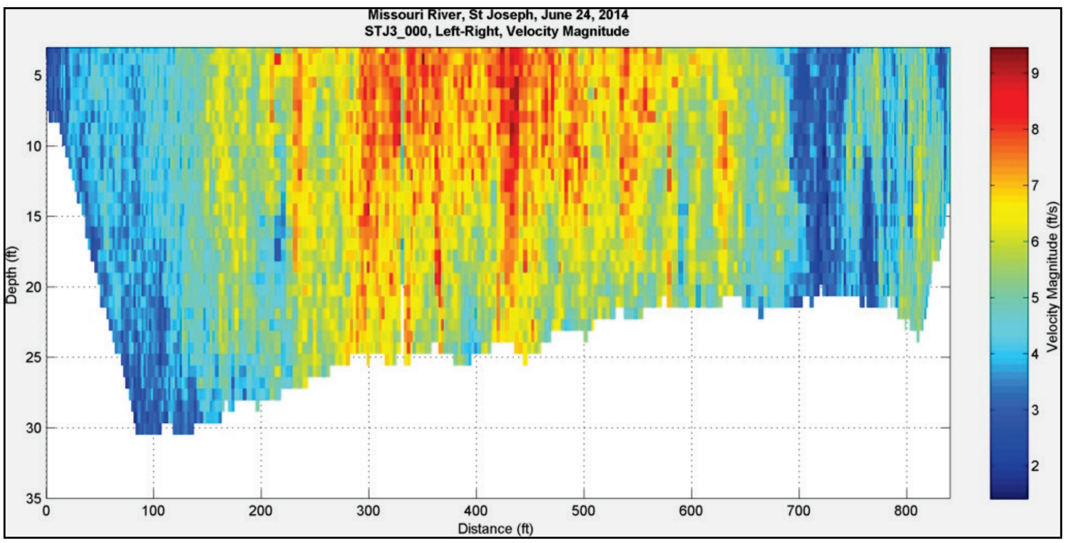

6.2 Water surface elevation and slope

Water surface elevation measurements were taken upstream and downstream of the multi-beam survey area. Figure 117 shows the upstream elevations, at distance zero, connected to the downstream elevations, at a distance of 1,500 ft, for each data collection date. Table 38 presents the slope values for the St. Joseph, MO, location for the three dates. The measured data are available at Appendix IV-b.

Figure 117. Water surface elevation at St. Joseph, MO – from upstream to downstream.

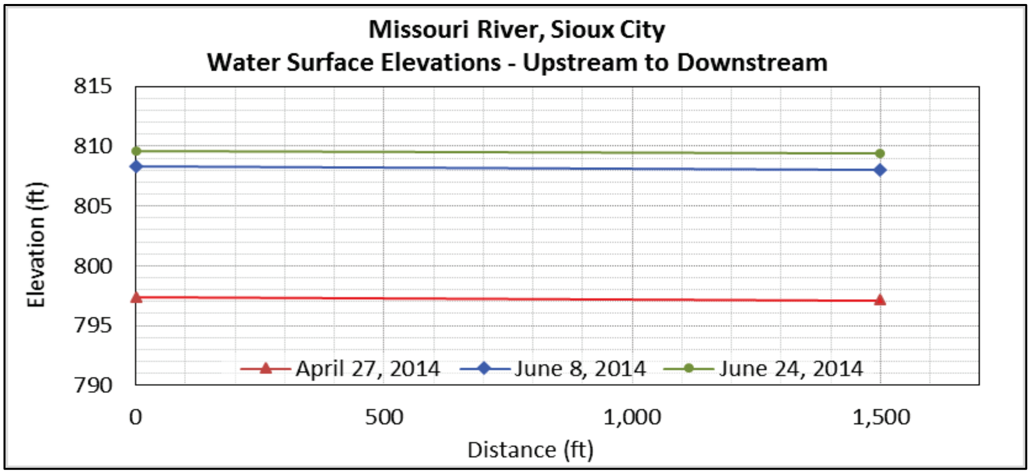

Table 38. Water surface slopes at St. Joseph, MO.

Date	Water Surface Slope (%)
April 27, 2014	0.00020
June 8, 2014	0.00020
June 24, 2014	0.00013

6.3 Water temperature

Table 39 presents the average temperature for each date (see Appendix IV-g for the measured values).

Table 39. Water temperature at St. Joseph, MO.

Date	Temperature (F)
April 27, 2014	59.8
June 8, 2014	72
June 24, 2014	76.6

6.4 Multi-beam surveys

The initial multi-beam survey performed at St. Joseph, MO, included the full extent of the channel from bank to bank, as shown in Figure 118 where the dark blue areas are deeper and the red areas are shallower. This survey is used to determine the location of the sand waves throughout the study area and to then decide where to run the ISSDOTv2 swaths according to the location of the active sand transport portion of the channel. The selected area with swath lines and numbers displayed in red is shown in Figure 119. This shows the actual area that was used for the ISSDOTv2 bed-load computations. The length of the multi-beam swaths is approximately 1,500 ft for all three data collection dates.

Figure 118. Multi-beam survey extent at St. Joseph, MO – April 27, 2014.

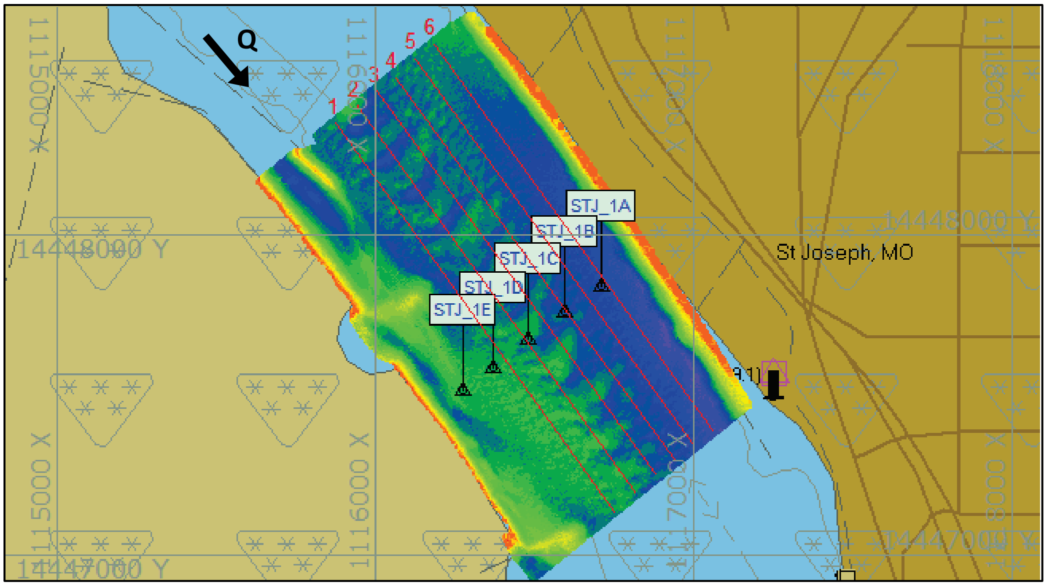

Figure 119. Multi-beam survey extent at St. Joseph, MO – June 8 and June 24, 2014.

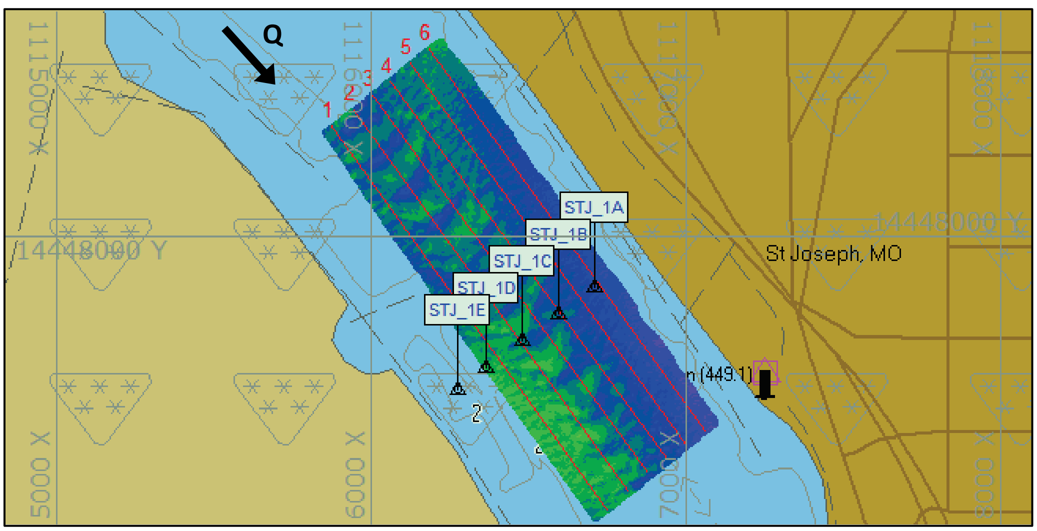

6.5 Bed material samples

Five sediment sample stations were positioned equidistant from each other along the cross section, as presented on Figure 120, which is the same location at which the suspended sediment samples and the ADCP velocity data were obtained. The first station, Station A, was positioned on the left descending bank, and the last station, Station E, on the right descending bank. Table 40 provides the locations of sample stations according to NAD83. See Appendix IV-c for the coordinates using the UTM Grid System.

Table 40. Sediment sample stations NAD83 coordinates at St. Joseph, MO.

Station	NAD83 Latitude	NAD83 Longitude
STJ A	39° 46' 6.1451" N	94° 51' 49.3072" W
STJ B	39° 46' 5.2911" N	94° 51' 50.7516" W
STJ C	39° 46' 4.4257" N	94° 51' 52.1872" W
STJ D	39° 46' 3.5602" N	94° 51' 53.6228" W
STJ E	39° 46' 2.8406" N	94° 51' 54.8102" W

Figure 120. Sediment sample stations at the Missouri River – St. Joseph, MO.

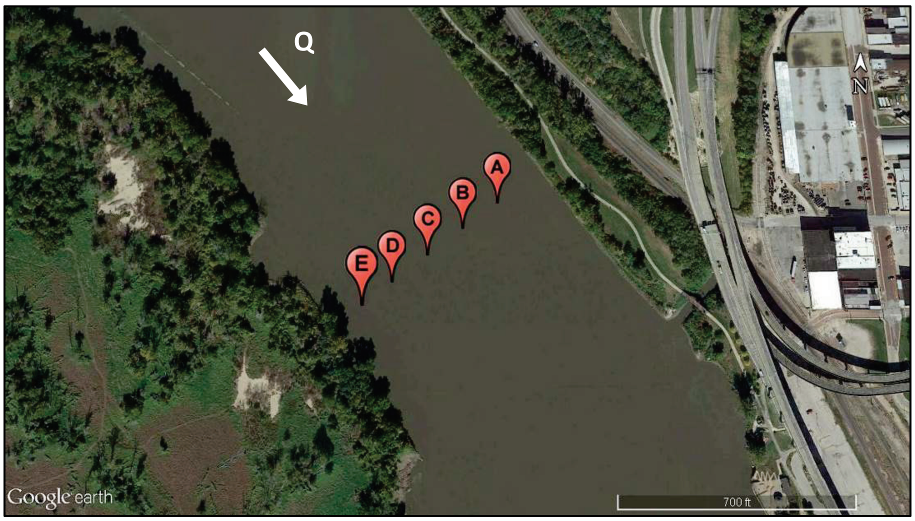

The grain size distribution for the five bed material samples of the first collection date, April 27, 2014, is provided at Figure 121. Figure 122 and Figure 123 present the gradation analysis for the second and third collected samples, respectively. The measured data are available in Appendix IV-d.

Figure 121. Bed material grain size distribution for St. Joseph, MO – April 27, 2014.

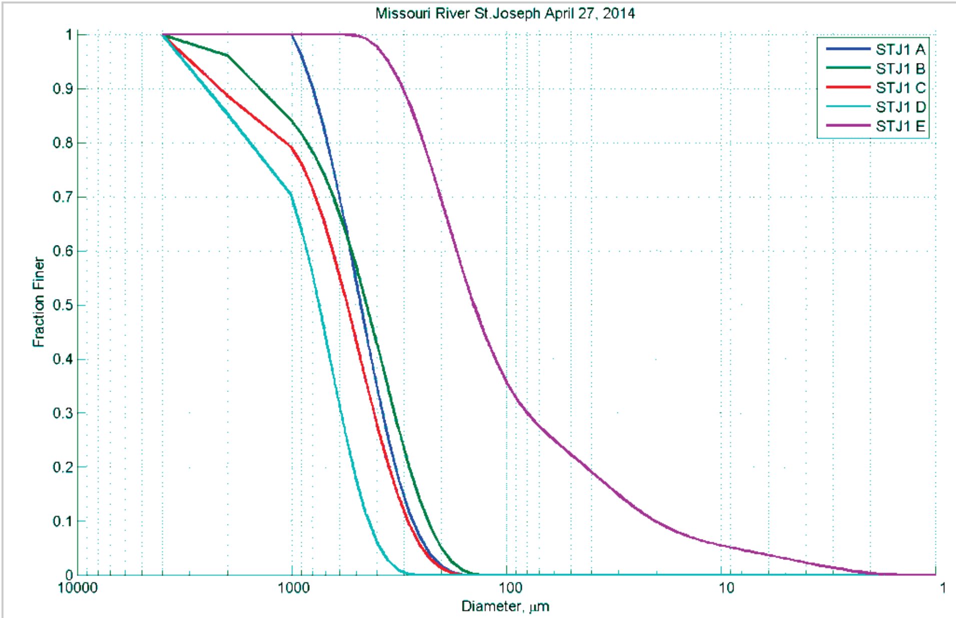

Figure 122. Bed material grain size distribution for St. Joseph, MO – June 8, 2014.

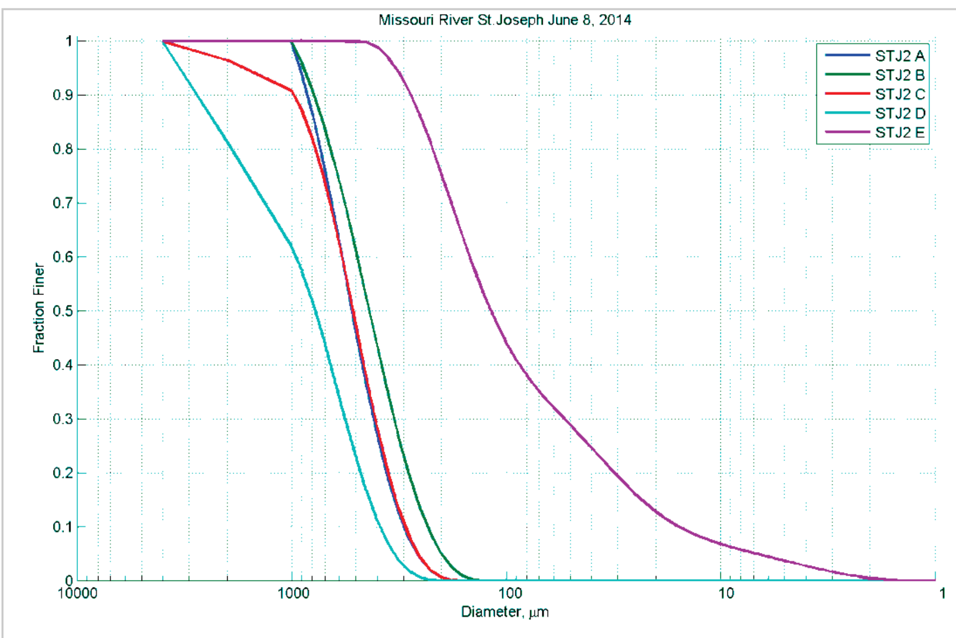

Figure 123. Bed material grain size distribution for St. Joseph, MO – June 24, 2014.

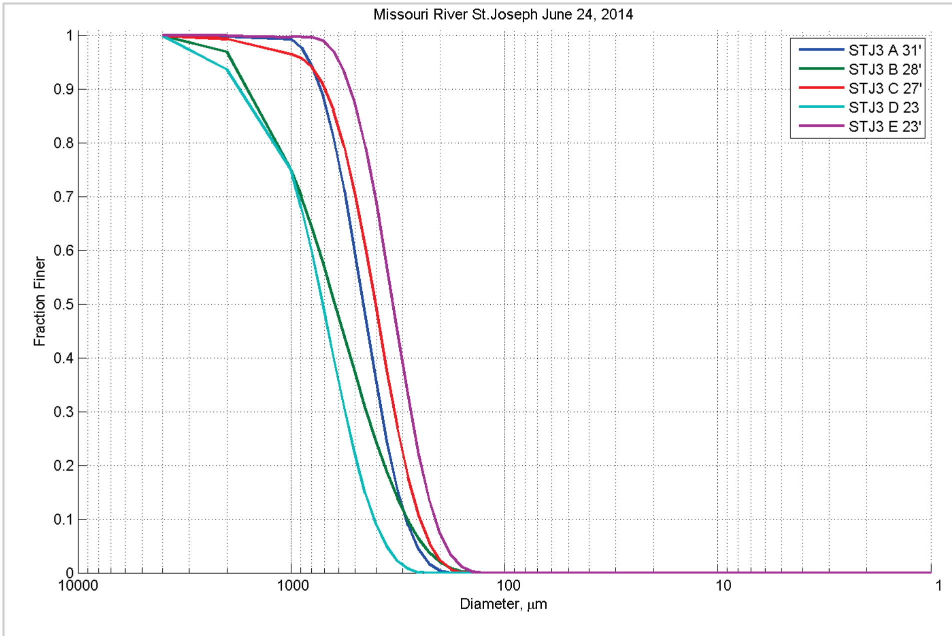

6.6 Suspended sediment

Suspended sediment samples at different depths in a column were taken at the five stations shown in Figure 120, for each data collection date. A particle size analysis was conducted for the samples of each station and date. The results are presented in this report as Figure 124 to Figure 138, and the measured data are available at Appendix IV-e.

Particle size distribution for the first data collection date, April 27, 2014, is shown in Figure 124 to Figure 128. It is organized starting from the station closer to the left descending bank, Station A, to the station closer to the right descending bank, Station E.

Figure 124. Particle size distribution at different depths (feet) in Station A - April 27, 2014.

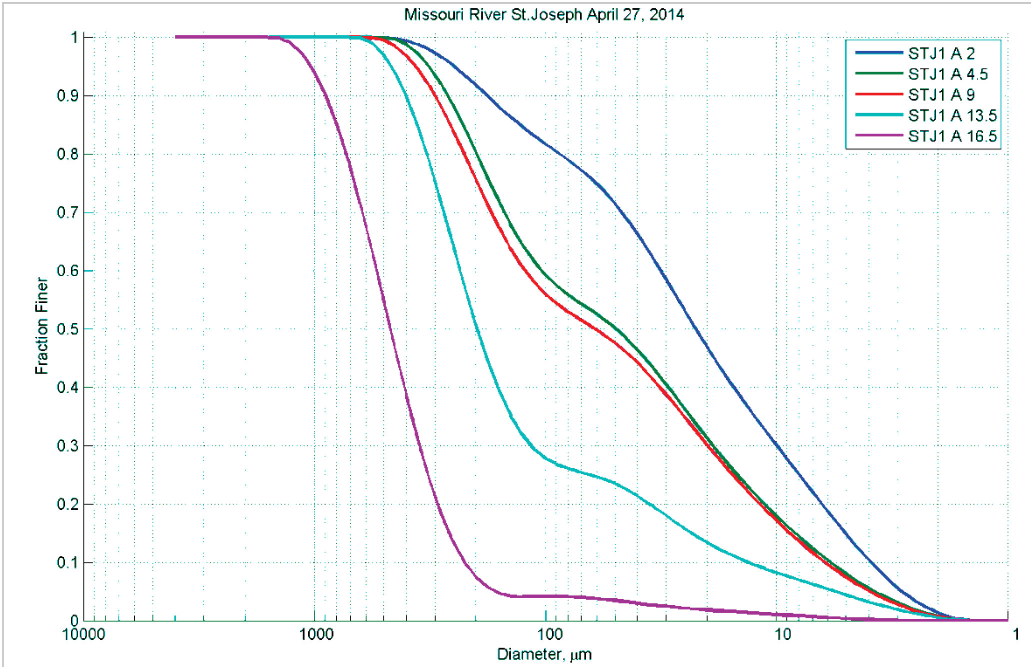

Figure 125. Particle size distribution at different depths (feet) in Station B - April 27, 2014.

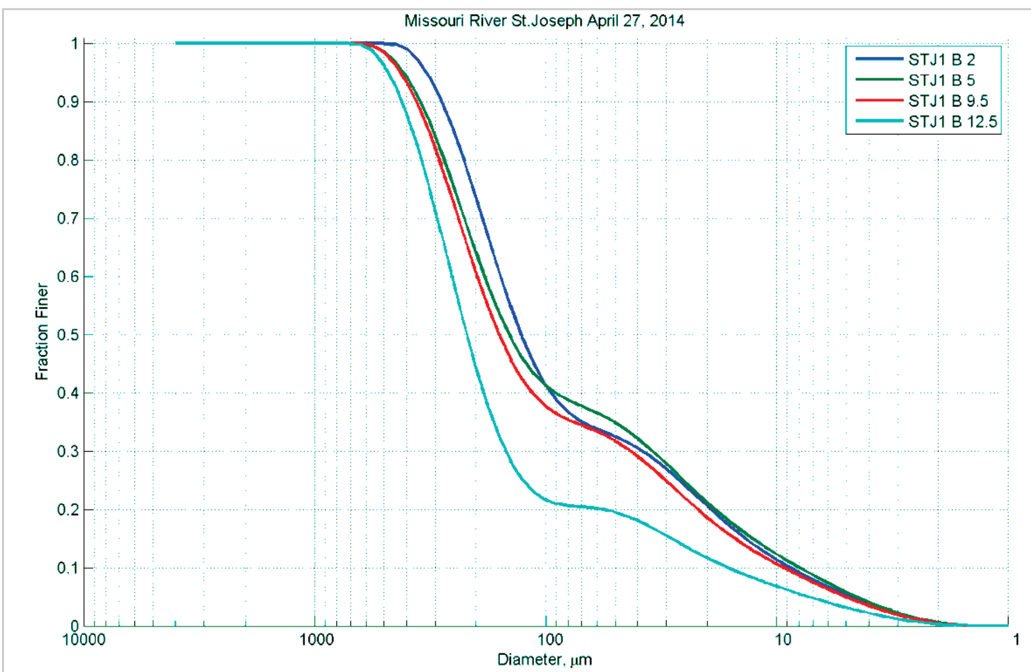

Figure 126. Particle size distribution at different depths (feet) in Station C - April 27, 2014.

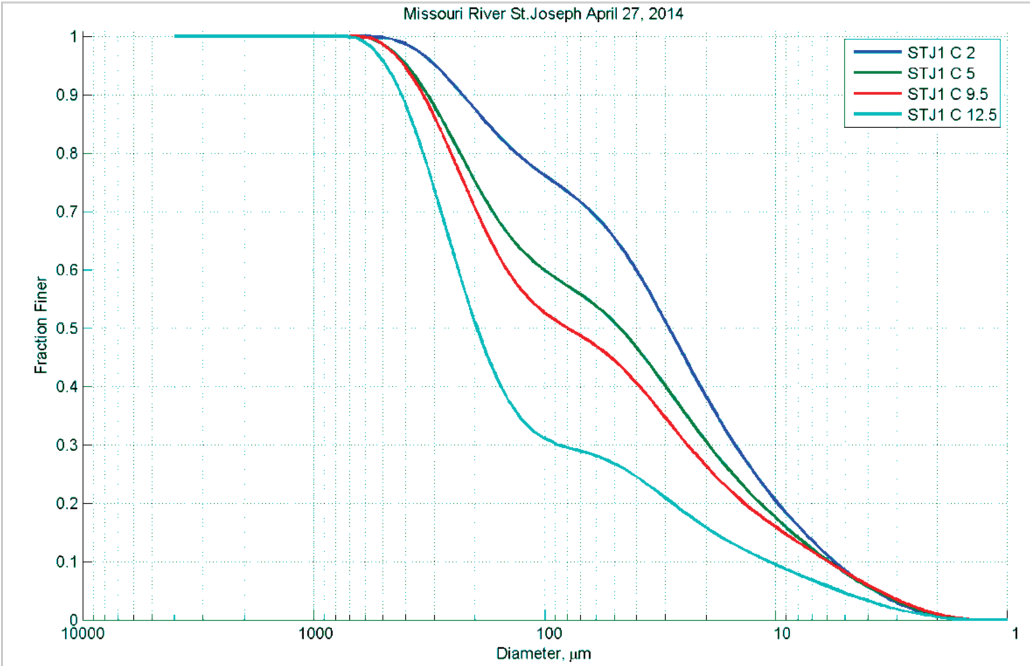

Figure 127. Particle size distribution at different depths (feet) in Station D - April 27, 2014.

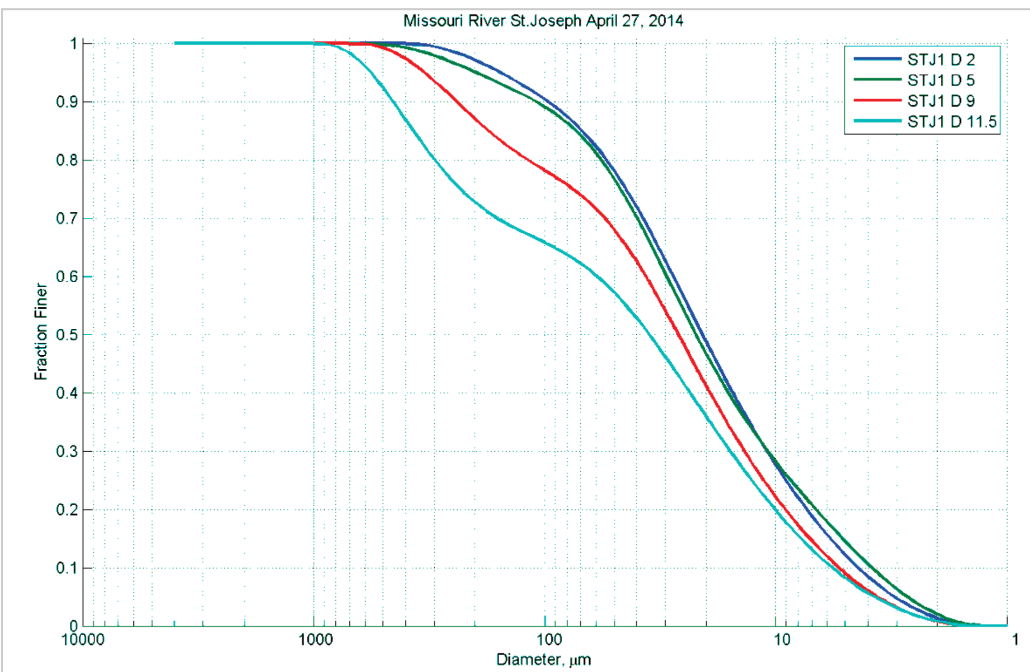

Figure 128. Particle size distribution at different depths (feet) in Station E - April 27, 2014.

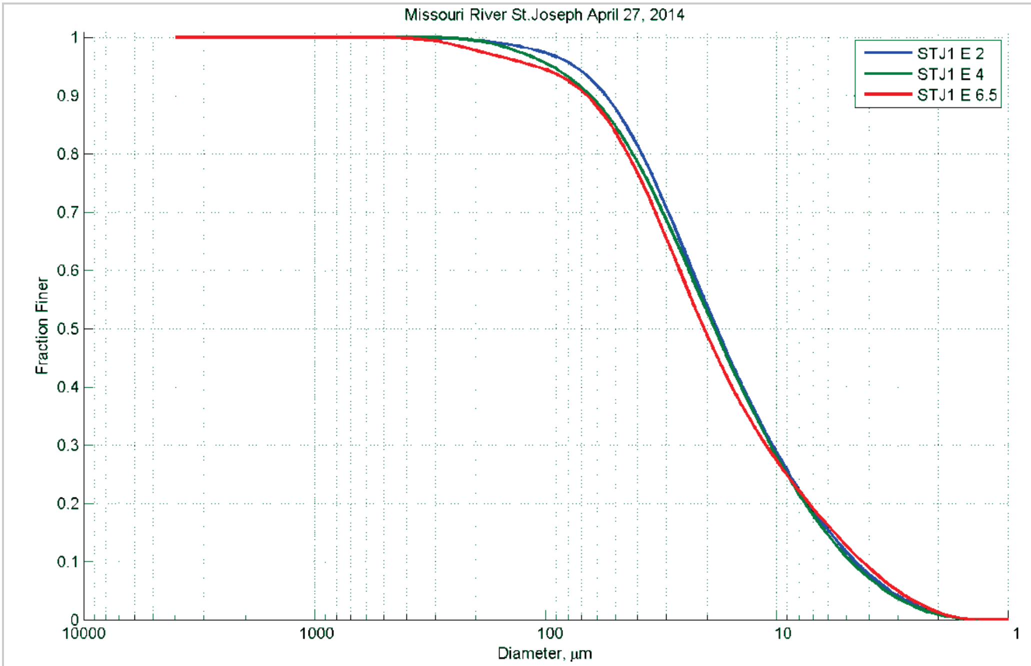

Particle size distribution for the second data collection date, June 8, 2014, are shown in Figure 129 to Figure 133.

Figure 129. Particle size distribution at different depths (feet) in Station A – June 8, 2014.

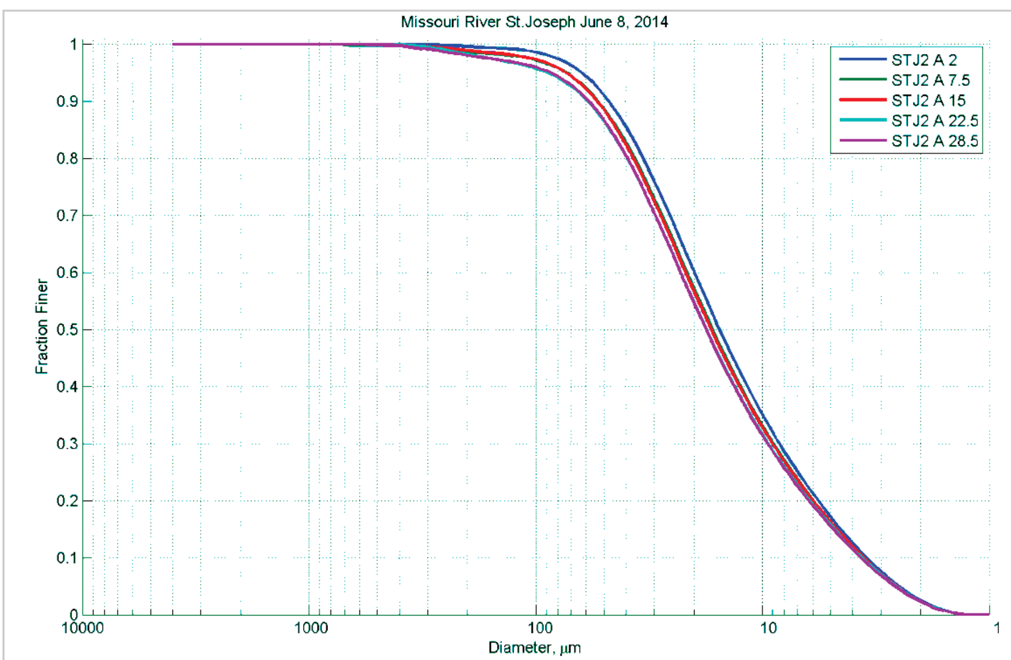

Figure 130. Particle size distribution at different depths (feet) in Station B – June 8, 2014.

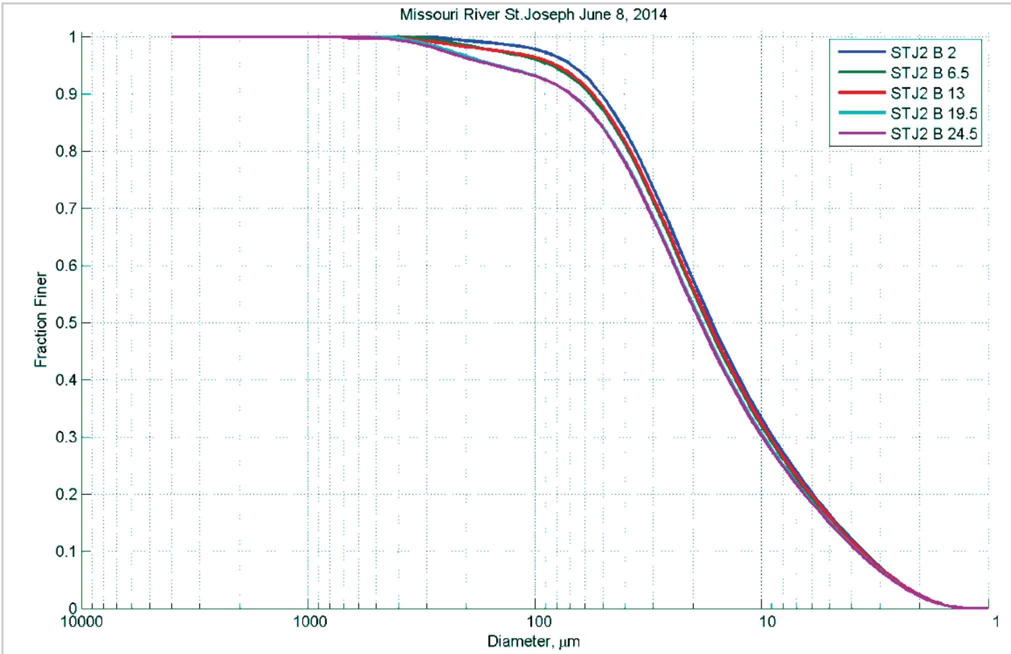

Figure 131. Particle size distribution at different depths (feet) in Station C – June 8, 2014.

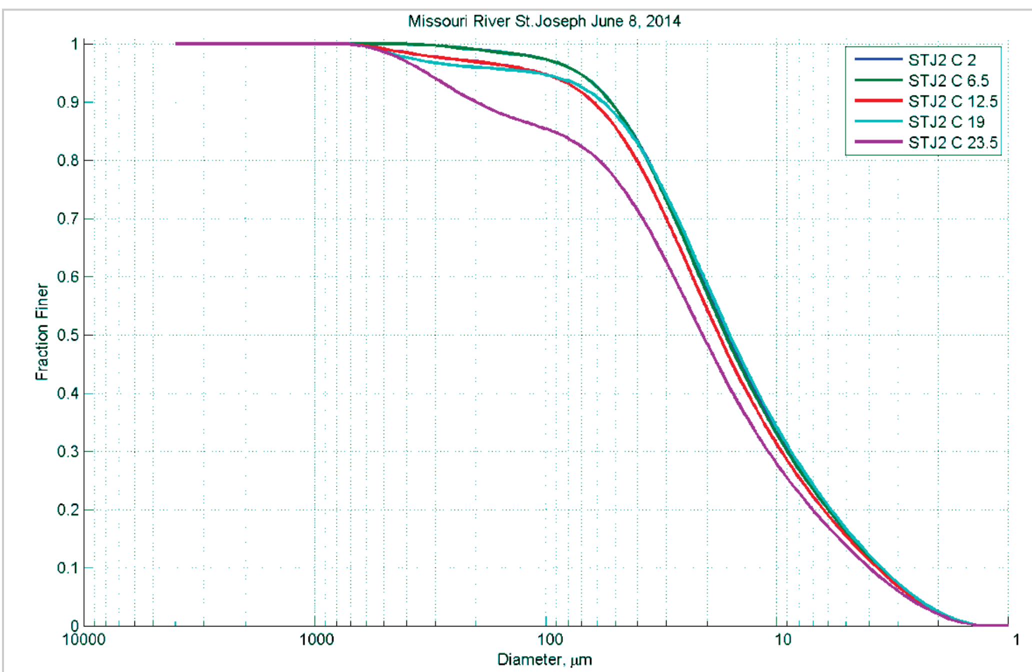

Figure 132. Particle size distribution at different depths (feet) in Station D – June 8, 2014.

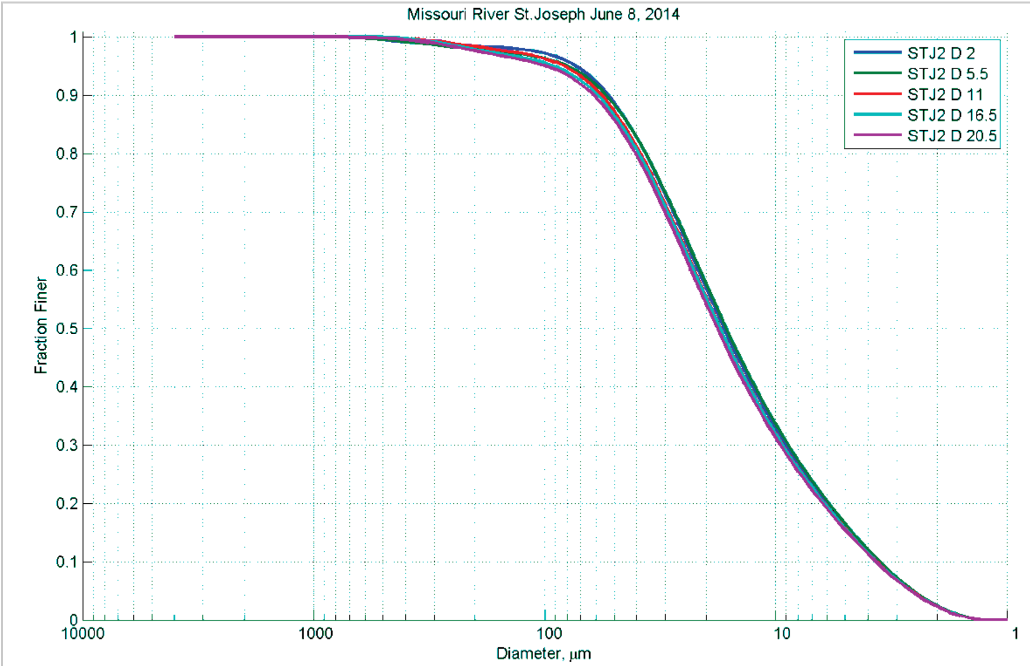

Figure 133. Particle size distribution at different depths (feet) in Station E – June 8, 2014.

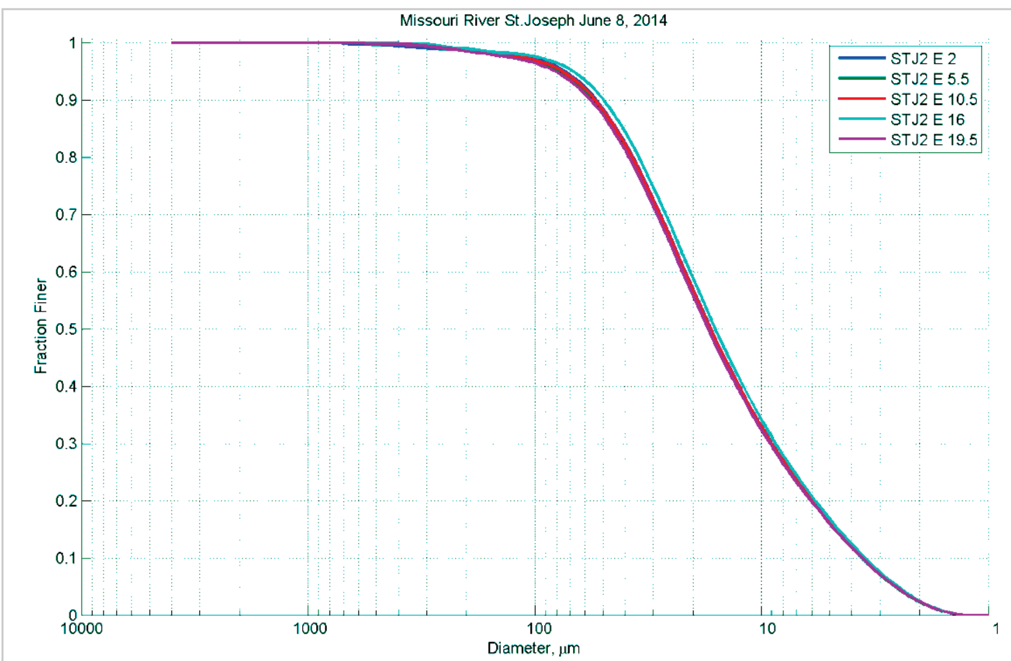

Particle size distribution for the third data collection date, June 24, 2014, is shown in Figure 134 to Figure 138.

Figure 134. Particle size distribution at different depths (feet) in Station A – June 24, 2014.

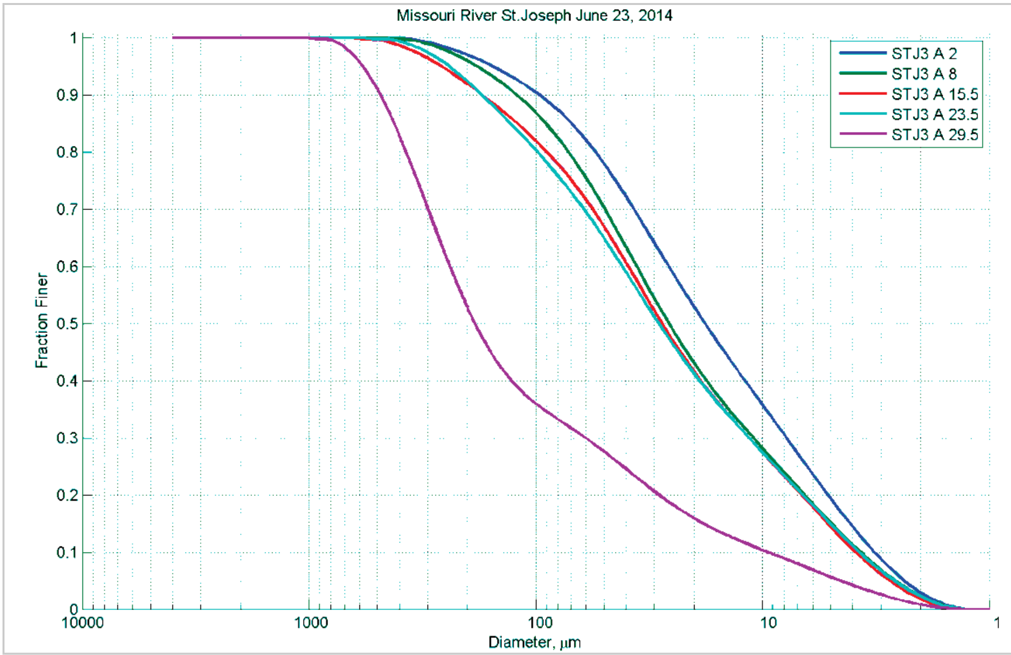

Figure 135. Particle size distribution at different depths (feet) in Station B – June 24, 2014.

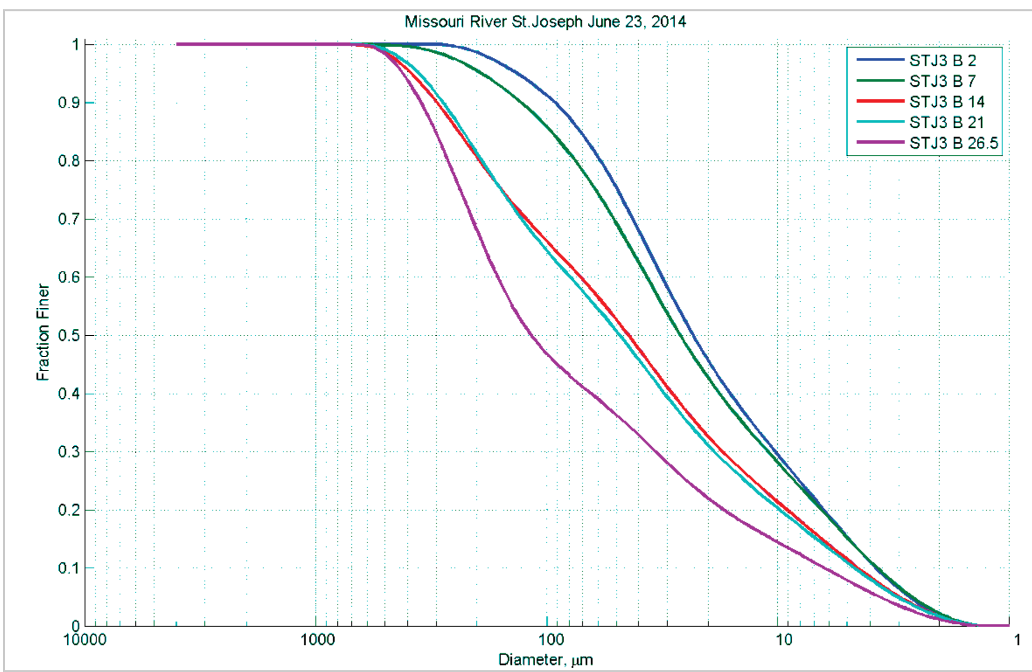

Figure 136. Particle size distribution at different depths (feet) in Station C – June 24, 2014.

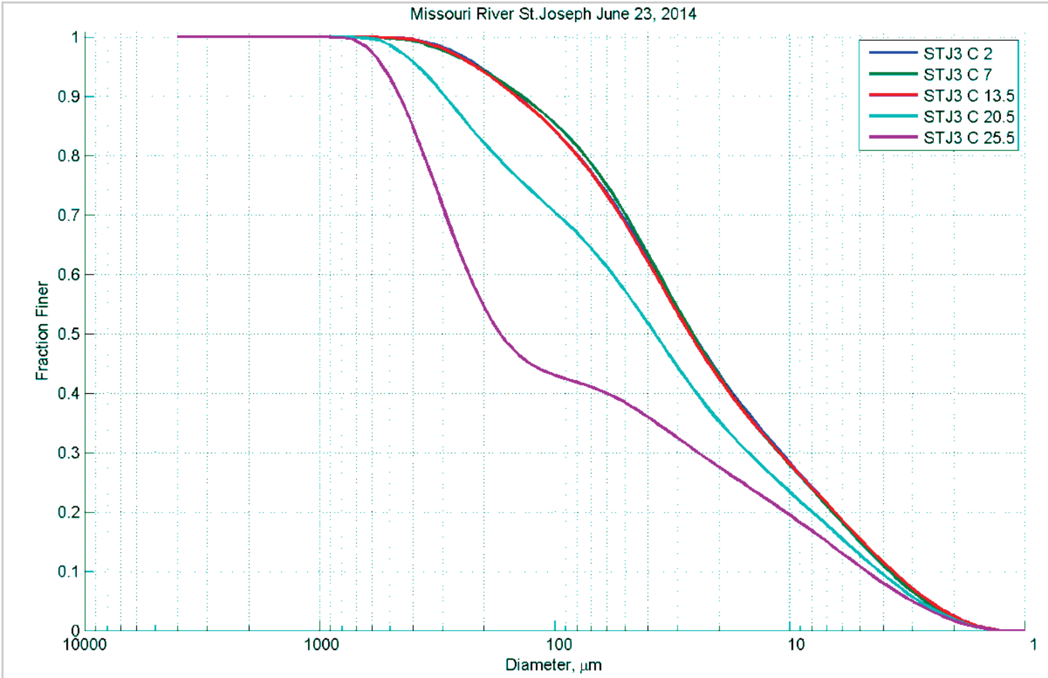

Figure 137. Particle size distribution at different depths (feet) in Station D – June 24, 2014.

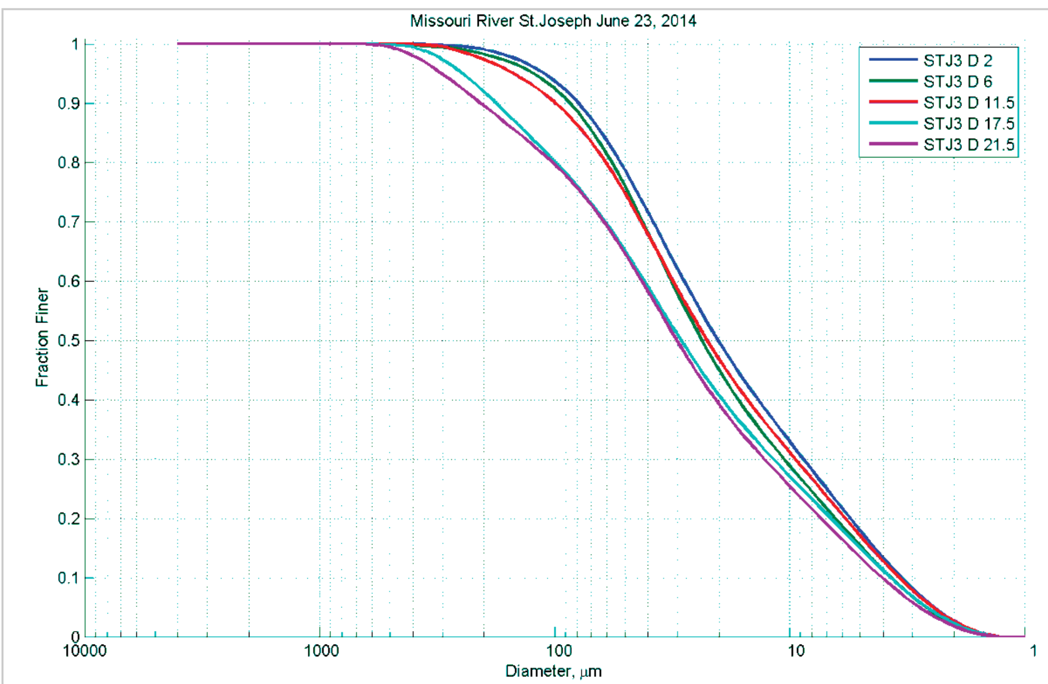

Figure 138. Particle size distribution at different depths (feet) in Station E – June 24, 2014.

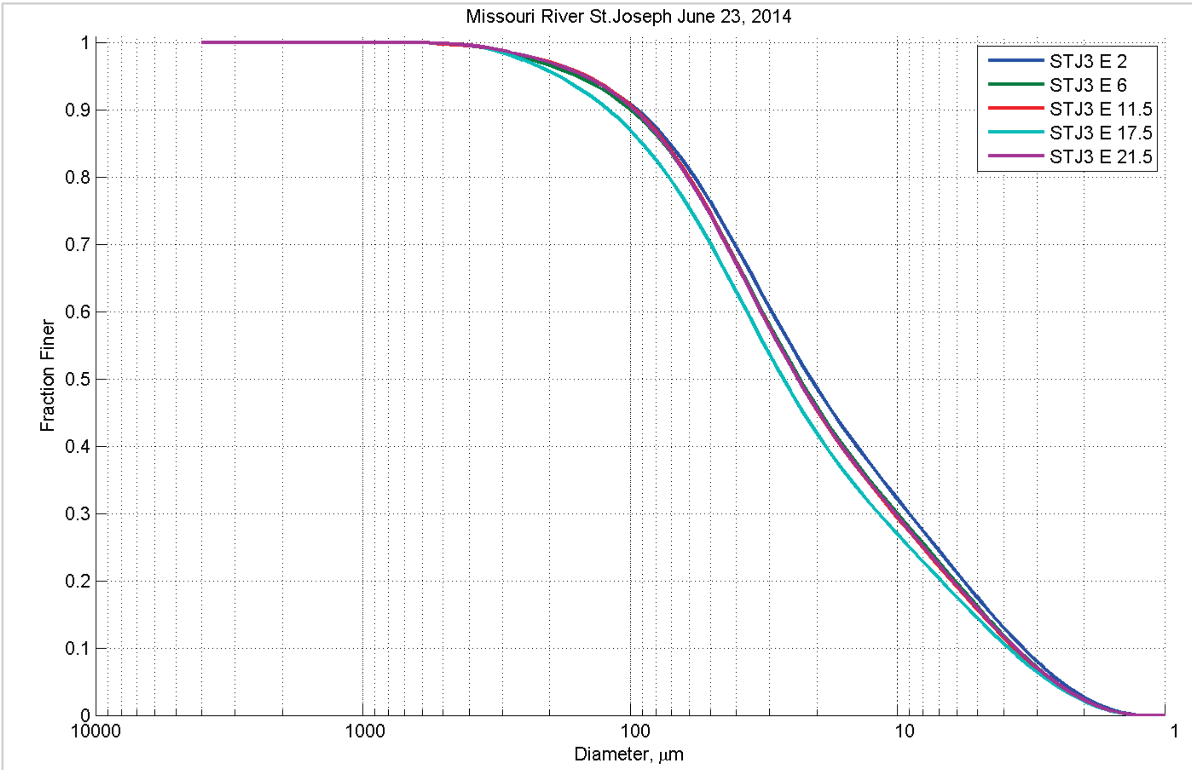

Suspended sediment concentration was also measured from the collected samples. Table 41 to Table 43 present the concentration values for each data collection date. At location STJ1A at a depth of 16.5 ft, bad data were obtained, so no value is recorded. The erroneous value was not used in the ADCP calibration for station A. Suspended sediment concentration profiles were created using the measured data, presented in Figure 139 to Figure 141. See Appendix IV-f for more details about the measured data.

Table 41. Suspended sediment concentration at St. Joseph, MO – April 27, 2014.

Station	Depth (ft)	Concentration (mg/L)
STJ 1A	2	122.33
STJ 1A	4.5	118.28
STJ 1A	9	217.39
STJ 1A	13.5	243.17
STJ 1A	16.5	No data
Total depth	17.2	(Bottom)
STJ 1B	2	161.47
STJ 1B	5	213.78
STJ 1B	9.5	300.98
STJ 1B	12.5	291.32
Total depth	14.5	(Bottom)
STJ 1C	2	127.77
STJ 1C	5	146.00
STJ 1C	9.5	220.81
STJ 1C	12.5	238.55
Total depth	14.9	(Bottom)
STJ 1D	2	90.99
STJ 1D	5	91.72
STJ 1D	9	110.32
STJ 1D	11.5	91.94
Total depth	13.2	(Bottom)
STJ 1E	2	93.50
STJ 1E	4	81.36
STJ 1E	6.5	77.57
Total depth	9.4	(Bottom)

Table 42. Suspended sediment concentration at St. Joseph, MO – June 8, 2014.

Station	Depth (ft)	Concentration (mg/L)
STJ2A	2	4,618.37
STJ2A	7.5	4,854.29
STJ2A	15	4,926.67
STJ2A	22.5	5,088.29
STJ2A	28.5	4,944.87
Total depth	29.7	(Bottom)
STJ2B	2	4,817.38
STJ2B	6.5	4,970.27
STJ2B	13	5,024.68
STJ2B	19.5	5,191.83
STJ2B	24.5	5,356.00
Total depth	26.3	(Bottom)
STJ2C	2	4,600.00
STJ2C	6.5	4,795.79
STJ2C	12.5	5,012.12
STJ2C	19	4,898.59
STJ2C	23.5	5,596.03
Total depth	24.2	(Bottom)
STJ2D	2	4,391.29
STJ2D	5.5	4,385.38
STJ2D	11	4,571.65
STJ2D	16.5	4,659.00
STJ2D	20.5	5,409.49
Total depth	22.3	(Bottom)
STJ2E	2	4,161.96
STJ2E	5.5	4,179.60
STJ2E	10.5	4,240.37
STJ2E	16	4,247.06
STJ2E	19.5	4,388.28
Total depth	21.4	(Bottom)

Table 43. Suspended Sediment Concentration at St. Joseph, MO – June 24, 2014.

Station	Depth (ft)	Concentration (mg/L)
STJ 3A	2	1,073.40
STJ 3A	8	1,074.72
STJ 3A	15.5	1,157.81
STJ 3A	23.5	1,262.70
STJ 3A	29.5	1,558.99
Total depth	31.3	(Bottom)
STJ 3B	2	1,086.42
STJ 3B	7	1,285.58
STJ 3B	14	1,367.96
STJ 3B	21	1,606.20
STJ 3B	26.5	1,728.98
Total depth	28.8	(Bottom)
STJ 3C	2	1,112.47
STJ 3C	7	1,154.75
STJ 3C	13.5	1,158.57
STJ 3C	20.5	1,193.09
STJ 3C	25.5	1,550.77
Total depth	27.1	(Bottom)
STJ 3D	2	1,064.42
STJ 3D	6	1,141.49
STJ 3D	11.5	1,158.57
STJ 3D	17.5	1,333.86
STJ 3D	21.5	1,253.33
Total depth	24.2	(Bottom)
STJ 3E	2	1,074.07
STJ 3E	6	1,125.24
STJ 3E	11.5	1,114.83
STJ 3E	17.5	1,129.44
STJ 3E	21.5	1,240.51
Total depth	24.3	(Bottom)

Figure 139. Suspended sediment concentration at St. Joseph, MO – April 27, 2014.

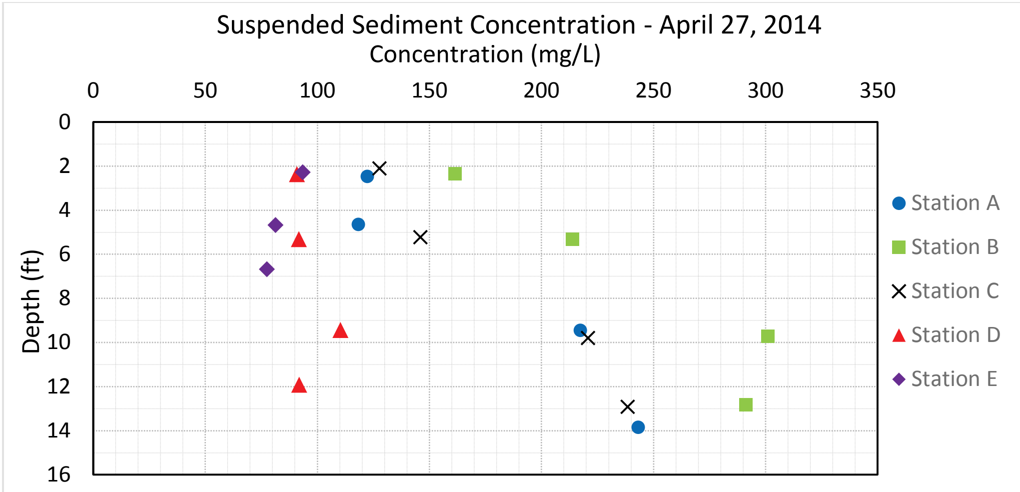

Figure 140. Suspended sediment concentration at St. Joseph, MO– June 8, 2014.

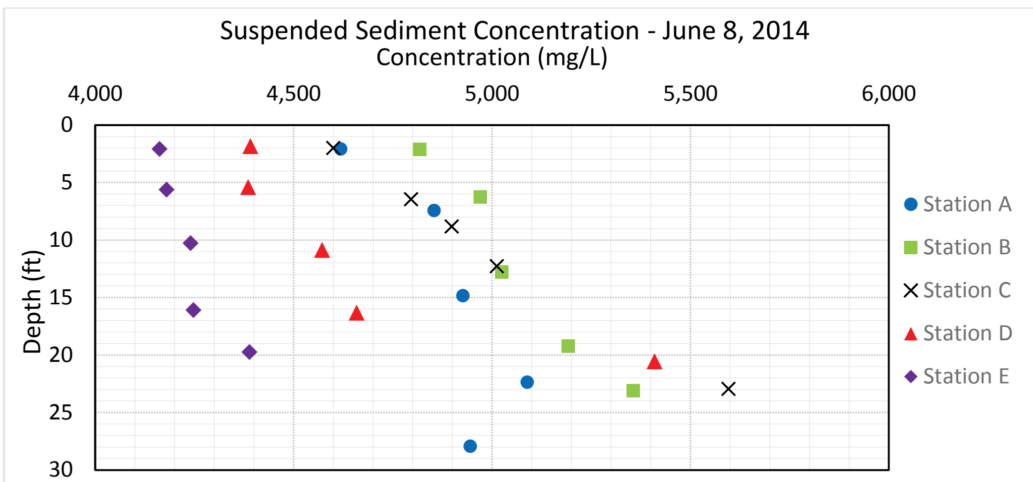

Figure 141. Suspended sediment concentration at St. Joseph, MO – June 24, 2014.

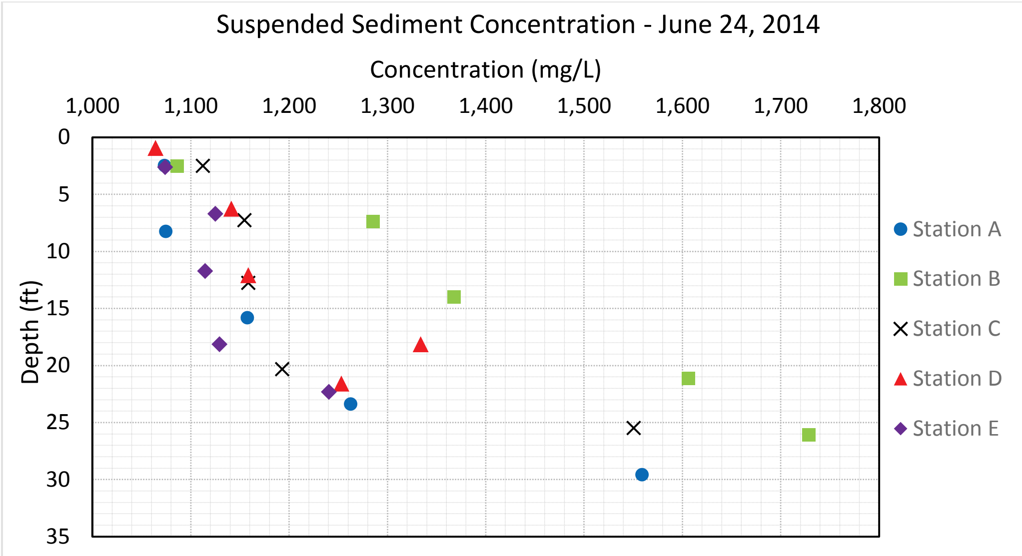

The suspended sediment concentration data were used to calibrate the ADCP acoustic backscatter and develop suspended sediment concentration profiles across the channel. Figure 142 to Figure 144 show the suspended sediment concentration profiles for the first left-to-right ADCP pass for each data collection date. To see the other profiles, see Appendix IV-f.

Figure 142. Suspended sediment concentration profile at St. Joseph, MO - April 27, 2014.

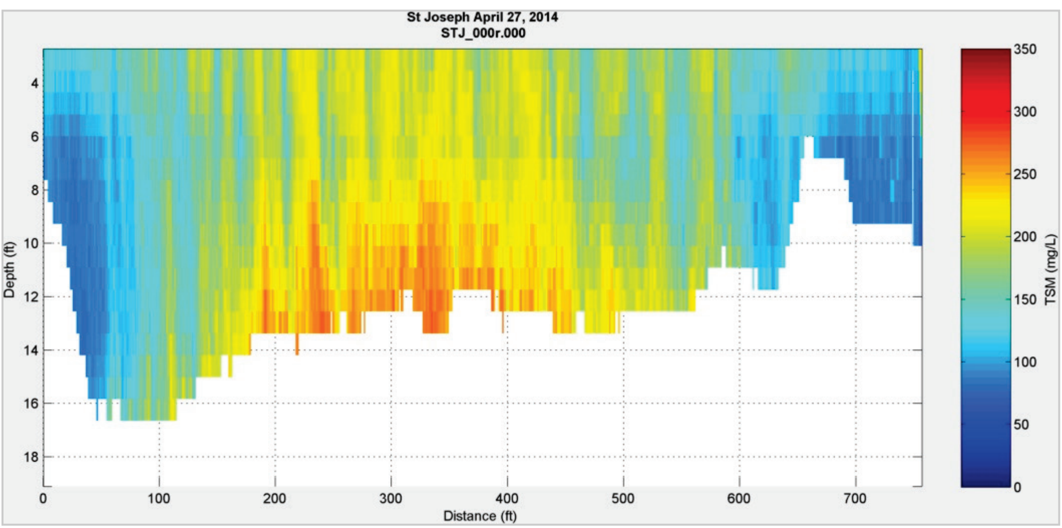

Figure 143. Suspended sediment concentration profile at St. Joseph, MO – June 8, 2014.

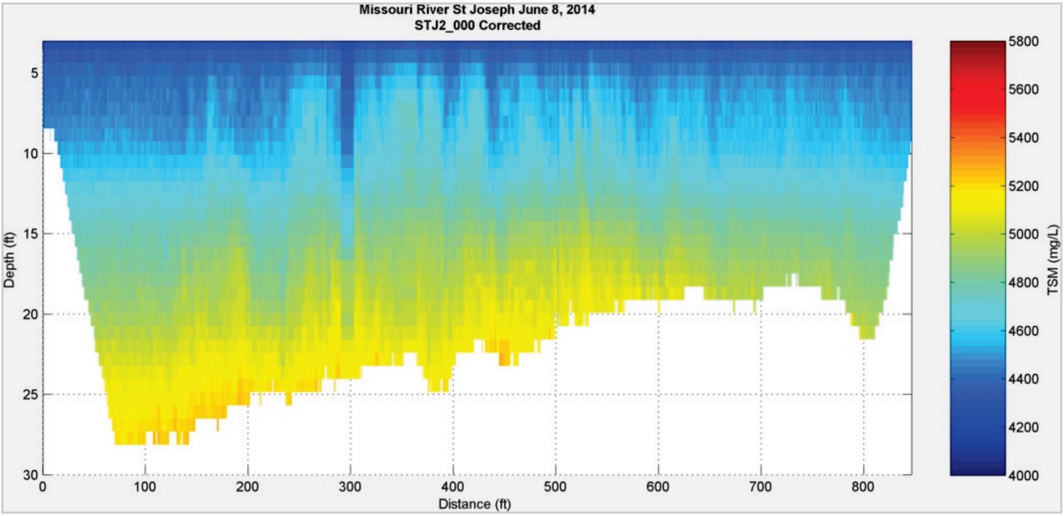

Figure 144. Suspended sediment concentration profile at St. Joseph, MO – June 24, 2014.

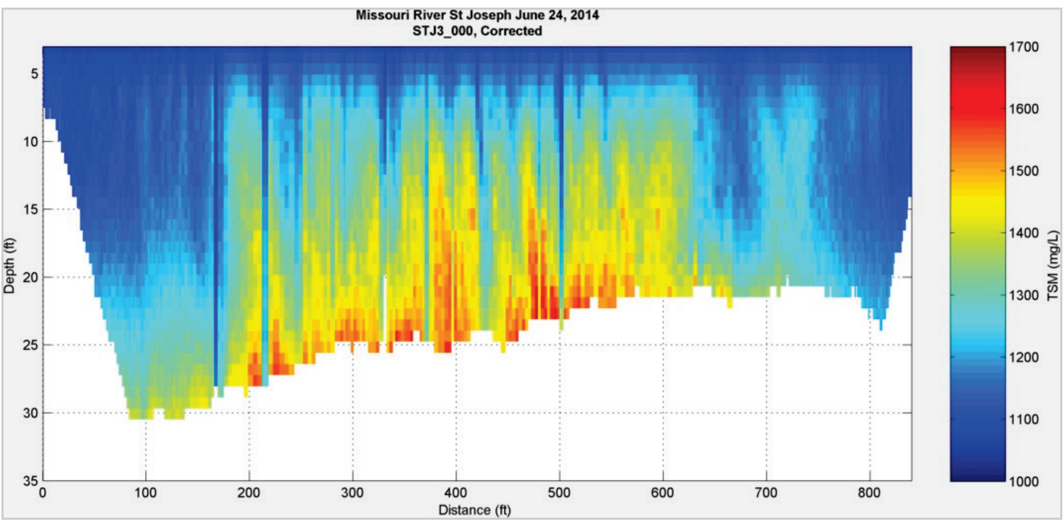

The suspended sediment concentration cross-section profiles obtained from the ADCP measurements were combined with the flow discharges, also obtained from the ADCP, to obtain the suspended sediment transport load, in tons per day. The method used for this study is explained in Heath et al. (2015, 13–14). The suspended sediment load can be divided classifying the suspended material by size and soil type. Table 44 presents the suspended sediment transport load, according to both classifications, for the first data collection date April 27, 2014. Table 45 and Table 46 present the same information for the second and third data collection dates, respectively. In all three tables, the categories under the Soil Type Classification were determined as follows: Clay Flux groups the size fractions 0.0001 to 0.0004 mm, Silt Flux 0.0004 to 0.0625 mm, and Sand Flux 0.0625 to 2.00 mm.

Table 44. Suspended sediment load distributed by grain size and soil type – April 27, 2014.

Classification System	Category	Sediment Flux (tons/day)
Total load		16,431.81
Sediment size classification	0.001 - 0.004 mm	850.05
	0.004 - 0.008 mm	1,401.17
	0.008 - 0.016 mm	1,977.07
	0.016 - 0.031 mm	2,491.95
	0.031 - 0.063 mm	2,243.52
	0.063 - 0.125 mm	1,289.09
	0.125 - 0.250 mm	2,746.92
	0.250 - 0.500 mm	2,731.42
	0.500 - 1.00 mm	635.82
	1.00 - 2.00 mm	64.80
Soil type classification	Clay	850.05
	Silt	8,113.71
	Sand	7,468.05

Table 45. Suspended sediment load distributed by grain size and soil type – June 8, 2014.

Classification System	Category	Sediment Flux (tons/day)
Total load		1,262,207.10
Sediment size Classification	0.001 - 0.004 mm	136,061.36
	0.004 - 0.008 mm	181,110.30
	0.008 - 0.016 mm	258,419.45
	0.016 - 0.031 mm	318,010.28
	0.031 - 0.063 mm	252,526.71
	0.063 - 0.125 mm	73,422.52
	0.125 - 0.250 mm	23,053.37
	0.250 - 0.500 mm	16,556.37
	0.500 - 1.00 mm	3,046.75
	1.00 - 2.00 mm	0.00
Soil type classification	Clay	136,061.36
	Silt	1,010,066.74
	Sand	116,079.01

Table 46. Suspended sediment load distributed by grain size and soil type – June 24, 2014.

Classification System	Category	Sediment Flux (tons/day)
Total load		381,224.42
Sediment size classification	0.001 - 0.004 mm	37,221.72
	0.004 - 0.008 mm	45,155.52
	0.008 - 0.016 mm	48,820.31
	0.016 - 0.031 mm	60,151.21
	0.031 - 0.063 mm	73,145.07
	0.063 - 0.125 mm	47,934.74
	0.125 - 0.250 mm	37,343.18
	0.250 - 0.500 mm	27,015.52
	0.500 - 1.00 mm	4,435.07
	1.00 - 2.00 mm	2.11
Soil type classification	Clay	37,221.72
	Silt	227,272.11
	Sand	116,730.62

6.7 Bed load transport

The ISSDOTv2 method was used for computing the bed-load transport. Table 47 shows the values obtained for the bed load, as well as the other sediment quantities determined from the suspended sediment samples at the St. Joseph site. It provides a breakdown of the various measured sediment transport components, based on sediment size classification.

Table 47. Bed-load transport values from St. Joseph, MO.

Data collection date	27-Apr-14	8-Jun-14	24-Jun-14
Flow (cfs)	36,857	97,663	113,735
Bed load (tons/day)	2,019	6,564	8,512
Suspended BML (tons/day)	7,468	116,079	116,731
Total BML (tons/day)	9,487	122,643	125,243
Bed load fraction (%)	21.3%	5.4%	6.8%
Wash load (tons/day)	8,964	1,146,128	264,494
Total load	18,451	1,268,771	389,737

In Table 47, *bed load* is defined as the bed material moving at the bottom of the river in bed-forms; *suspended BML* refers to the suspended material with grain size higher than 0.063 mm; *total BML* is the sum of bed load and suspended BML; *bed load fraction* is the percentage of the total bed

material moving as bed load; *wash load* is fine sediments that never settle in the bed, with grain size of 0.063 or less; and *total load* combines the quantity of total BML and wash load.

A bed-load rating curve was prepared for this site by plotting the bed-load transport in tons per day versus the river flowrate. This graph is shown in Figure 145. In this case, trip 1 was a much lower flow than trips 2 and 3, as shown in Table 47. Accordingly, the bed-load transport for the last two trips is noticeably higher. The bed-load fraction also falls off considerably since more BML is going into suspension at the higher flows.

Figure 145. Bed-load rating curve for St. Joseph, MO.

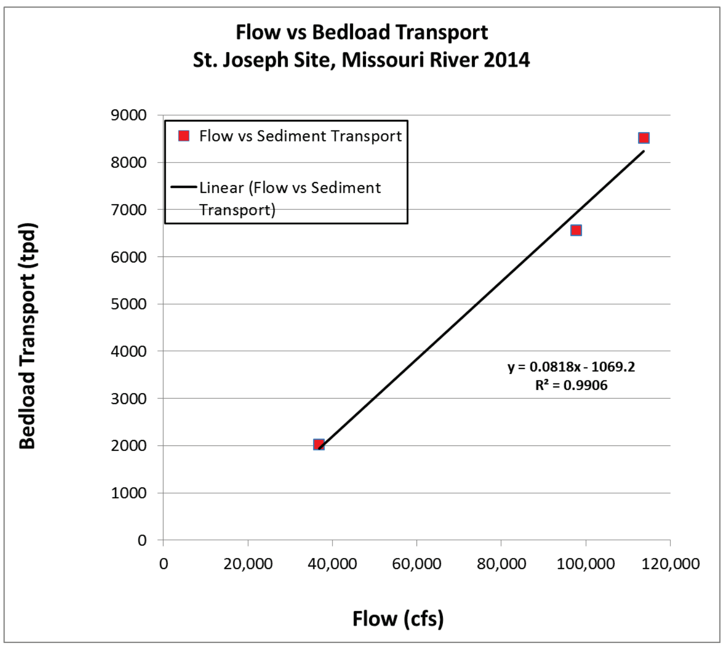

Bed-load transport values were also computed for this site using two analytic transport functions. One is the MPM formula, and the other is the Einstein formula. They were computed for each swath of bathymetric data. For instance, Figure 146 shows the bathymetry of this site with the six swath numbers (S1 to S6) labeled on it, indicating the lateral position where each swath was located. The hydraulic and sediment parameters obtained in the field data collection effort discussed before were extracted for each of these swaths.

Figure 146. Bathymetry for Missouri River at St. Joseph showing swath locations.

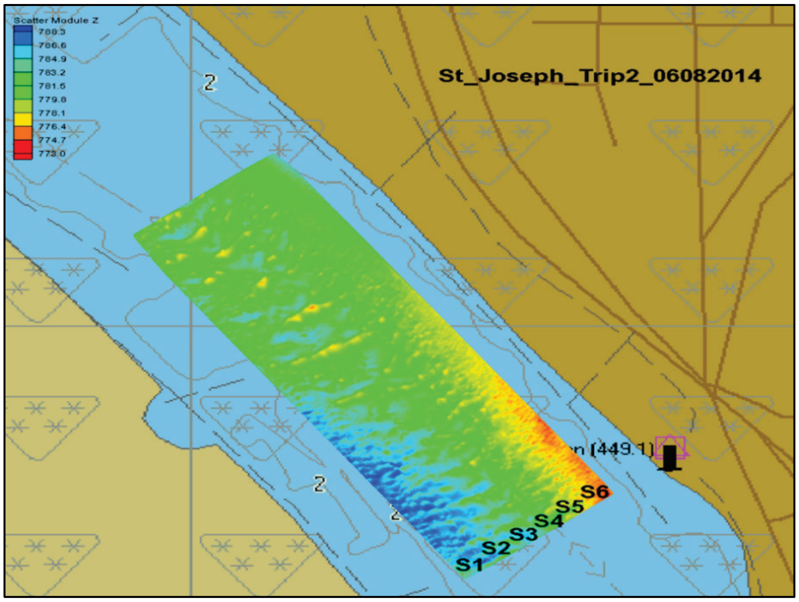

Flow, average velocity, and water depth were obtained from the ADCP data by a separate program written for that specific purpose. Water slope and water temperature were obtained from each appropriate data appendix. Bed sediment gradations used were selected based on their proximity to a given swath. The SAM Hydraulic Design Package for Channels program was then used with these data to compute the bed-load values for each swath. This software package has provisions for entering hydraulic and sediment input parameters and can then compute bed-load transport values for several commonly used transport functions.

The results are plotted in Figure 147 to Figure 149 and show how the transport function values compare to the ISSDOTv2 measured values. They also show the lateral variability across the measured section from the left side to the right side of the channel.

Figure 147. Bed-load transport at St. Joseph, MO – April 27, 2014: ISSDOTv2 values compared to transport function computed values.

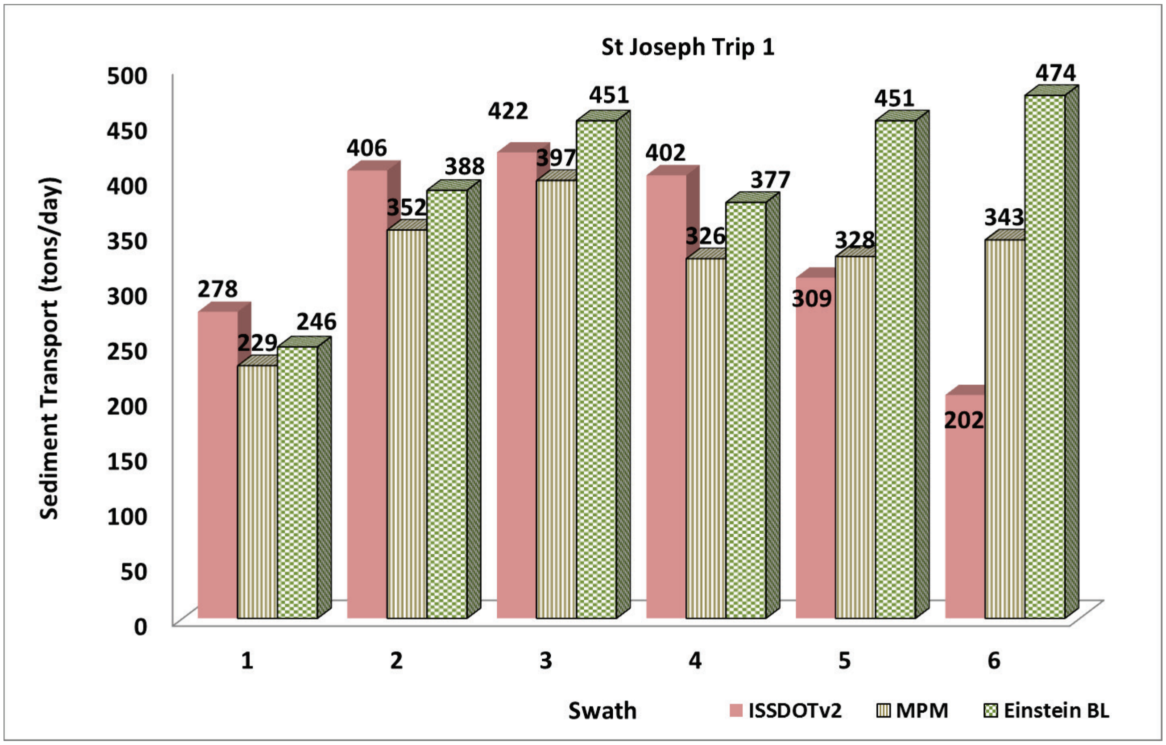

Figure 148. Bed-load transport at St. Joseph, MO – June 8, 2014: ISSDOTv2 values compared to transport function computed values.

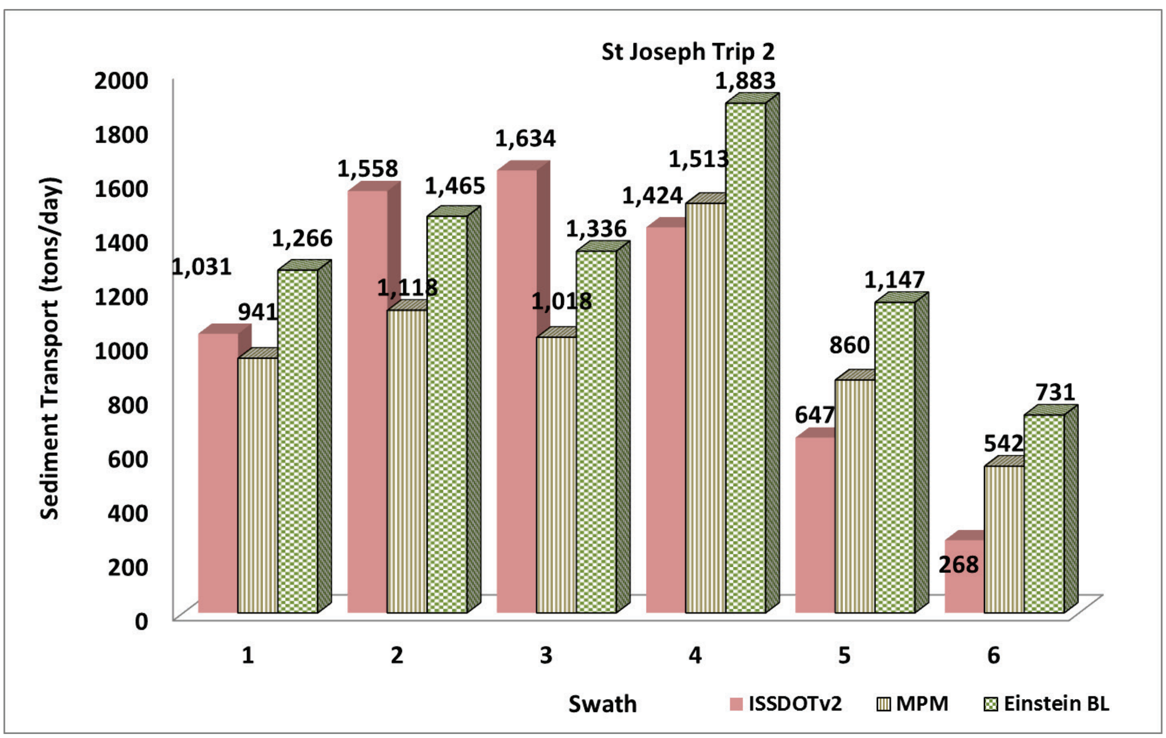

Figure 149. Bed-load transport at St. Joseph, MO – June 24, 2014: ISSDOTv2 values compared to transport function computed values.

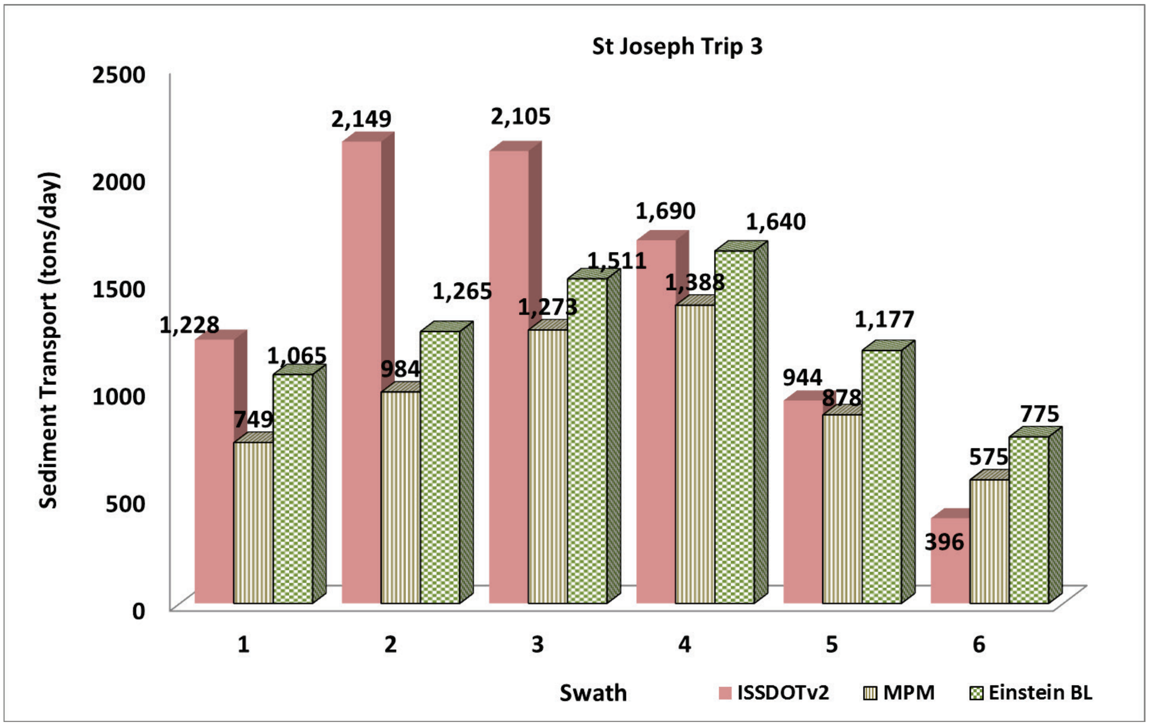

7 Site 5: Kansas City, Missouri

Multi-beam surveys, ADCP flow and velocity measurements, bed and suspended material sampling and testing, and water temperature, water surface elevation, and slope measurements were performed during each data collection date at Kansas City, MO. The measuring area is shown on Figure 150 as the green polygon. The approximate location of the USGS gage station near the data collection site is also shown as the blue pin. This location might not be accurate in the figure. Coordinates for the gage site as given in the USGS web site are listed in Table 3. The red line indicates the cross section where ADCP measurements were conducted and suspended and bed load material samples were collected. The bank-to-bank width of the river at this location is estimated to range between 805 and 950 ft; the length of the study area was approximately 2,900 ft. The data collection dates for Kansas City were April 26, 2014; June 9, 2014; and June 24, 2014.

Figure 150. Kansas City data collection site.

7.1 ADCP flow and velocity

The velocity and discharge for each data collection date, and site, were measured using an ADCP. Table 48 presents the cross-section average flow (ft^3/s), area (ft^2), and average velocity (ft/s) for each date, calculated from the measured data. See Appendix V-a for the measured data.

Table 48. Total flow, area, and average velocity on the given dates at Kansas City, MO.

Date	Total Flow, Q (ft^3/s)	Total Area, A (ft^2)	Velocity Q/A (ft/s)
April 26, 2014	40,624	12,502	3.25
June 9, 2014	97,068	18,024	5.39
June 24, 2014	116,525	21,315	5.47

Real-time vertical profiles of instantaneous velocities are also obtained from the ADCP measurements. Figure 151 to Figure 153 present the velocity magnitude, before the multi-beam measurements, from left to right. In the figures, the velocity magnitude is quantified by the range of colors shown on the right side of each figure, where the higher velocities are denoted by red and the lower velocities by blue. The velocity profiles for after the multi-beam measurements are available at Appendix V-a.

Figure 151. Velocity magnitude at Kansas City, MO – April 26, 2014, 17:19:53.

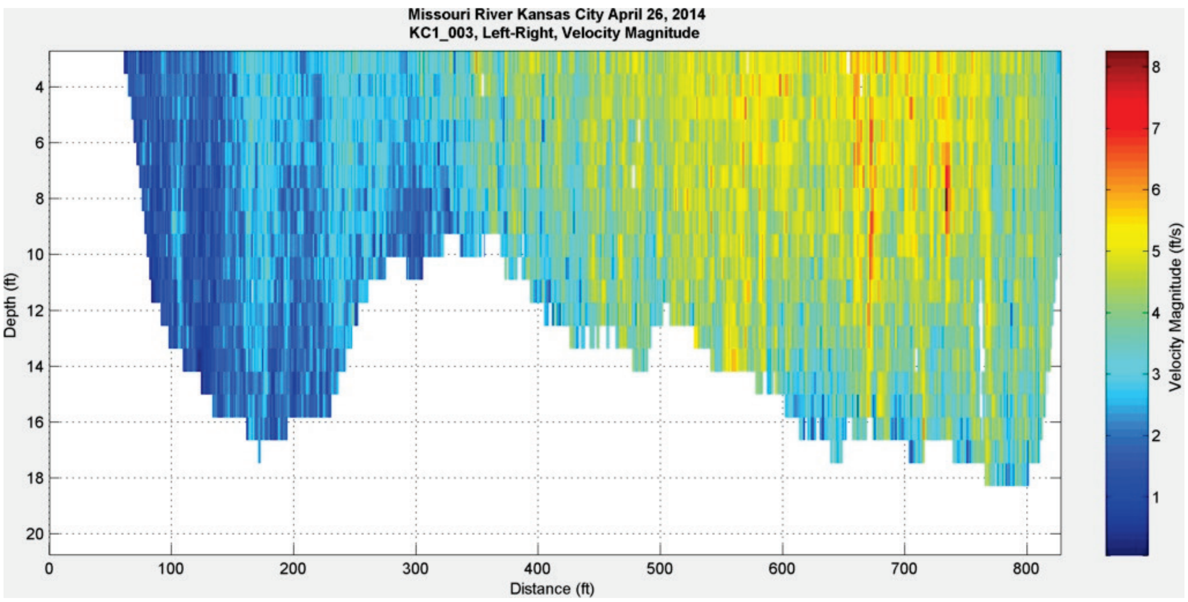

Figure 152. Velocity magnitude at Kansas City, MO – June 9, 2014, 17:21:41.

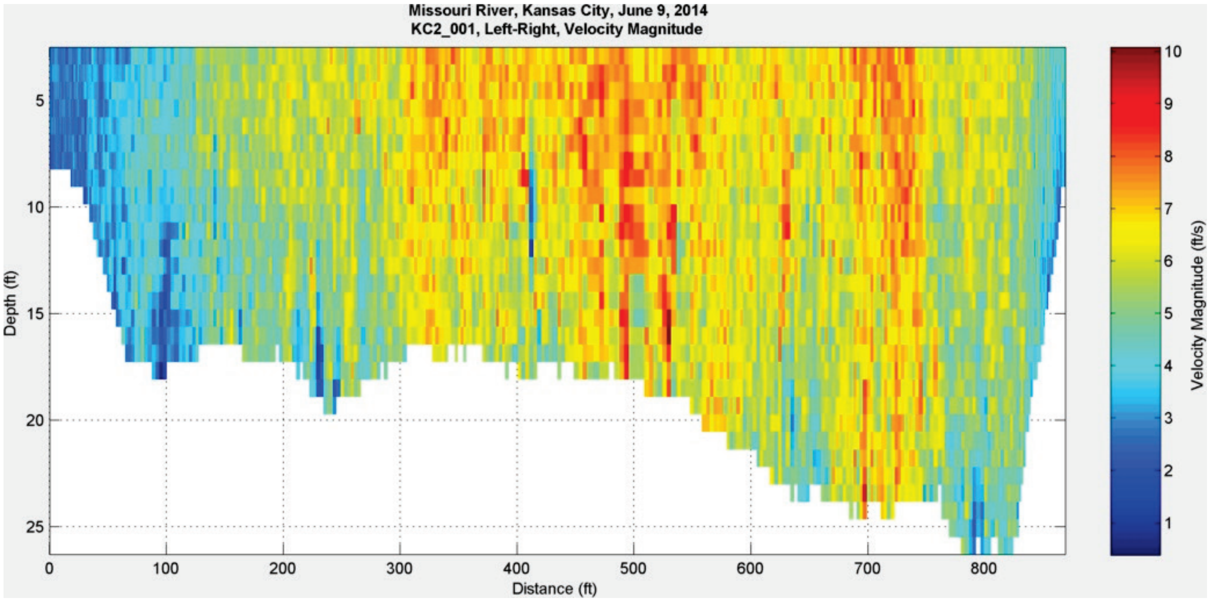

Figure 153. Velocity magnitude at Kansas City, MO – June 24, 2014, 18:38:11.

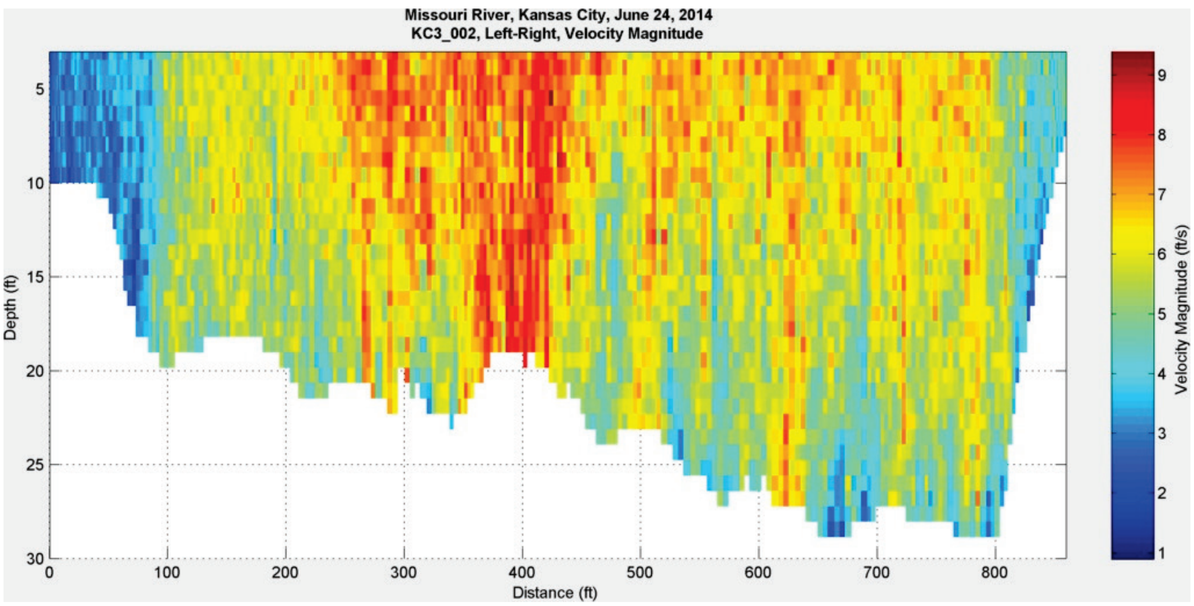

7.2 Water surface elevation and slope

Water surface elevation measurements were taken upstream and downstream of the multi-beam survey area. Figure 154 shows the upstream elevations, at distance zero, connected to the downstream elevations, at a distance of 2,900 ft, for each data collection date. Table 49 presents the slope values for the Kansas City, MO, location for the three dates. The measured data are available at Appendix V-b.

Figure 154. Water surface elevation at Kansas City, MO – from upstream to downstream.

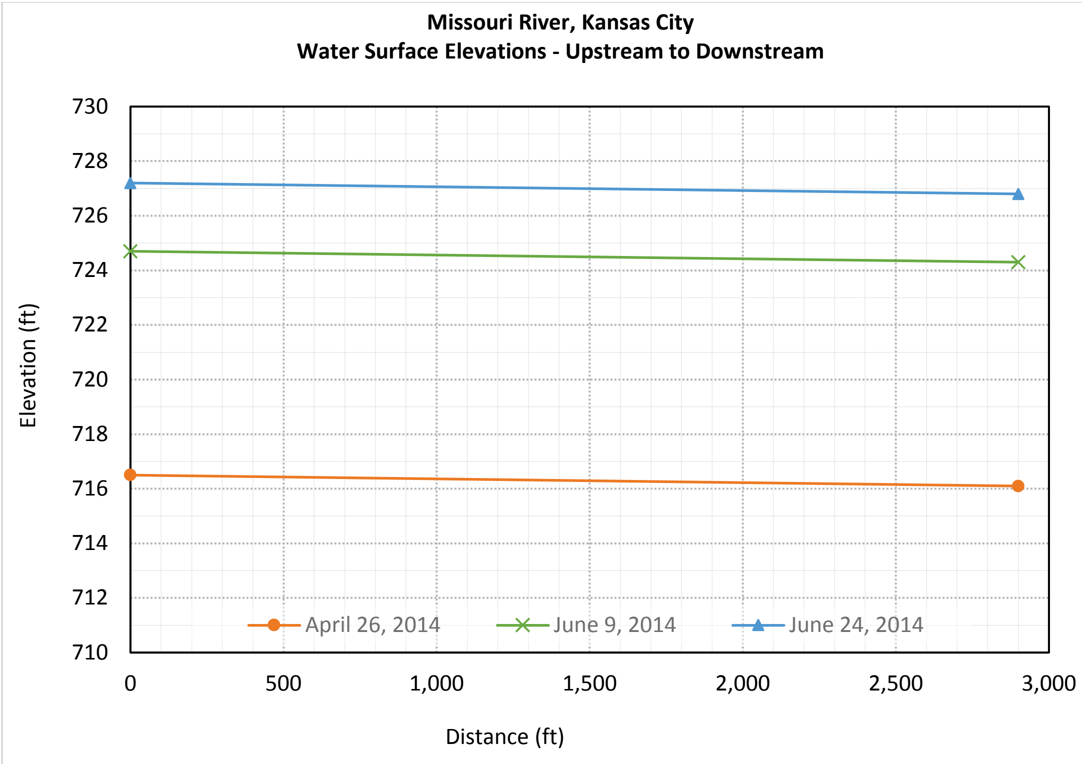

Table 49. Water surface slopes at Kansas City, MO.

Date	Water Surface Slope (%)
April 26, 2014	0.00014
June 9, 2014	0.00014
June 24, 2014	0.00014

7.3 Water temperature

Table 50 presents the average temperature for each date (see Appendix V-g for the measured values).

Table 50. Water temperature at Kansas City, MO.

Date	Temperature (F)
April 26, 2014	60
June 9, 2014	72.3
June 24, 2014	77.7

7.4 Multi-beam surveys

The initial multi-beam survey performed at Kansas City, MO. included the full extent of the channel from bank to bank, as shown in Figure 155 where the dark blue areas are deeper and the red areas are shallower. This survey is used to determine the location of the sand waves throughout the study area and to then decide where to run the ISSDOTv2 swaths according to the location of the active sand transport portion of the channel. The selected area with swath lines and numbers displayed in red is shown in Figure 156. This shows the actual area that was used for the ISSDOTv2 bed-load computations. The length of the multi-beam swaths is approximately 2,900 ft for all three data collection dates.

Figure 155. Multi-beam survey extent at Kansas City, MO – April 26, 2014.

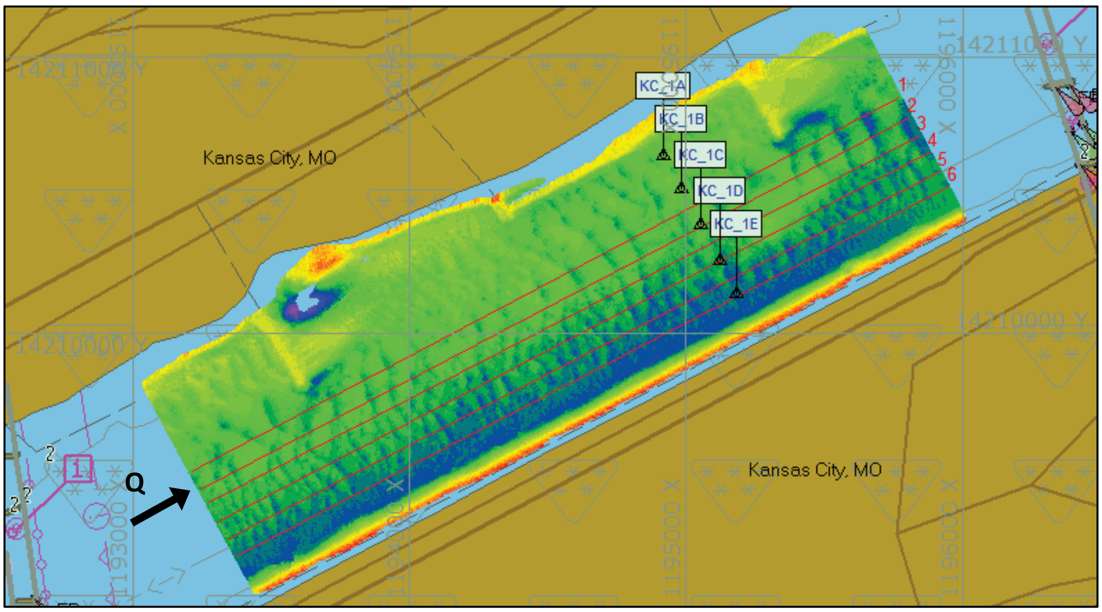

Figure 156. Multi-beam survey extent at Kansas City, MO – June 9 and June 24, 2014.

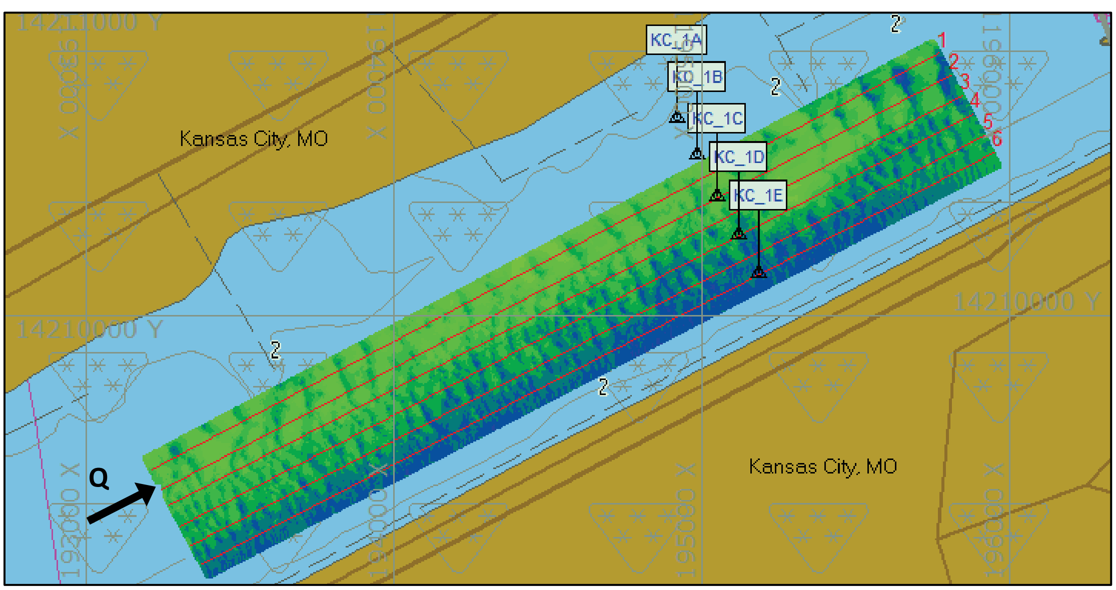

7.5 Bed material samples

Five sediment sample stations were positioned equidistant from each other along the cross section, as presented on Figure 157, which is the same location at which the suspended sediment samples and the ADCP velocity data were obtained. The first station, Station A, was positioned on the left descending bank, and the last station, Station E, on the right descending bank. Table 51 provides the locations of sample stations according to NAD83. See Appendix V-c for the coordinates using the UTM Grid System.

Table 51. Sediment sample stations NAD83 coordinates at Kansas City, MO.

Station	NAD83 Latitude	NAD83 Longitude
KC A	39° 07' 16.7233" N	94° 34' 14.8328" W
KC B	39° 07' 15.5584" N	94° 34' 14.0" W
KC C	39° 07' 14.2589" N	94° 34' 13.1015" W
KC D	39° 07' 13.0" N	94° 34' 12.1859" W
KC E	39° 07' 11.815" N	94° 34' 11.3543" W

Figure 157. Sediment sample stations at the Missouri River – Kansas City, MO.

The grain size distribution for the five bed material samples of the first collection date, April 26, 2014, is provided at Figure 158. Figure 159 and Figure 160 present the gradation analysis for the second and third collected samples, respectively. The measured data are available in Appendix V-d.

Figure 158. Bed material grain size distribution for Kansas City, MO – April 26, 2014.

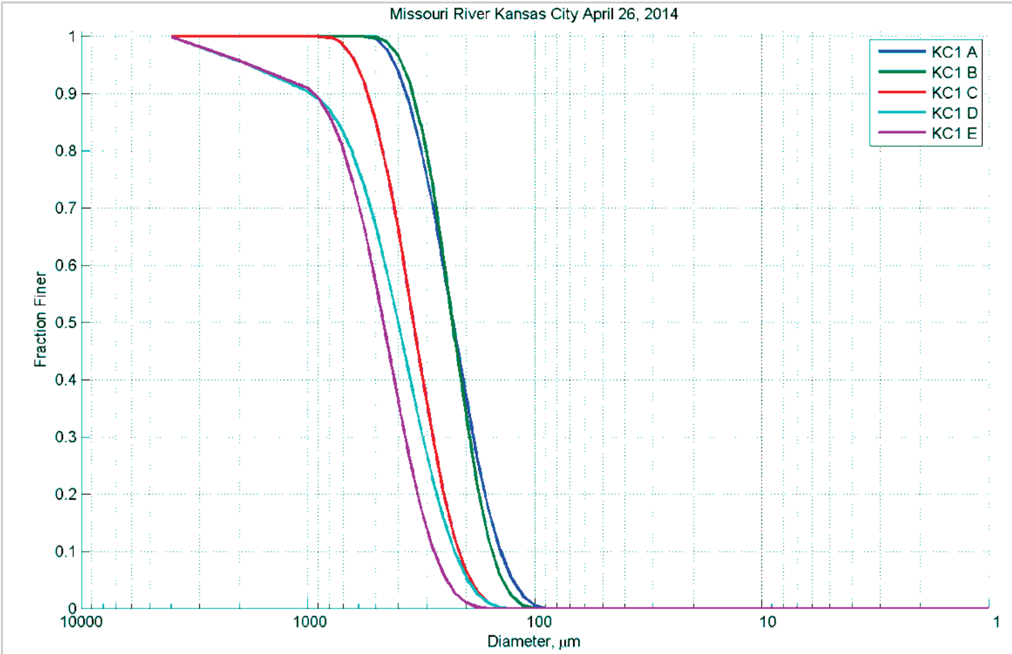

Figure 159. Bed material grain size distribution for Kansas City, MO – June 9, 2014.

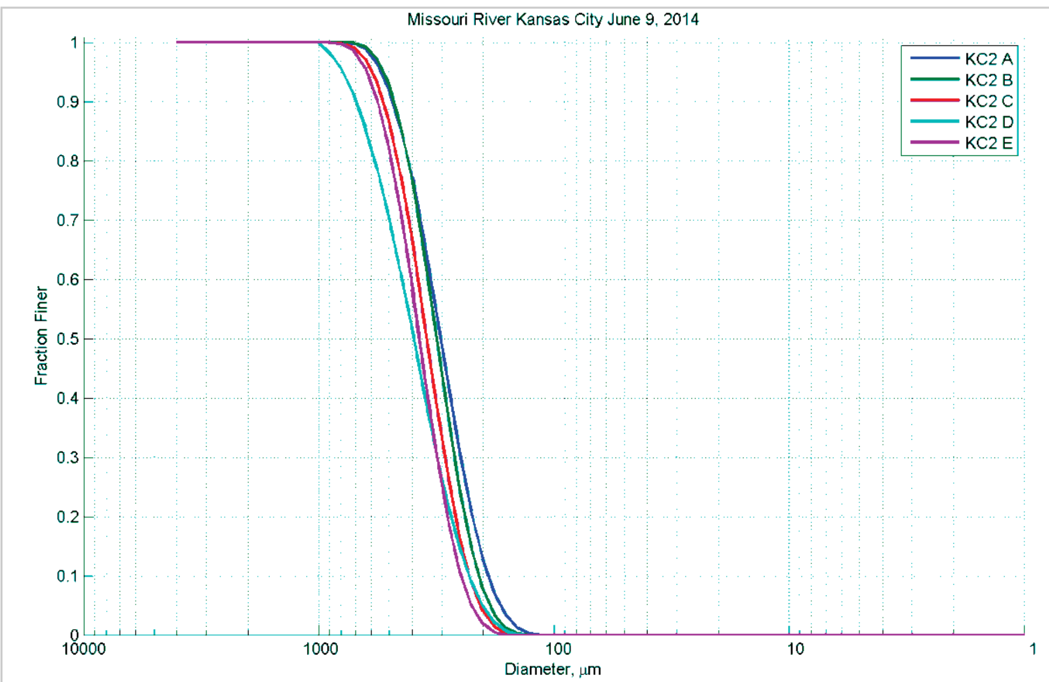

Figure 160. Bed material grain size distribution for Kansas City, MO – June 24, 2014.

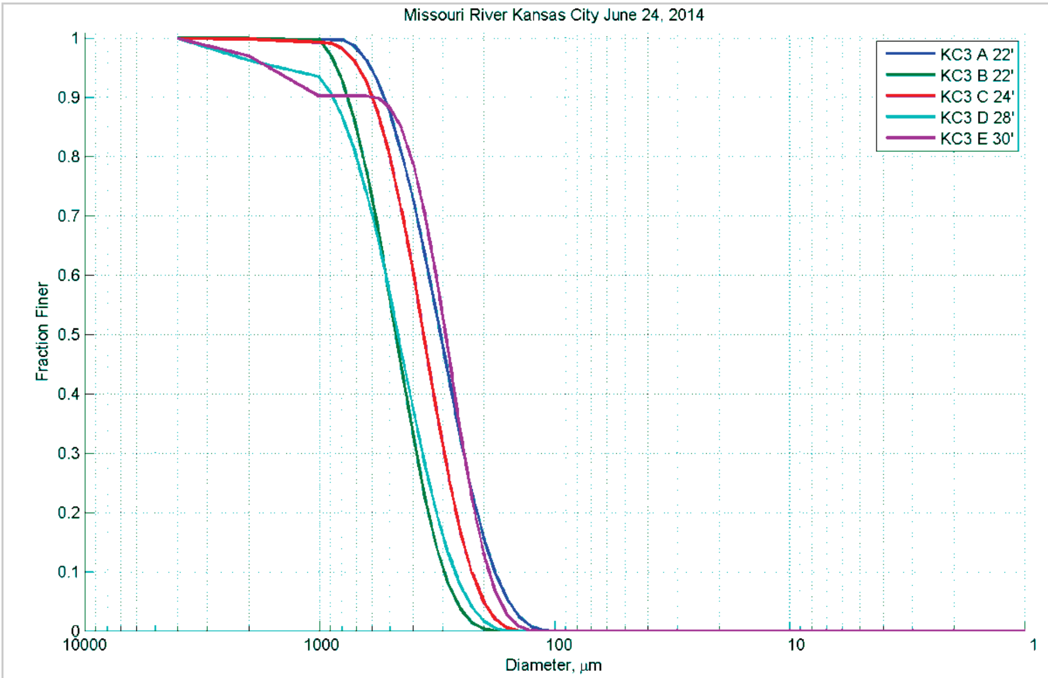

7.6 Suspended sediment

Suspended sediment samples at different depths in a column were taken at the five stations shown in Figure 157, for each data collection date. A particle size analysis was conducted for the samples of each station and date. The results are presented in this report as Figure 161 to Figure 175, and the measured data are available at Appendix V-e.

Particle size distribution for the first data collection date, April 26, 2014, is shown in Figure 161 to Figure 165. It is organized starting from the station closer to the left descending bank, Station A, to the station closer to the right descending bank, Station E.

Figure 161. Particle size distribution at different depths (feet) in Station A - April 26, 2014.

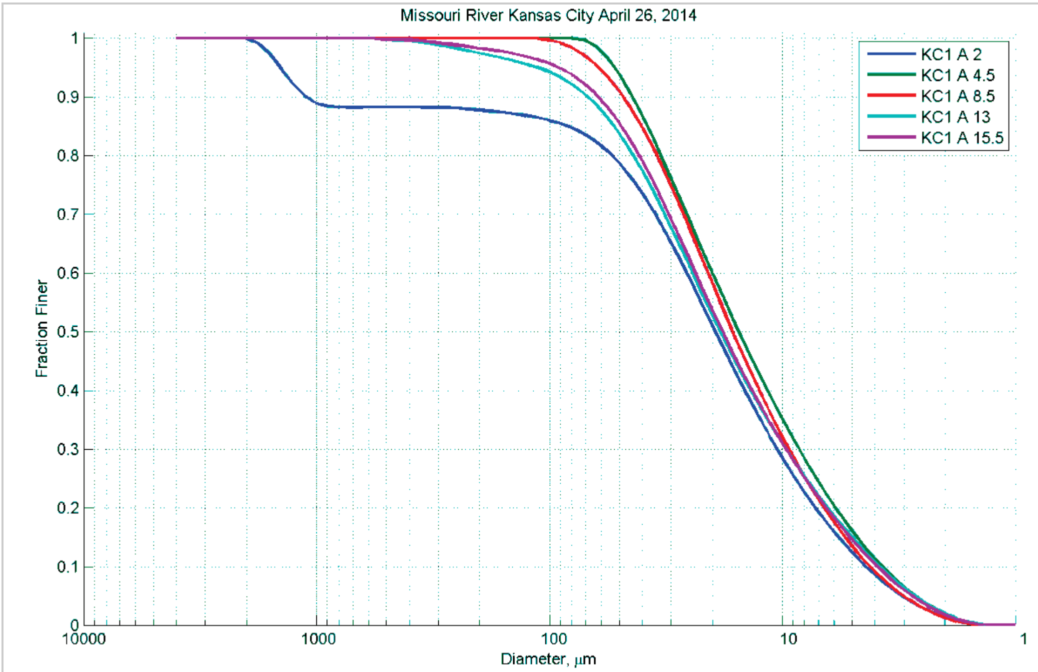

Figure 162. Particle size distribution at different depths (feet) in Station B - April 26, 2014.

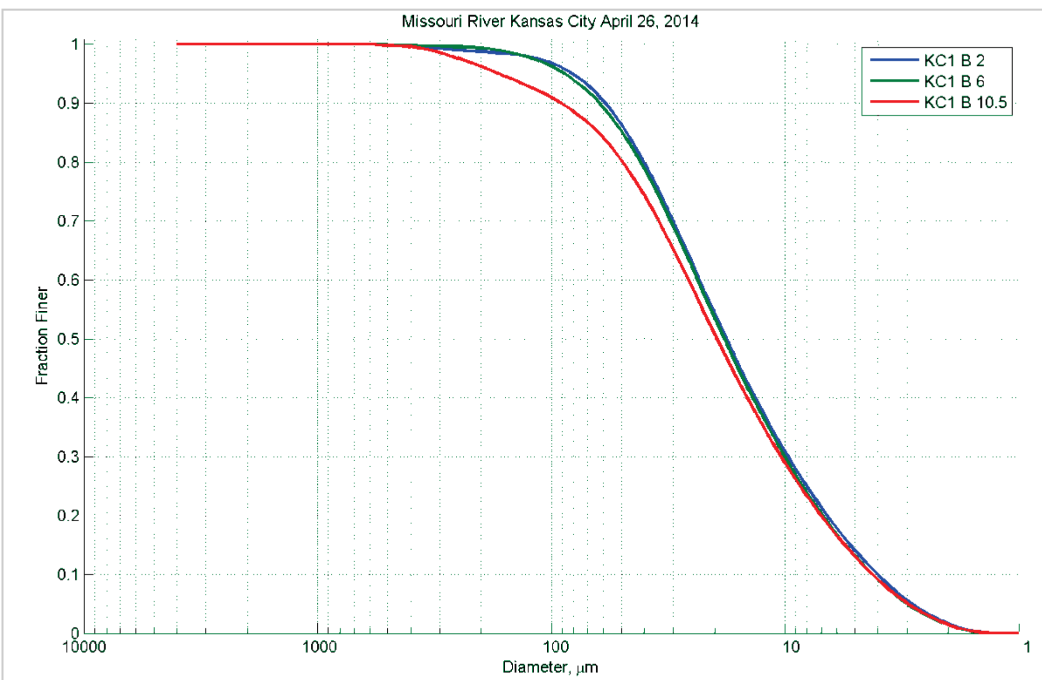

Figure 163. Particle size distribution at different depths (feet) in Station C - April 26, 2014.

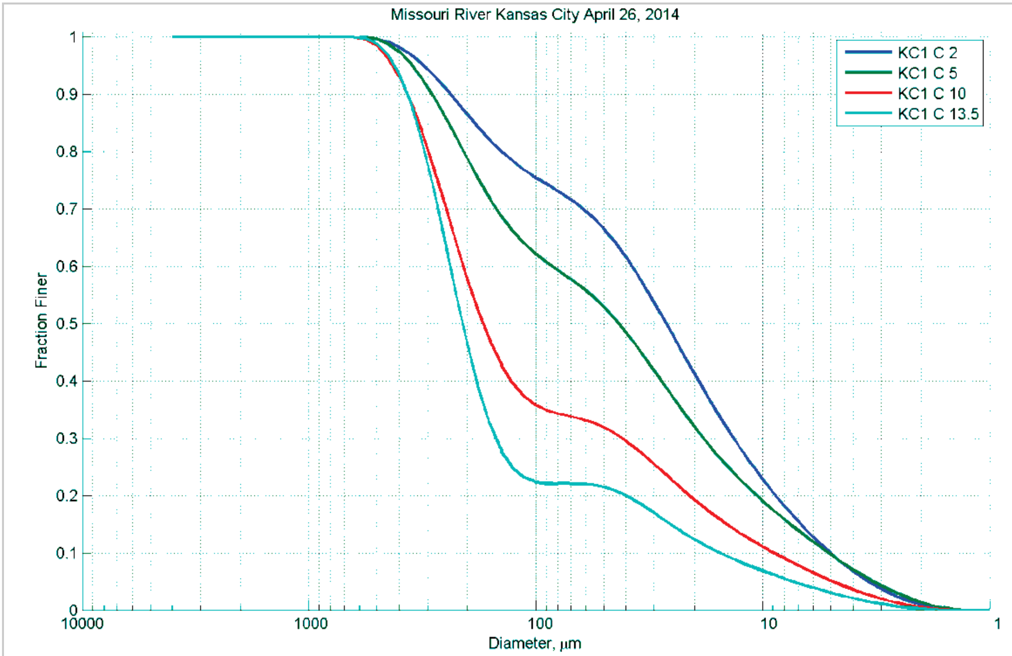

Figure 164. Particle size distribution at different depths (feet) in Station D - April 26, 2014.

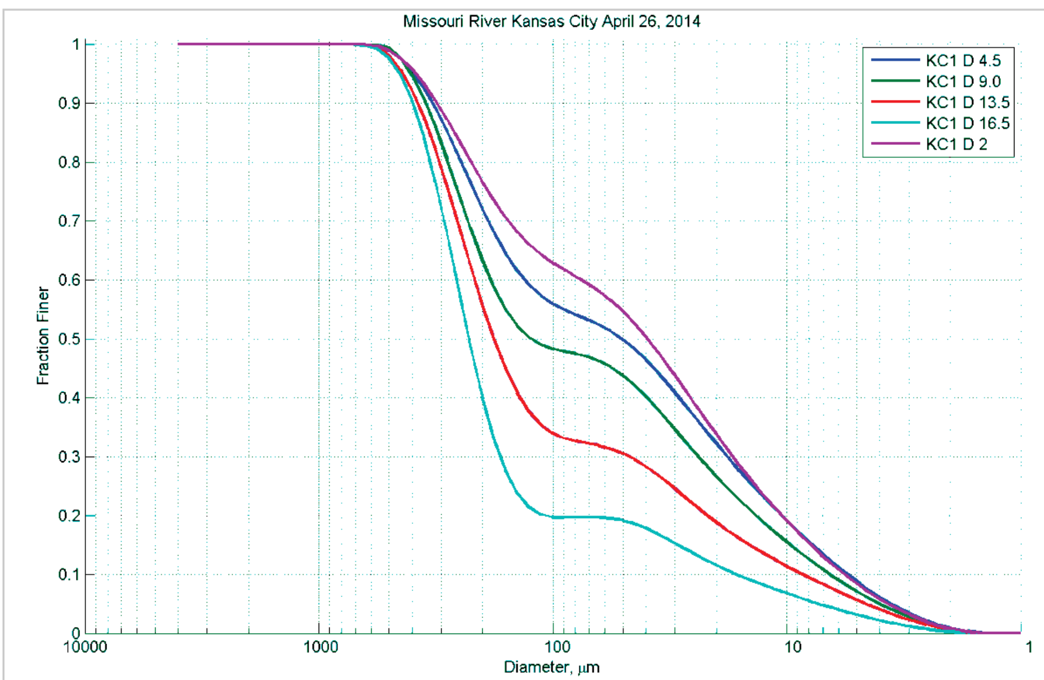

Figure 165. Particle size distribution at different depths (feet) in Station E - April 26, 2014.

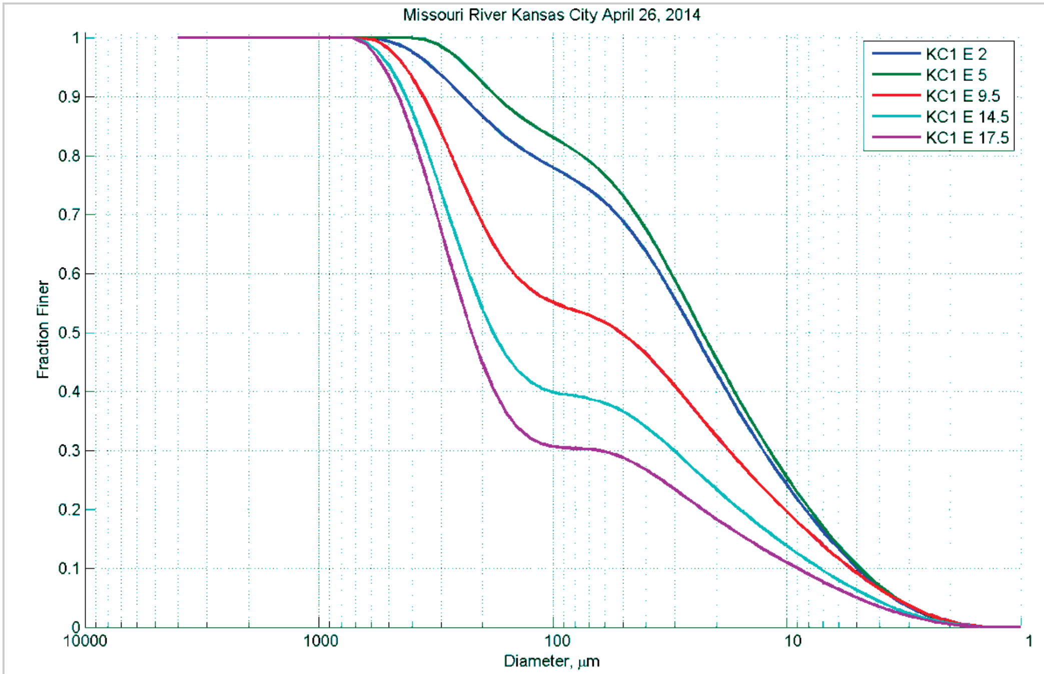

Particle size distribution for the second data collection date, June 9, 2014, is shown in Figure 166 to Figure 170.

Figure 166. Particle size distribution at different depths (feet) in Station A – June 9, 2014.

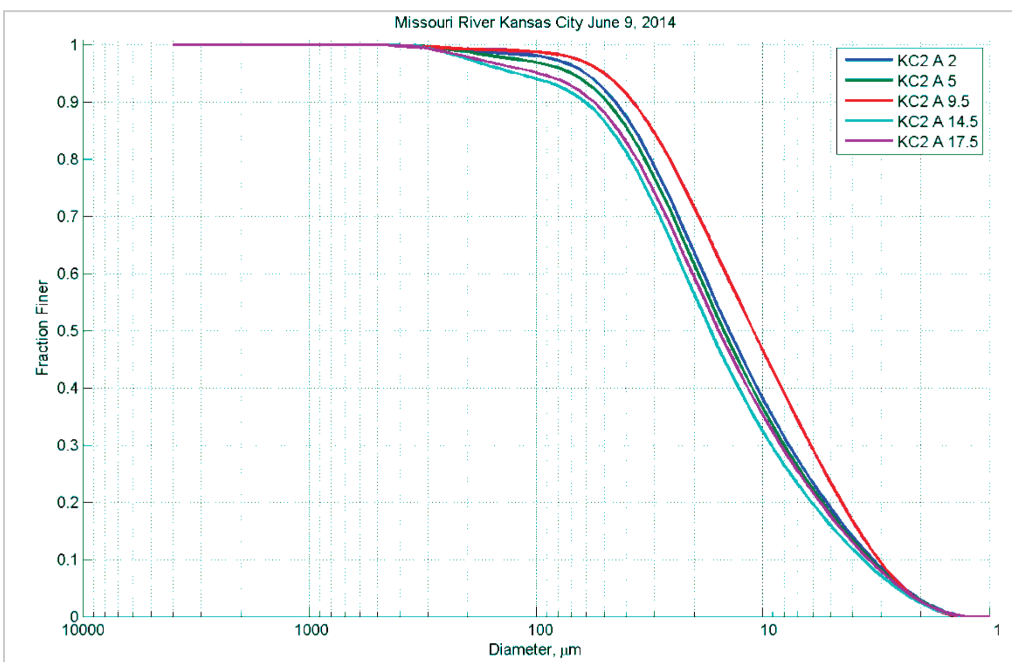

Figure 167. Particle size distribution at different depths (feet) in Station B – June 9, 2014.

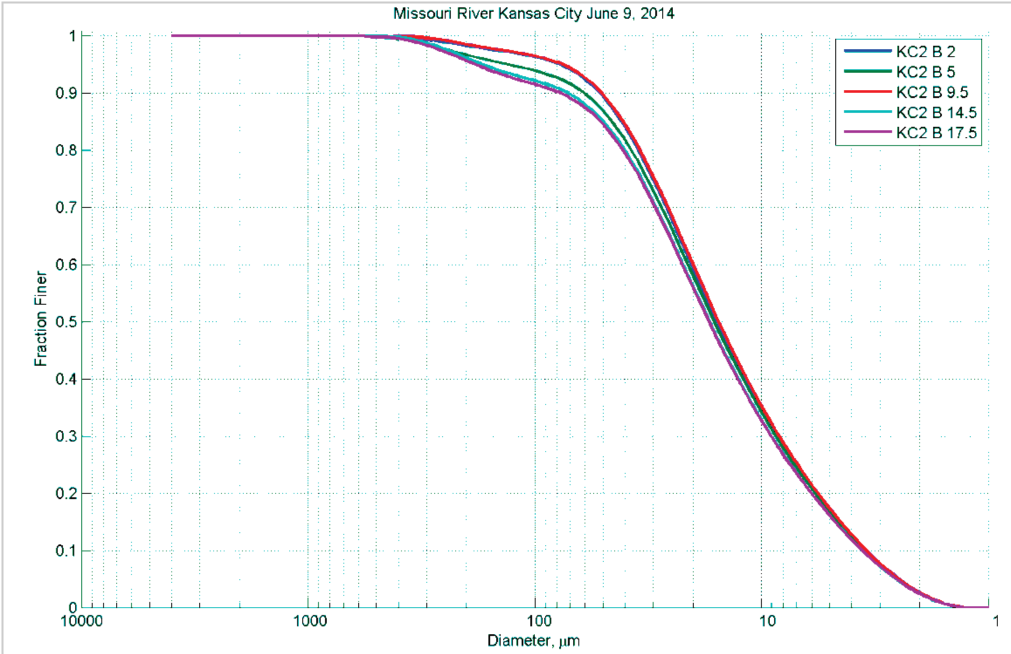

Figure 168. Particle size distribution at different depths (feet) in Station C – June 9, 2014.

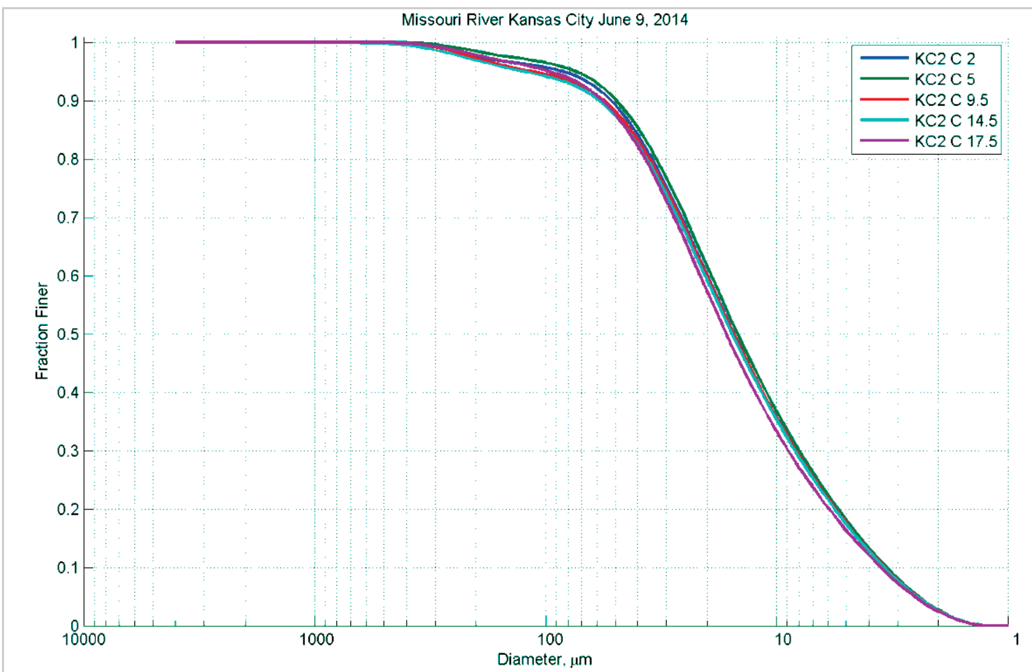

Figure 169. Particle size distribution at different depths (feet) in Station D – June 9, 2014.

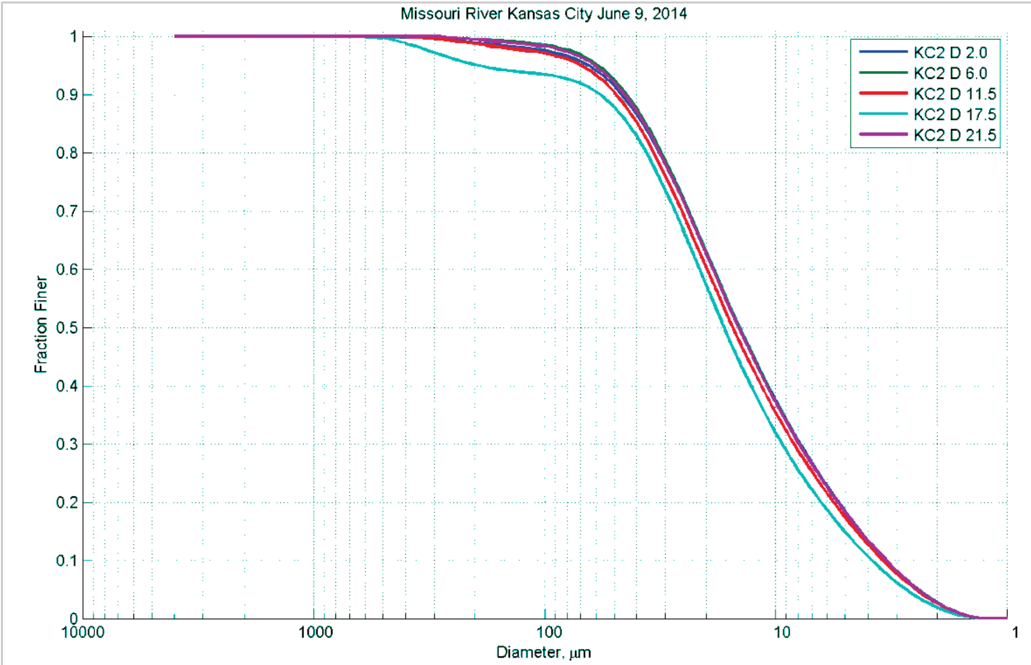

Figure 170. Particle size distribution at different depths (feet) in Station E – June 9, 2014.

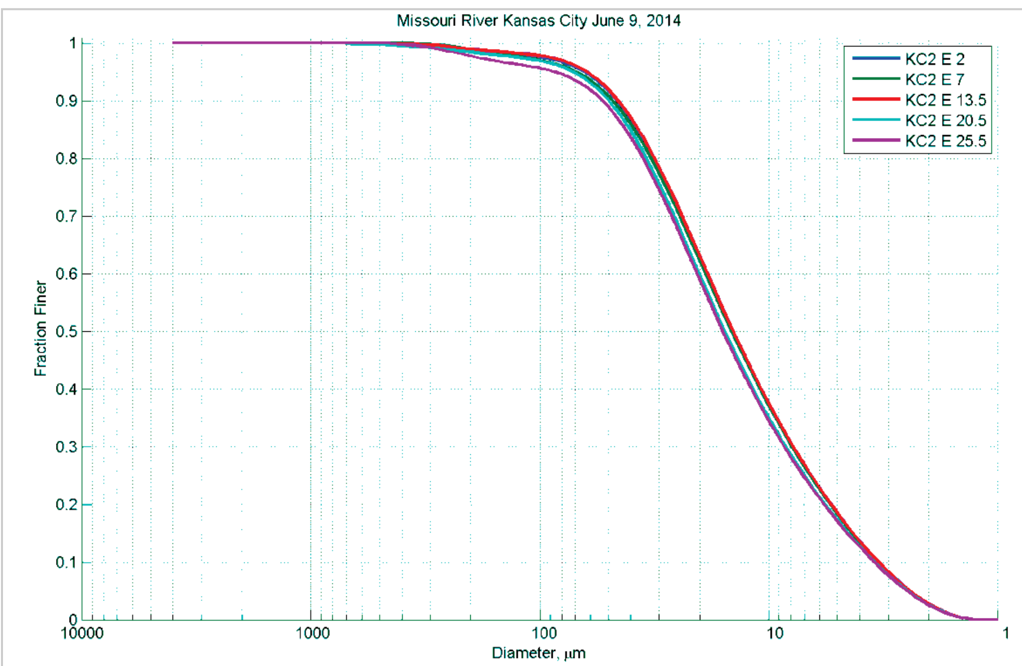

Particle size distribution for the third data collection date, June 24, 2014, is shown in Figure 171 to Figure 175.

Figure 171. Particle size distribution at different depths (feet) in Station A – June 24, 2014.

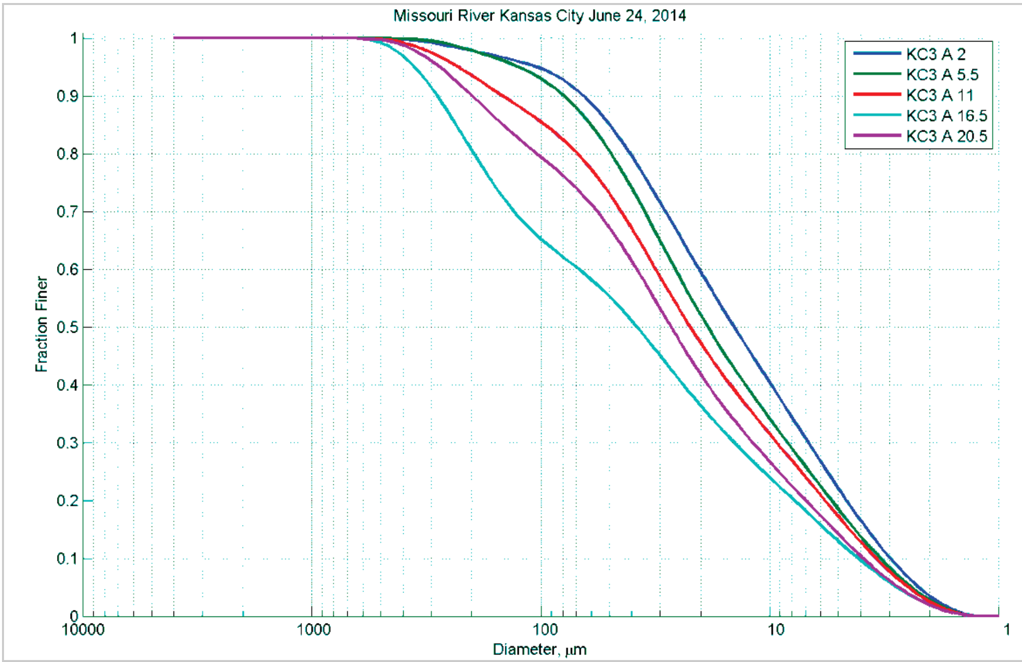

Figure 172. Particle size distribution at different depths (feet) in Station B – June 24, 2014.

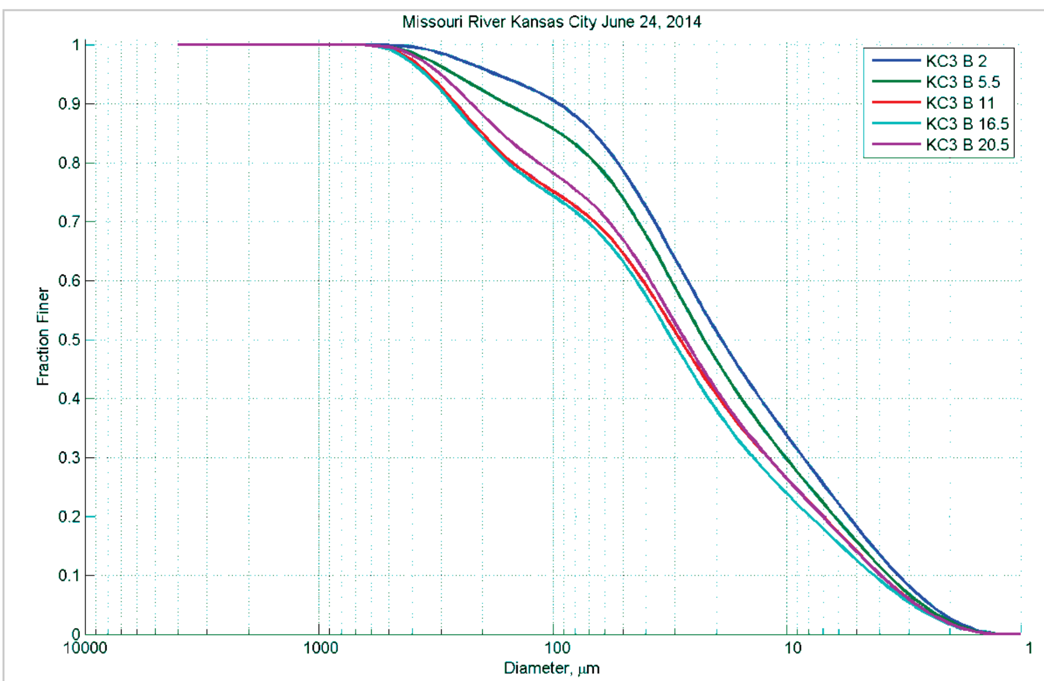

Figure 173. Particle size distribution a different depths (feet) in t Station C – June 24, 2014.

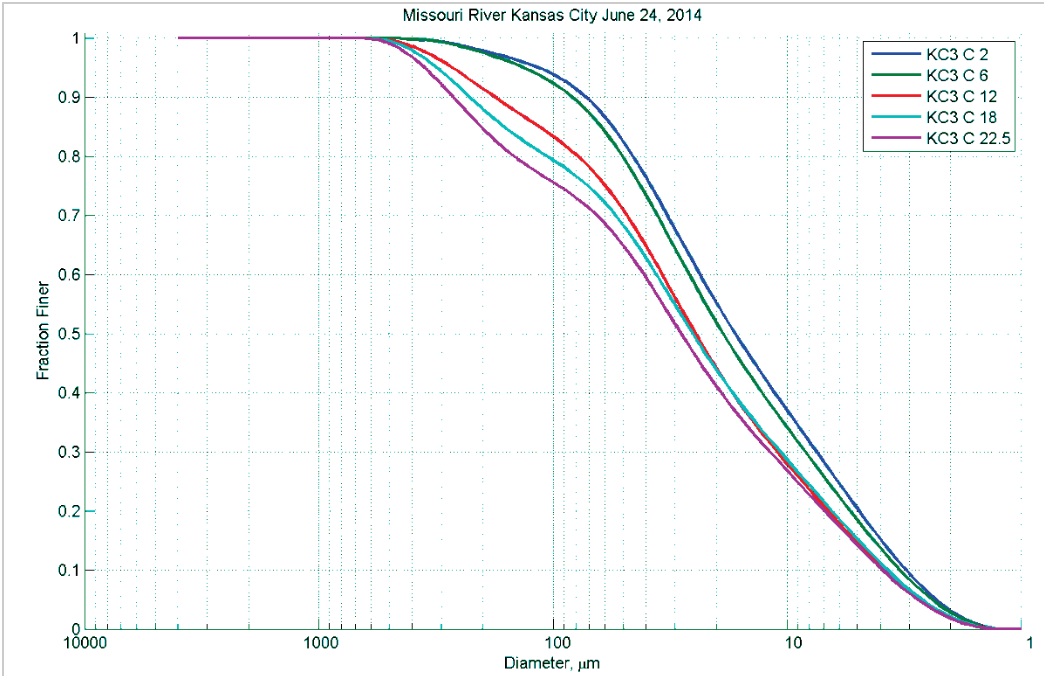

Figure 174. Particle size distribution at different depths (feet) in Station D – June 24, 2014.

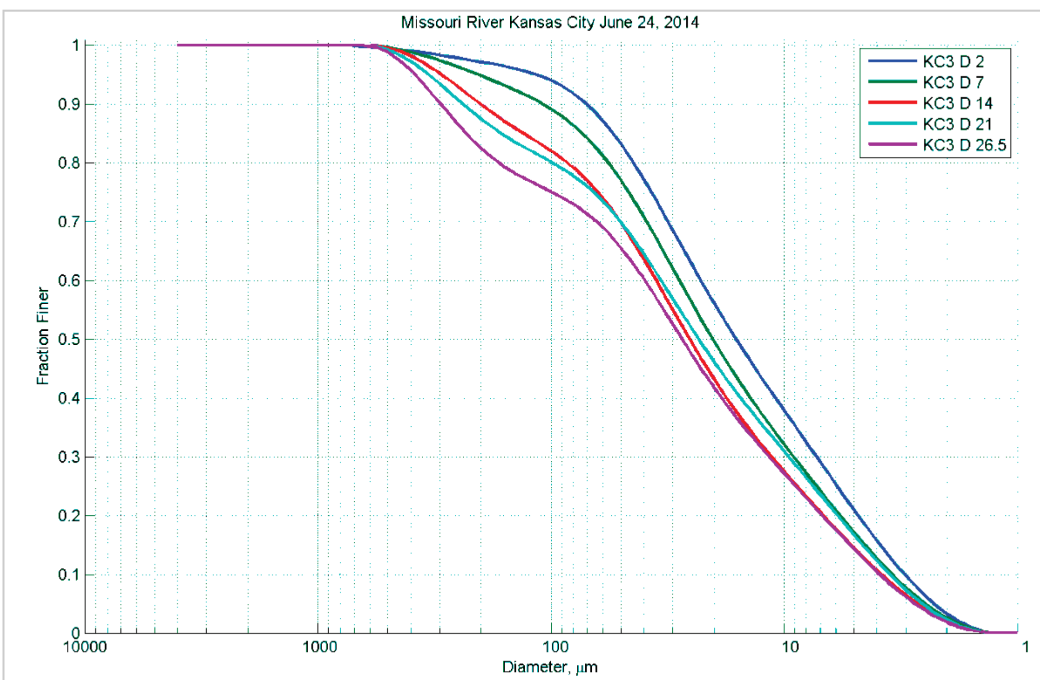

Figure 175. Particle size distribution at different depths (feet) in Station E – June 24, 2014.

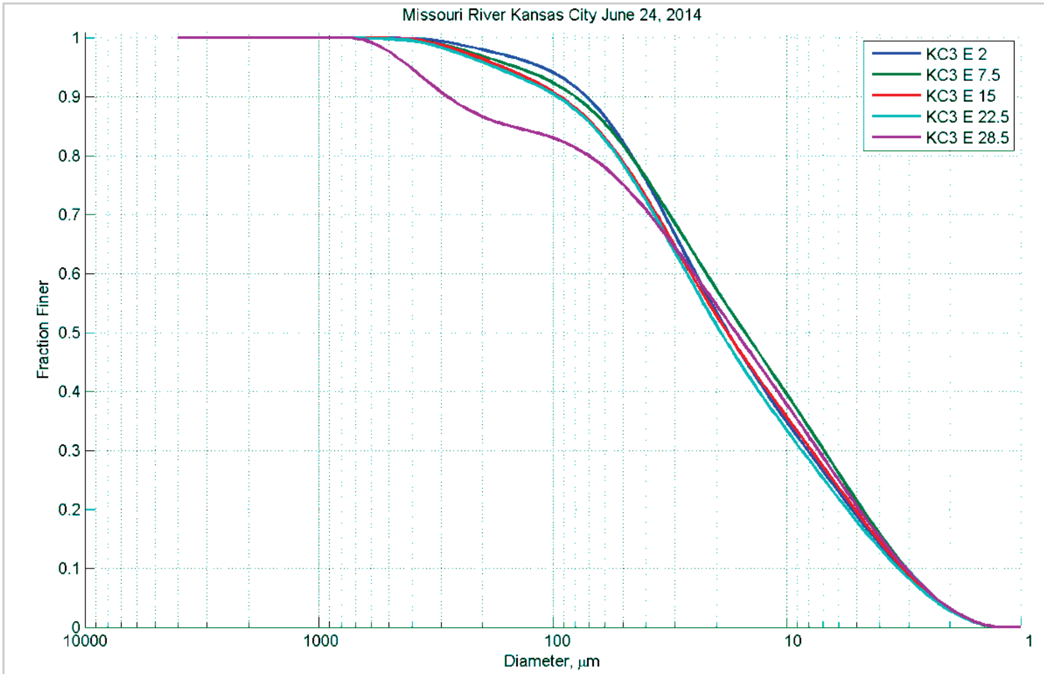

Suspended sediment concentration was also measured from the collected samples. Table 52 to Table 54 present the concentration values for each data collection date. Suspended sediment concentration profiles were created using the measured data, presented in Figure 176 to Figure 178. See Appendix V-f for more details about the measured data.

Table 52. Suspended sediment concentration at Kansas City, MO – April 26, 2014.

Station	Depth (ft)	Concentration (mg/L)
KC 1A	2	93.9
KC 1A	4.5	94.71
KC 1A	8.5	97.48
KC 1A	13	102.37
KC 1A	15.5	111.23
Total depth	17.3	(Bottom)
KC 1B	2	107.21
KC 1B	6	130.17
KC 1B	10.5	177.40
Total depth	13.7	(Bottom)
KC 1C	2	149.12
KC 1C	5	165.03
KC 1C	10	252.46
KC 1C	13.5	465.78
Total depth	14.2	(Bottom)
KC 1D	2	113.54
KC 1D	4.5	155.65
KC 1D	9	209.84
KC 1D	13.5	321.29
KC 1D	16.5	582.55
Total depth	17.3	(Bottom)
KC 1E	2	97.12
KC 1E	5	152.12
KC 1E	9.5	127.39
KC 1E	14.5	206.81
KC 1E	17.5	289.62
Total depth	19.3	(Bottom)

Table 53. Suspended sediment concentration at Kansas City, MO – June 9, 2014.

Station	Depth (ft)	Concentration (mg/L)
KC 2A	2	3,650.30
KC 2A	5	3,803.31
KC 2A	9.5	3,726.56
KC 2A	14.5	3,994.04
KC 2A	17.5	4,153.39
Total depth	22.4	(Bottom)
KC 2B	2	3,581.28
KC 2B	5	3,889.33
KC 2B	9.5	3,992.63
KC 2B	14.5	4,043.46
KC 2B	17.5	4,160.00
Total depth	19.3	(Bottom)
KC 2C	2	3,662.28
KC 2C	5	3,772.67
KC 2C	9.5	3,943.62
KC 2C	14.5	4,028.52
KC 2C	17.5	4,167.75
Total depth	19.9	(Bottom)
KC 2D	2	3,650.00
KC 2D	6	3,615.04
KC 2D	11.5	3,573.70
KC 2D	17.5	3,752.55
KC 2D	21.5	3,961.60
Total depth	24.7	(Bottom)
KC 2E	2	3,338.41
KC 2E	7	3,390.00
KC 2E	13.5	3,557.76
KC 2E	20.5	3,704.60
KC 2E	25.5	3,956.20
Total depth	26.9	(Bottom)

Table 54. Suspended sediment concentration at Kansas City, MO – June 24, 2014

Station	Depth (ft)	Concentration (mg/L)
KC 3A	2	1,535.23
KC 3A	5.5	1,553.20
KC 3A	11	1,596.57
KC 3A	16.5	1,904.32
KC 3A	20.5	1,878.03
Total depth	22.7	(Bottom)
KC 3B	2	1,473.93
KC 3B	5.5	1,693.13
KC 3B	11	1,759.13
KC 3B	16.5	1,945.95
KC 3B	20.5	2,187.48
Total depth	24.7	(Bottom)
KC 3C	2	1,432.78
KC 3C	6	1,620.47
KC 3C	12	1,703.08
KC 3C	18	1,673.59
KC 3C	22.5	2,022.39
Total depth	25.2	(Bottom)
KC 3D	2	1,433.33
KC 3D	7	1,511.71
KC 3D	14	1,483.06
KC 3D	21	1,671.79
KC 3D	26.5	1,919.19
Total depth	29	(Bottom)
KC 3E	2	1,335.28
KC 3E	7.5	1,481.70
KC 3E	15	1,409.38
KC 3E	22.5	1,546.56
KC 3E	28.5	1,666.96
Total depth	30.9	(Bottom)

Figure 176. Suspended sediment concentration at Kansas City, MO – April 26, 2014.

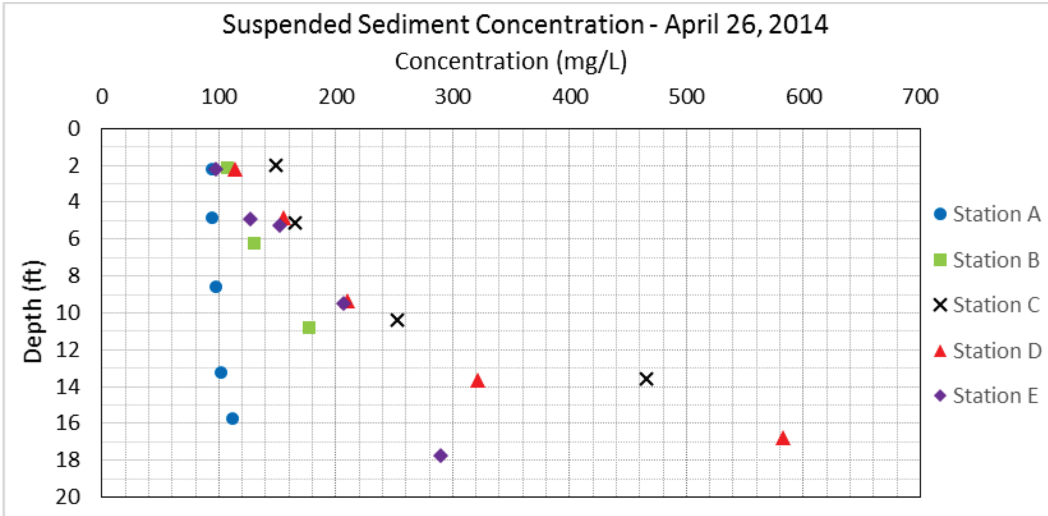

Figure 177. Suspended sediment concentration at Kansas City, MO – June 9, 2014.

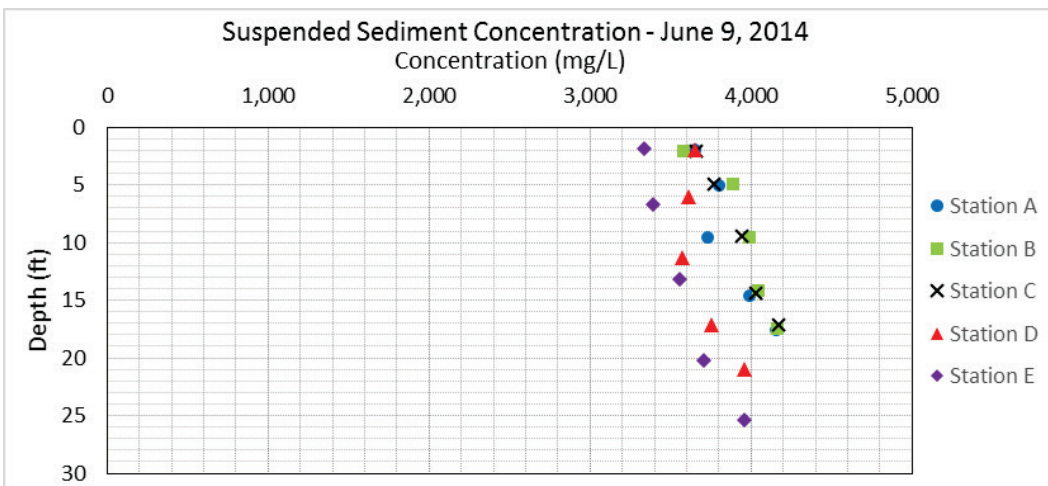

Figure 178. Suspended sediment concentration at Kansas City, MO – June 24, 2014.

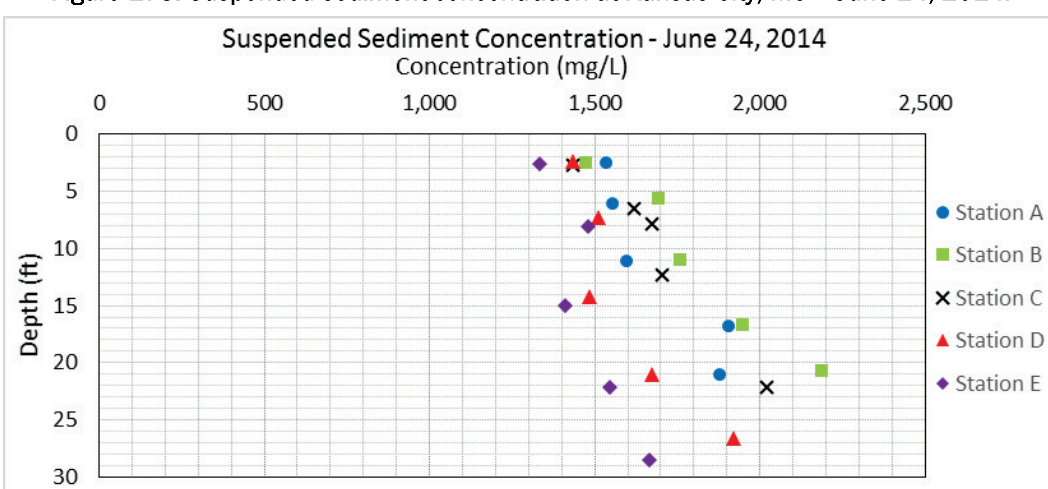

The suspended sediment concentration data were used to calibrate the ADCP acoustic backscatter and develop suspended sediment concentration profiles across the channel. Figure 179 to Figure 181 show the suspended sediment concentration profiles for the first left-to-right ADCP pass, for each data collection date. To see the other profiles, see Appendix V-f.

Figure 179. Suspended sediment concentration profile at Kansas City, MO – April 26, 2014.

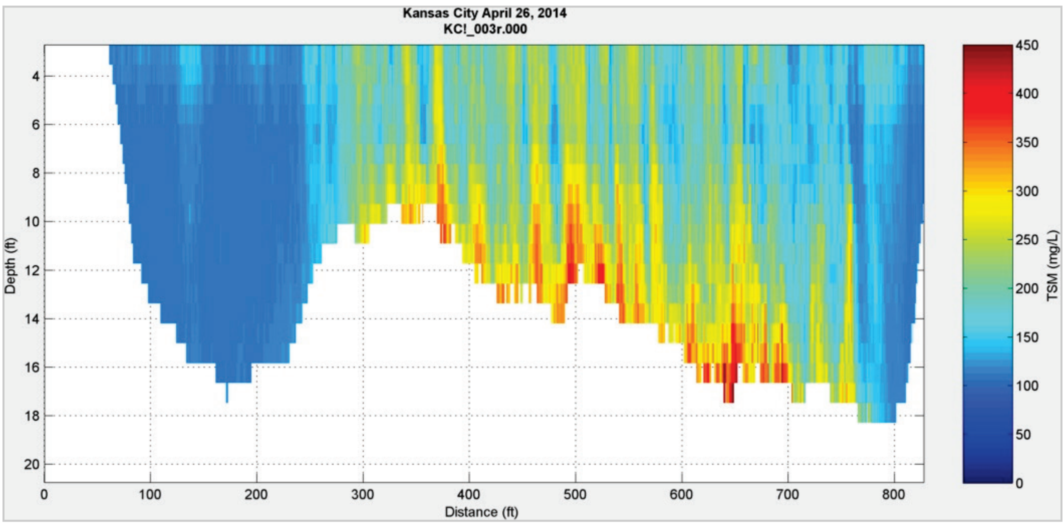

Figure 180. Suspended sediment concentration profile at Kansas City, MO – June 9, 2014.

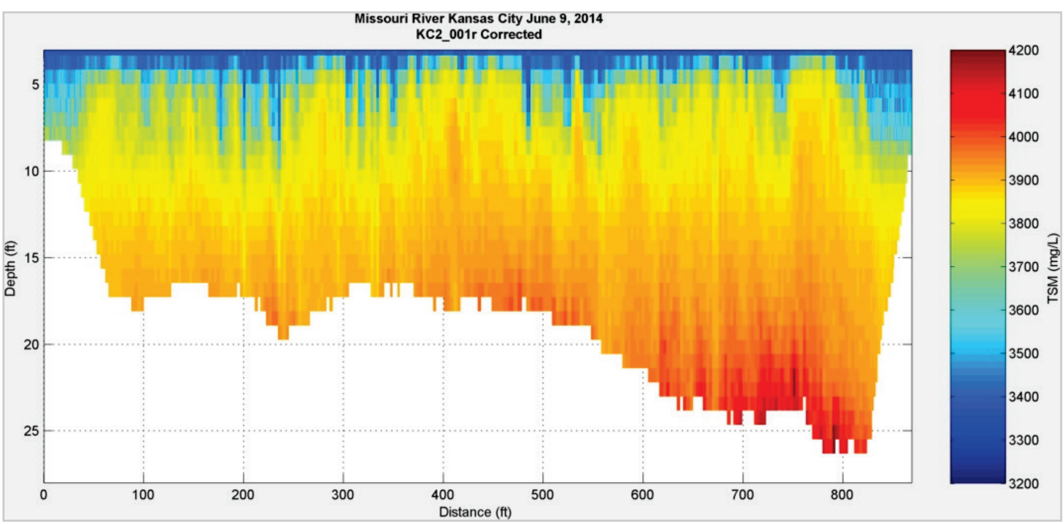

Figure 181. Suspended sediment concentration profile at Kansas City, MO – June 24, 2014.

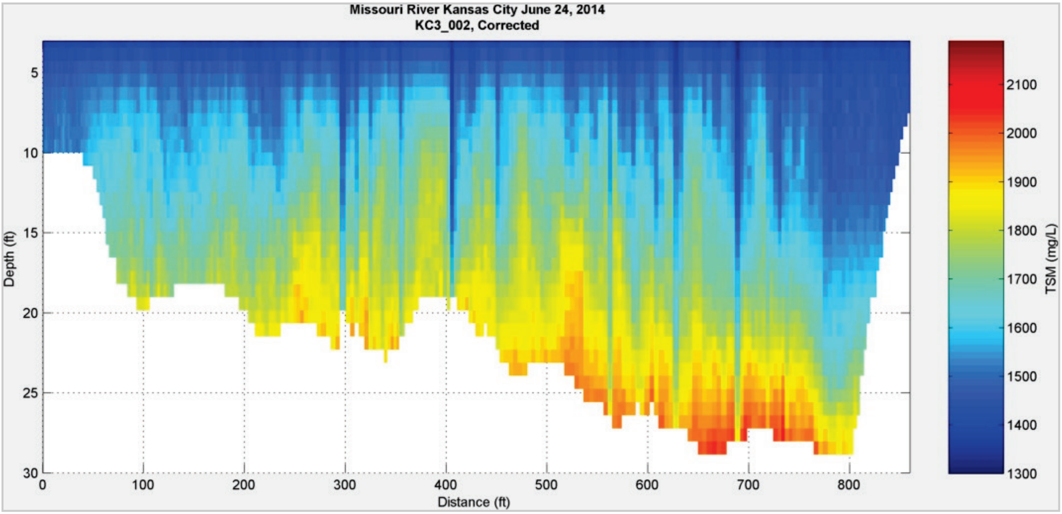

The suspended sediment concentration cross-section profiles obtained from the ADCP measurements were combined with the flow discharges, also obtained from the ADCP, to obtain the suspended sediment transport load, in tons per day. The method used for this study is explained in Heath et al. (2015, 13–14. The suspended sediment load can be divided classifying the suspended material by size and soil type. Table 55 presents the suspended sediment transport load, according to both classifications, for the first data collection date April 26, 2014. Table 56 and Table 57 present the same information for the second and third data collection dates, respectively. In all three tables, the categories under the Soil Type Classification were determined as follows: Clay Flux groups the size fractions 0.0001 to 0.0004 mm, Silt Flux 0.0004 to 0.0625 mm, and Sand Flux 0.0625 to 2.00 mm.

Table 55. Suspended sediment load distributed by grain size and soil type – April 26, 2014.

Classification System	Category	Sediment Flux (tons/day)
Total load		20,308.77
Sediment size classification	0.001 - 0.004 mm	1,254.18
	0.004 - 0.008 mm	2,063.19
	0.008 - 0.016 mm	2,909.61
	0.016 - 0.031 mm	3,471.09
	0.031 - 0.063 mm	2,945.79
	0.063 - 0.125 mm	1,166.23
	0.125 - 0.250 mm	2,880.16
	0.250 - 0.500 mm	3,176.83
	0.500 - 1.00 mm	341.21
	1.00 - 2.00 mm	100.47
Soil type Classification	Clay	1,254.18
	Silt	11,389.68
	Sand	7,664.90

Table 56. Suspended sediment load distributed by grain size and soil type – June 9, 2014.

Classification System	Category	Sediment Flux (tons/day)
Total load		1,028,912.40
Sediment size classification	0.001 - 0.004 mm	122,949.78
	0.004 - 0.008 mm	163,798.03
	0.008 - 0.016 mm	227,458.45
	0.016 - 0.031 mm	257,189.57
	0.031 - 0.063 mm	178,974.69
	0.063 - 0.125 mm	43,413.34
	0.125 - 0.250 mm	21,533.74
	0.250 - 0.500 mm	13,220.45
	0.500 - 1.00 mm	374.36
	1.00 - 2.00 mm	0.00
Soil type classification	Clay	122,949.78
	Silt	827,420.74
	Sand	78,541.89

Table 57. Suspended sediment load distributed by grain size and soil type – June 24, 2014.

Classification System	Category	Sediment Flux (tons/day)
Total load		524,323.74
Sediment size classification	0.001 - 0.004 mm	60,656.37
	0.004 - 0.008 mm	73,786.45
	0.008 - 0.016 mm	80,340.54
	0.016 - 0.031 mm	93,700.62
	0.031 - 0.063 mm	96,911.76
	0.063 - 0.125 mm	48,093.20
	0.125 - 0.250 mm	37,198.76
	0.250 - 0.500 mm	30,554.71
	0.500 - 1.00 mm	3,081.32
	1.00 - 2.00 mm	0.00
Soil Type classification	Clay	60,656.37
	Silt	344,739.37
	Sand	118,927.99

7.7 Bed load transport

The ISSDOTv2 method was used for computing the bed-load transport. Table 58 shows the values obtained for the bed load, as well as the other sediment quantities determined from the suspended sediment samples at the Kansas City site. It provides a breakdown of the various measured sediment transport components, based on sediment size classification.

Table 58. Bed-load transport values from Kansas City, MO.

Data collection date	26-Apr-14	9-Jun-14	24-Jun-14
Flow (cfs)	40,624	97,068	116,525
Bed load (tons/day)	1,756	4,282	7,935
Suspended BML (tons/day)	7,665	78,542	118,928
Total BML (tons/day)	9,421	82,824	126,863
Bed load fraction (%)	18.6%	5.2%	6.3%
Wash load (tons/day)	12,644	950,371	405,396
Total load	22,065	1,033,194	532,259

In Table 58, *bed load* is defined as the bed material moving at the bottom of the river in bed-forms; *suspended BML* refers to the suspended material with grain size higher than 0.063 mm; *total BML* is the sum of bed load and suspended BML; *bed load fraction* is the percentage of the total bed

material moving as bed load; *wash load* is fine sediments that never settle in the bed, with grain size of 0.063 or less; and *total load* combines the quantity of total BML and wash load.

As in the case of the St. Joseph data, Kansas City trip 1 was a much lower flow than trips 2 and 3, as shown in Table 58. Accordingly, the bed-load transport for the last two trips is noticeably higher. The bed-load fraction also falls off considerably since more BML is going into suspension at the higher flows

A bed-load rating curve was prepared for this site by plotting the bed-load transport in tons per day versus the river flowrate. This graph is shown in Figure 182. The R-squared value of 0.9677 shows a high correlation for a linear trend considering the range of flows. One additional bed-load value was obtained at the Kansas City site prior to the 2014 measurement effort during the high-flow event of 2011. The latest version of the ISSDOTv2 code that was used in computing the 2014 bed-load values was also used to re-compute the 2011 value. It was added to the rating curve as noted in the legend of Figure 182.

Figure 182. Bed-load rating curve for Kansas City, MO.

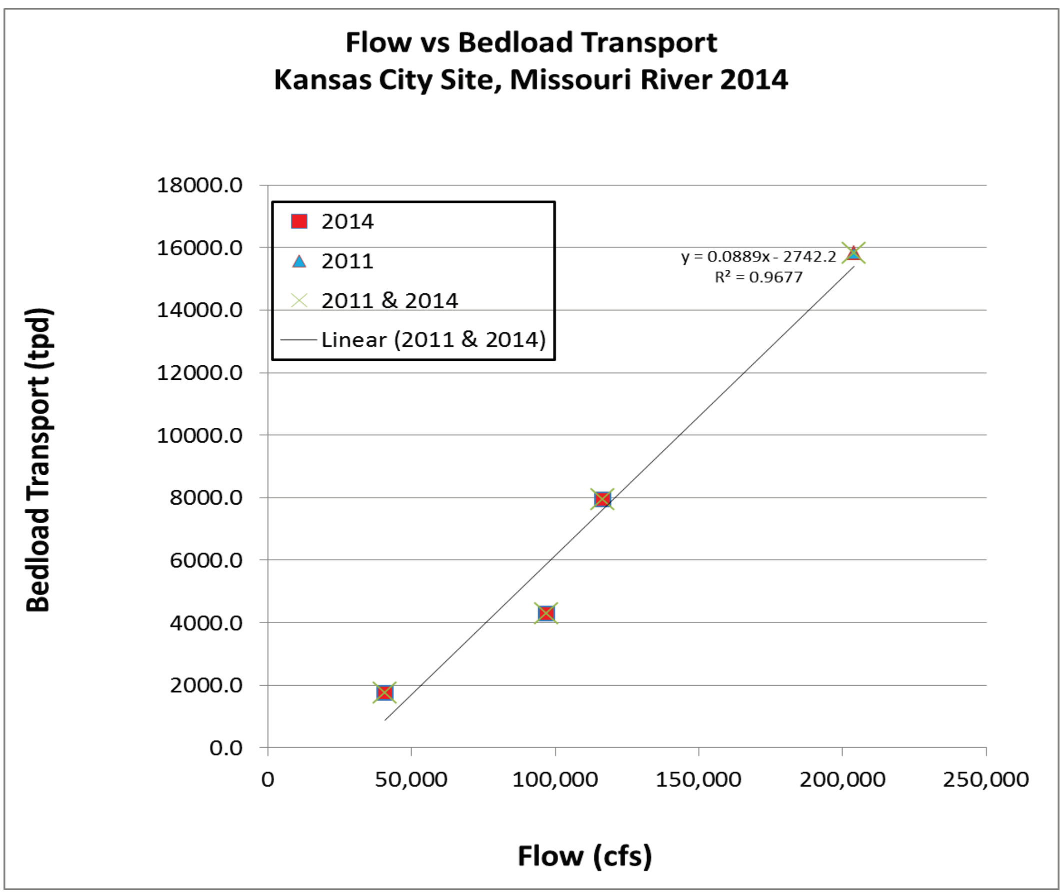

Bed-load transport values were also computed for this site using two analytic transport functions. One is the MPM formula, and the other is the Einstein formula. They were computed for each swath of bathymetric data. For instance, Figure 183 shows the bathymetry of this site with the six swath numbers (S1 to S6) labeled on it, indicating the lateral position where each swath was located. The hydraulic and sediment parameters obtained in the field data collection effort discussed before were extracted for each of these swaths.

Figure 183. Bathymetry for Kansas City showing swath locations.

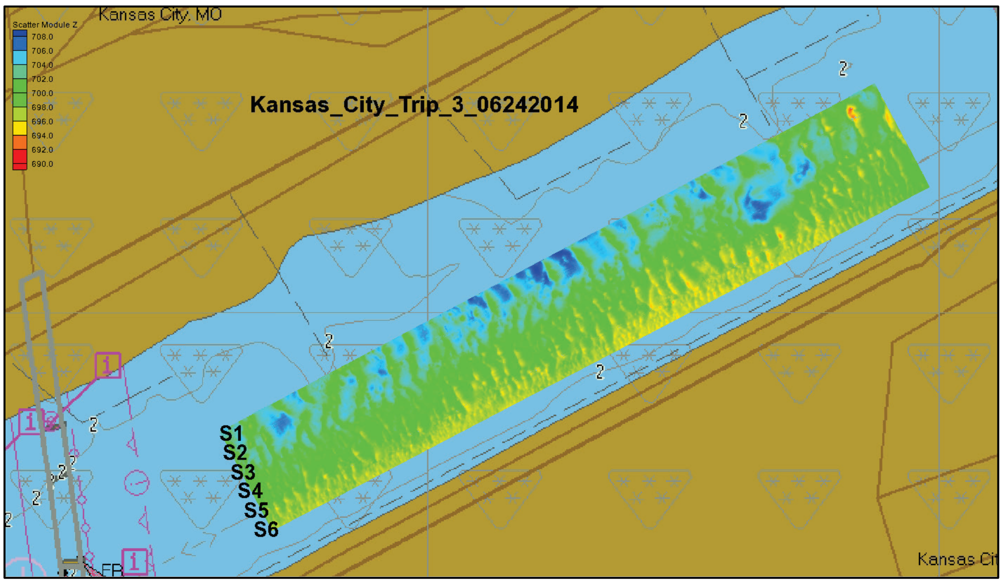

Flow, average velocity, and water depth were obtained from the ADCP data by a separate program written for that specific purpose. Water slope and water temperature were obtained from each appropriate data appendix. Bed sediment gradations used were selected based on their proximity to a given swath. The SAM Hydraulic Design Package for Channels program was then used with these data to compute the bed-load values for each individual swath. This software package has provisions for entering hydraulic and sediment input parameters and can then compute bed-load transport values for several commonly used transport functions.

The results are plotted in Figure 184 to Figure 186 and show how the transport function values compare to the ISSDOTv2 measured values. They also show the lateral variability across the measured section from the left side to the right side of the channel. The red number in Figure 185 indicates an interpolated value.

Figure 184. Bed-load transport at Kansas City, MO – April 26, 2014: ISSDOTv2 values compared to transport function computed values.

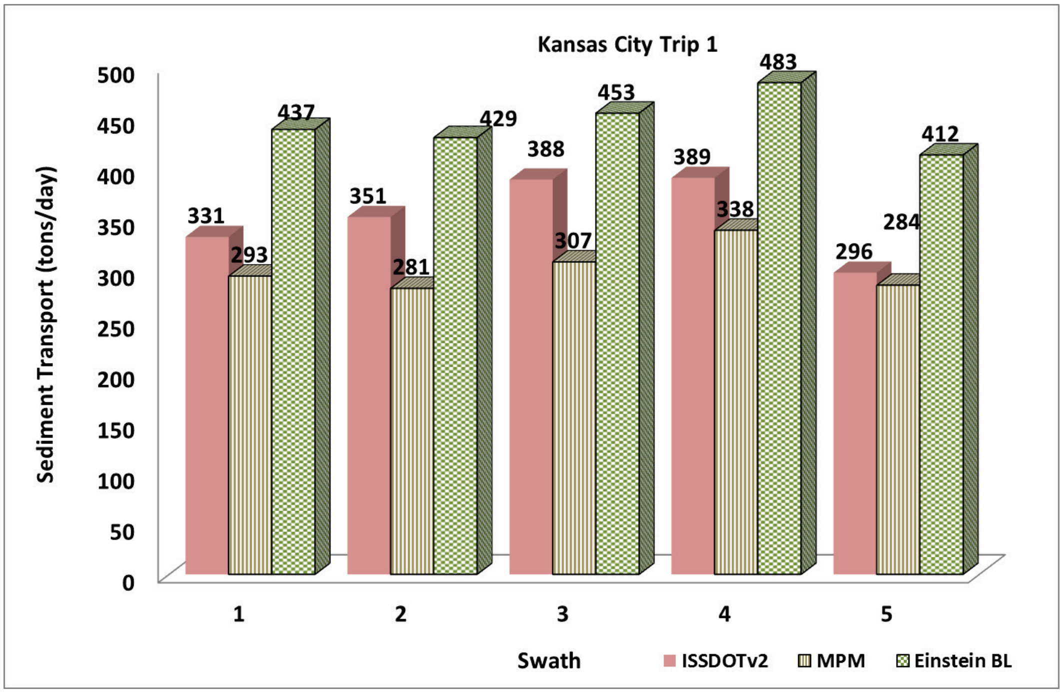

Figure 185. Bed-load transport at Kansas City, MO – June 9, 2014: ISSDOTv2 values compared to transport function computed values, where red indicates an interpolated value.

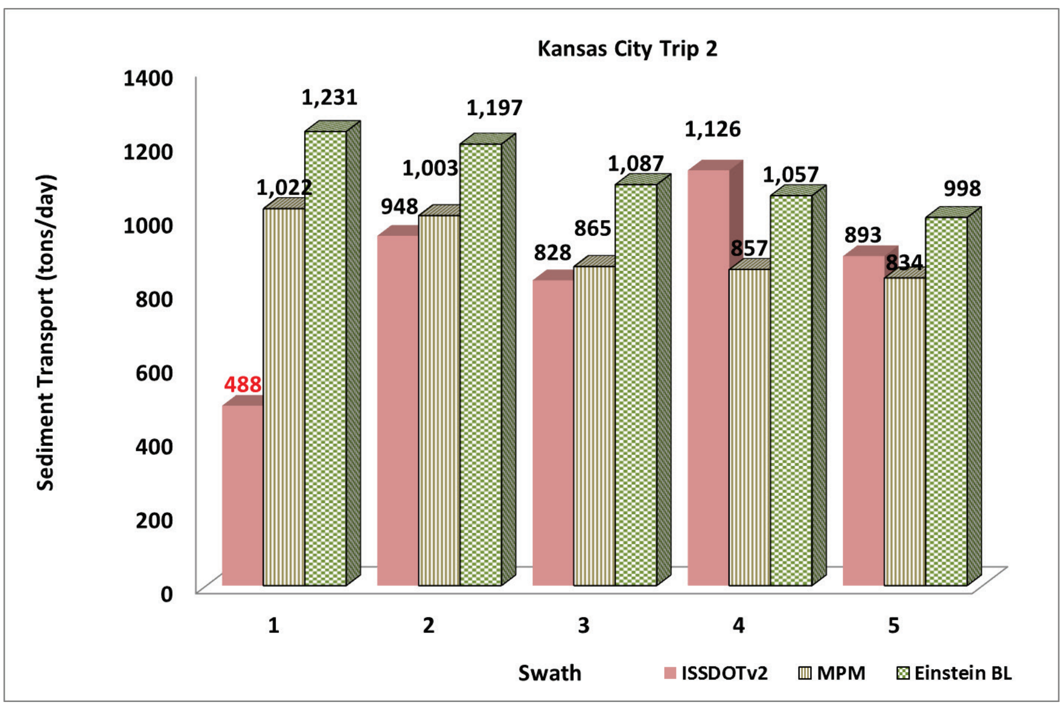

Figure 186. Bed-load transport at Kansas City, MO – June 26, 2014: ISSDOTv2 values compared to transport function computed values.

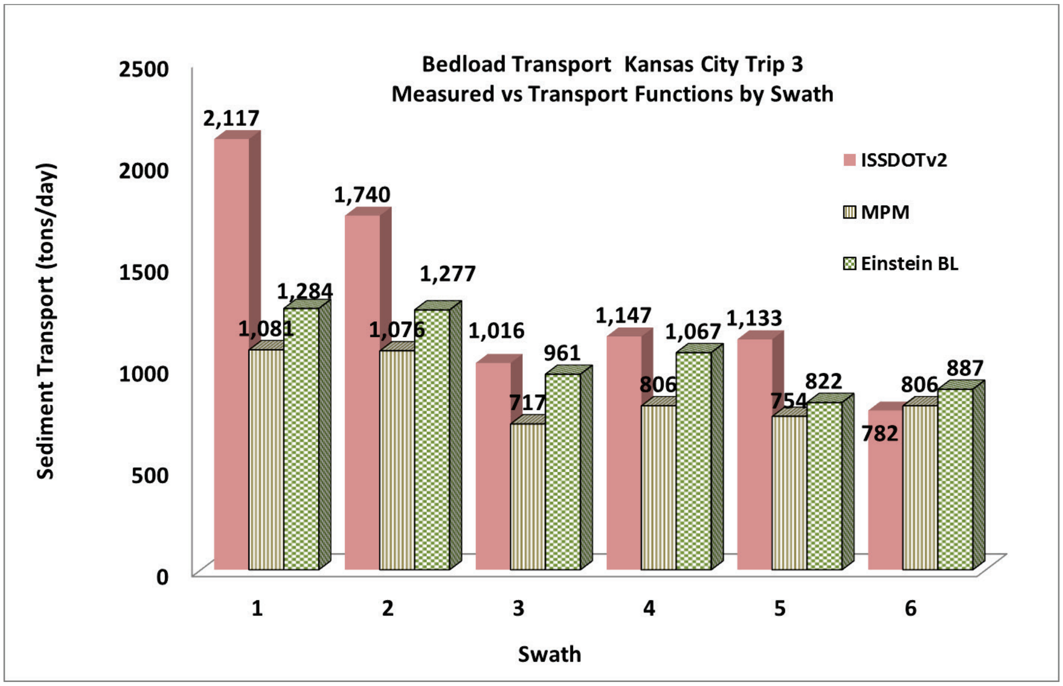

8 Site 6: Waverly, Missouri

Multi-beam surveys, ADCP flow and velocity measurements, bed and suspended material sampling and testing, and water temperature, water surface elevation, and slope measurements were performed during each data collection date at Waverly, MO. The measuring area is shown on Figure 187 as the green polygon. The approximate location of the USGS gage station near the data collection site is also shown as the blue pin. This location might not be accurate in the figure. Coordinates for the gage site as given in the USGS web site are listed in Table 3. The red line indicates the cross section where ADCP measurements were conducted and suspended and bed load material samples were collected. The bank-to-bank width of the river at this location is estimated to range between 1,000 and 1,100 ft, and the length of the study area was approximately 2,000 ft. The data collection dates for Kansas City were April 25, 2014; June 10, 2014; and June 25, 2014.

Figure 187. Waverly, MO, data collection site.

8.1 ADCP flow and velocity

The velocity and discharge for each data collection date, and site, were measured using an ADCP. Table 59 presents the cross-section average flow (ft^3/s), area (ft^2), and average velocity (ft/s) for each date, calculated from the measured data. See Appendix VI-a for the measured data.

Table 59. Total flow, area, and average velocity on the given dates at Waverly, MO.

Date	Total Flow, Q (ft^3/s)	Total Area, A (ft^2)	Velocity Q/A (ft/s)
April 25, 2014	43,566	13,371	3.26
June 10, 2014	100,478	22,218	4.52
June 25, 2014	117,347	23,809	4.93

Real-time vertical profiles of instantaneous velocities are also obtained from the ADCP measurements. Figure 188 to Figure 190 present the velocity magnitude, before the multi-beam measurements, from left to right. In the figures, the velocity magnitude is quantified by the range of colors shown on the right side of each figure, where the higher velocities are denoted by red and the lower velocities by blue. The velocity profiles for after the multi-beam measurements are available at Appendix VI-a.

Figure 188. Velocity magnitude at Waverly, MO – April 25, 2014, 17:31:13.

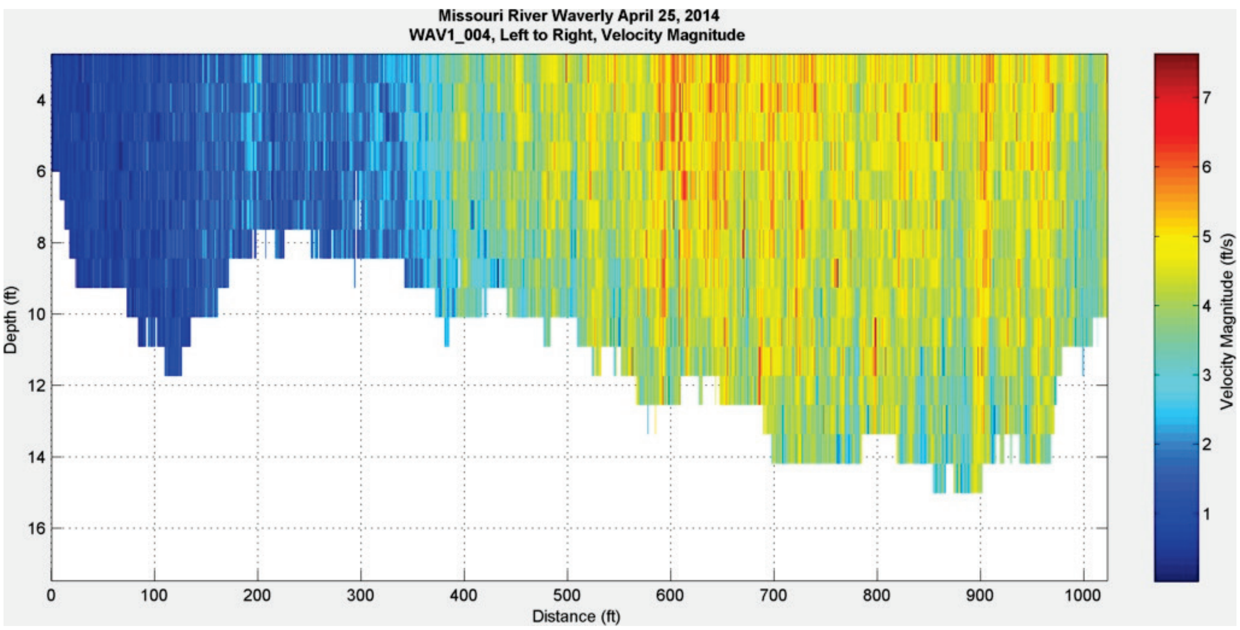

Figure 189. Velocity magnitude at Waverly, MO – June 10, 2014, 16:44:16.

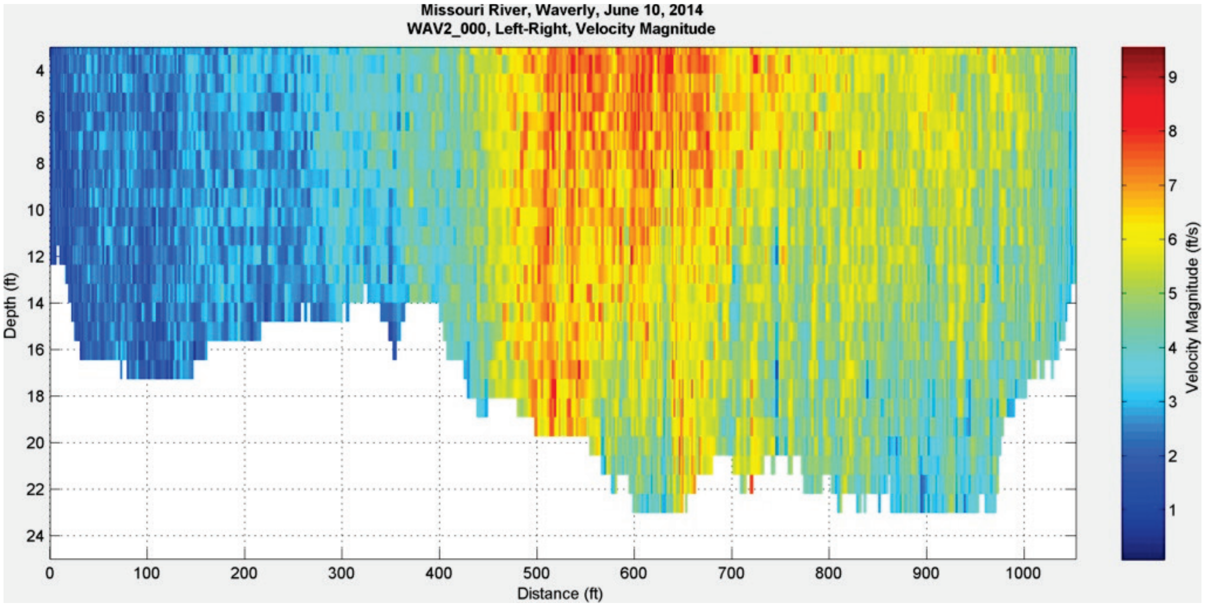

Figure 190. Velocity magnitude at Waverly, MO – June 25, 2014, 16:26:28.

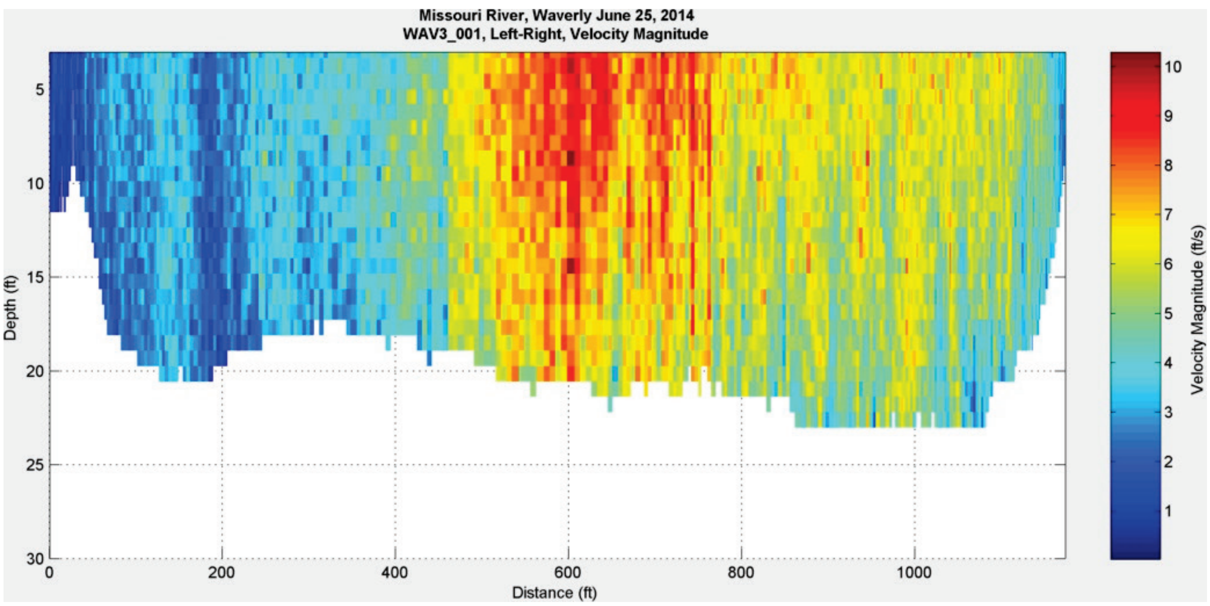

8.2 Water surface elevation and slope

Water surface elevation measurements were taken upstream and downstream of the multi-beam survey area. Figure 191 shows the upstream elevations, at distance zero, connected to the downstream elevations, at a distance of 2,000 ft, for each data collection date. Table 60 presents the slope values for the Waverly, MO, location for the three dates. The measured data are available at Appendix VI-b.

Figure 191. Water surface elevation at Waverly, MO – from upstream to downstream.

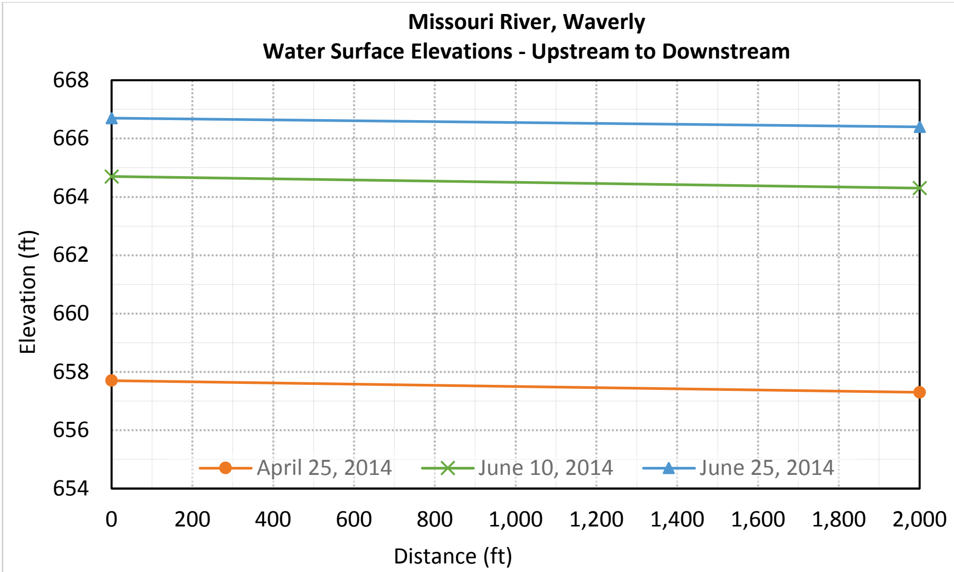

Table 60. Water surface slopes at Waverly, MO.

Date	Water Surface Slope (%)
April 25, 2014	0.00020
June 10, 2014	0.00020
June 25, 2014	0.00015

8.3 Water temperature

Table 61 presents the average temperature for each date (see Appendix VI-g for the measured values).

Table 61. Water temperature at Waverly, MO.

Date	Temperature (F)
April 25, 2014	60.1
June 10, 2014	71.6
June 25, 2014	78.3

8.4 Multi-beam surveys

The initial multi-beam survey performed at Waverly, MO, included the full extent of the channel from bank to bank, as shown in Figure 192 where the dark blue areas are deeper and the red areas are shallower. This survey is used to determine the location of the sand waves throughout the study area and to then decide where to run the ISSDOTv2 swaths according to the location of the active sand transport portion of the channel. The selected area with swath lines and numbers displayed in red is shown in

Figure 193. This shows the actual area that was used for the ISSDOTv2 bed-load computations. The length of the multi-beam swaths is approximately 2,000 ft for all three data collection dates.

Figure 192. Multi-beam survey extent at Waverly, MO – April 25, 2014.

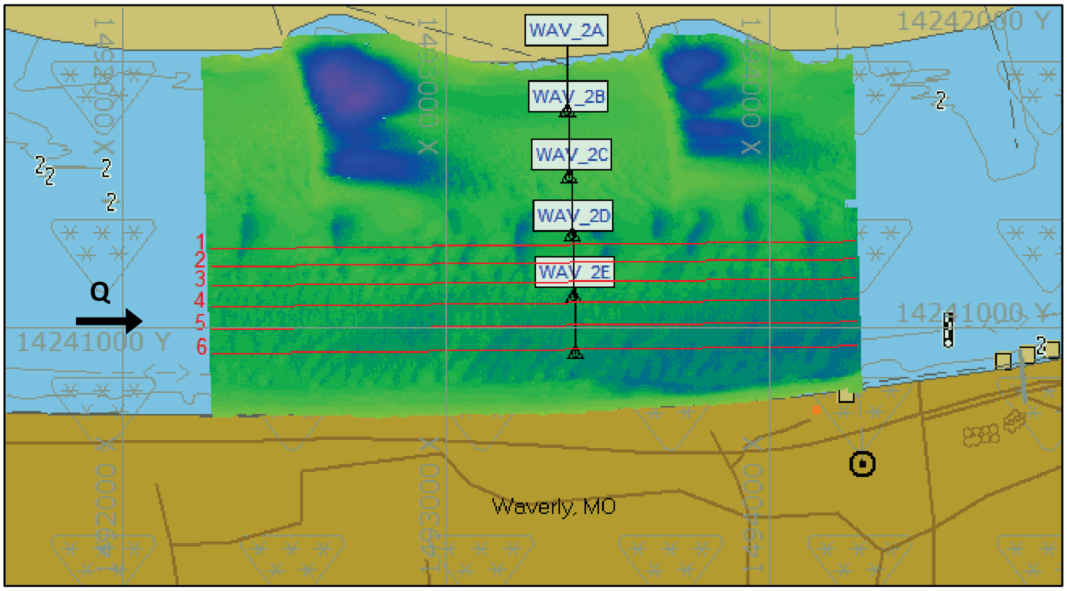

Figure 193. Multi-beam survey extent at Waverly, MO – June 10 and June 25, 2014.

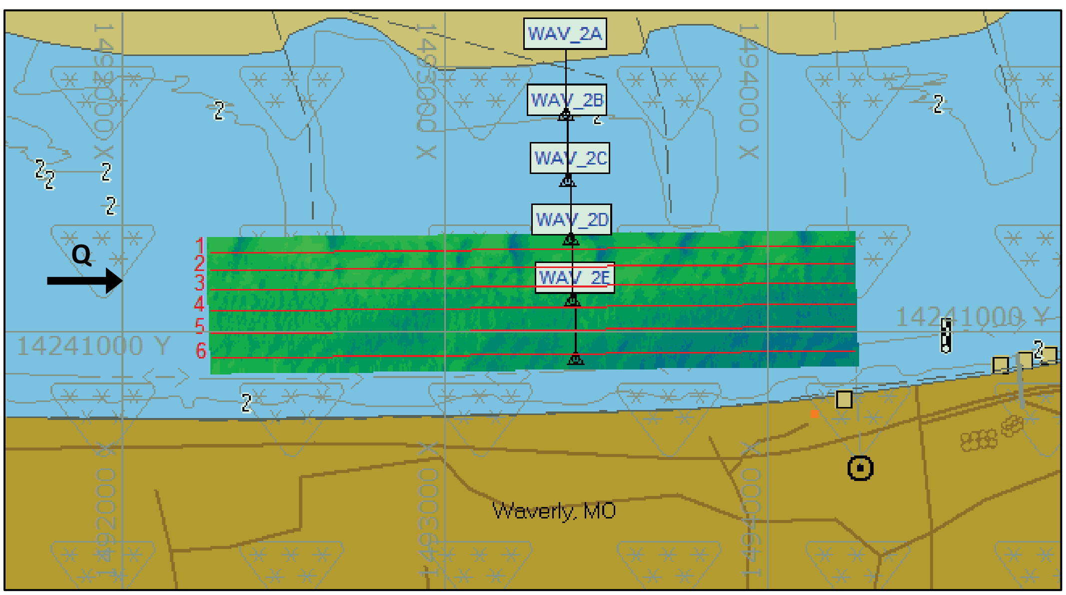

8.5 Bed material samples

Five sediment sample stations were positioned equidistant from each other along the cross section, as presented on Figure 194, which is the same location at which the suspended sediment samples and the ADCP velocity data were obtained. The first station, Station A, was positioned on the left descending bank, and the last station, Station E, on the right descending bank. Table 62 provides the locations of sample stations according to NAD83. See Appendix VI-c for the coordinates using the UTM Grid System.

Table 62. Sediment sample stations NAD83 Coordinates at Waverly, MO.

Station	NAD83 Latitude	NAD83 Longitude
WAV A	39° 12' 57.4103" N	93° 31' 9.0" W
WAV B	39° 12' 55.3939" N	93° 31' 8.9109" W
WAV C	39° 12' 53.6115" N	93° 31' 8.8038" W
WAV D	39° 12' 51.7268" N	93° 31' 8.6960" W
WAV E	39° 12' 49.9881" N	93° 31' 8.6081" W

Figure 194. Sediment sample stations at the Missouri River – Waverly, MO

The grain size distribution for the five bed material samples of the first collection date, April 25, 2014, is provided at Figure 195. Figure 196 and Figure 197 present the gradation analysis for the second and third collected samples, respectively. The measured data are available in Appendix VI-d.

Figure 195. Bed material grain size distribution for Waverly, MO – April 25, 2014.

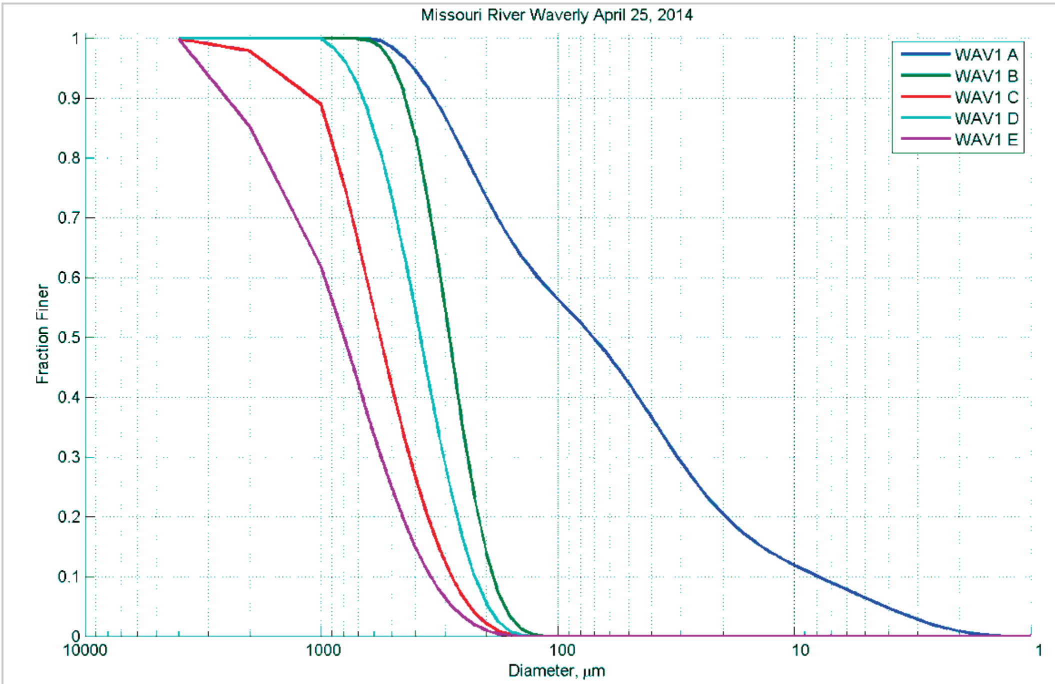

Figure 196. Bed material grain size distribution for Waverly, MO – June 10, 2014.

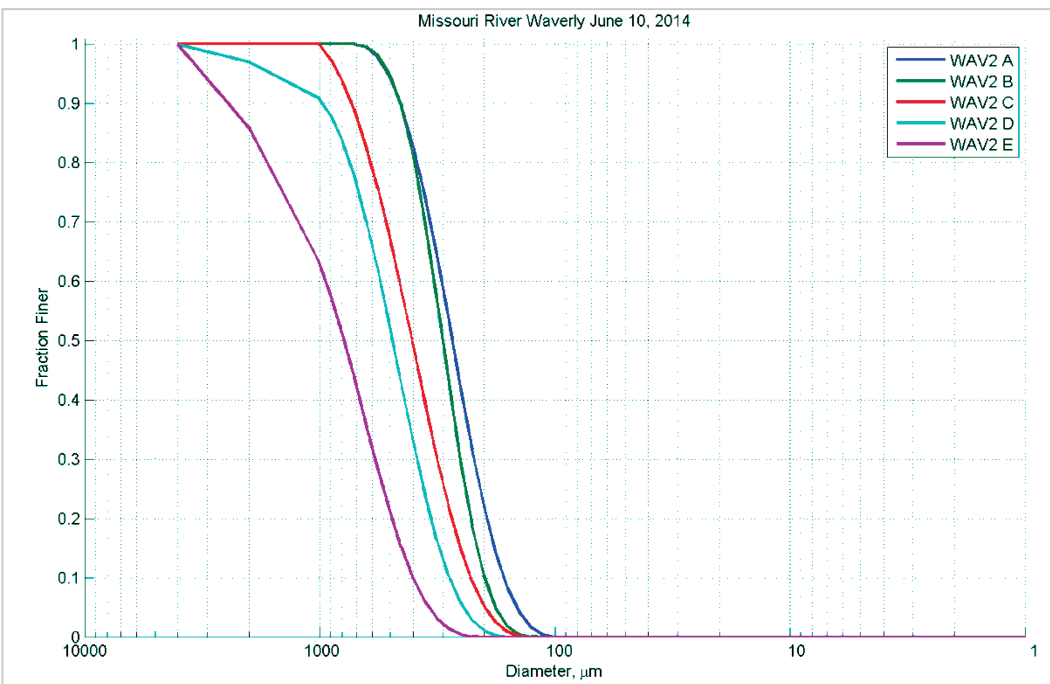

Figure 197. Bed material grain size distribution for Waverly, MO – June 25, 2014.

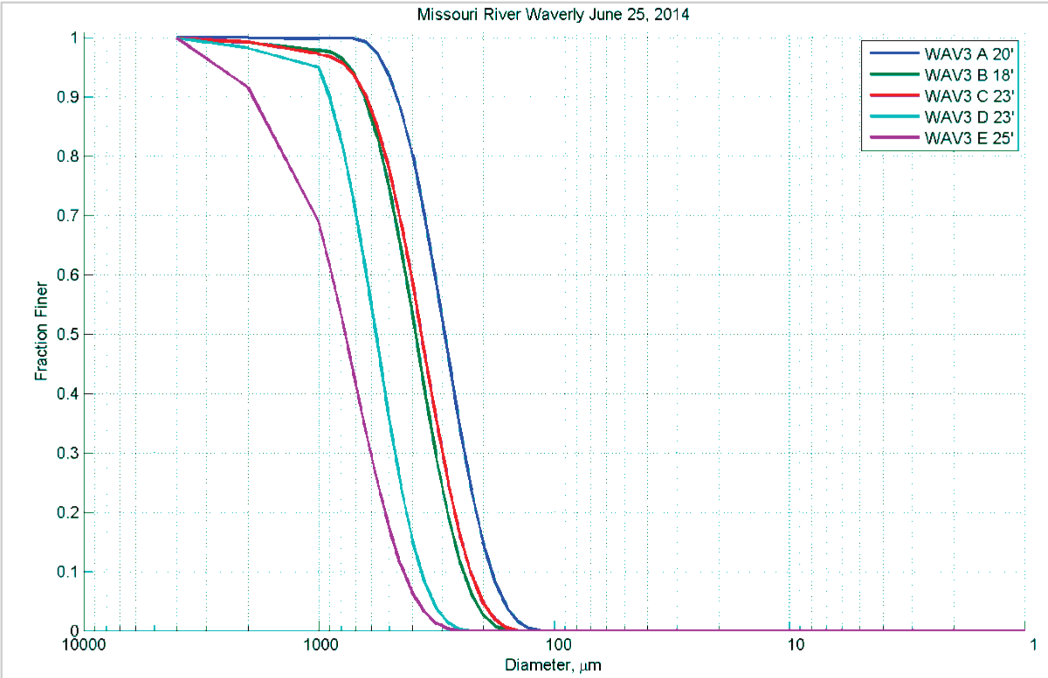

8.6 Suspended sediment

Suspended sediment samples at different depths in a column were taken at the five stations shown in Figure 194, for each data collection date. A particle size analysis was conducted for the samples of each station and date. The results are presented in this report as Figure 198 to Figure 212, and the measured data are available at Appendix VI-e.

Particle size distribution for the first data collection date, April 25, 2014, is shown in Figure 198 to Figure 202. It is organized starting from the station closer to the left descending bank, Station A, to the station closer to the right descending bank, Station E.

Figure 198. Particle Size Distribution at Station A - April 25, 2014.

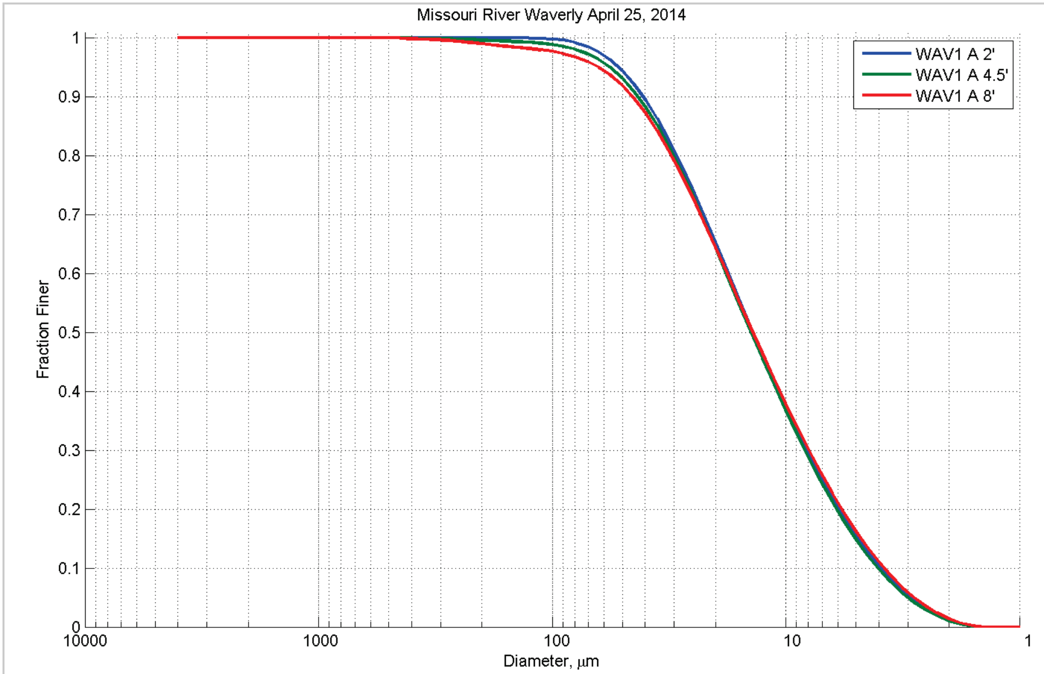

Figure 199. Particle size distribution at different depths (feet) in Station B - April 25, 2014.

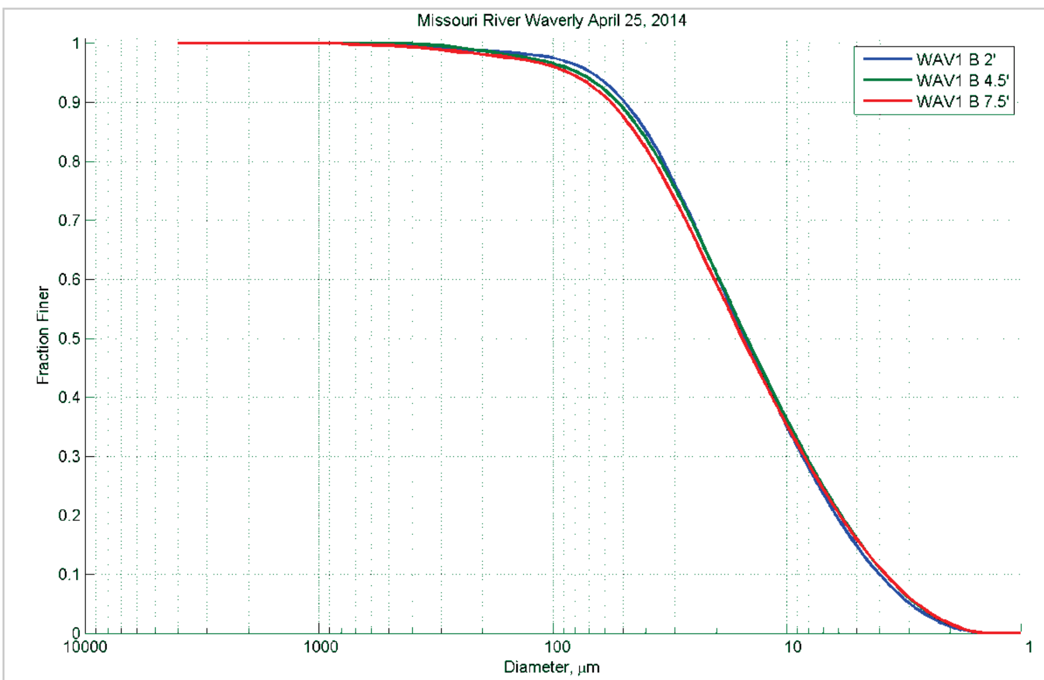

Figure 200. Particle size distribution at different depths (feet) in Station C - April 25, 2014.

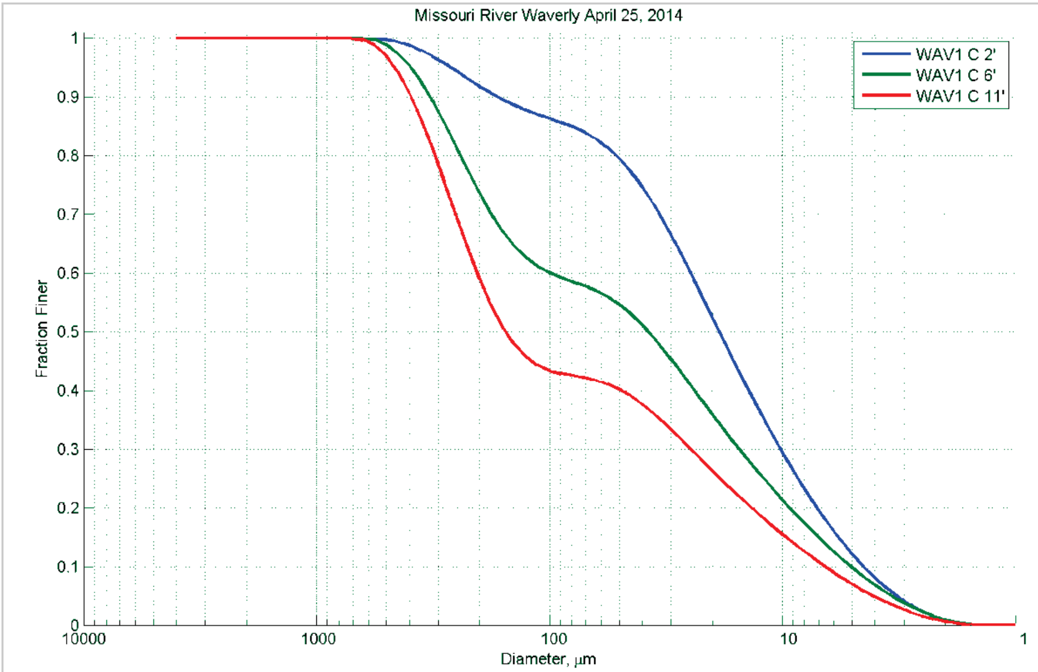

Figure 201. Particle size distribution at different depths (feet) in Station D - April 25, 2014.

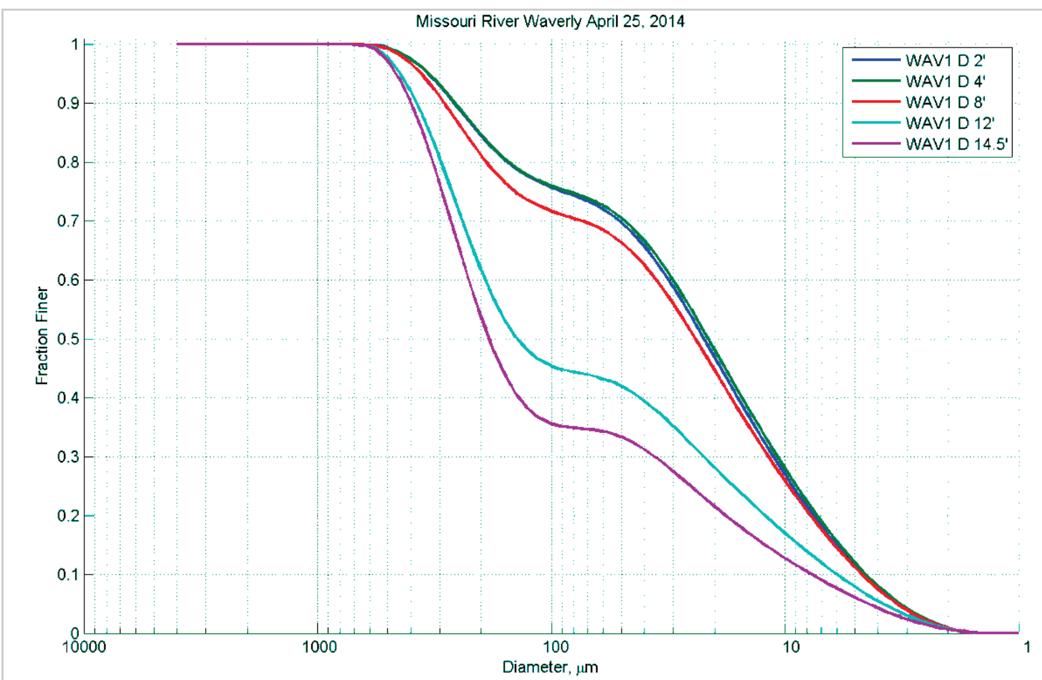

Figure 202. Particle size distribution at different depths (feet) in Station E - April 25, 2014.

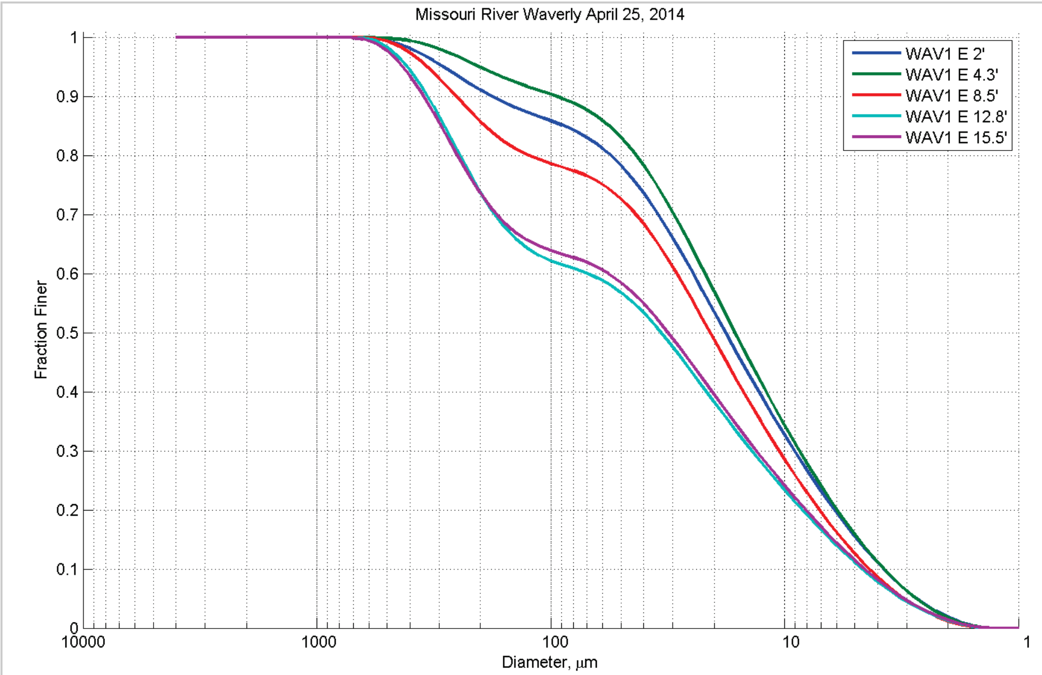

Particle size distribution for the second data collection date, June 10, 2014, is shown in Figure 203 to Figure 207.

Figure 203. Particle size distribution at different depths (feet) in Station A – June 10, 2014.

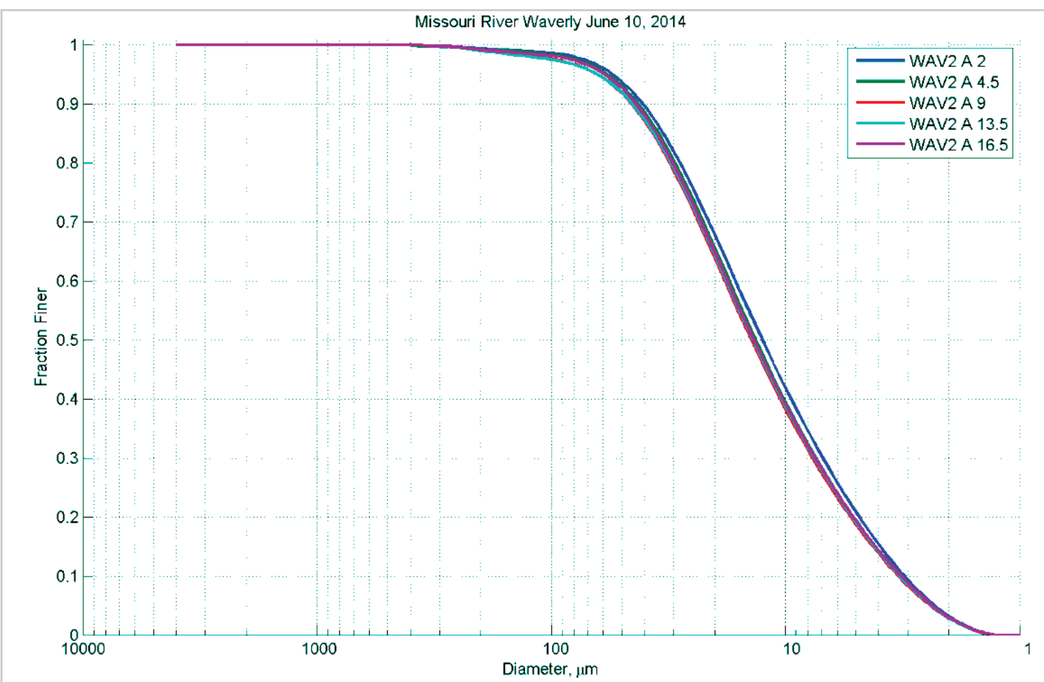

Figure 204. Particle size distribution at different depths (feet) in Station B – June 10, 2014.

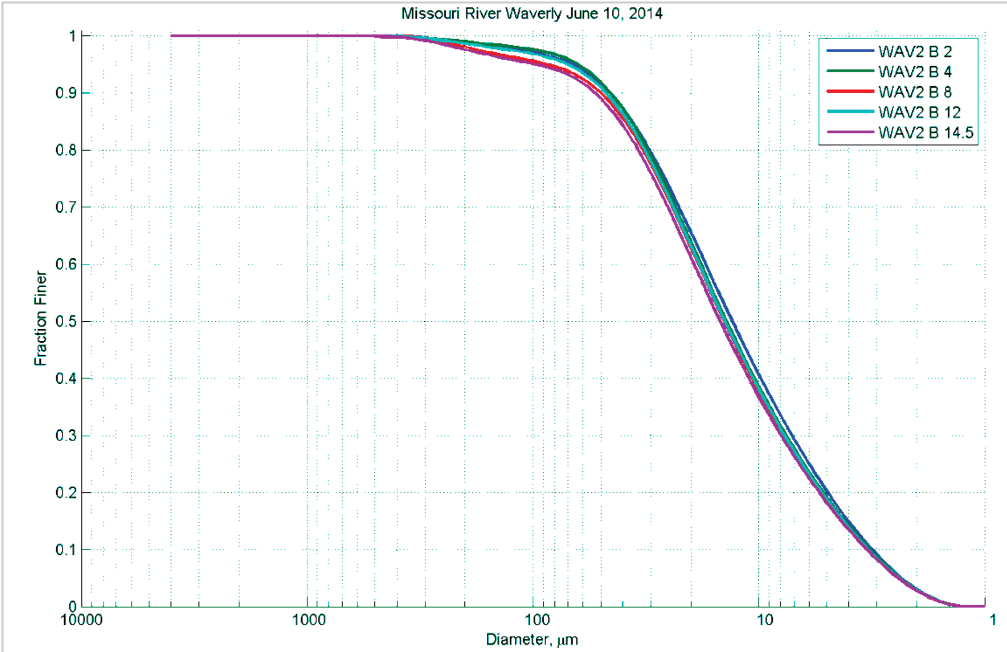

Figure 205. Particle size distribution at different depths (feet) in Station C – June 10, 2014.

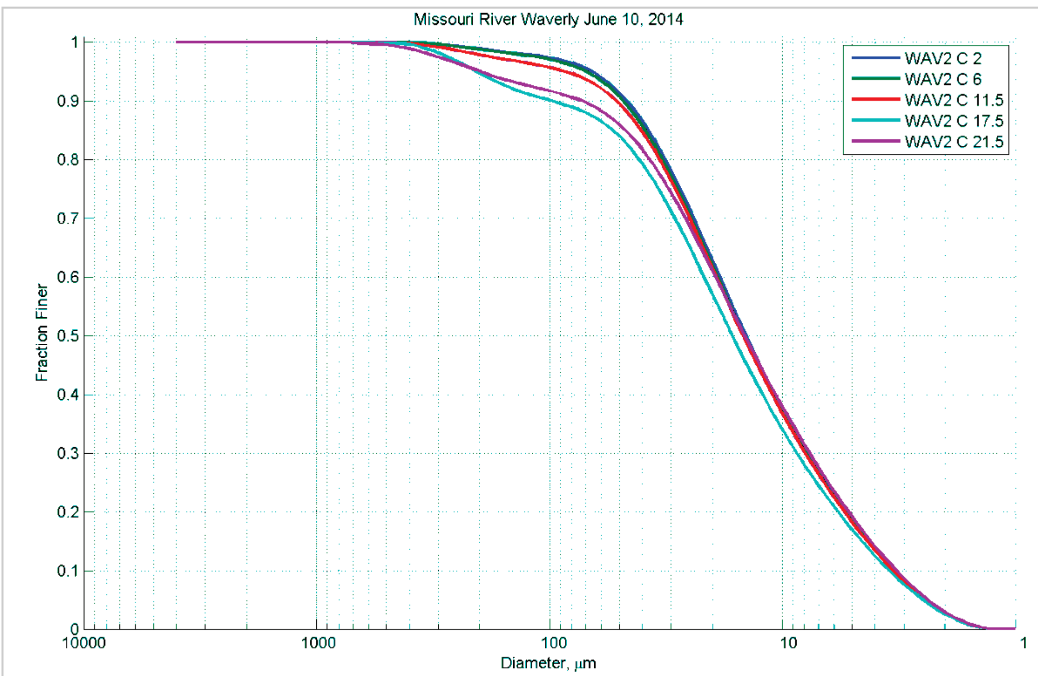

Figure 206. Particle size distribution at different depths (feet) in Station D – June 10, 2014.

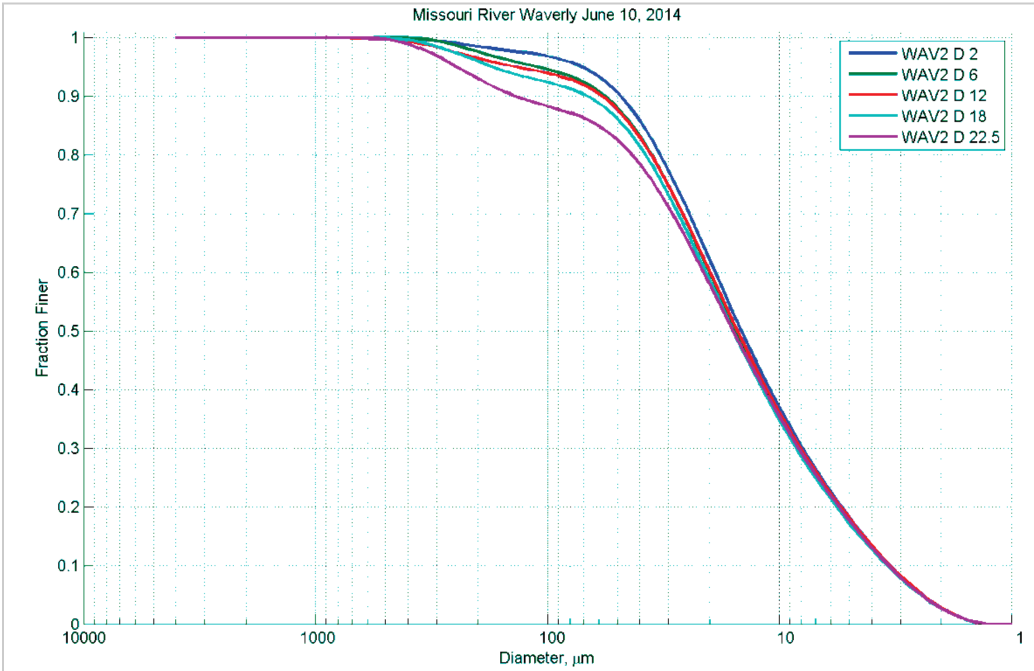

Figure 207. Particle size distribution at different depths (feet) in Station E – June 10, 2014.

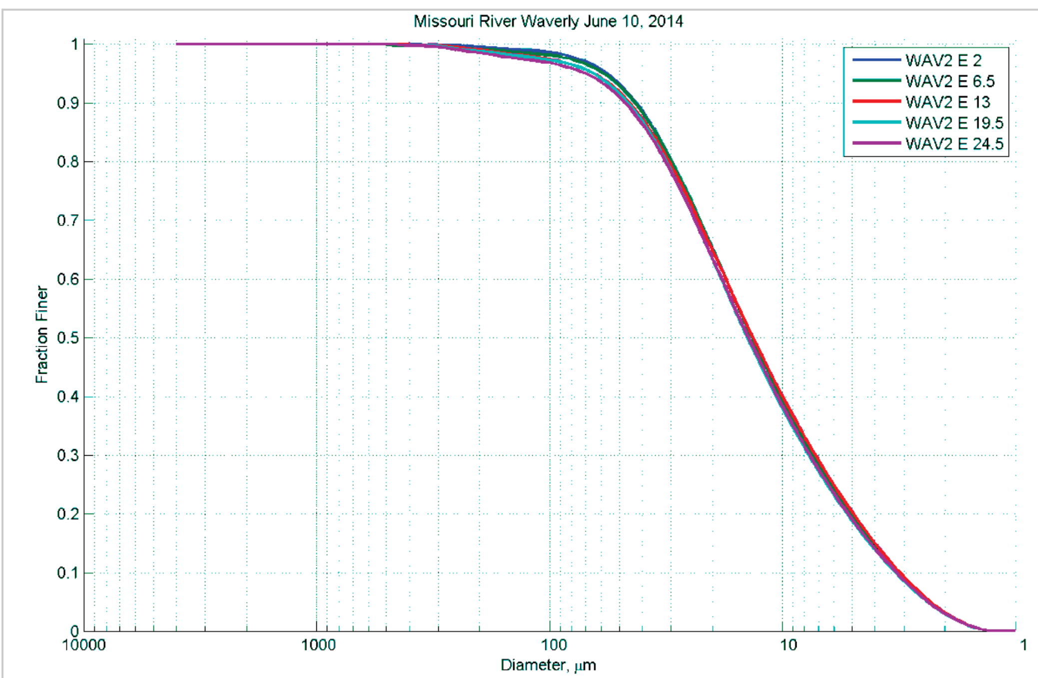

Particle size distribution for the third data collection date, June 25, 2014, is shown in Figure 208 to Figure 212.

Figure 208. Particle size distribution at different depths (feet) in Station A – June 25, 2014.

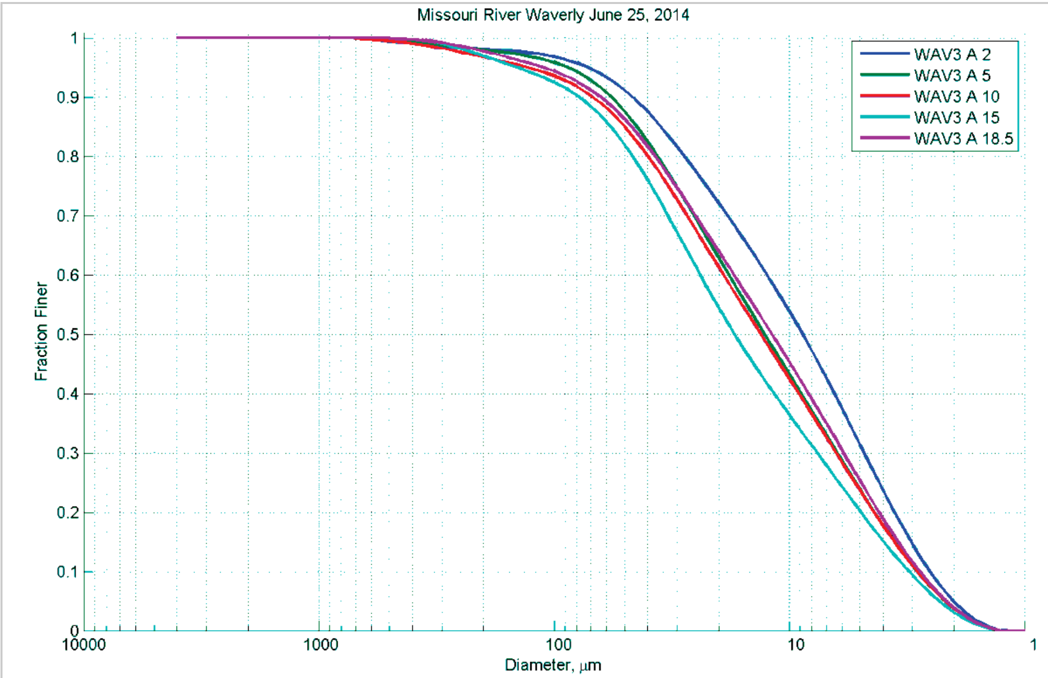

Figure 209. Particle size distribution at different depths (feet) in Station B – June 25, 2014.

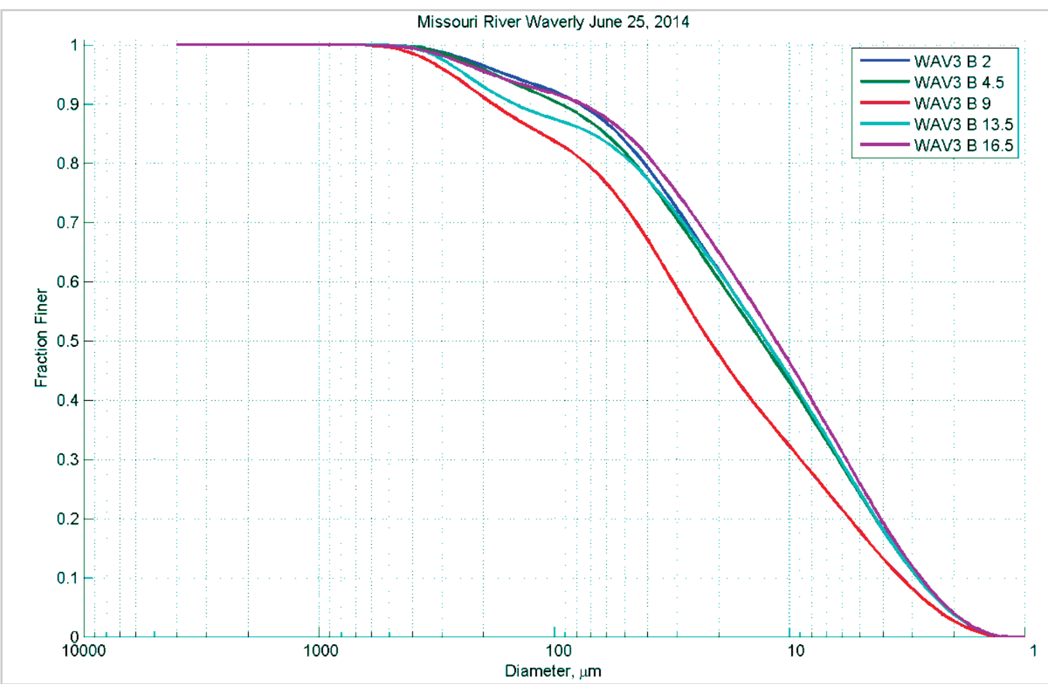

Figure 210. Particle size distribution at different depths (feet) in Station C – June 25, 2014.

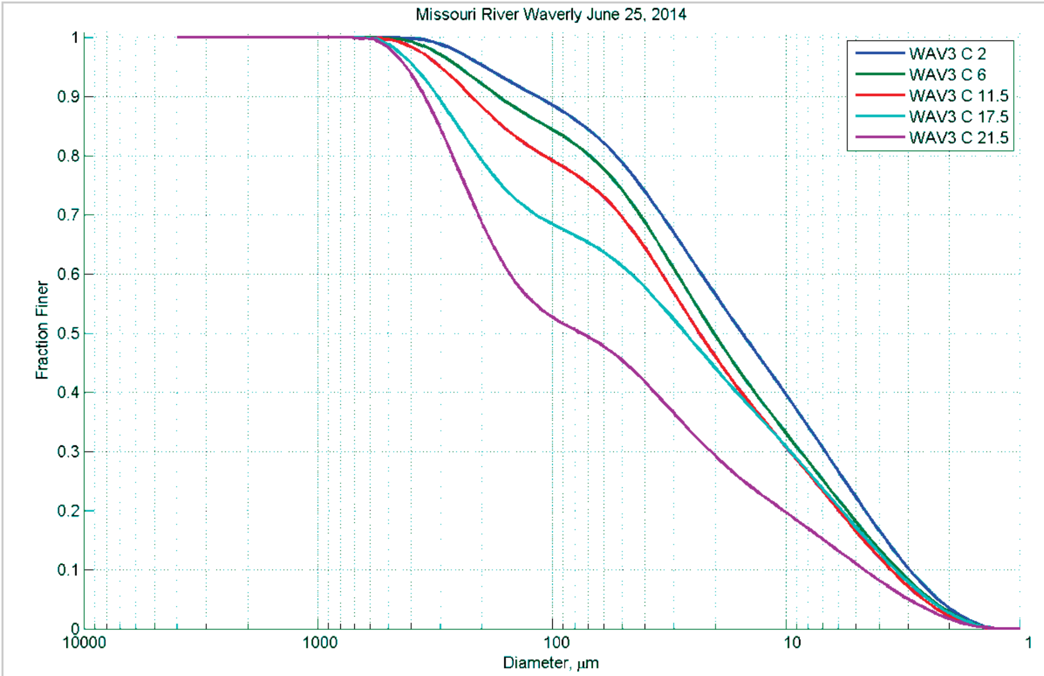

Figure 211. Particle size distribution at different depths (feet) in Station D – June 25, 2014.

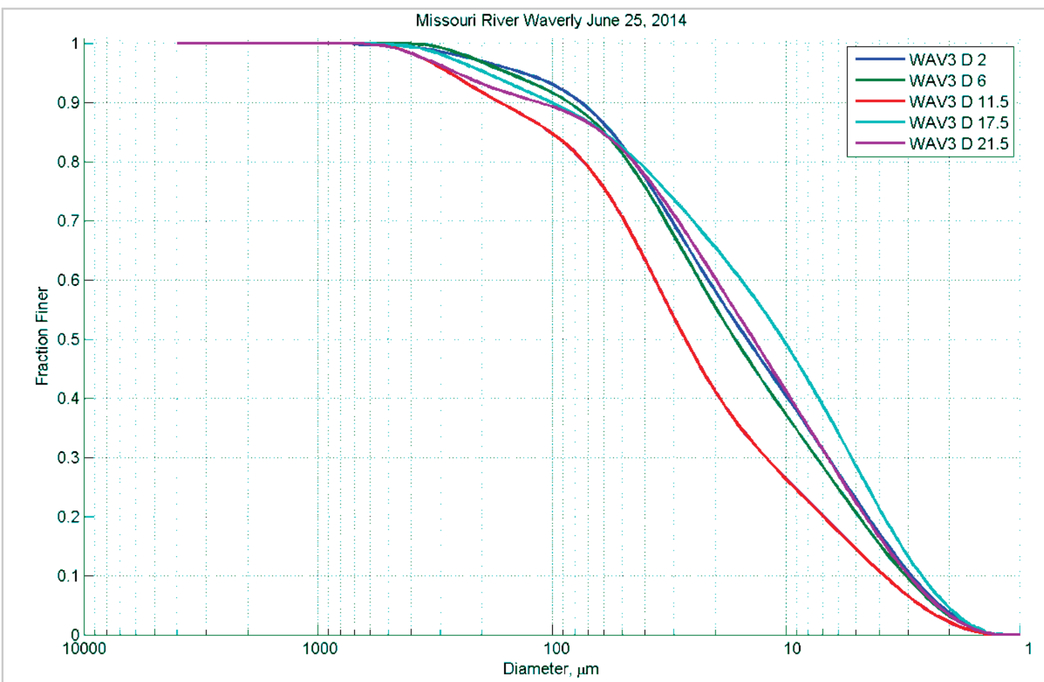

Figure 212. Particle size distribution at different depths (feet) in Station E – June 25, 2014.

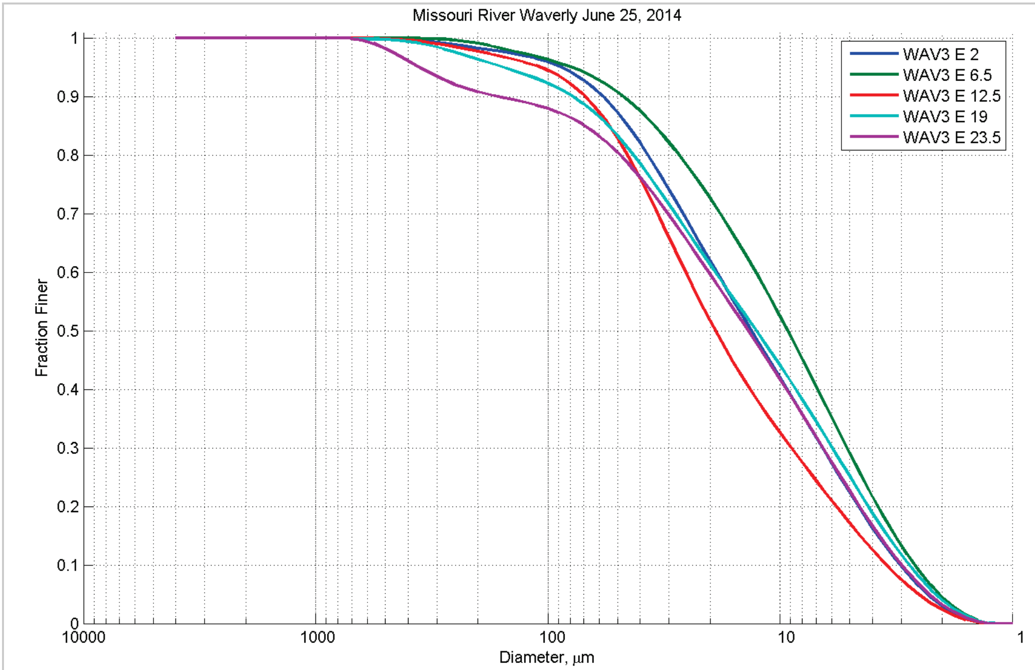

Suspended sediment concentration was also measured from the collected samples. Table 63 to Table 65 present the concentration values, for each data collection date. Suspended sediment concentration profiles were created using the measured data, presented in Figure 213 to Figure 215. See Appendix VI-f for more details about the measured data.

Table 63. Suspended sediment concentration at Waverly, MO – April 25, 2014.

Station	Depth (ft)	Concentration (mg/L)
WAV 1A	2	97.25
WAV 1A	4.5	96.67
WAV 1A	8	99.67
Total depth	12.7	(Bottom)
WAV 1B	2	106.03
WAV 1B	4.5	104.44
WAV 1B	7.5	112.87
Total depth	10.3	(Bottom)
WAV 1C	2	150.38
WAV 1C	6	191.58
WAV 1C	11	346.57
Total depth	13.2	(Bottom)
WAV 1D	2	167.81
WAV 1D	4	181.24
WAV 1D	8	221.58
WAV 1D	12	280.72
WAV 1D	14.5	341.15
Total depth	16.7	(Bottom)
WAV 1E	2	160.51
WAV 1E	4.3	162.86
WAV 1E	8.5	170.68
WAV 1E	12.8	197.61
WAV 1E	15.5	272.43
Total depth	17.3	(Bottom)

Table 64. Suspended sediment concentration at Waverly, MO – June 10, 2014.

Station	Depth (ft)	Concentration (mg/L)
WAV 2A	2	3,022.92
WAV 2A	4.5	3,026.48
WAV 2A	9	3,034.23
WAV 2A	13.5	2,703.64
WAV 2A	16.5	3,124.07
Total depth	19.2	(Bottom)
WAV 2B	2	3,135.25
WAV 2B	4	3,262.48
WAV 2B	8	3,274.48
WAV 2B	12	3,287.33
WAV 2B	14.5	3,497.02
Total depth	16.7	(Bottom)
WAV 2C	2	3,079.78
WAV 2C	6	3,391.11
WAV 2C	11.5	3,547.95
WAV 2C	17.5	3,932.97
WAV 2C	21.5	3,898.05
Total depth	23.1	(Bottom)
WAV 2D	2	3,219.75
WAV 2D	6	3,225.80
WAV 2D	12	3,422.95
WAV 2D	18	3,538.49
WAV 2D	22.5	3,532.57
Total depth	24.9	(Bottom)
WAV 2E	2	3,035.83
WAV 2E	6.5	3,054.22
WAV 2E	13	3,072.98
WAV 2E	19.5	3,154.61
WAV 2E	24.5	3,196.83
Total depth	26.2	(Bottom)

Table 65. Suspended sediment concentration at Waverly, MO – June 25, 2014.

Station	Depth (ft)	Concentration (mg/L)
WAV 3A	2	1,400.55
WAV 3A	5	1,400.48
WAV 3A	10	1,407.42
WAV 3A	15	1,443.53
WAV 3A	18.5	1,510.19
Total depth	21.4	(Bottom)
WAV 3B	2	1,519.30
WAV 3B	4.5	1,560.84
WAV 3B	9	1,612.44
WAV 3B	13.5	1,721.34
WAV 3B	16.5	1,773.26
Total depth	20.3	(Bottom)
WAV 3C	2	1,493.78
WAV 3C	6	1,337.12
WAV 3C	11.5	1,194.31
WAV 3C	17.5	1,804.44
WAV 3C	21.5	2,072.75
Total depth	24.3	(Bottom)
WAV 3D	2	1,470.92
WAV 3D	6	1,636.29
WAV 3D	11.5	1,698.54
WAV 3D	17.5	1,675.89
WAV 3D	21.5	1,778.93
Total depth	24.3	(Bottom)
WAV 3E	2	1,418.51
WAV 3E	6.5	1,443.15
WAV 3E	12.5	1,449.36
WAV 3E	19	1,511.53
WAV 3E	23.5	1,806.04
Total depth	26.7	(Bottom)

Figure 213. Suspended sediment concentration at Waverly, MO – April 25, 2014.

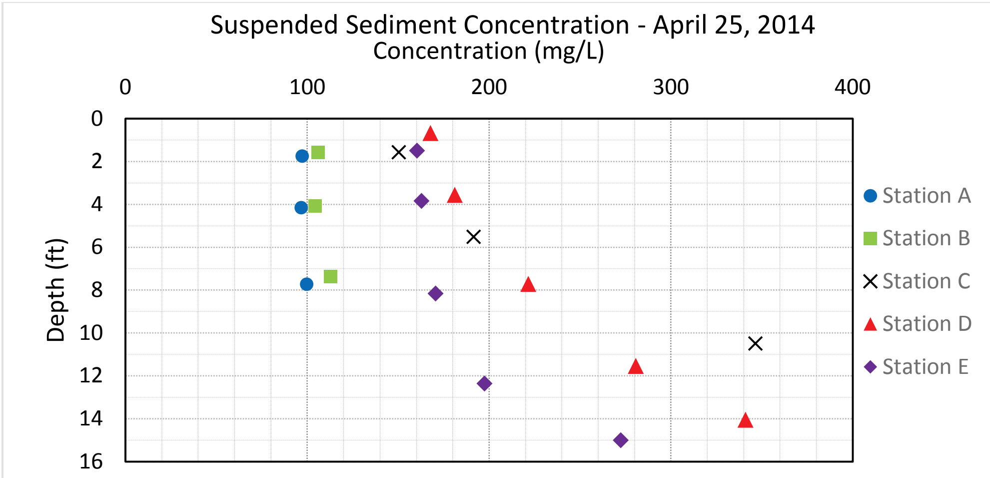

Figure 214. Suspended Sediment concentration at Waverly, MO – June 10, 2014.

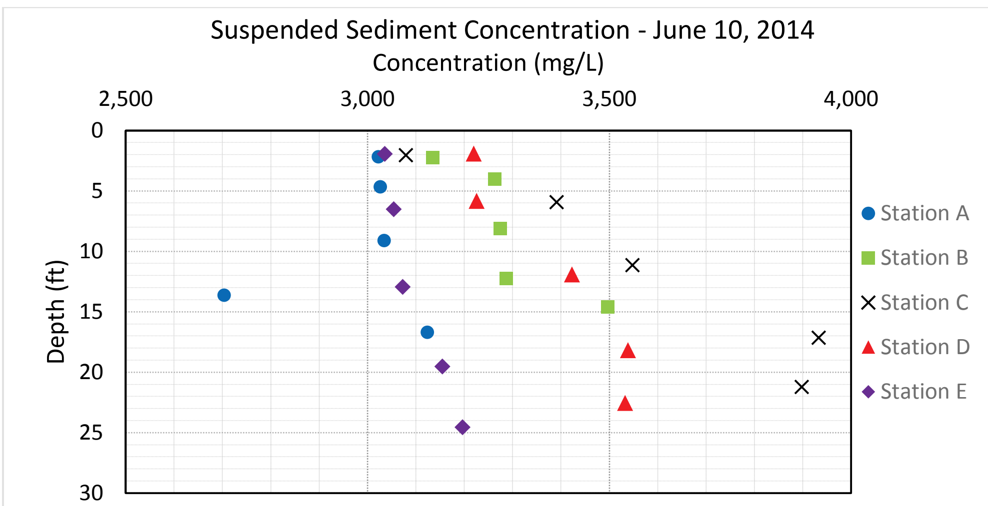

Figure 215. Suspended sediment concentration at Waverly, MO – June 25, 2014.

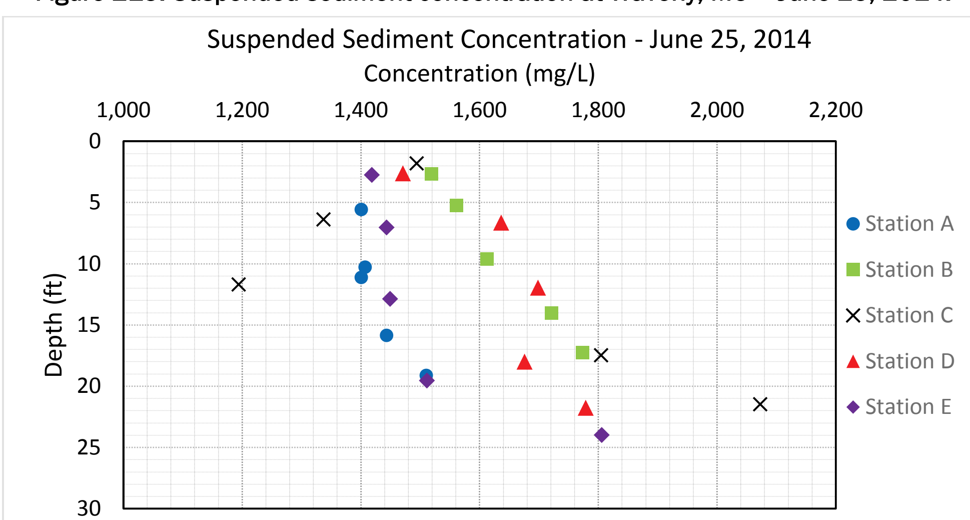

The suspended sediment concentration data were used to calibrate the ADCP acoustic backscatter and develop suspended sediment concentration profiles across the channel. Figure 216 to Figure 218 show the suspended sediment concentration profiles for the first left-to-right ADCP pass, for each data collection date. To see the other profiles, see Appendix VI-f.

Figure 216. Suspended sediment concentration profile at Waverly, MO – April 25, 2014.

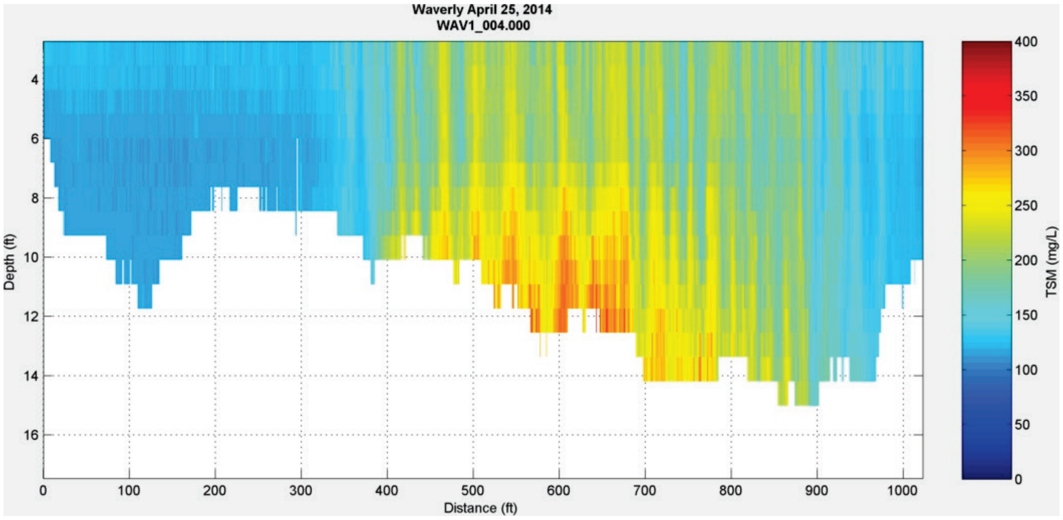

Figure 217. Suspended sediment concentration profile at Waverly, MO – June 10, 2014.

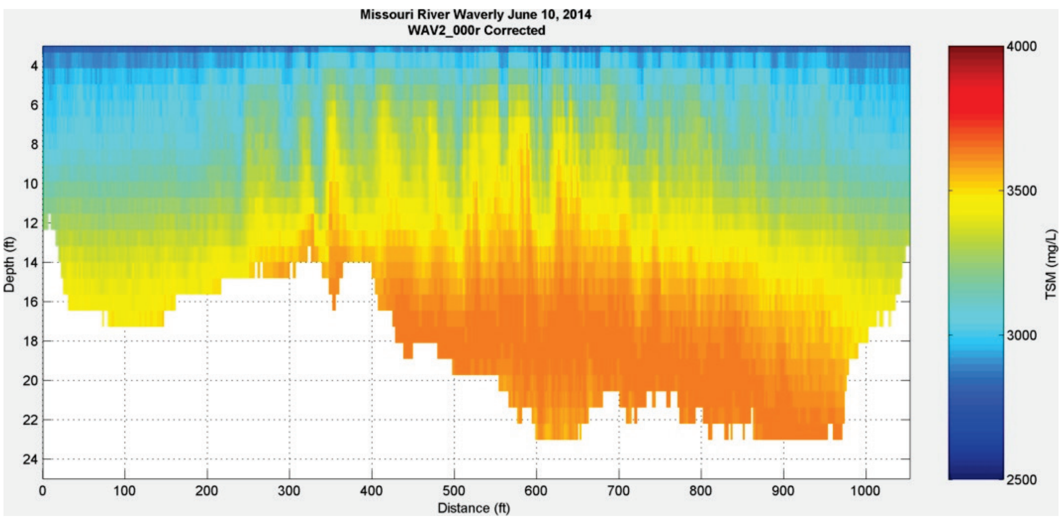

Figure 218. Suspended sediment concentration profile at Waverly, MO – June 25, 2014.

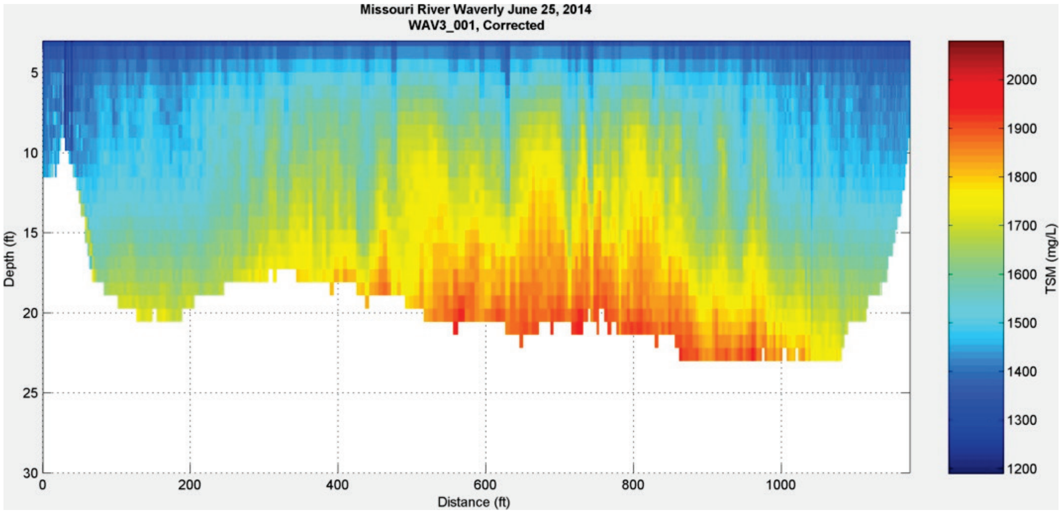

The suspended sediment concentration cross-section profiles obtained from the ADCP measurements were combined with the flow discharges, also obtained from the ADCP, to obtain the suspended sediment transport load, in tons per day. The method used for this study is explained in Heath et al. (2015, 13–14). The suspended sediment load can be divided classifying the suspended material by size and soil type. Table 66 presents the suspended sediment transport load, according to both classifications, for the first data collection date April 30, 2014. Table 67 and Table 68 present the same information for the second and third data collection dates, respectively. In all three tables, the categories under the Soil Type Classification were determined as follows: Clay Flux groups the size fractions 0.0001 to 0.0004 mm, Silt Flux 0.0004 to 0.0625 mm, and Sand Flux 0.0625 to 2.00 mm.

Table 66. Suspended sediment load distributed by grain size and soil type – April 25, 2014.

Classification System	Category	Sediment Flux (tons/day)
Total load		22,078.59
Sediment size classification	0.001 - 0.004 mm	1,713.42
	0.004 - 0.008 mm	3,016.98
	0.008 - 0.016 mm	4,100.20
	0.016 - 0.031 mm	4,300.82
	0.031 - 0.063 mm	3,087.95
	0.063 - 0.125 mm	1,015.39
	0.125 - 0.250 mm	2,121.62
	0.250 - 0.500 mm	2,434.15
	0.500 - 1.00 mm	288.07
	1.00 - 2.00 mm	0.00
Soil type classification	Clay	1,713.42
	Silt	14,505.95
	Sand	5,859.23

Table 67. Suspended sediment load distributed by grain size and soil type – June 10, 2014.

Classification System	Category	Sediment Flux (tons/day)
Total load		890,008.59
Sediment size classification	0.001 - 0.004 mm	113,908.73
	0.004 - 0.008 mm	148,930.57
	0.008 - 0.016 mm	202,881.72
	0.016 - 0.031 mm	216,836.07
	0.031 - 0.063 mm	142,353.71
	0.063 - 0.125 mm	34,223.26
	0.125 - 0.250 mm	18,861.66
	0.250 - 0.500 mm	11,600.02
	0.500 - 1.00 mm	412.84
	1.00 - 2.00 mm	0.00
Soil type classification	Clay	113,908.73
	Silt	711,002.07
	Sand	65,097.78

Table 68. Suspended sediment load distributed by grain size and soil type – June 25, 2014.

Classification System	Category	Sediment Flux (tons/day)
Total load		507,574.54
Sediment size classification	0.001 - 0.004 mm	77,140.90
	0.004 - 0.008 mm	88,893.20
	0.008 - 0.016 mm	87,697.16
	0.016 - 0.031 mm	86,732.06
	0.031 - 0.063 mm	79,260.94
	0.063 - 0.125 mm	35,335.76
	0.125 - 0.250 mm	27,996.53
	0.250 - 0.500 mm	22,287.52
	0.500 - 1.00 mm	2,230.48
	1.00 - 2.00 mm	0.00
Soil type classification	Clay	77,140.90
	Silt	342,583.36
	Sand	87,850.29

8.7 Bed load transport

The ISSDOTv2 method was used for computing the bed-load transport. Table 69 shows the values obtained for the bed load, as well as the other sediment quantities determined from the suspended sediment samples at the Waverly site. It provides a breakdown of the various measured sediment transport components, based on sediment size classification.

Table 69. Bed-load transport values from Waverly, MO.

Data Collection Date	25-Apr-14	10-Jun-14	25-Jun-14
Flow (cfs)	43,566	100,478	117,347
Bed Load (tons/day)	1,734	5,648	5,288
Suspended BML (tons/day)	5,859	65,098	87,850
Total BML (tons/day)	7,593	70,745	93,139
Bed Load Fraction (%)	22.8%	8.0%	5.7%
Wash Load (tons/day)	16,219	824,911	419,724
Total Load	23,812	895,656	512,863

In Table 69, *bed load* is defined as the bed material moving at the bottom of the river in bed-forms; *suspended BML* refers to the suspended material with grain size higher than 0.063 mm; *total BML* is the sum of bed load and suspended BML; *bed load fraction* is the percentage of the total bed

material moving as bed load; *wash load* is fine sediments that never settle in the bed, with grain size of 0.063 or less; and *total load* combines the quantity of total BML and wash load.

A bed-load rating curve was prepared for this site by plotting the bed-load transport in tons per day versus the river flowrate. This graph is shown in Figure 219. As in the case of the St. Joseph and Kansas City data, trip 1 was a much lower flow than trip 2 and 3, as shown in Table 69. Accordingly, the bed-load transport for the last two trips is noticeably higher. The bed-load fraction also falls off considerably since more BML is going into suspension at the higher flows. However, the three points do not show the same strong linearity as the St. Joseph data, and the bed-load transport rate at the highest flow (trip3) is slightly lower than trip 2.

Figure 219. Bed-load rating curve for Waverly, MO.

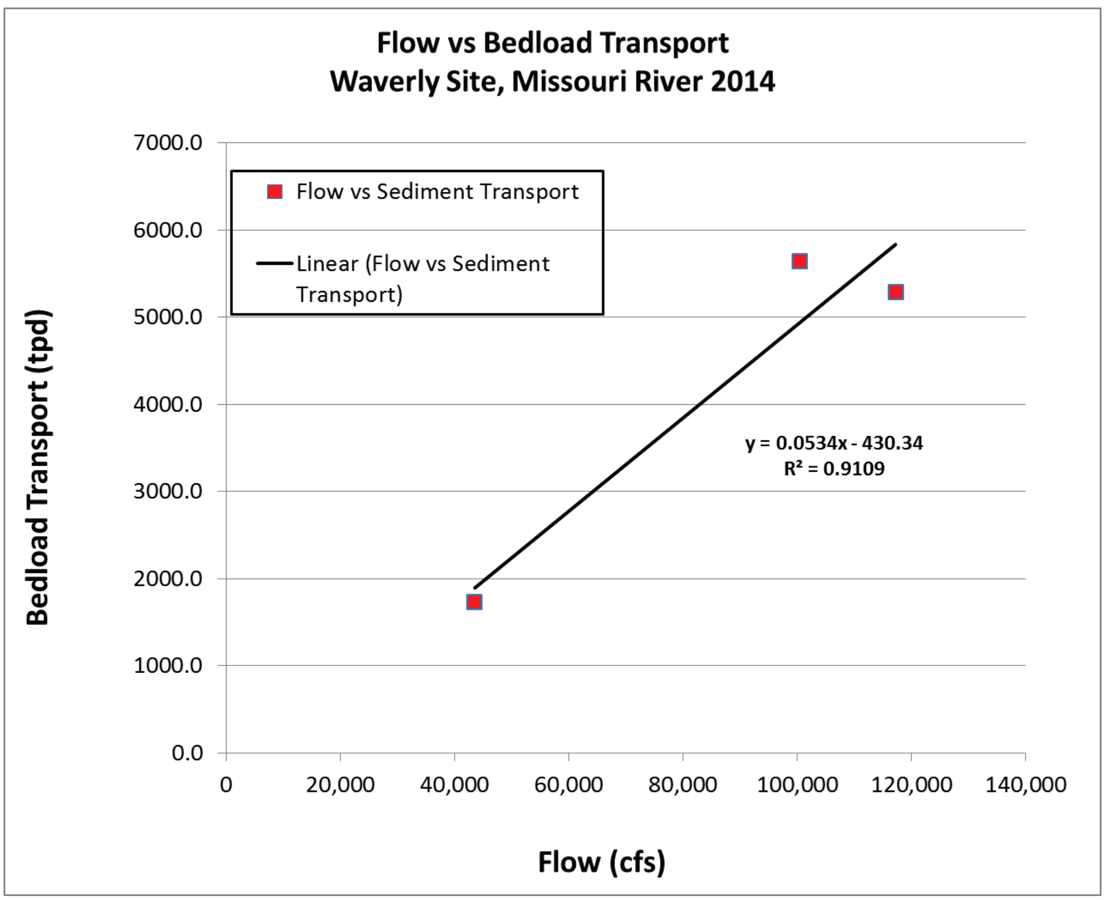

Bed-load transport values were also computed for this site using two analytic transport functions. One is the MPM formula, and the other is the Einstein formula. They were computed for each swath of bathymetric data.

For instance, Figure 220 shows the bathymetry of this site with the six swath numbers (S1 to S6) labeled on it, indicating the lateral position where each swath was located. The hydraulic and sediment parameters obtained in the field data collection effort discussed before were extracted for each of these swaths.

Figure 220. Bathymetry for Missouri River at Waverly, MO, showing swath locations.

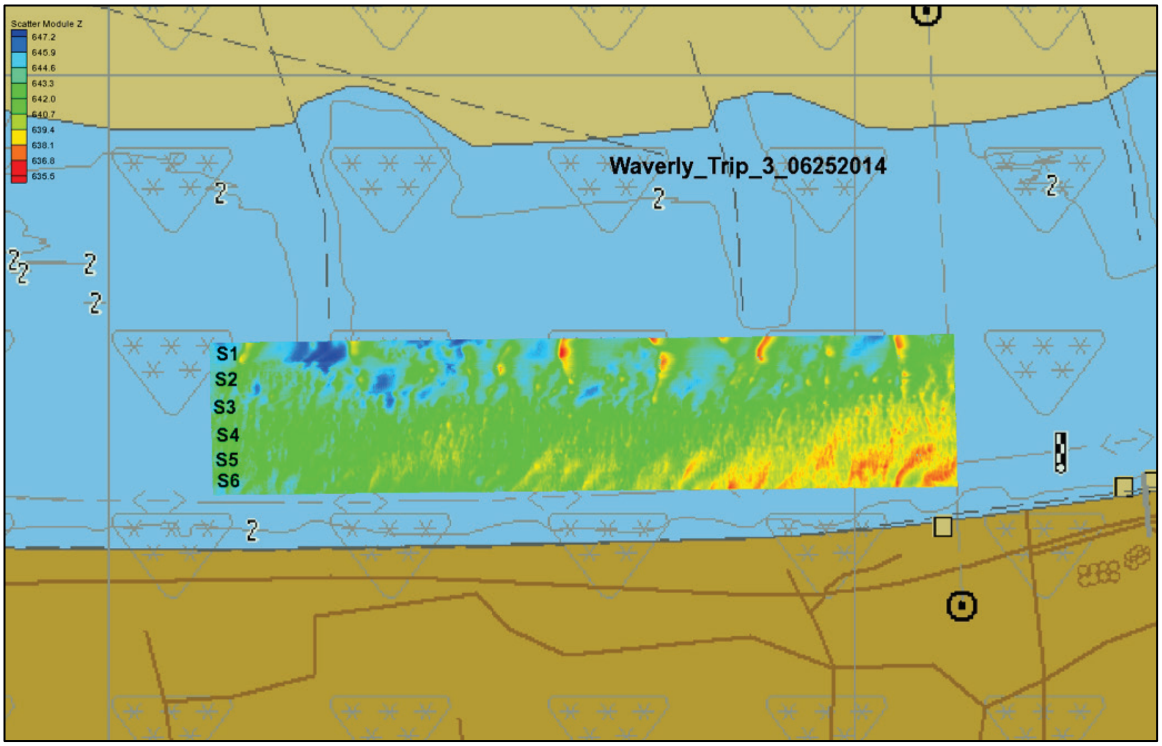

Flow, average velocity, and water depth were obtained from the ADCP data by a separate program written for that specific purpose. Water slope and water temperature were obtained from each appropriate data appendix. Bed sediment gradations used were selected based on their proximity to a given swath. The SAM Hydraulic Design Package for Channels program was then used with these data to compute the bed-load values for each swath. This software package has provisions for entering hydraulic and sediment input parameters and can then compute bed-load transport values for several commonly used transport functions.

The results are plotted in Figure 221 to Figure 223 and show how the transport function values compare to the ISSDOTv2 measured values. They also show the lateral variability across the measured section from the left side to the right side of the channel.

Figure 221. Bed-load transport at Waverly, MO – April 25, 2014: ISSDOTv2 values compared to transport function computed values.

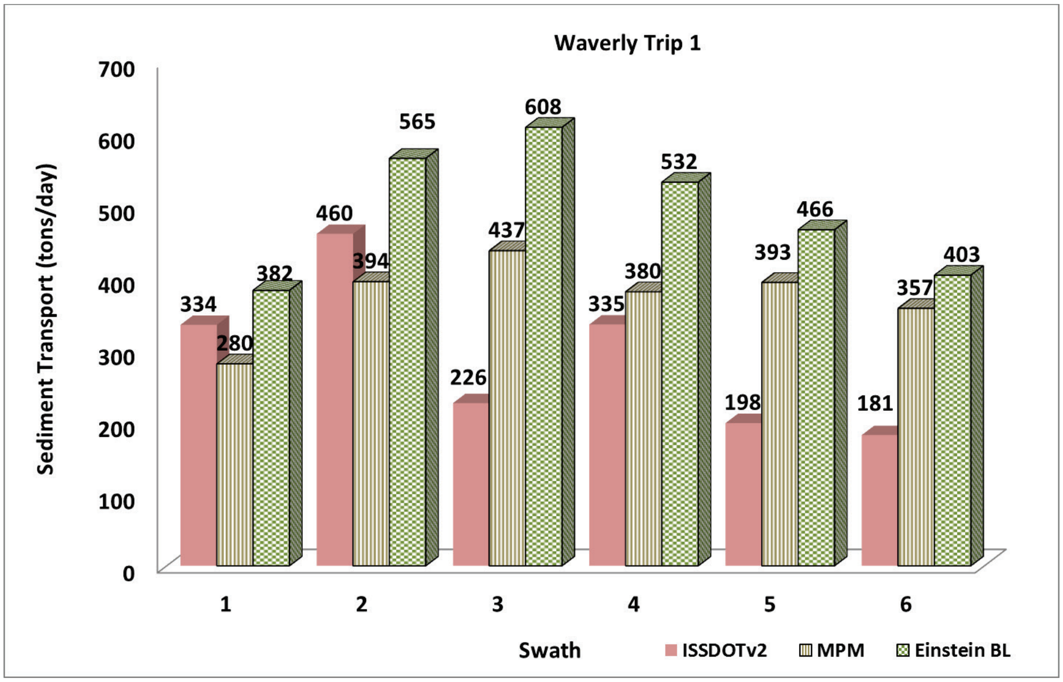

Figure 222. Bed-load transport at Waverly, MO – June 10, 2014: ISSDOTv2 values compared to transport function computed values.

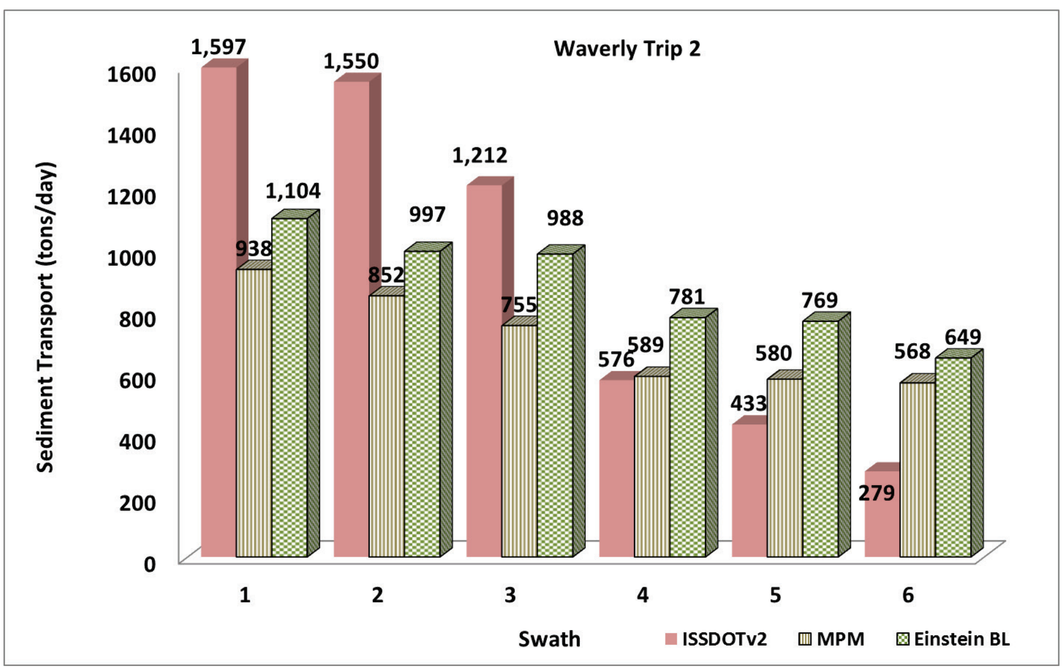

Figure 223. Bed-load transport at Waverly, MO – June 25, 2014: ISSDOTv2 values compared to transport function computed values.

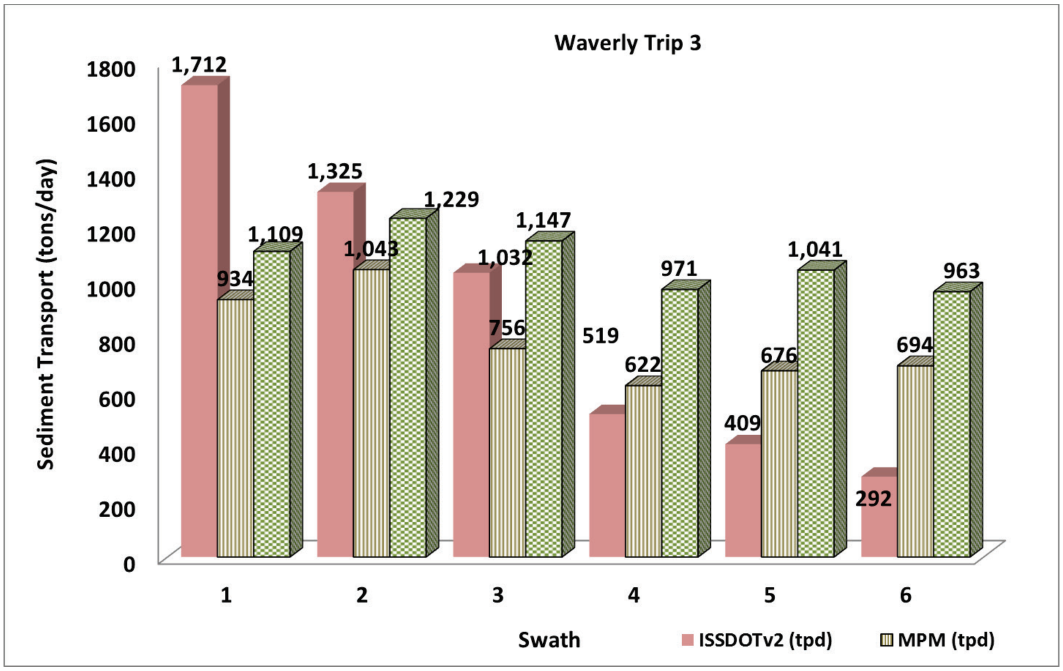

9 Site 7: Hermann, Missouri

Multi-beam surveys, ADCP flow and velocity measurements, bed and suspended material sampling and testing, and water temperature, water surface elevation, and slope measurements were performed during each data collection date at Hermann, MO. The measuring area is shown on Figure 224 as the green polygon. The approximate location of the USGS gage station near the data collection site is also shown as the blue pin. This location might not be accurate in the figure. Coordinates for the gage site as given in the USGS web site are listed in Table 3. The red line indicates the cross section where ADCP measurements were conducted and suspended and bed load material samples were collected. The bank-to-bank width of the river at this location is estimated to range between 990 and 1,200 ft, and the length of the study area was approximately 2,000 ft. The data collection dates for this site were April 24, 2014; June 11, 2014; and June 26, 2014.

Figure 224. Hermann, MO, data collection site.

9.1 ADCP flow and velocity

The velocity and discharge for each data collection date, and site, were measured using an ADCP. Table 70 presents the cross-section average flow (ft^3/s), area (ft^2), and average velocity (ft/s) for each date, calculated from the measured data. See Appendix VI-a for the measured data.

Table 70. Total flow, area, and average velocity on the given dates at Hermann, MO.

Date	Total Flow, Q (ft^3/s)	Total Area, A (ft^2)	Velocity Q/A (ft/s)
April 24, 2014	48,771	14,656	3.33
June 11, 2014	191,044	31,843	6.0
June 26, 2014	131,327	26,032	5.05

Real-time vertical profiles of instantaneous velocities are also obtained from the ADCP measurements. Figure 225 to Figure 227 present the velocity magnitude, before the multi-beam measurements, from left to right. In the figures, the velocity magnitude is quantified by the range of colors shown on the right side of each figure, where the higher velocities are denoted by red and the lower velocities by blue. The velocity profiles for after the multi-beam measurements are available at Appendix VI-a.

Figure 225. Velocity magnitude at Hermann, MO – April 24, 2014, 16:48:52.

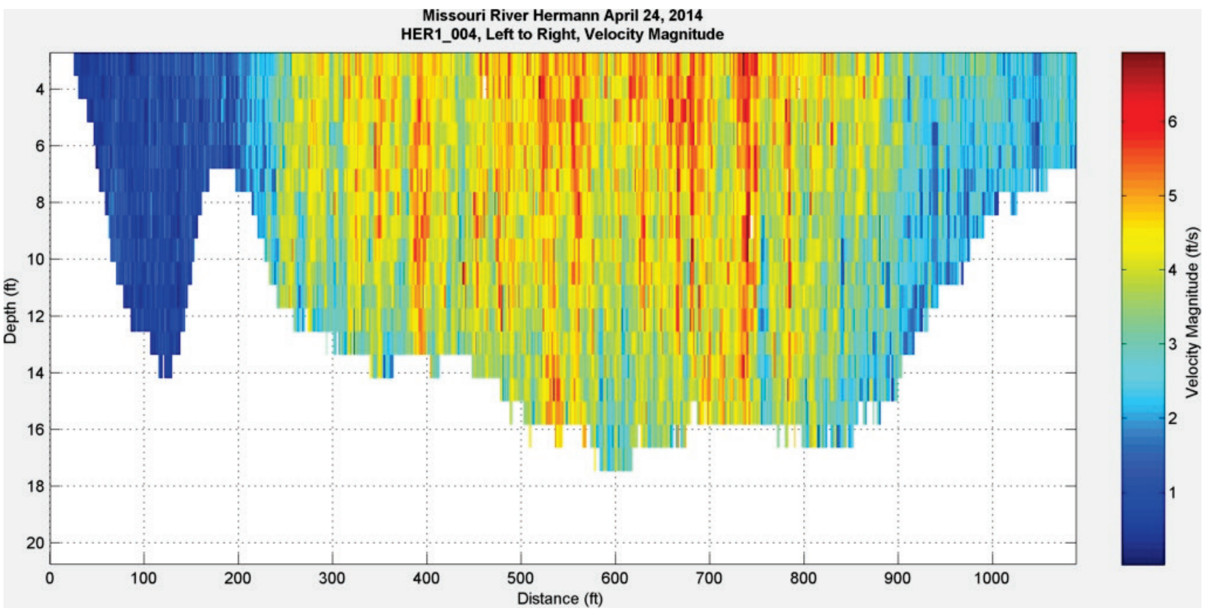

Figure 226. Velocity magnitude at Hermann, MO – June 11, 2014, 16:38:54.

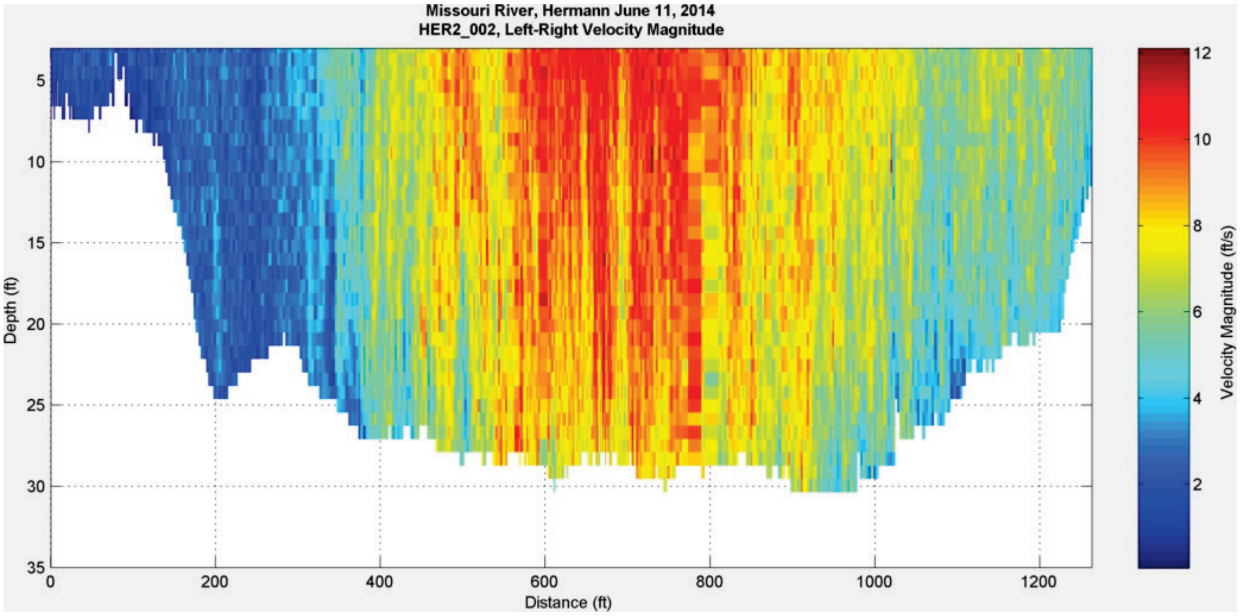

Figure 227. Velocity magnitude at Hermann, MO – June 26, 2014, 16:40:20.

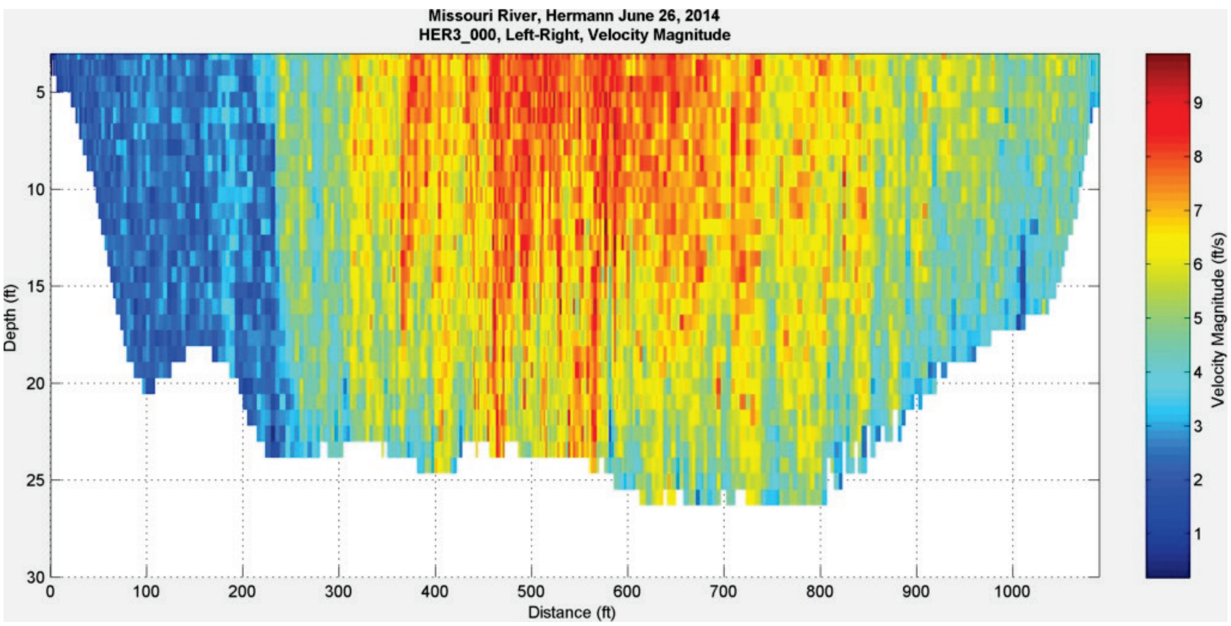

9.2 Water surface elevation and slope

Water surface elevation measurements were taken upstream and downstream of the multi-beam survey area. Figure 228 shows the upstream elevations, at distance zero, connected to the downstream elevations, at a distance of 2,000 ft, for each data collection date. Table 71 presents the slope values for the Hermann, MO, location for the three dates. The measured data are available at Appendix VI-b.

Figure 228. Water surface elevation at Hermann, MO – from upstream to downstream.

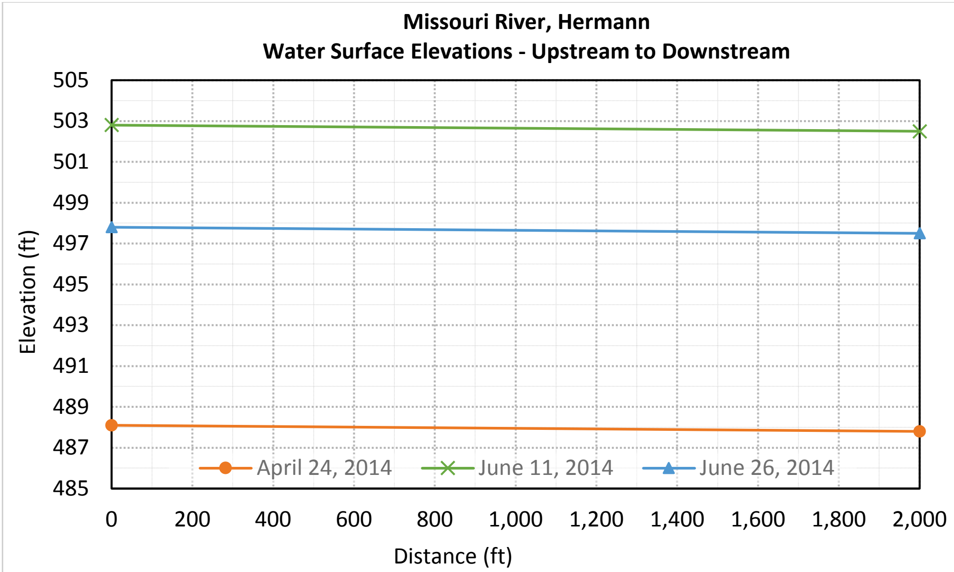

Table 71. Water surface slopes at Hermann, MO.

Date	Water Surface Slope (%)
April 25, 2014	0.00015
June 10, 2014	0.00015
June 25, 2014	0.00015

9.3 Water temperature

Table 72 presents the average temperature for each date, see Appendix VI-g for the measured values.

Table 72. Water temperature at Hermann, MO.

Date	Temperature (F)
April 24, 2014	59.8
June 11, 2014	71.4
June 26, 2014	80

9.4 Multi-beam surveys

The initial multi-beam survey performed at Hermann, MO, included the full extent of the channel from bank to bank, as shown in Figure 229 where the dark blue areas are deeper and the red areas are shallower. This survey is used to determine the location of the sand waves throughout the study area and to then decide where to run the ISSDOTv2 swaths according to the location of the active sand transport portion of the channel. The selected area with swath lines and numbers displayed in red is shown in Figure 230.

This shows the actual area that was used for the ISSDOTv2 bed-load computations. The length of the multi-beam swaths is approximately 2,000 ft for all three data collection dates.

Figure 229. Multi-beam survey extent at Hermann, MO – April 24, 2014.

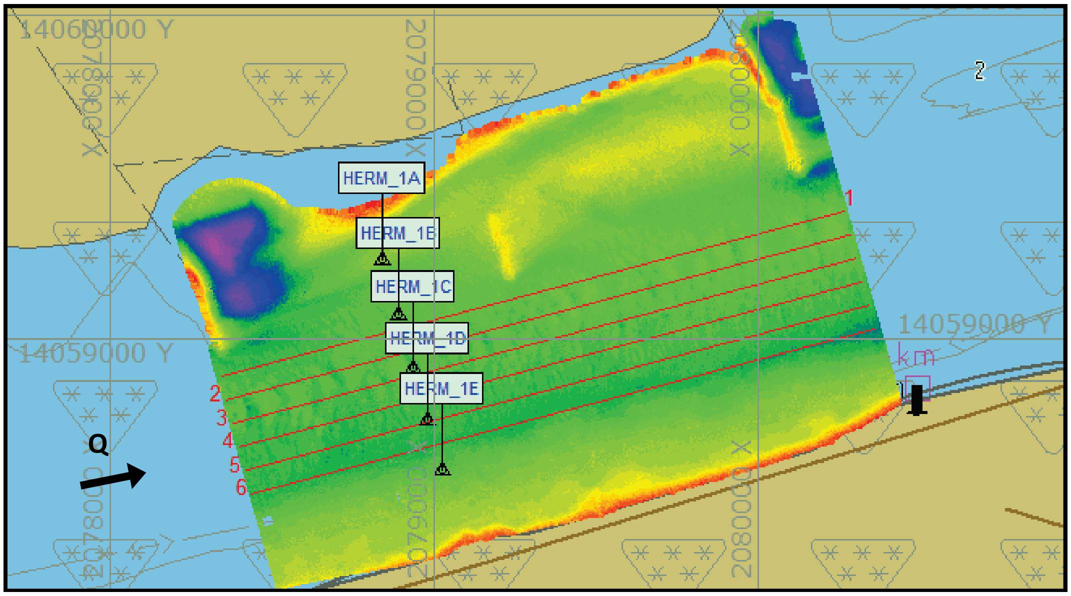

Figure 230. Multi-beam survey extent at Waverly, MO – June 11 and June 26, 2014.

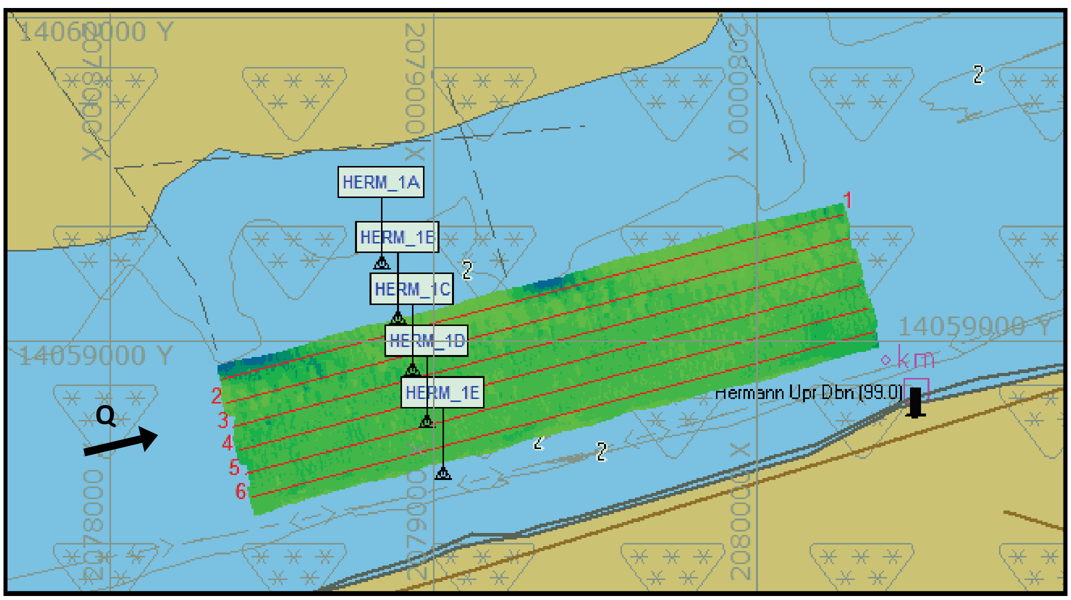

9.5 Bed material samples

Five sediment sample stations were positioned equidistant from each other along the cross section, as presented on Figure 231, which is the same location at which the suspended sediment samples and the ADCP velocity data were obtained. The first station, Station A, was positioned on the left descending bank and the last station, Station E, on the right descending bank. Table 73 provides the locations of sample stations according to NAD83. See Appendix VI-c for the coordinates using the UTM Grid System.

Table 73. Sediment sample stations NAD83 coordinates at Hermann, MO.

Station	NAD83 Latitude	NAD83 Longitude
HER A	38° 42' 21.3707" N	91° 27' 47.3025" W
HER B	38° 42' 19.6835" N	91° 27' 46.7247" W
HER C	38° 42' 18.0727" N	91° 27' 46.1988" W
HER D	38° 42' 16.483" N	91° 27' 45.6583" W
HER E	38° 42' 14.9143" N	91° 27' 45.1033" W

Figure 231. Sediment sample stations at the Missouri River – Hermann, MO.

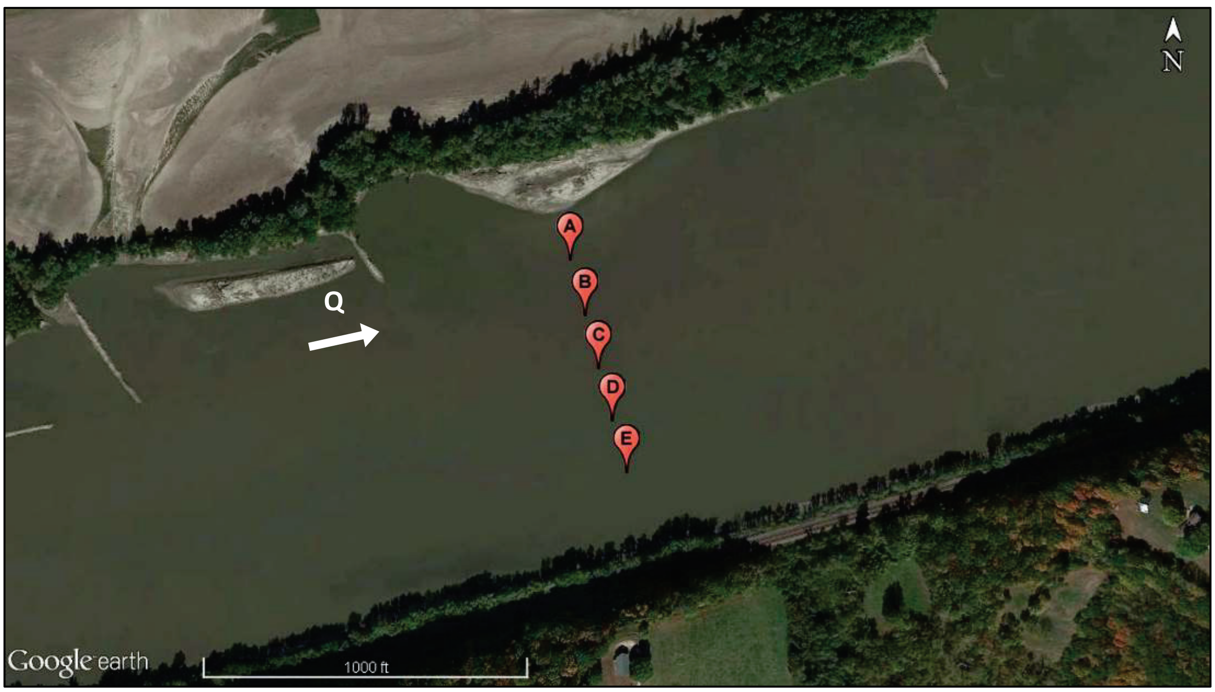

The grain size distribution for the five bed material samples of the first collection date, April 24, 2014, is provided at Figure 232. Figure 233 and Figure 234 present the gradation analysis for the second and third collected samples, respectively. The measured data are available in Appendix VI-d.

Figure 232. Bed material grain size distribution for Hermann, MO – April 24, 2014.

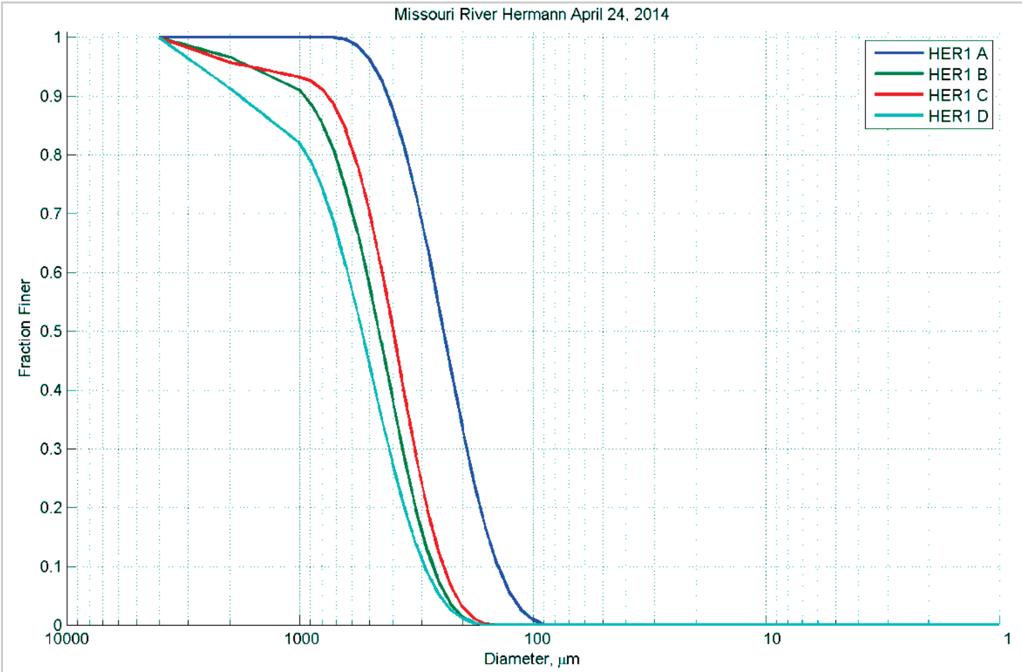

Figure 233. Bed material grain size distribution for Hermann, MO – June 11, 2014.

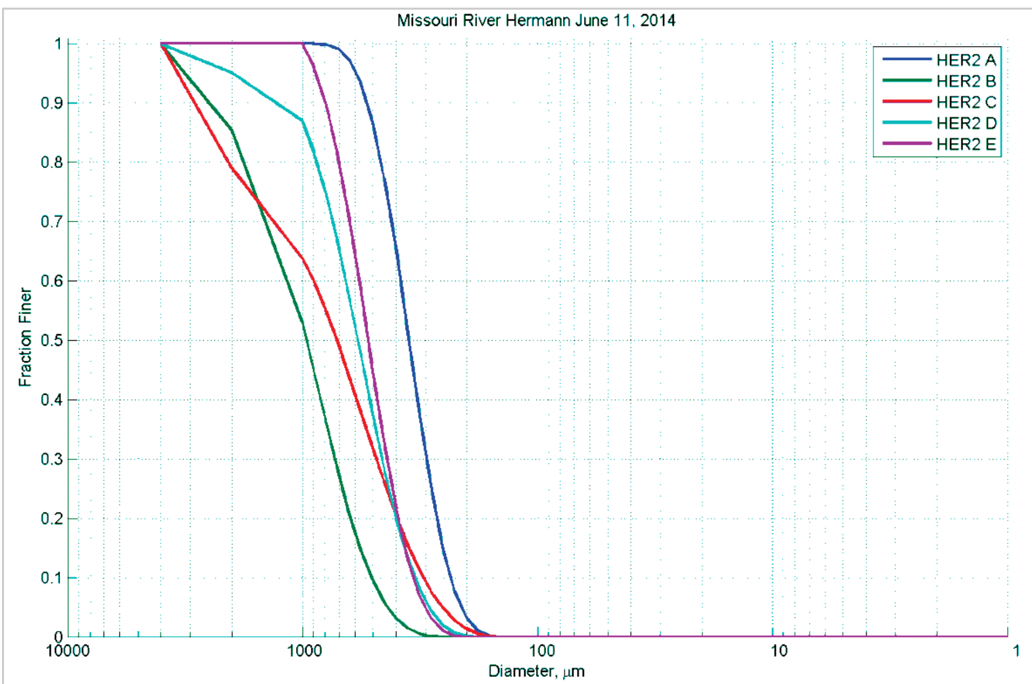

Figure 234. Bed material grain size distribution for Hermann, MO – June 26, 2014.

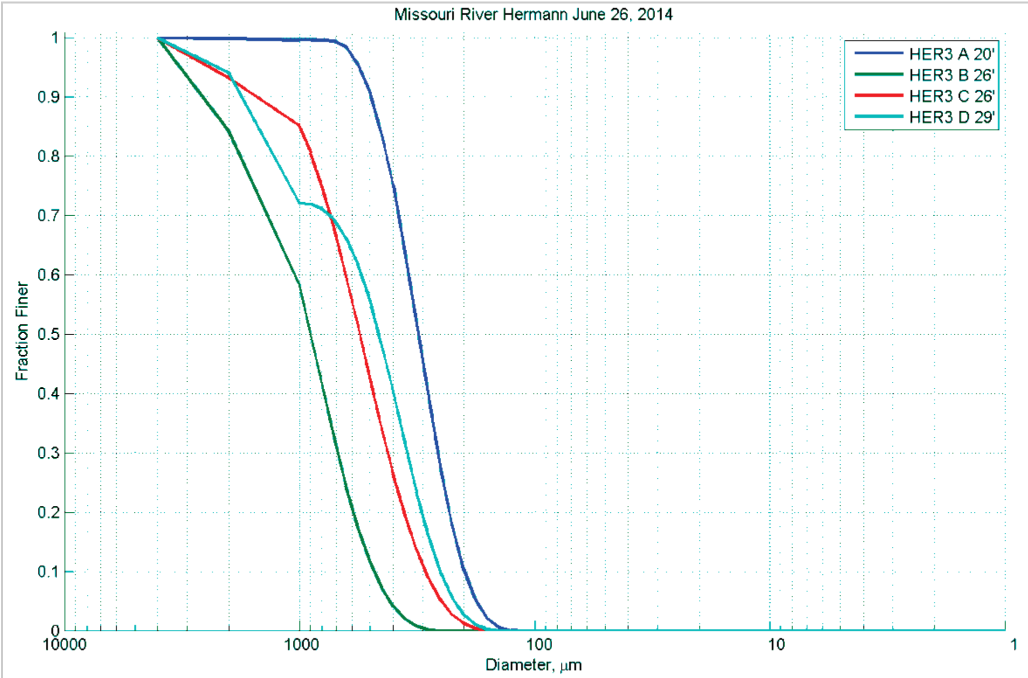

9.6 Suspended sediment

Suspended sediment samples at different depths in a column were taken at the five stations shown in Figure 231, for each data collection date. A particle size analysis was conducted for the samples of each station and date. The results are presented in this report as Figure 235 to Figure 249, and the measured data are available at Appendix VI-e.

Particle size distribution for the first data collection date, April 24, 2014, is shown in Figure 235 to Figure 239. It is organized starting from the station closer to the left descending bank, Station A, to the station closer to the right descending bank, Station E.

Figure 235. Particle size distribution at different depths (feet) in Station A - April 24, 2014.

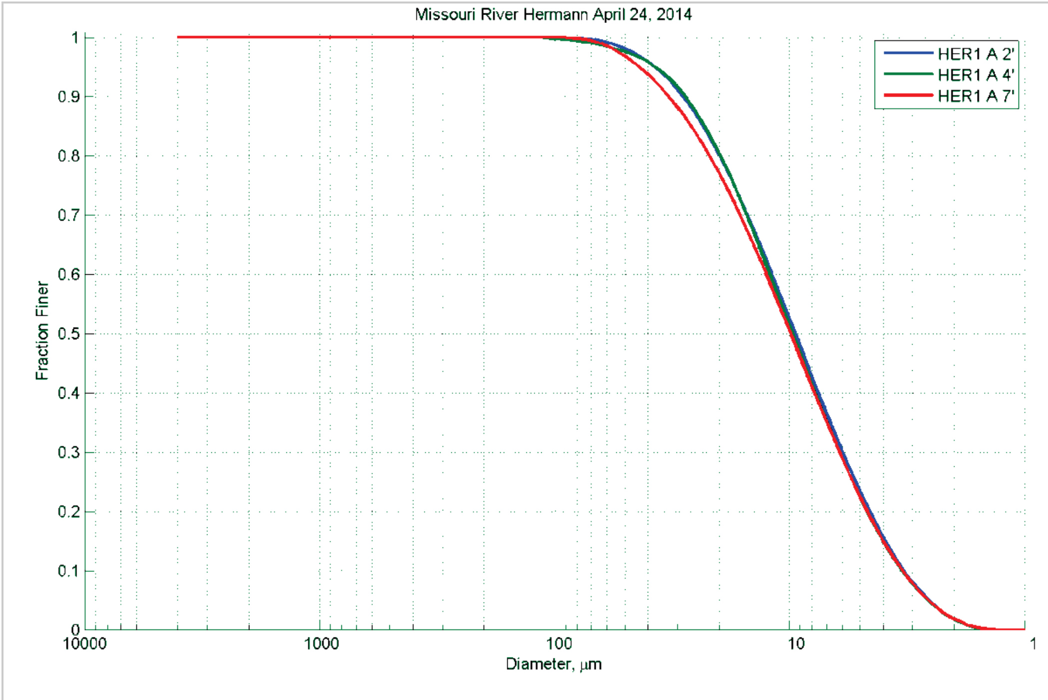

Figure 236. Particle size distribution at different depths (feet) in Station B - April 24, 2014.

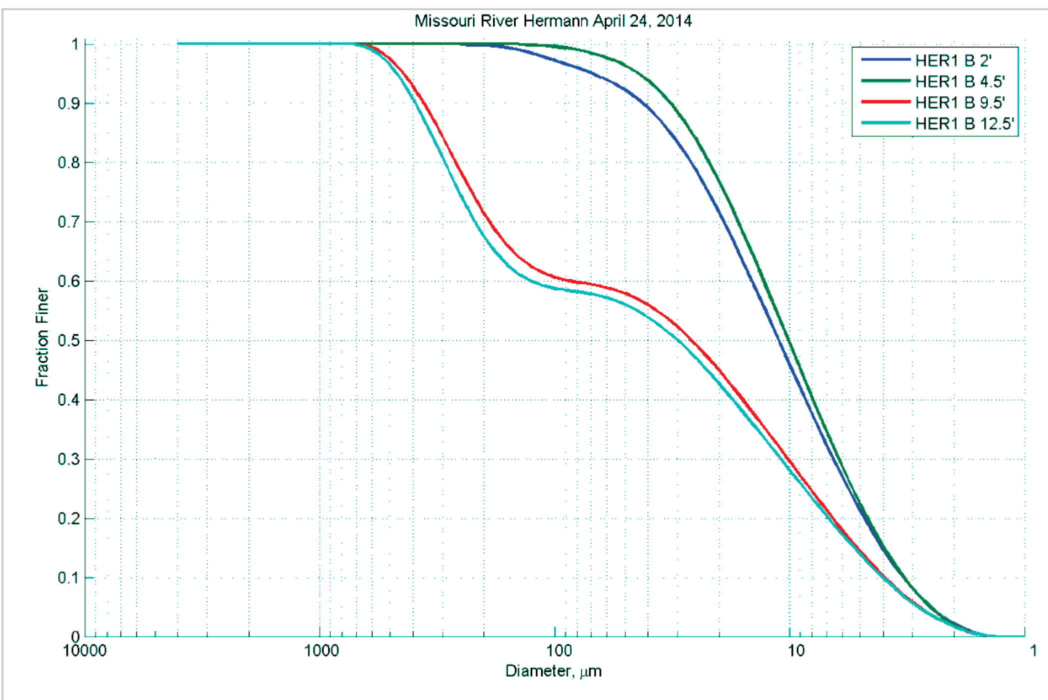

Figure 237. Particle size distribution at different depths (feet) in Station C - April 24, 2014.

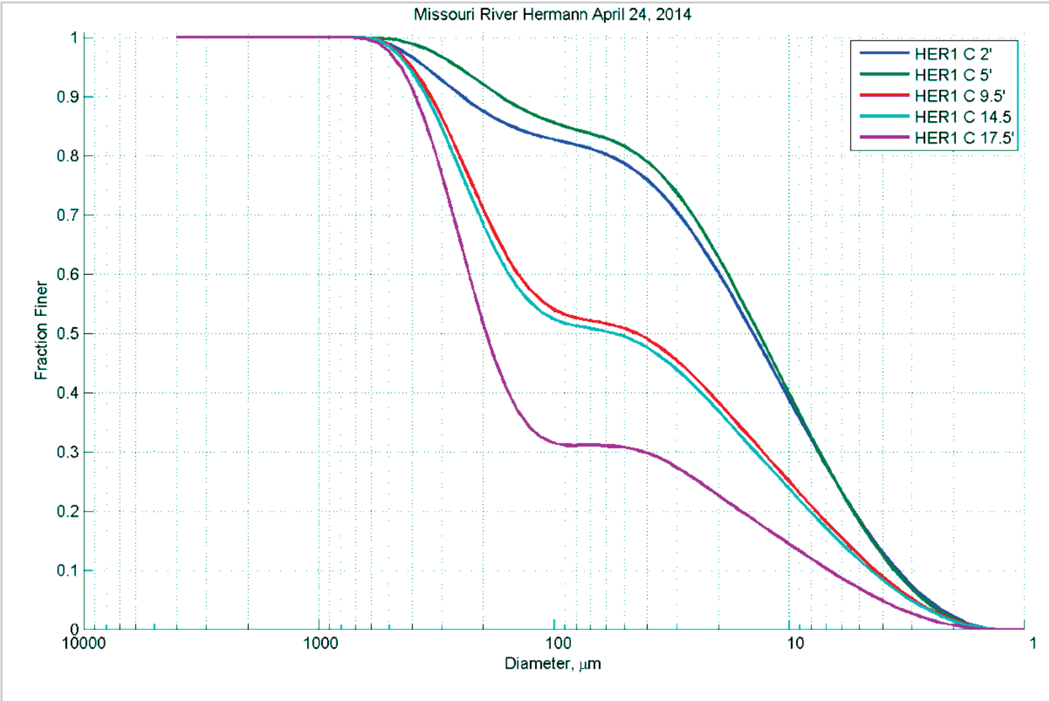

Figure 238. Particle size distribution at different depths (feet) in Station D - April 24, 2014.

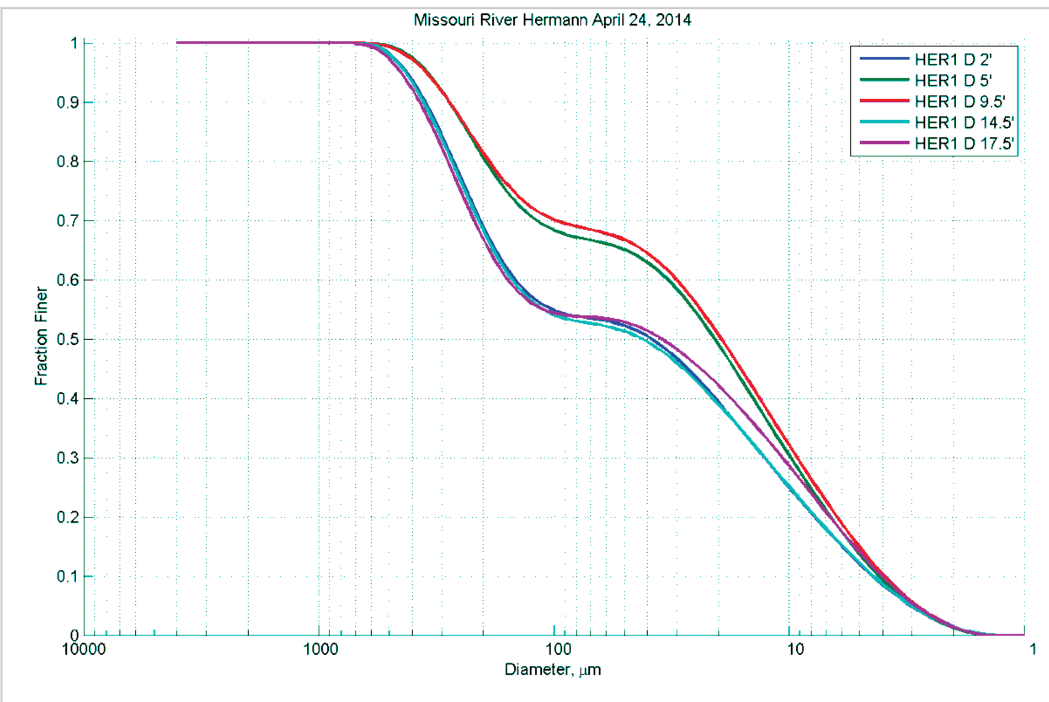

Figure 239. Particle size distribution at different depths (feet) in Station E - April 24, 2014.

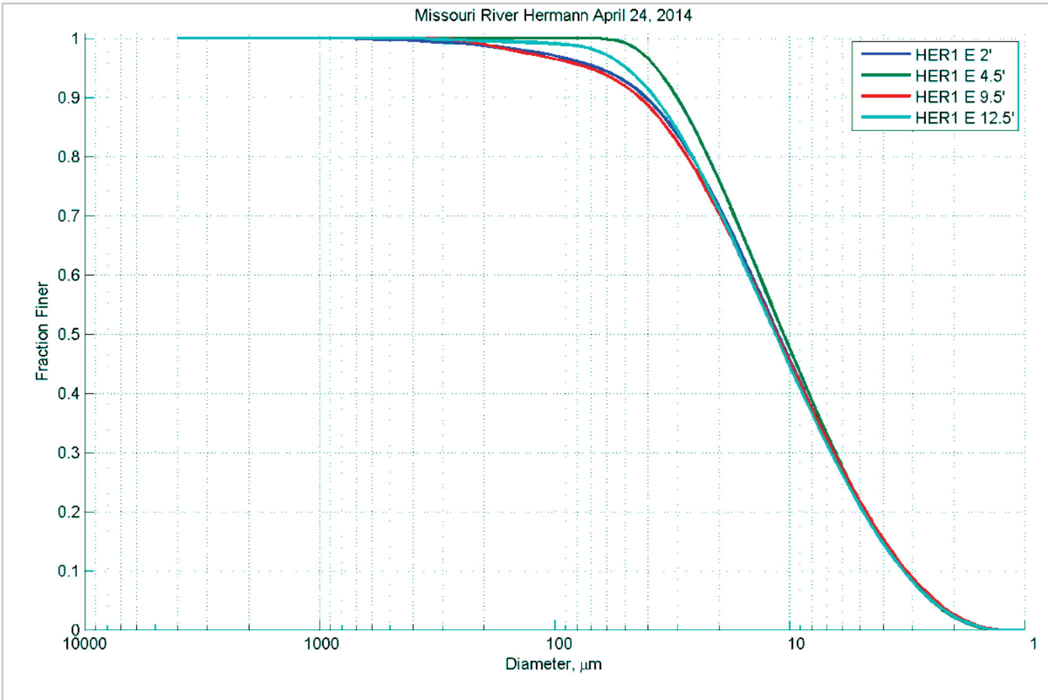

Particle size distribution for the second data collection date, June 11, 2014, are shown in Figure 240 to Figure 244.

Figure 240. Particle size distribution at different depths (feet) in Station A – June 11, 2014.

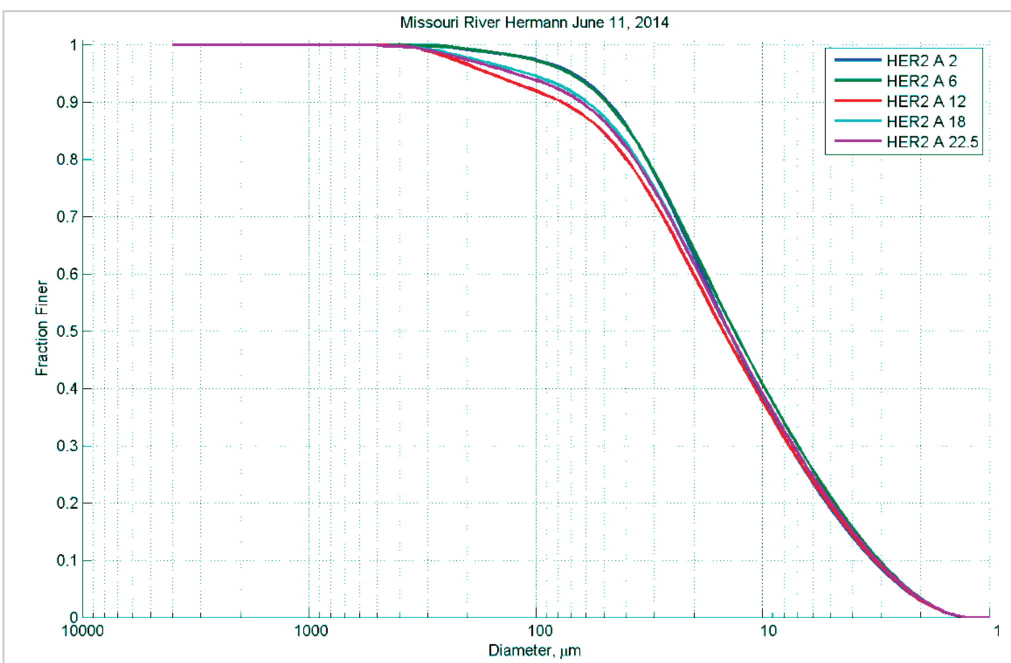

Figure 241. Particle size distribution at different depths (feet) in Station B – June 11, 2014.

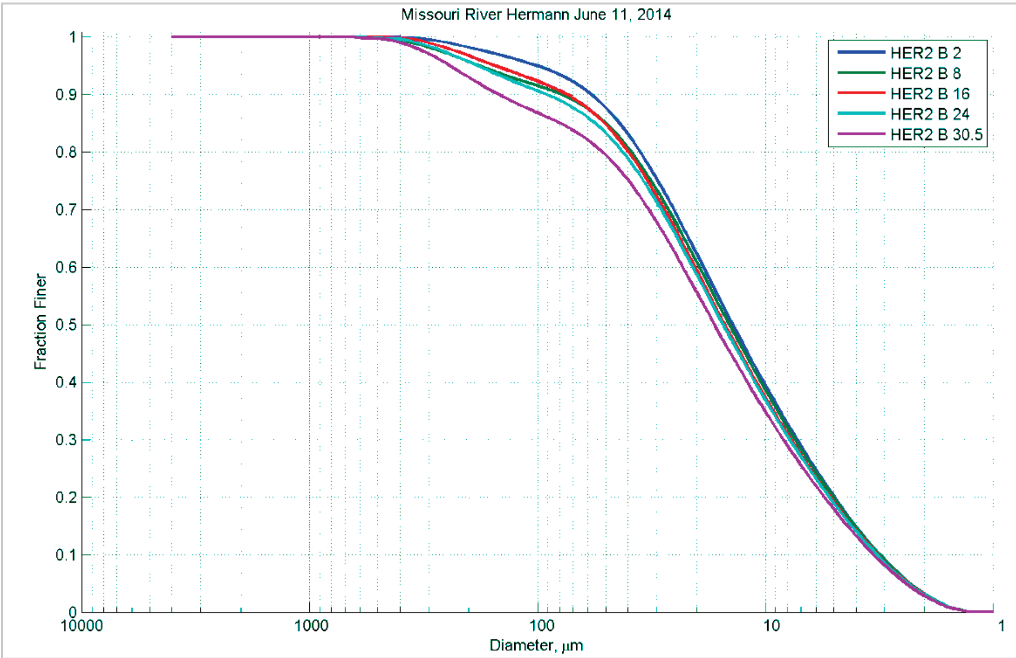

Figure 242. Particle size distribution at different depths (feet) in Station C – June 11, 2014.

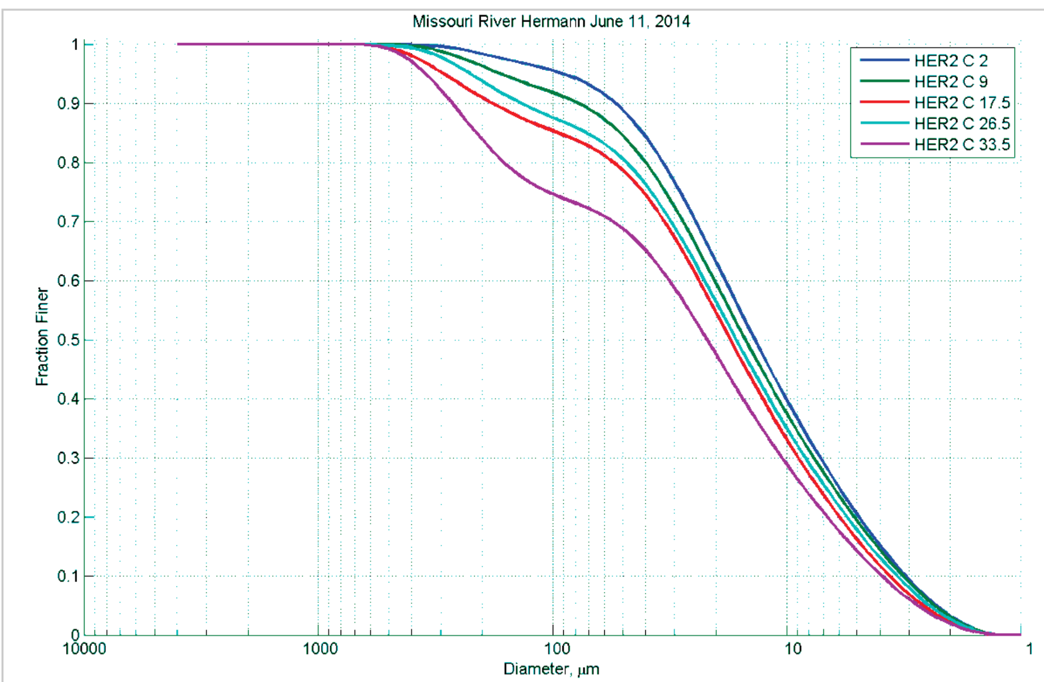

Figure 243. Particle size distribution at different depths (feet) in Station D – June 11, 2014.

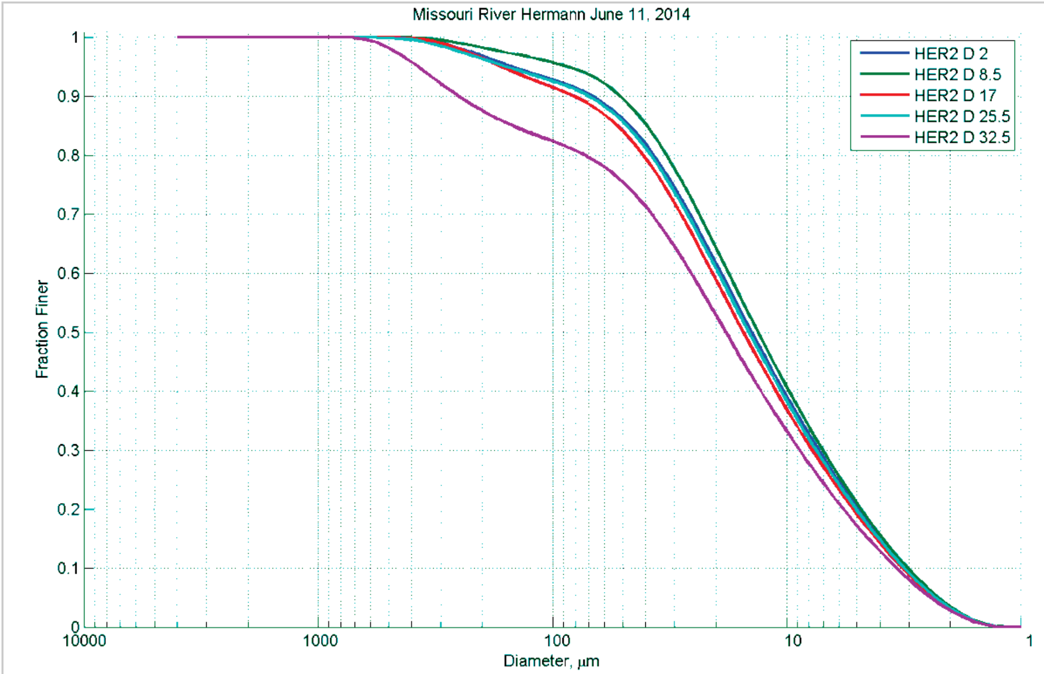

Figure 244. Particle size distribution at different depths (feet) in Station E – June 11, 2014.

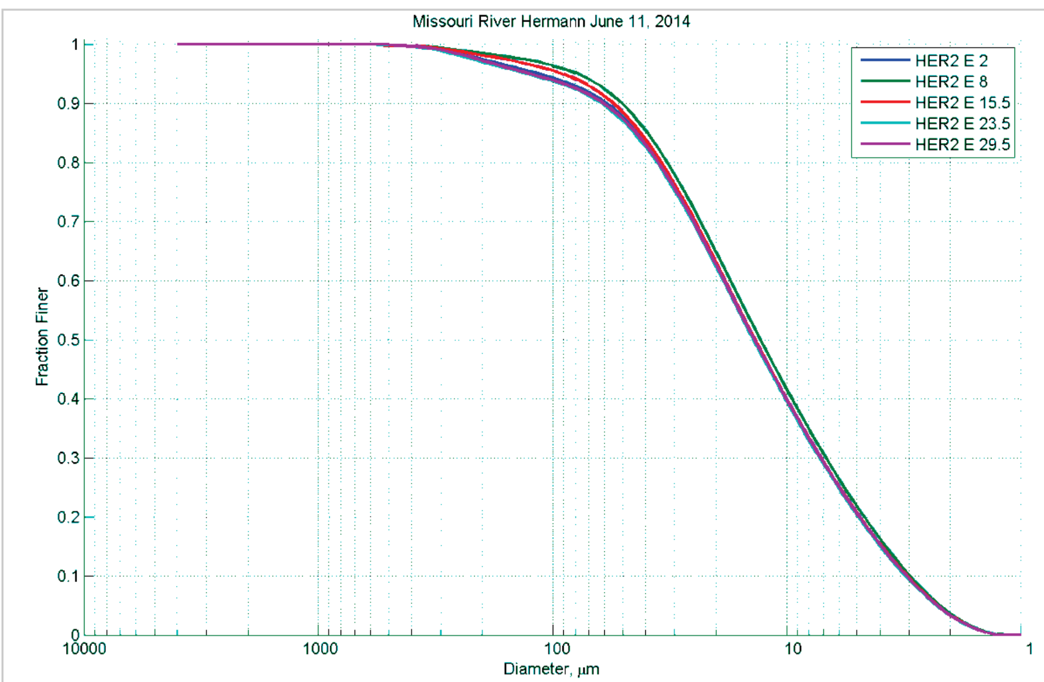

Particle size distribution for the third data collection date, June 26, 2014, is shown in Figure 245 to Figure 249.

Figure 245. Particle size distribution at different depths (feet) in Station A – June 26, 2014.

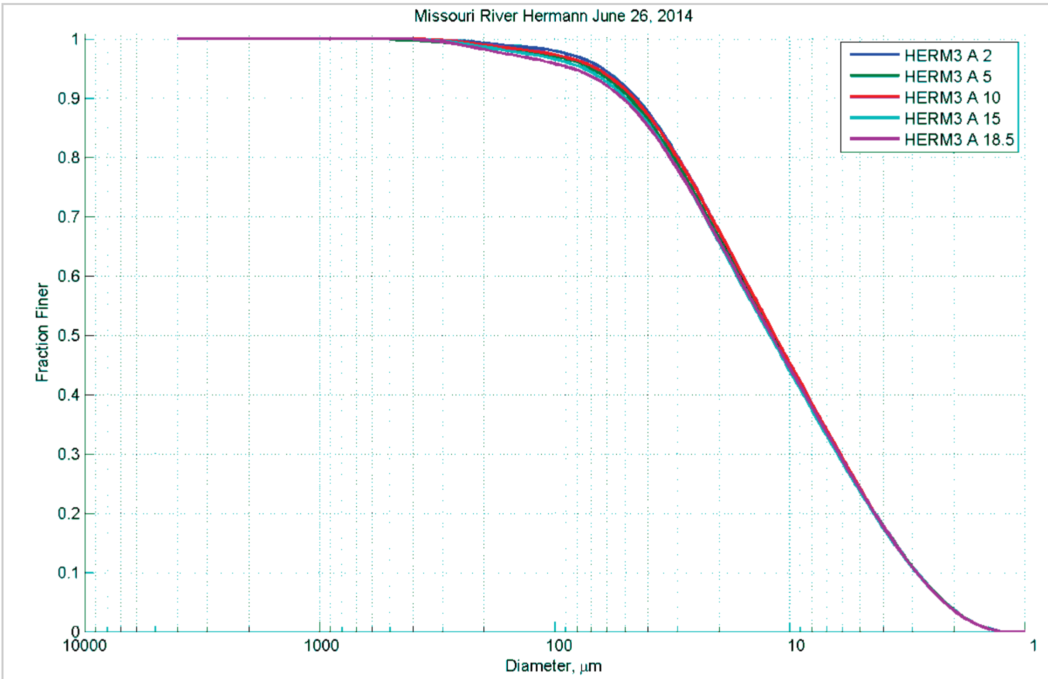

Figure 246. Particle size distribution at different depths (feet) in Station B – June 26, 2014.

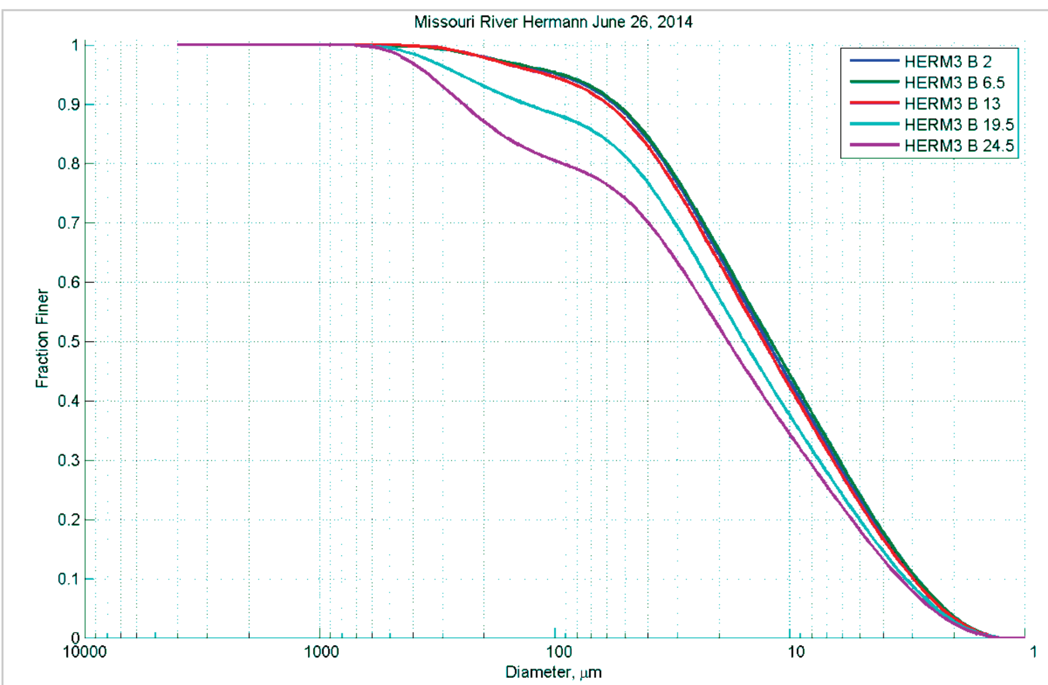

Figure 247. Particle size distribution at different depths (feet) in Station C – June 26, 2014.

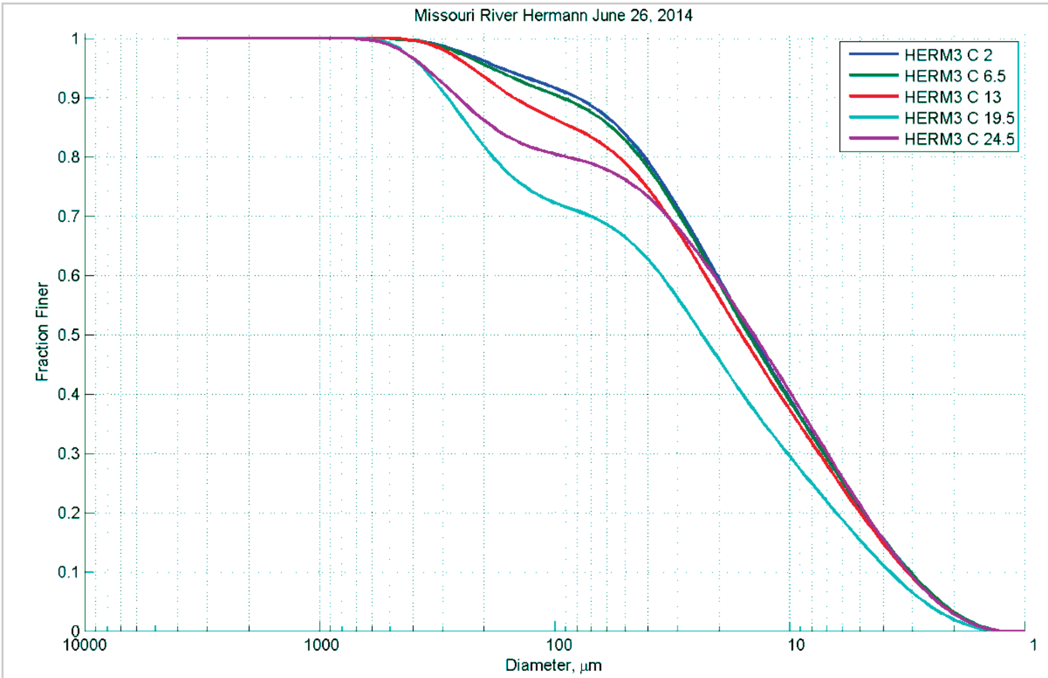

Figure 248. Particle size distribution at different depths (feet) in Station D – June 26, 2014.

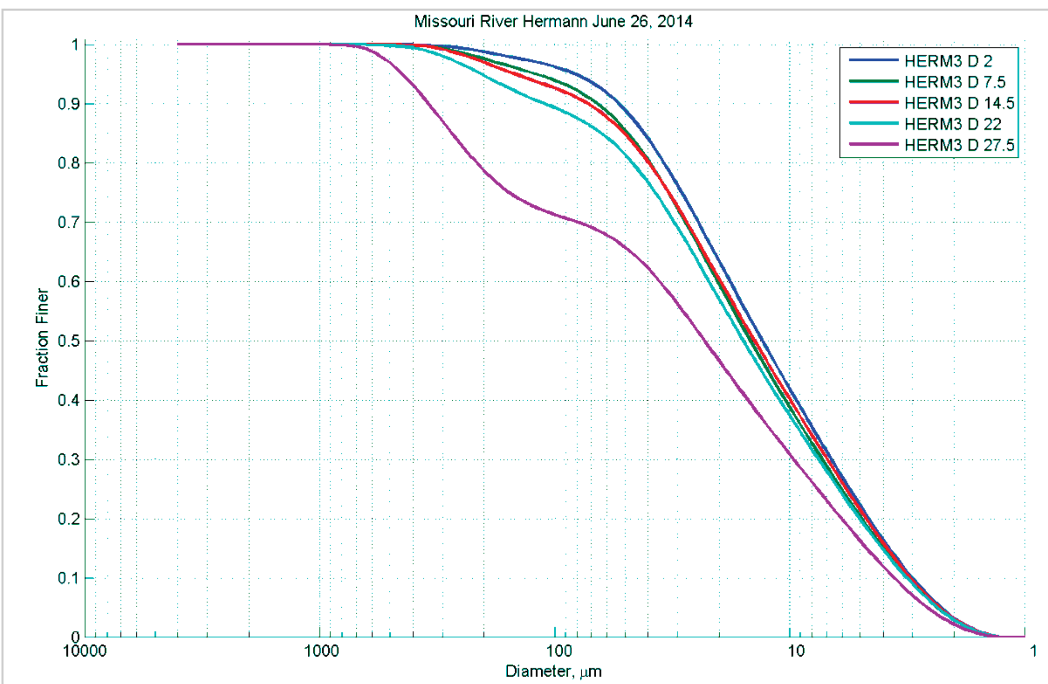

Figure 249. Particle size distribution at different depths (feet) in Station E – June 26, 2014.

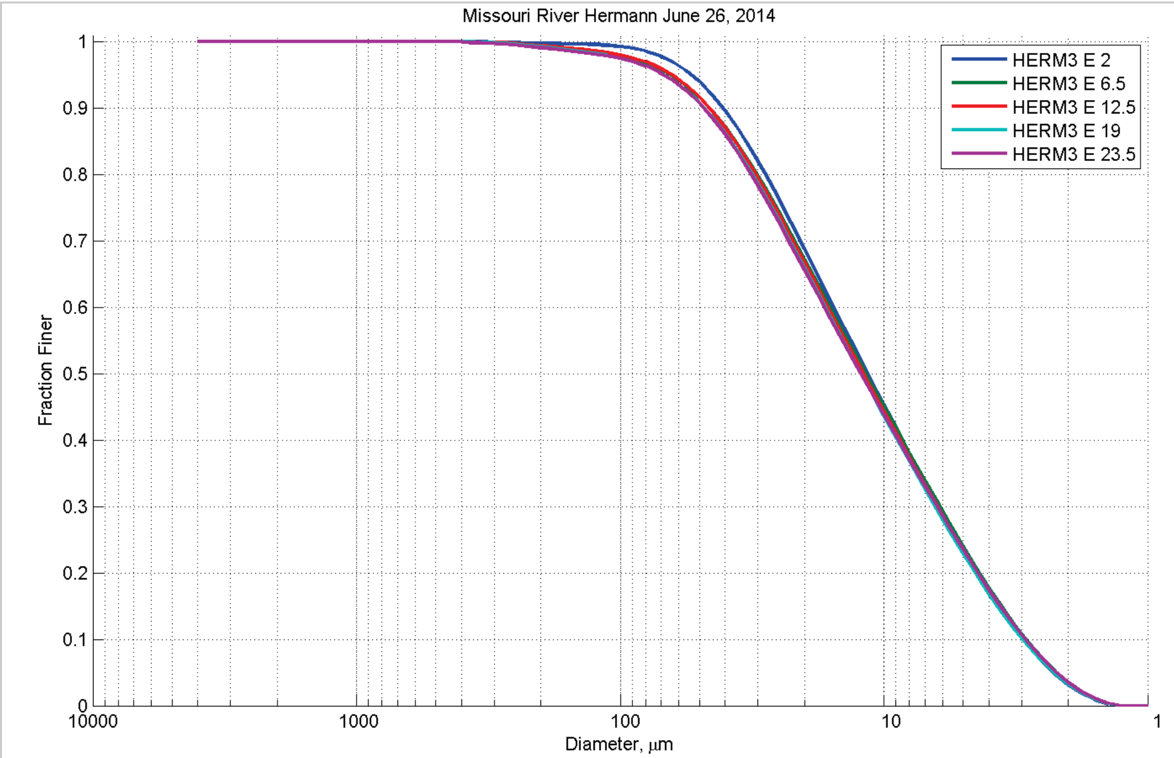

Suspended sediment concentration was also measured from the collected samples. Table 74 to Table 76 present the concentration values for each data collection date. Suspended sediment concentration profiles were created using the measured data, presented in Figure 250 to Figure 252. See Appendix VI-f for more details about the measured data.

Table 74. Suspended sediment concentration at Hermann, MO – April 24, 2014.

Station	Depth (ft)	Concentration (mg/L)
HER 1A	2	106.17
HER 1A	4	108.33
HER 1A	7	105.00
Total depth	8.7	(Bottom)
HER 1B	2	155.83
HER 1B	4.5	130.17
HER 1B	9.5	173.33
HER 1B	12.5	227.83
Total depth	15.5	(Bottom)
HER 1C	2	128.17
HER 1C	5	161.16
HER 1C	9.5	167.13
HER 1C	14.5	248.50
HER 1C	17.5	502.83
Total depth	18.7	(Bottom)
HER 1D	2	108.44
HER 1D	5	126.72
HER 1D	9.5	144.38
HER 1D	14.5	218.33
HER 1D	17.5	283.40
Total depth	18.7	(Bottom)
HER 1E	2	84.49
HER 1E	4.5	88.18
HER 1E	9.5	94.63
HER 1E	12.5	110.00
Total depth	16.1	(Bottom)

Table 75. Suspended sediment concentration at Hermann, MO – June 11, 2014.

Station	Depth (ft)	Concentration (mg/L)
HER 2A	2	2,178.94
HER 2A	6	2,182.93
HER 2A	12	2,153.39
HER 2A	18	2,243.13
HER 2A	22.5	2,402.41
Total depth	25.5	(Bottom)
HER 2B	2	2,264.25
HER 2B	8	2,262.02
HER 2B	16	2,430.00
HER 2B	24	2,395.22
HER 2B	30.5	2,611.86
Total depth	31.2	(Bottom)
HER 2C	2	2,140.20
HER 2C	9	2,273.11
HER 2C	17.5	2,377.02
HER 2C	26.5	2,659.84
HER 2C	33.5	3,171.65
Total depth	34.5	(Bottom)
HER 2D	2	2,147.41
HER 2D	8.5	2,270.88
HER 2D	17	2,309.45
HER 2D	25.5	2,377.01
HER 2D	32.5	2,640.16
Total depth	35.1	(Bottom)
HER2E	2	2,012.28
HER2E	8	2,033.80
HER2E	15.5	2,086.61
HER2E	23.5	2,152.24
HER2E	29.5	2,102.35
Total depth	31.5	(Bottom)

Table 76. Suspended sediment concentration at Hermann, MO – June 26, 2014.

Station	Depth (ft)	Concentration (mg/L)
HER 3A	2	1,339.47
HER 3A	5	1,374.17
HER 3A	10	1,345.60
HER 3A	15	1,370.93
HER 3A	18.5	1,361.69
Total depth	21.8	(Bottom)
HER 3B	2	1,462.93
HER 3B	6.5	1,433.83
HER 3B	13	1,505.43
HER 3B	19.5	1,594.08
HER 3B	24.5	1,950.89
Total depth	27	(Bottom)
HER 3C	2	1,473.90
HER 3C	6.5	1,648.53
HER 3C	13	1,722.86
HER 3C	19.5	1,770.57
HER 3C	24.5	1,893.22
Total depth	28.1	(Bottom)
HER 3D	2	1,339.18
HER 3D	7.5	1,414.38
HER 3D	14.5	1,468.57
HER 3D	22	1,552.84
HER 3D	27.5	1,624.65
Total depth	29	(Bottom)
HER 3E	2	1,259.42
HER 3E	6.5	1,253.52
HER 3E	12.5	1,285.67
HER 3E	19	1,266.61
HER 3E	23.5	1,299.70
Total depth	26.6	(Bottom)

Figure 250. Suspended sediment concentration at Hermann, MO – April 24, 2014.

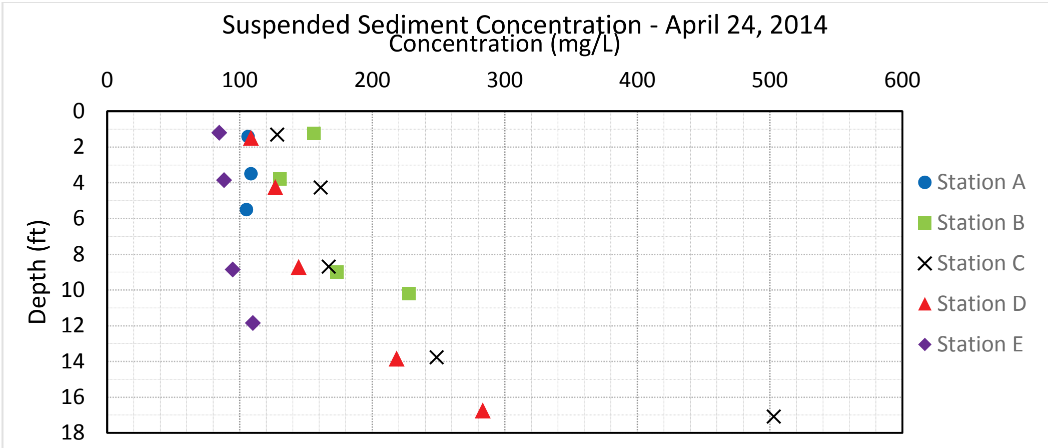

Figure 251. Suspended sediment concentration at Hermann, MO – June 11, 2014.

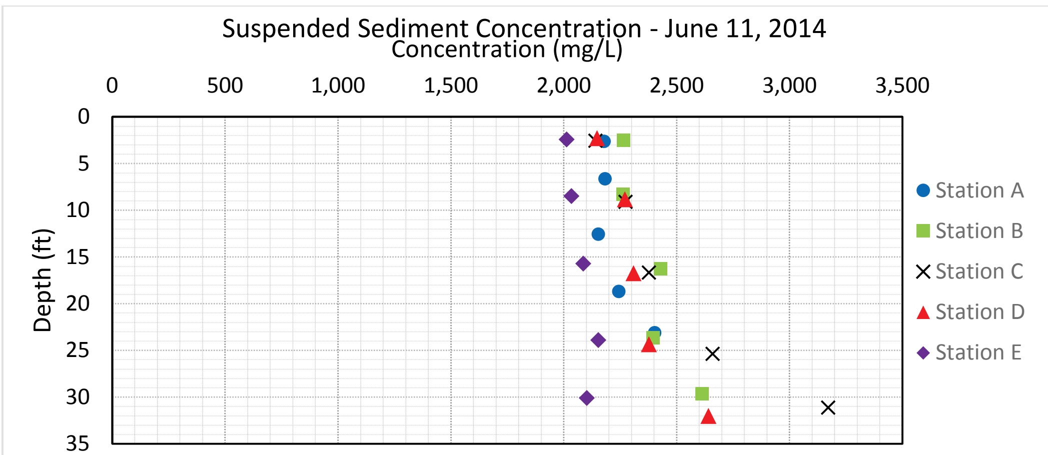

Figure 252. Suspended sediment concentration at Hermann, MO – June 26, 2014.

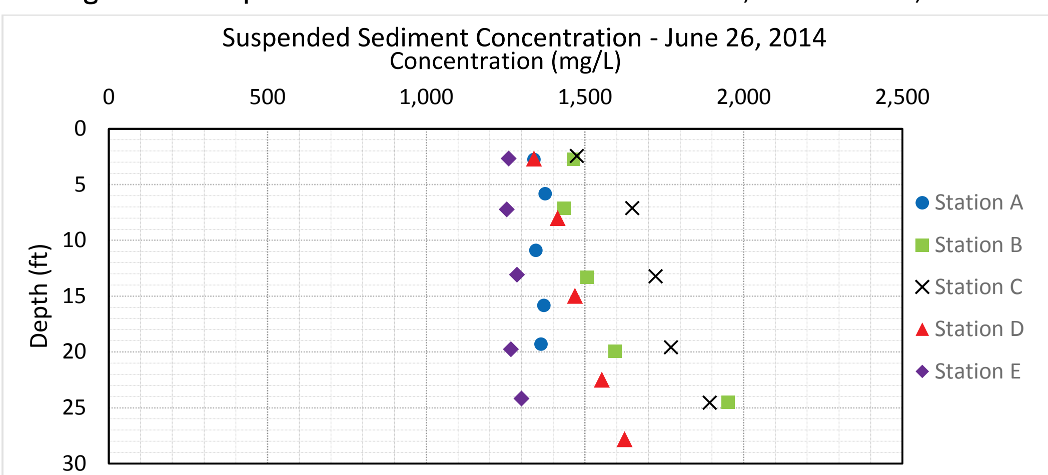

The suspended sediment concentration data were used to calibrate the ADCP acoustic backscatter and develop suspended sediment concentration profiles across the channel. Figure 253 to Figure 255 show the suspended sediment concentration profiles for the first left-to-right ADCP pass, for each data collection date. To see the other profiles, see Appendix VI-f.

Figure 253. Suspended sediment concentration profile at Hermann, MO – April 24, 2014.

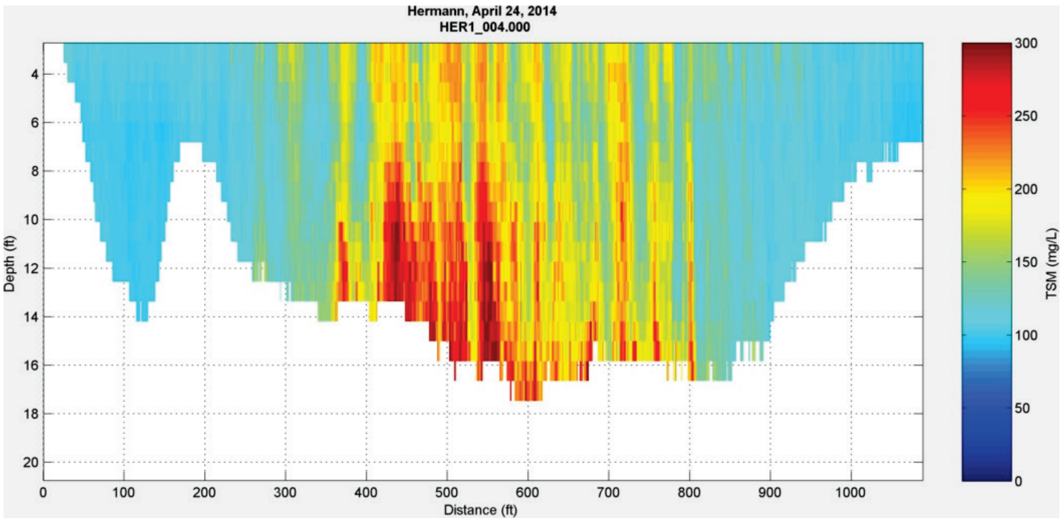

Figure 254. Suspended sediment concentration profile at Hermann, MO – June 11, 2014.

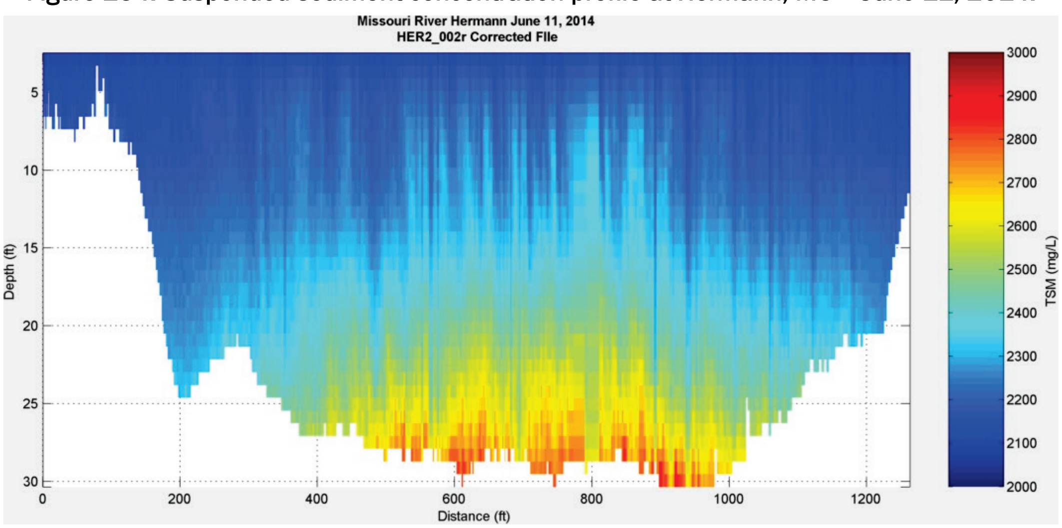

Figure 255. Suspended sediment concentration profile at Hermann, MO – June 25, 2014.

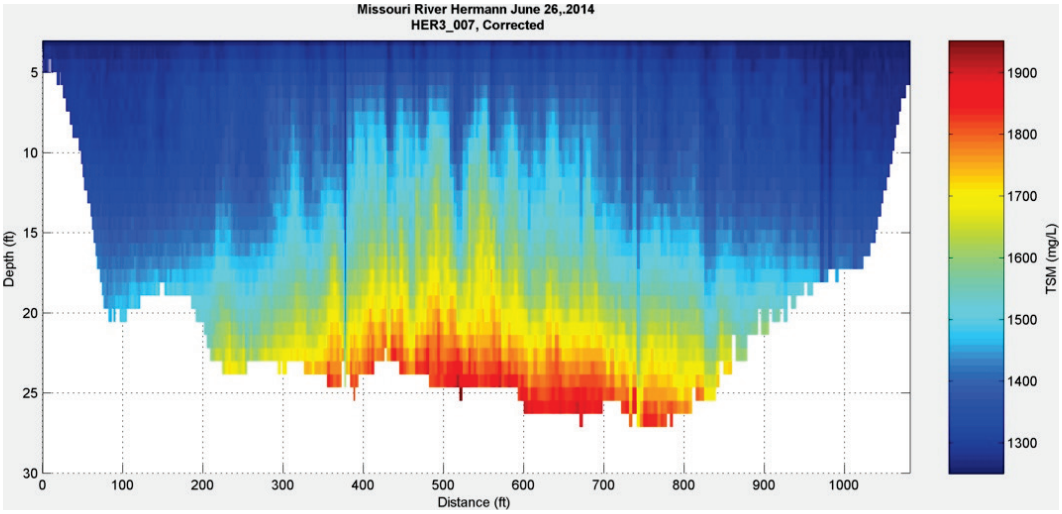

The suspended sediment concentration cross-section profiles obtained from the ADCP measurements were combined with the flow discharges, also obtained from the ADCP, to obtain the suspended sediment transport load, in tons per day. The method used for this study is explained in Heath et al. (2015, 13–14). The suspended sediment load can be divided classifying the suspended material by size and soil type. Table 77 presents the suspended sediment transport load, according to both classifications, for the first data collection date April 24, 2014. Table 78 and Table 79 present the same information for the second and third data collection dates, respectively. In all three tables, the categories under the Soil Type Classification were determined as follows: Clay Flux groups the size fractions 0.0001 to 0.0004 mm, Silt Flux 0.0004 to 0.0625 mm, and Sand Flux 0.0625 to 2.00 mm.

Table 77. Suspended sediment load distributed by grain size and soil type – April 24, 2014.

Classification System	Category	Sediment Flux (tons/day)
Total load		22,724.83
Sediment size classification	0.001 - 0.004 mm	2,454.19
	0.004 - 0.008 mm	4,020.55
	0.008 - 0.016 mm	4,772.66
	0.016 - 0.031 mm	3,876.29
	0.031 - 0.063 mm	1,962.43
	0.063 - 0.125 mm	640.77
	0.125 - 0.250 mm	2,202.08
	0.250 - 0.500 mm	2,482.23
	0.500 - 1.00 mm	313.65
	1.00 - 2.00 mm	0.00
Soil type classification	Clay	2,454.19
	Silt	14,631.93
	Sand	5,638.73

Table 78. Suspended sediment load distributed by grain size and soil type – June 11, 2014.

Classification System	Category	Sediment Flux (tons/day)
Total load		1,203,156.70
Sediment size classification	0.001 - 0.004 mm	159,997.51
	0.004 - 0.008 mm	200,411.04
	0.008 - 0.016 mm	251,832.32
	0.016 - 0.031 mm	258,494.28
	0.031 - 0.063 mm	182,571.35
	0.063 - 0.125 mm	64,019.72
	0.125 - 0.250 mm	50,212.99
	0.250 - 0.500 mm	33,283.58
	0.500 - 1.00 mm	2,333.89
	1.00 - 2.00 mm	0.00
Soil type classification	Clay	159,997.51
	Silt	893,308.99
	Sand	149,850.18

Table 79. Suspended sediment load distributed by grain size and soil type – June 26, 2014.

Classification System	Category	Sediment Flux (tons/day)
Total load		521,847.32
Sediment size classification	0.001 - 0.004 mm	77,114.13
	0.004 - 0.008 mm	95,253.89
	0.008 - 0.016 mm	104,723.37
	0.016 - 0.031 mm	103,210.01
	0.031 - 0.063 mm	77,360.87
	0.063 - 0.125 mm	25,827.54
	0.125 - 0.250 mm	20,428.72
	0.250 - 0.500 mm	16,046.82
	0.500 - 1.00 mm	1,881.97
	1.00 - 2.00 mm	0.00
Soil type classification	Clay	77,114.13
	Silt	380,548.14
	Sand	64,185.05

9.7 Bed load transport

The ISSDOTv2 method was used for computing the bed-load transport. Table 80 shows the values obtained for the bed load, as well as the other sediment quantities determined from the suspended sediment samples at the Hermann site. It provides a breakdown of the various measured sediment transport components, based on sediment size classification.

Table 80. Bed-load transport values from Hermann, MO.

Data Collection Date	24-Apr-14	11-Jun-14	26-Jun-14
Flow (cfs)	48,771	191,044	131,327
Bed load (tons/day)	1,849	16,260	6,509
Suspended BML (tons/day)	5,639	149,850	64,185
Total BML (tons/day)	7,488	166,110	70,694
Bed load Fraction (%)	24.7%	9.8%	9.2%
Wash load (tons/day)	17,086	1,053,307	457,662
Total load	24,574	1,219,417	528,356

In Table 80, *bed load* is defined as the bed material moving at the bottom of the river in bed-forms; *suspended BML* refers to the suspended material with grain size higher than 0.063 mm; *total BML* is the sum of bed load and suspended BML; *bed load fraction* is the percentage of the total bed

material moving as bed load; *wash load* is fine sediments that never settle in the bed, with grain size of 0.063 or less; and *total load* combines the quantity of total BML and wash load.

A bed-load rating curve was prepared for this site by plotting the bed-load transport in tons per day versus the river flowrate. This graph is shown in Figure 256. The flowrates for trips 1, 2, and 3 were somewhat evenly spaced with regards to magnitude. As can be seen in the graph, the magnitudes of the bed-load transport increased proportionately for increasing flows. Also, the bed-load fraction once again was smaller for larger flows as seen in Table 80.

Figure 256. Bed-load rating curve for Hermann, MO.

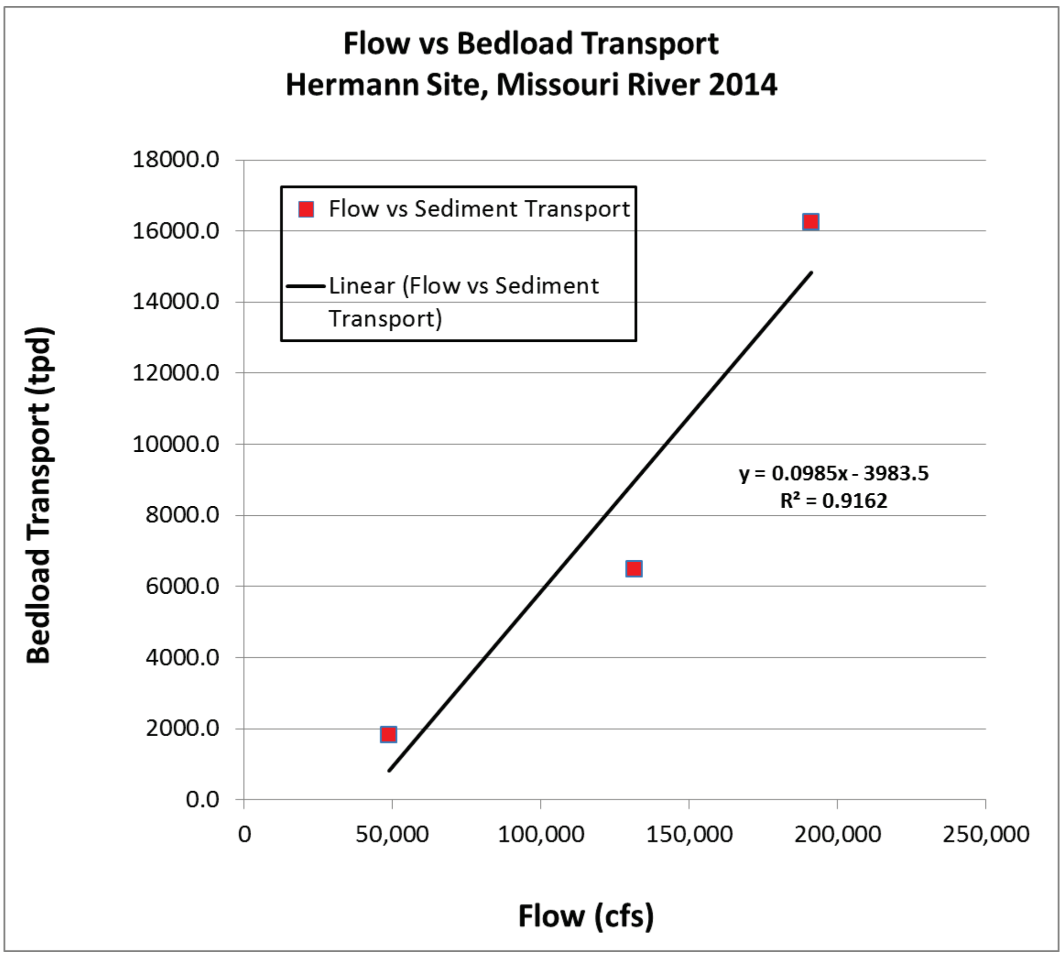

Bed-load transport values were also computed for this site using two analytic transport functions. One is the MPM formula, and the other is the Einstein formula. They were computed for each swath of bathymetric data. For instance, Figure 257 shows the bathymetry of this site with the six swath numbers (S1 to S6) labeled on it, indicating the lateral position where each swath was located. The hydraulic and sediment parameters obtained in the field data collection effort discussed before were extracted for each of these swaths.

Figure 257. Bathymetry for Missouri River at Hermann, MO, showing swath locations.

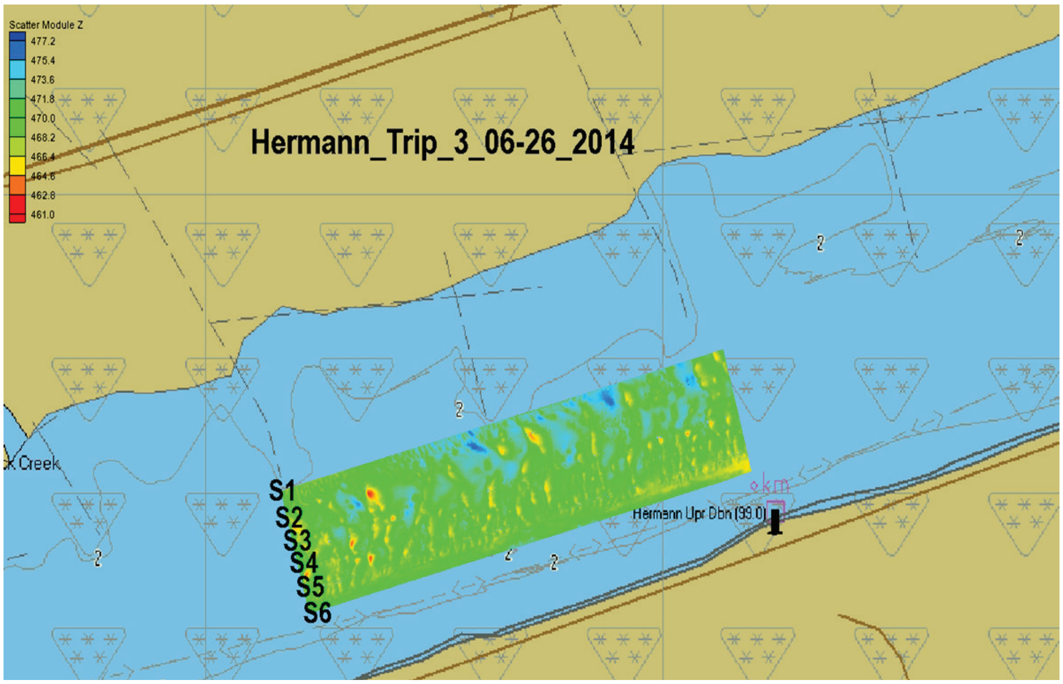

Flow, average velocity, and water depth were obtained from the ADCP data by a separate program written for that specific purpose. Water slope and water temperature were obtained from each appropriate data appendix. Bed sediment gradations used were selected based on their proximity to a given swath. The SAM Hydraulic Design Package for Channels program was then used with these data to compute the bed-load values for each swath. This software package has provisions for entering hydraulic and sediment input parameters and can then compute bed-load transport values for several commonly used transport functions.

The results are plotted in Figure 258 to Figure 260 and show how the transport function values compare to the ISSDOTv2 measured values. They also show the lateral variability across the measured section from the left side to the right side of the channel.

Figure 258. Bed-load transport at Hermann, MO – April 24, 2014: ISSDOTv2 values compared to transport function computed values.

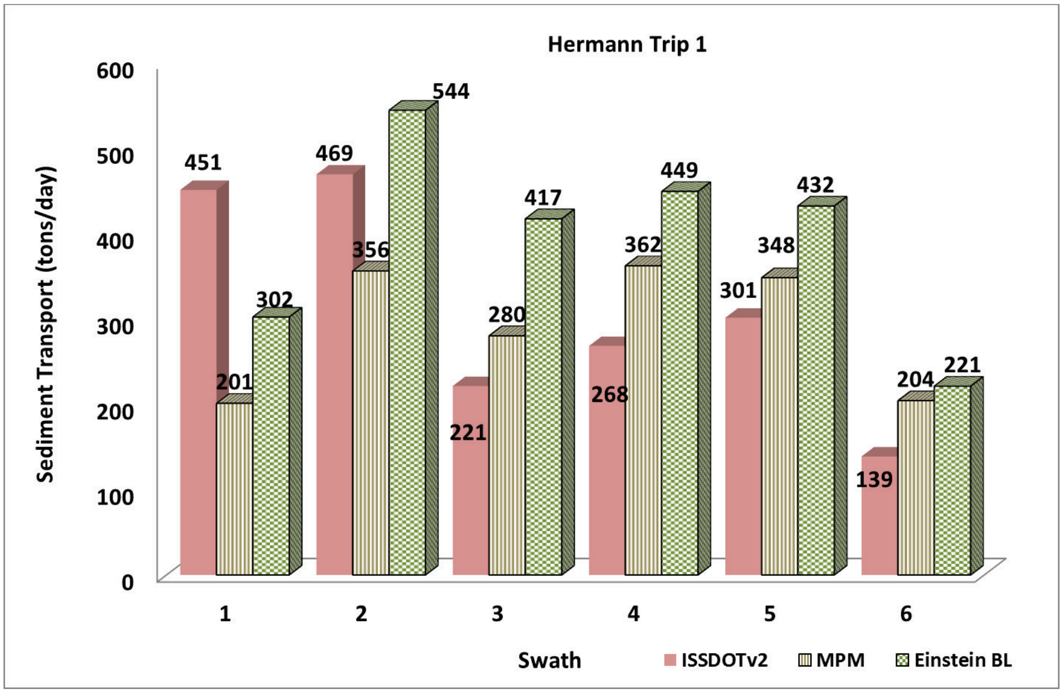

Figure 259. Bed-load transport at Hermann, MO– June 11, 2014: ISSDOTv2 values compared to transport function computed values.

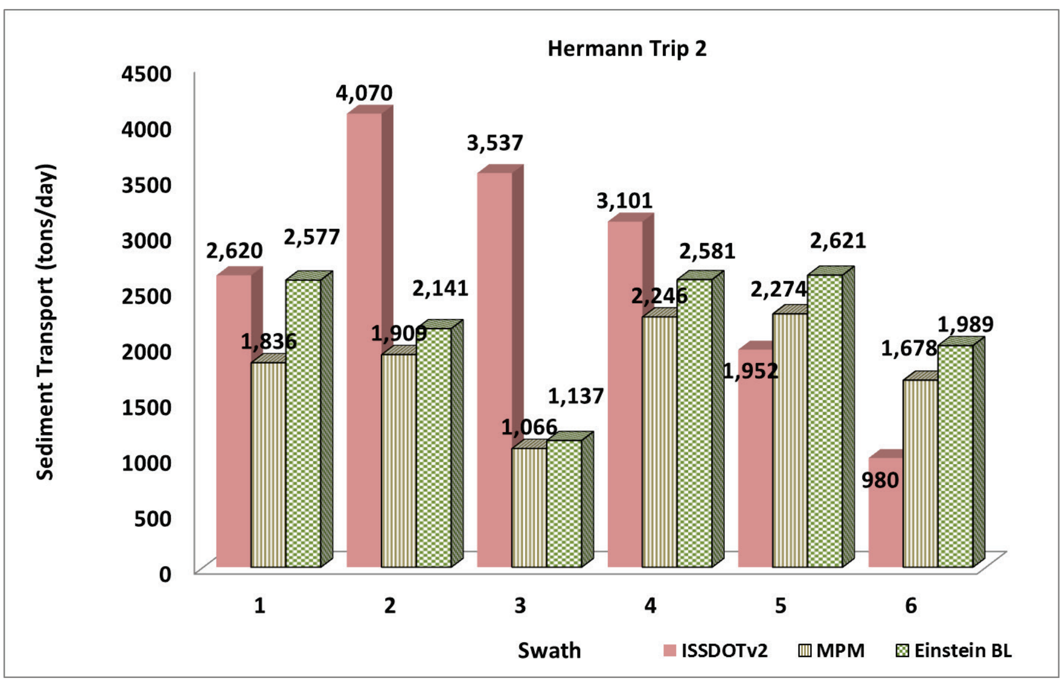

Figure 260. Bed-load transport at Hermann, MO – June 26, 2014: ISSDOTv2 values compared to transport function computed values.

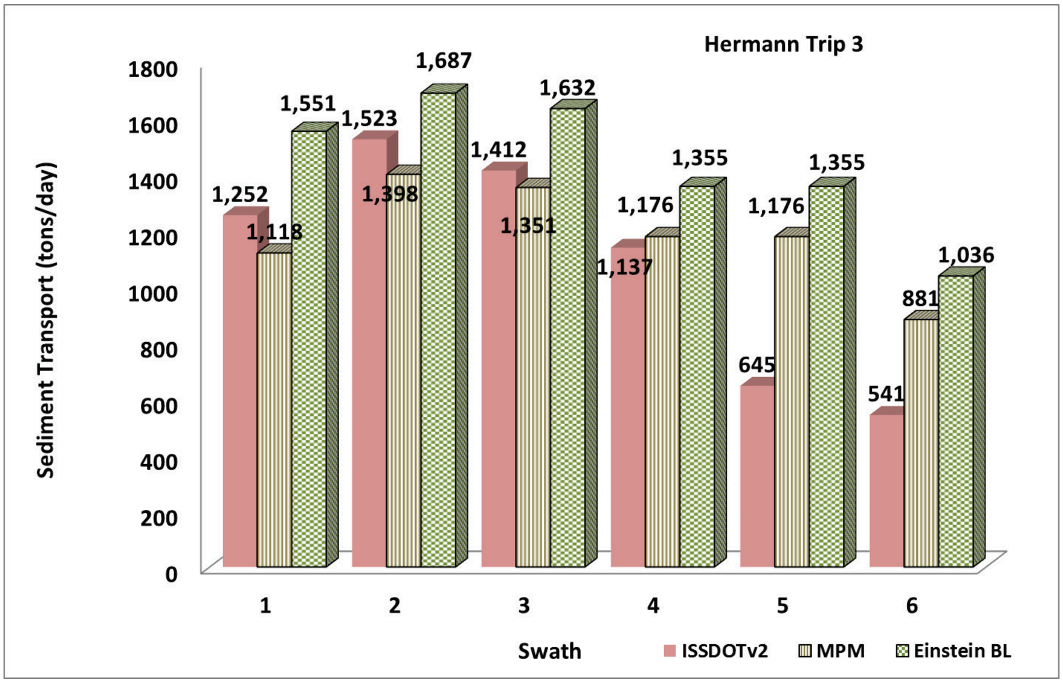

10 Previous Bed-Load Data

Table 81 shows a summary of previous bed-load measurements. These were obtained for the Kansas City and Omaha Districts during the period 2009 to 2011. The bed-load data in this sheet were computed using the same version of code as used on the 2014 Missouri River Data. In 2014, data were obtained at only two of the previous sites. They were the Nebraska City and Kansas City sites. The 2009 and 2011 data were incorporated into the rating curves at those two sites as appropriate.

Table 81. Previous bed-load values and site information.

Site	Trip	Collection Date(s)	River Mile	Notes	Flow (cfs)	Bed load (tons/day)
Barney	1	8/17/2009	551.7		39,212	1,829
Hamburg	1	8/16/2009	553.3		35,403	2,039
	1	8/14/2009			38,929	1,624
Nebraska City	2	6/27/2011	561.8		214,400	21,110
	1A	5/27/2009	67		140,425	2,694
	2a	6/25/2009			158,000	4,502
	3	8/9/2009			57,530	673
	4	10/13/2009		not used		
	4a	10/14/2009			121581	8397
	5	5/26/2010			209856	8619
Washington	6	7/7/2010			190392	9829
	1	5/29/2009			47507	marginal
	2	6/24/2009		bad data		
	3	6/26/2009			73290	marginal
	4	8/10/2009			44877	3324
	5	5/27/2010			67294	5189
Kansas City	6	7/9/2010			126936	13035
(by Old Airport)	7	6/28/2011	368.2		198000	18899
Kansas City Lower site	1	6/28/2011	365.8		204000	15812

In addition to the USACE data listed in this report, the USGS provided plots of other data collected and or computed at the various sites. These data are shown in Figure 261 to Figure 267. No USACE data were collected during the 2014 effort at Yankton, SD, but the USGS data at that location is presented for completeness and because it is in the vicinity of the Sioux City site. The data in these graphs were provided by written communication with David Heimann, Hydrologist at the USGS, Missouri Water Science Center, Kansas City Sub–District Office, February 2016. For more information on any of the sources of data points shown in these graphs, see the USGS Scientific Investigations Report 2015-5127.

Figure 261. USGS bed-load data - Maskell, NE.

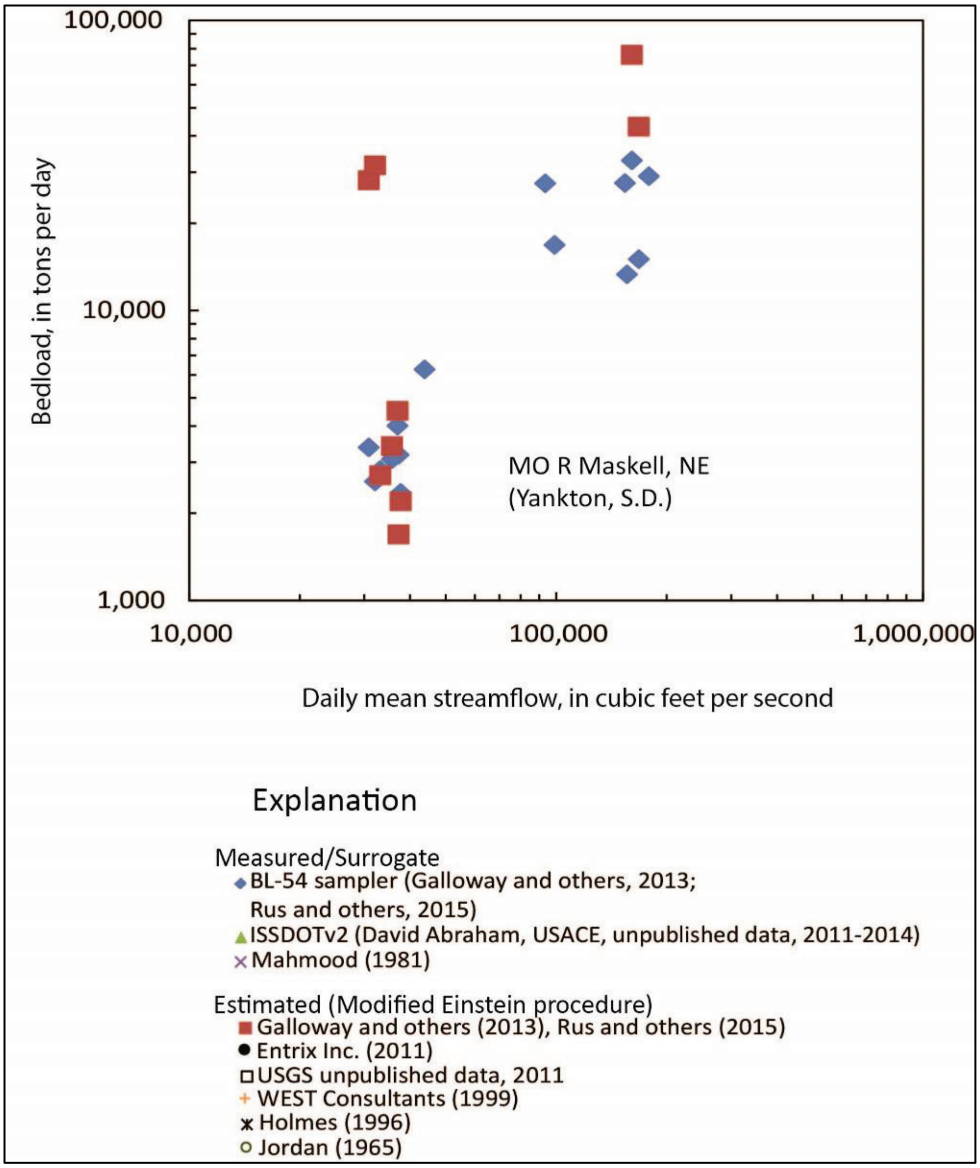

Figure 262. USGS bed-load data - Sioux City, IA.

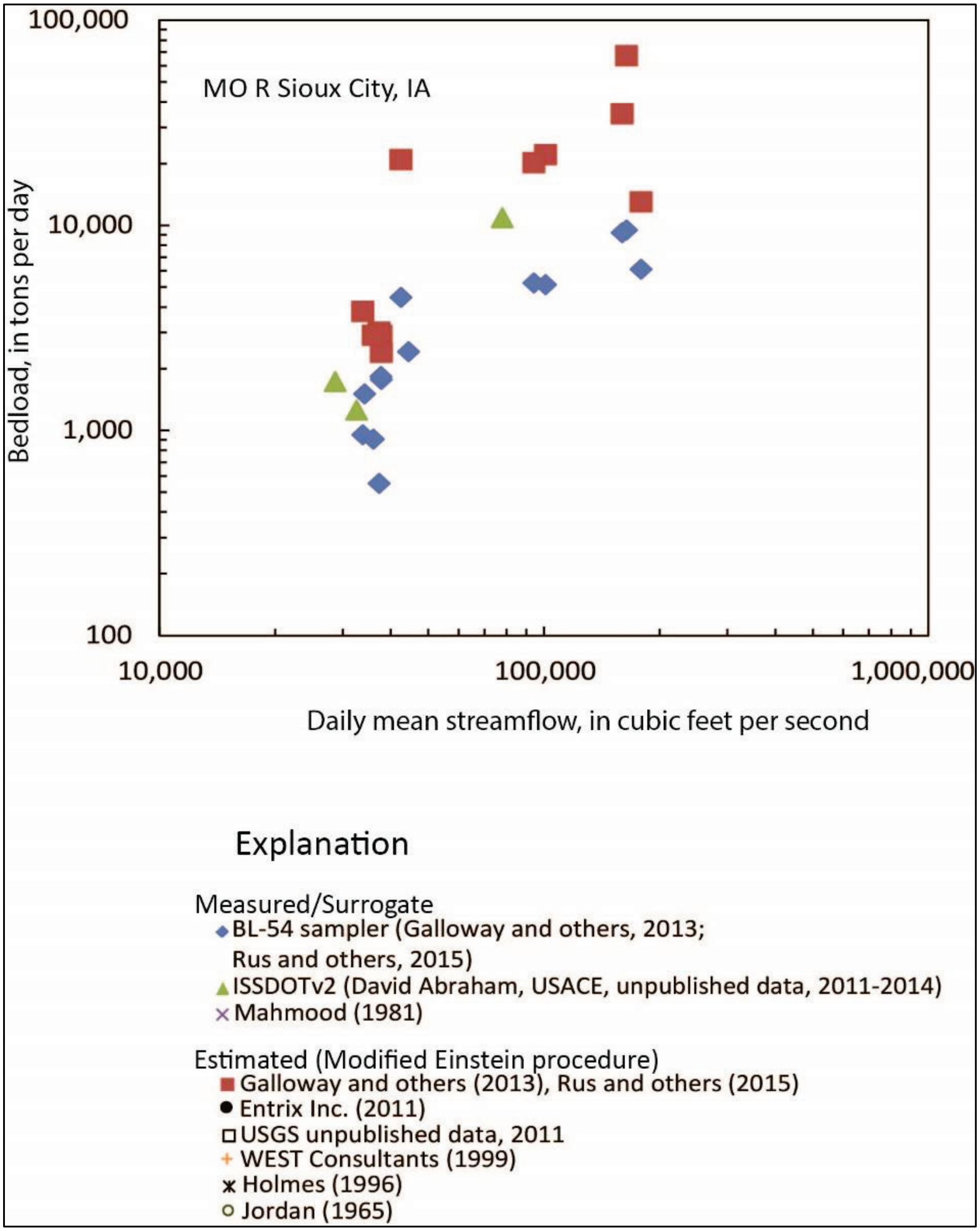

Figure 263. USGS bed-load data - Omaha, NE.

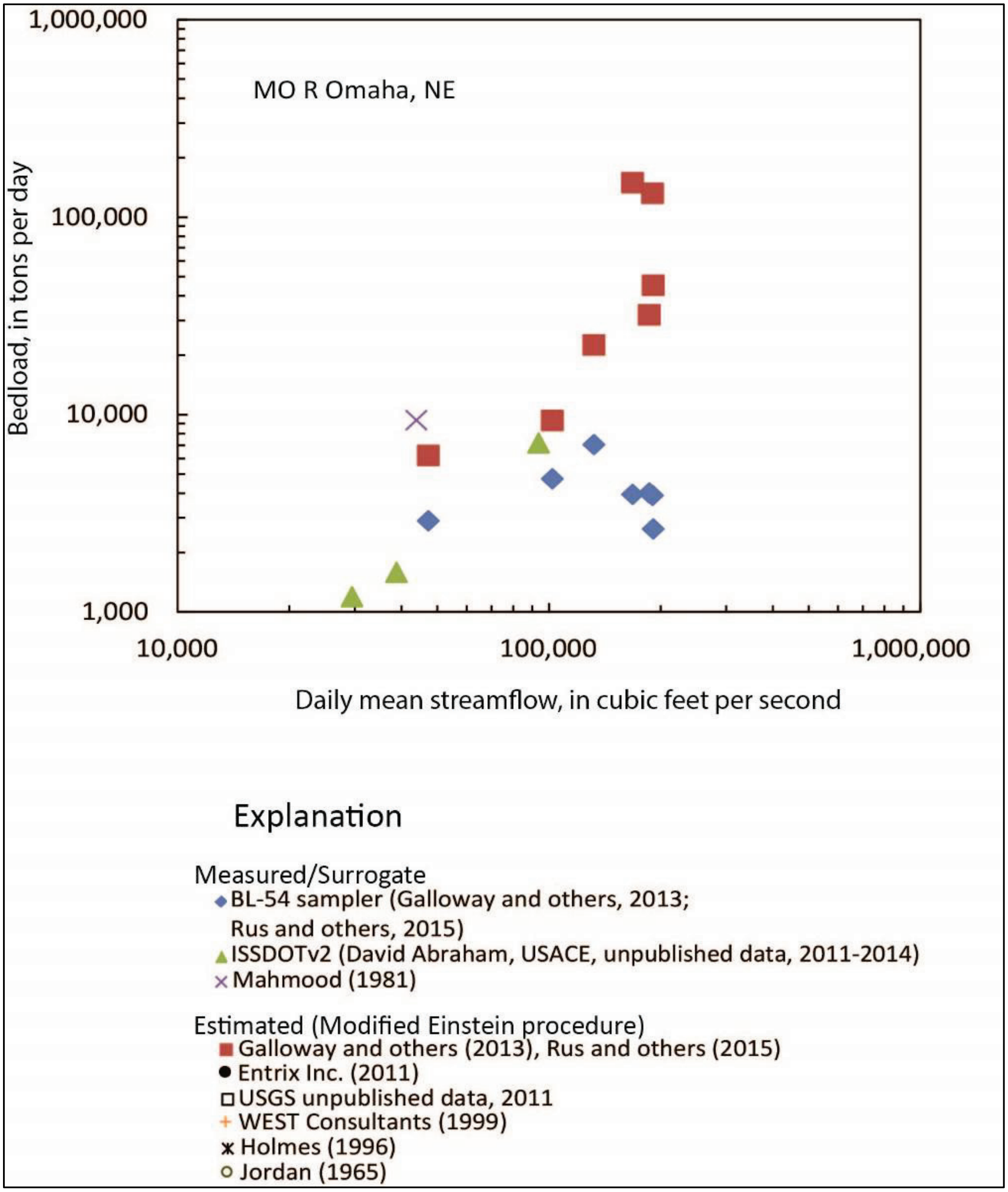

Figure 264. USGS bed-load data - Nebraska City, NE.

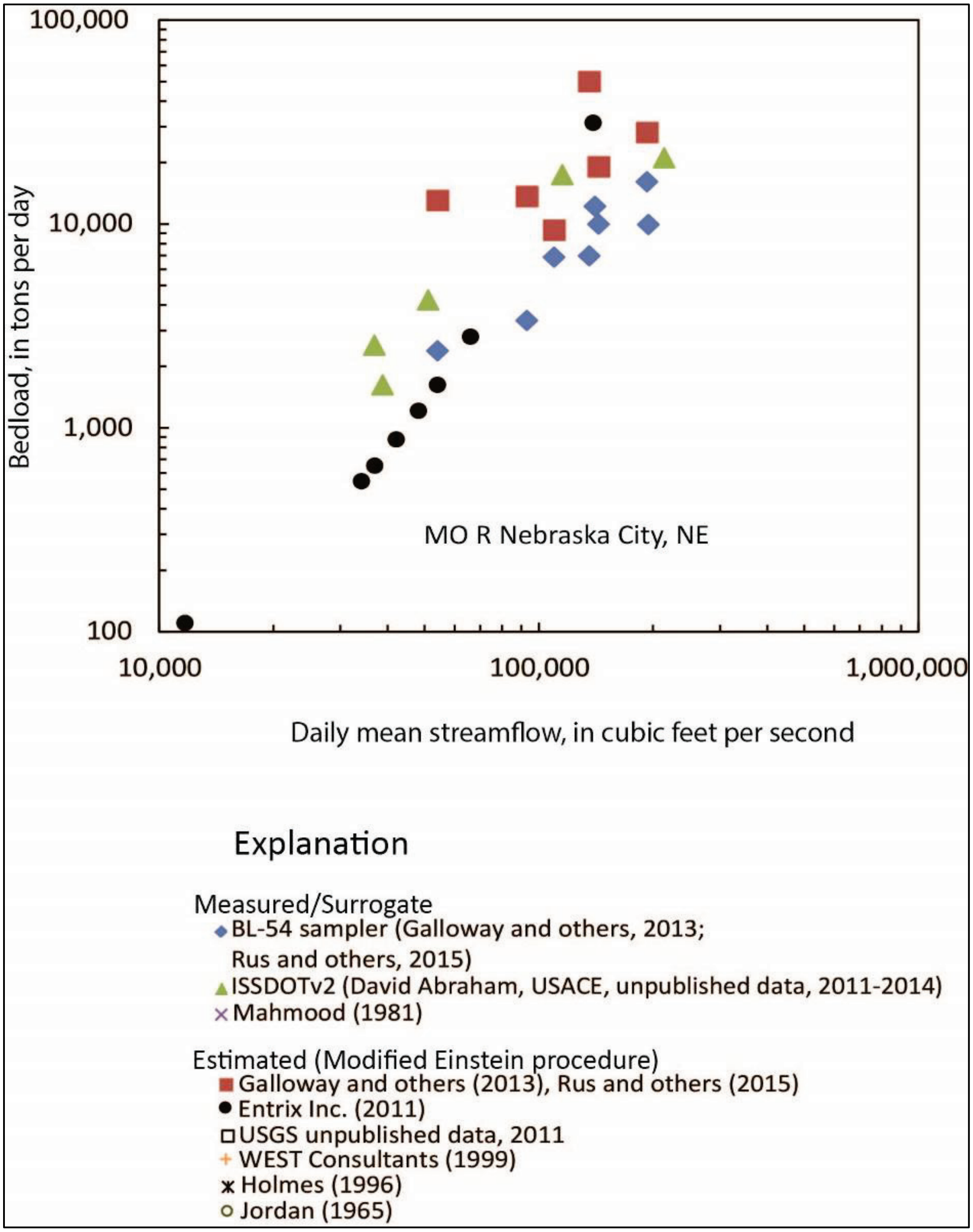

Figure 265. USGS bed-load data - St. Joseph, MO.

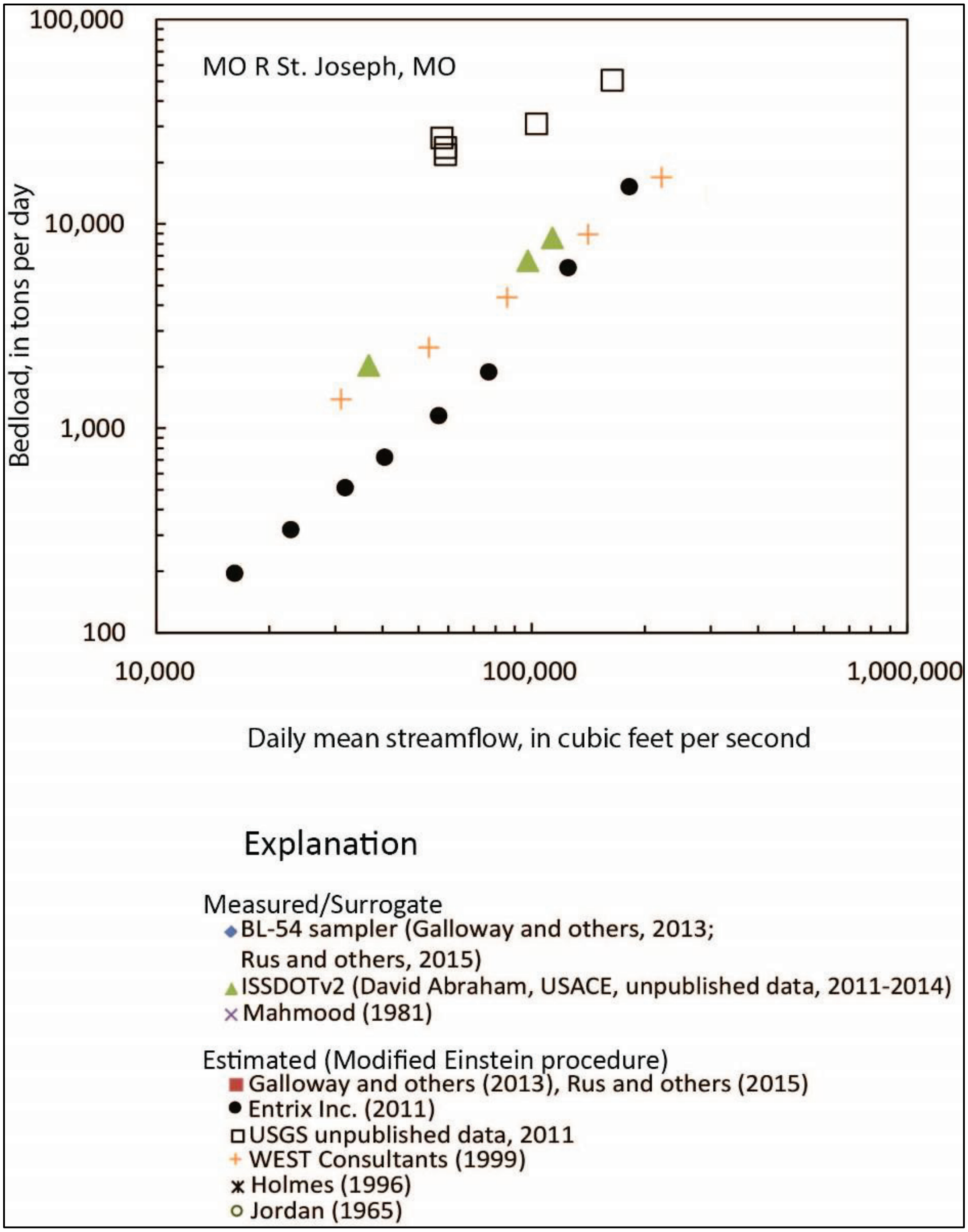

Figure 266. USGS bed-load data – Kansas City, MO.

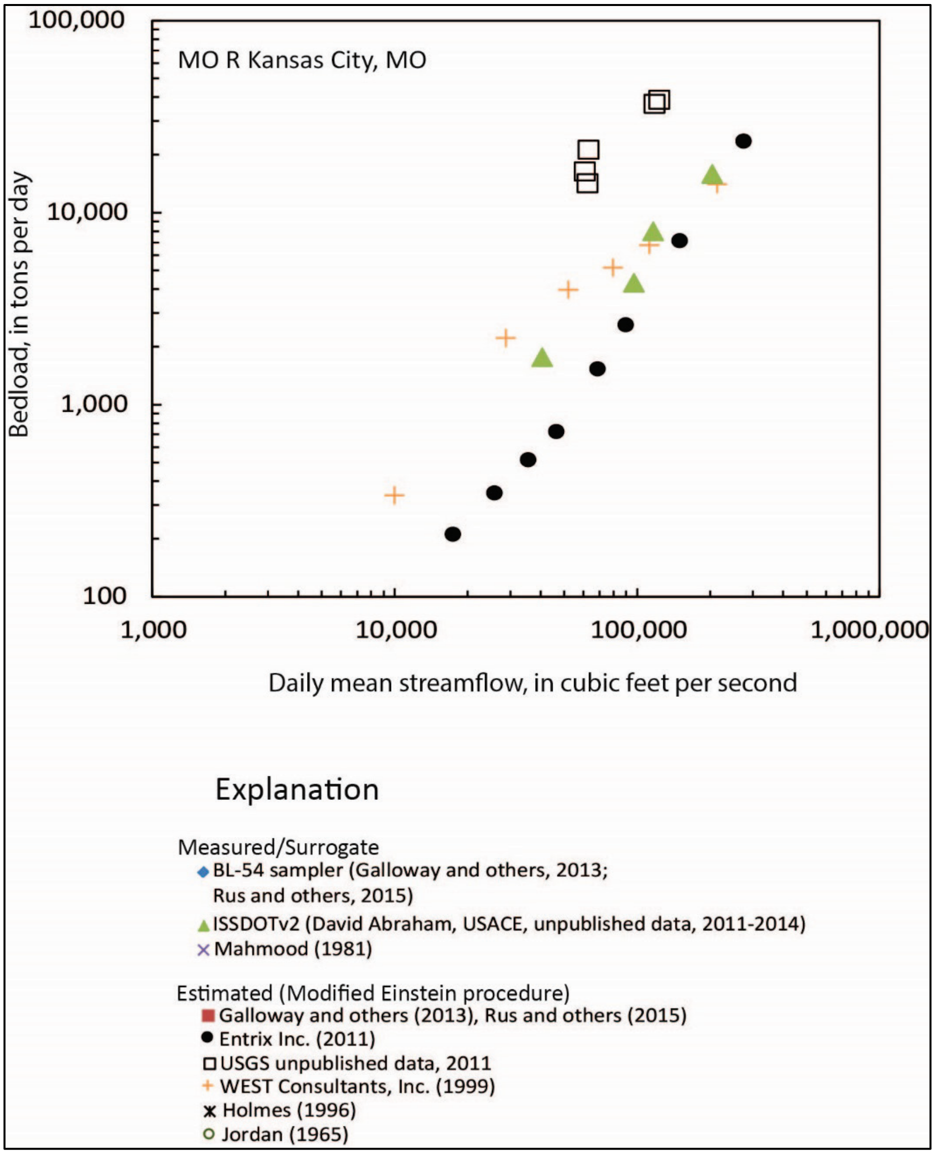

Figure 267. USGS bed-load data – Hermann, MO.

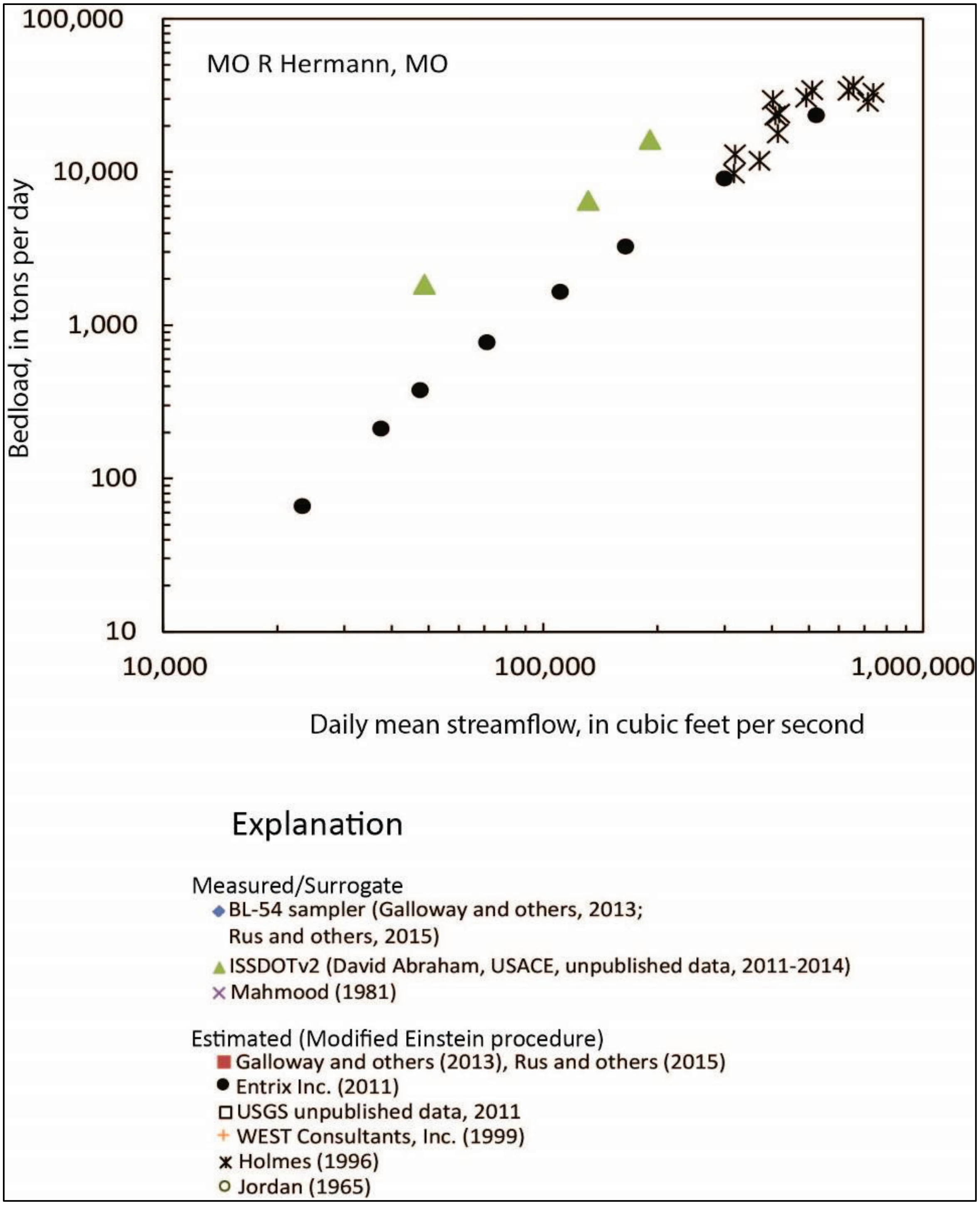

11 Summary

11.1 General comments

This report presents sediment and hydraulic data collected on the Missouri River. The time interval is for the period of April through June of 2014. The locations are from Sioux City, IA, River Mile (RM) 732 (northern most site) to Hermann, MO, at RM 99 (southern-most site). Data were collected at seven different sites, which are listed in Table 1.

Data collection equipment included a multi-beam fathometer, ADCP, a P-6 iso-kinetic suspended sediment sampler, and BM-54 bed material sampler.

The location of data types were recorded in the field via a GPS using NAD83. The coordinates provided in this study use the UTM Grid System.

Hydraulic related measurements that could be extracted from the collected data included flow, velocity, water depth, water surface elevation, water surface slope, and water temperature.

Sediment related parameters that could be extracted from the collected data included suspended sediment concentration vertical profiles at cross section stations, suspended sediment concentration two-dimensional (2D) profiles across a cross section, the separation of wash load from bed load, the grain size distribution of the BML, and the bed, the bed load, and a complete breakdown of various sediment loads.

These collected data provided a complete understanding of sediment transport magnitude and grain size as a function of flow at each site. Thus, for example and for the reader's convenience, Table 69 for the Waverly site is reproduced here. In Table 69, *bed load* is defined as the bed material moving at the bottom of the river in bed-forms; *suspended BML* refers to the suspended material with grain size higher than 0.063 mm; *total BML* is the sum of bed load and suspended BML; *bed load fraction* is the percentage of the total bed material moving as bed load; *wash load* is fine sediments that never settle in the bed, with grain size of 0.063 or less; and *total load* combines the quantity of total BML and wash load.

In the table, one can immediately see the effect of increasing or decreasing flow on the various transported quantities of sediment. In general, as flow increases, one would expect most of the parameters to increase, except the bed load fraction. The bed load fraction usually decreases as flow increases. This is because as flow increases, more of the BML becomes suspended. In going from a flow of 43,566 to 100,478 cfs, all measured quantities go up except the bed load fraction. The same is not true in going from a flow of 100,478 to 117,347 cfs. In that case, bed load stays approximately the same, suspended BML has a modest increase, and most surprising, wash load decreases by approximately one-half of its previous value. Suspended sediment data are notorious for the amount of scatter that occurs in field measurements. This could also be the case here, or it could also be that other actual physical causes are being measured. For instance, energy losses due to a receding hydrograph, or some other unsteady flow feature could have caused substantial deposition of fines in overbank areas.

Reproduction of bed-load transport values from Waverly, MO, (Table 69) shown below.

Data collection date	25-Apr-14	10-Jun-14	25-Jun-14
Flow (cfs)	43,566	100,478	117,347
Bed load (tons/day)	1,734	5,648	5,288
Suspended BML (tons/day)	5,859	65,098	87,850
Total BML (tons/day)	7,593	70,745	93,139
Bed load fraction (%)	22.8%	8.0%	5.7%
Wash load (tons/day)	16,219	824,911	419,724
Total load (tons/day)	23,812	895,656	512,863

After reviewing the tables for all the sites, a trend was noticed that when the percent change in flow from one measurement to the next was small, then the changes in measured sediment loads could be positive or negative. This could indicate that there was insufficient change to move the measured values out of the range of data scatter. This scatter could be due to measurement errors or due to unsteady flow or sediment conditions. However, in all instances where the flow differences between two dates were at or nearly doubled, then there was always an increase in measured sediment load with an increase in measured flow.

11.2 Applicability of bed-load transport functions at various scales

The next topic in this summary deals with the usage of bed load transport functions at a sub-cross-section scale. The intent of this discussion is (1) to present a comparison of measured bed load transport in a large sand bed river to values computed using analytic transport functions and (2) to compare values for the measured section on both a cross-section and sub-cross-sectional scale. The results presented made use of the detailed data and computations presented in the preceding parts of this report and from Abraham and Shelley et al. (2016).

The measured values versus computed values are considered first. The measured transport (computed using the multi-beam data via the ISSDOTv2 method) exhibits the expected lateral variability, with more transport occurring in the portion of the cross section with the higher velocities, as shown in Figure 268. There it can be seen that the highest velocities (shown in red) are in swath 1 (S1) and swath 2 (S2).

Figure 268. Cross section of measured velocities, Kansas City, trip 3.

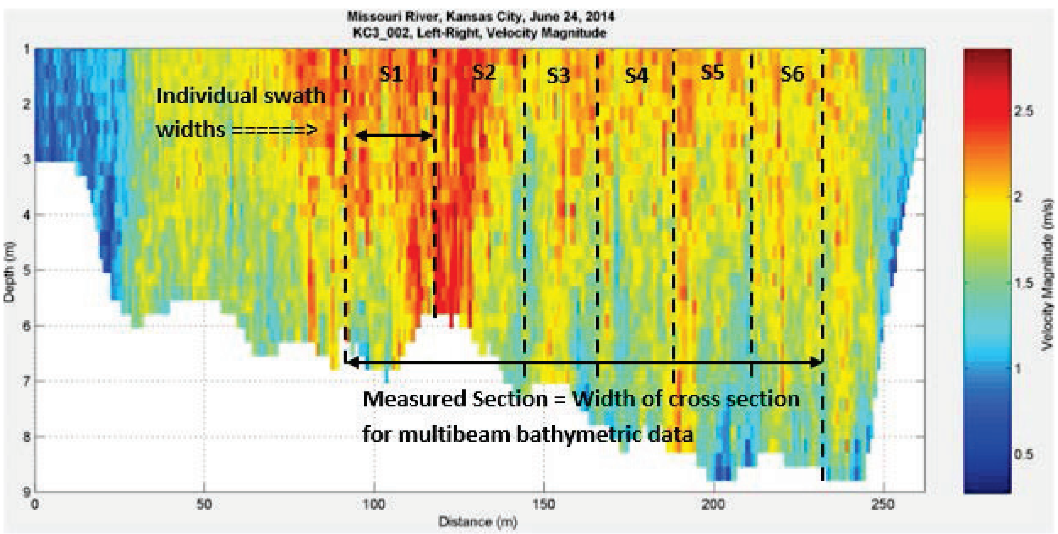

The highest bed load transport values also occur in swath 1 and 2 as shown in Figure 269, which is also for the Kansas City site, trip 3. The measured ISSDOTv2 bed load values provide a consistent data set against which to compare bed load transport values computed using the MPM and Einstein transport functions. An example of this is shown in Figure 269, in which the ISSDOTv2 values for each swath in the measured section are plotted in a bar chart versus the MPM and Einstein computed values.

Figure 269. Measured and computed values of bed load transport. Site is Kansas City, trip 3.

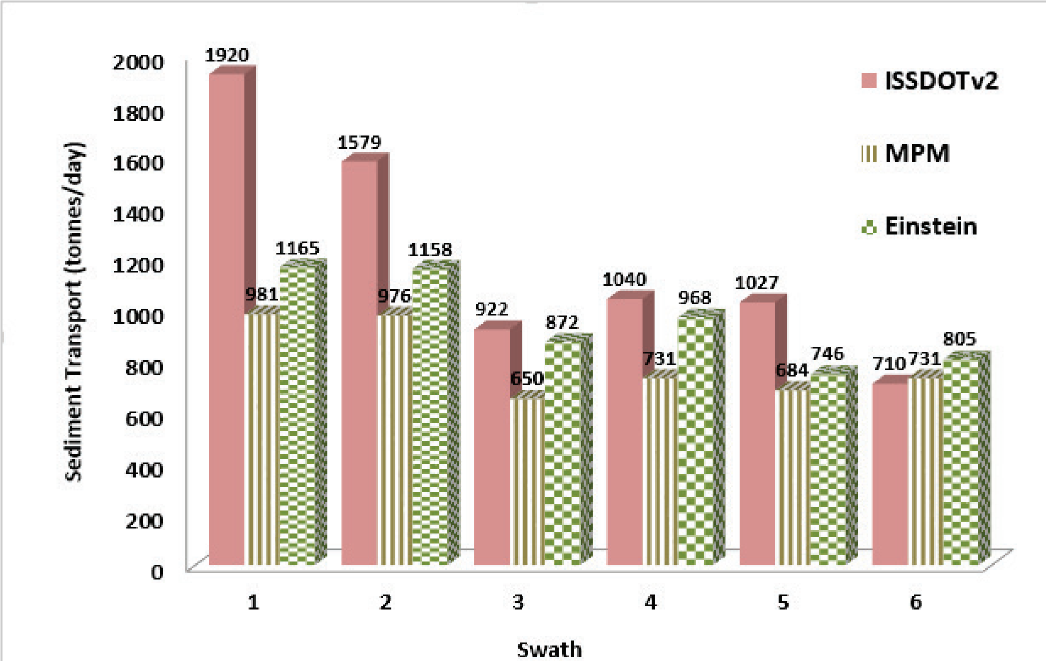

Both transport functions show the highest values of transport in swath one and two as does the measured ISSDOTv2 values; however, the MPM and Einstein functions significantly underestimate the bed load in those swaths by approximately 30% to 50%. The Kansas City trip 3 data were obtained at the highest flow rate for that site out of the three data collection trips. In observing all 119 values computed for the individual swaths (sub-cross sections) from all three trips and all seven sites in this report, one notes that at the lower flows (trips 1 and 2) the transport function's computed values are closer to the measured values. In general, the Einstein values are often larger, and the MPM values are somewhat smaller as compared to the ISSDOTv2 measurements. This can be seen in viewing the entire data set, plotted in Figure 270.

The line of equality plots the ISSDOTv2 values on both the horizontal and vertical axis. They are shown as green diamonds in this plot. The distance from each transport function data point to the line of equality is a visual representation of its closeness to the measured (ISSDOTv2) value. It can be seen that for the lower values, the MPM transport function produced bed load values that were reasonably close to the measured values while the Einstein function tended to overestimate the value. At the highest values, both functions underpredict compared to the measured values. The values shown in the graph were obtained using 114 of the 119 sub-cross sections. (Poor data quality prevented the calculation of bed load transport in five swaths of the measured data).

Figure 270. MPM and Einstein transport rates compared to ISSDOTv2 measurements at the sub-cross-section scale.

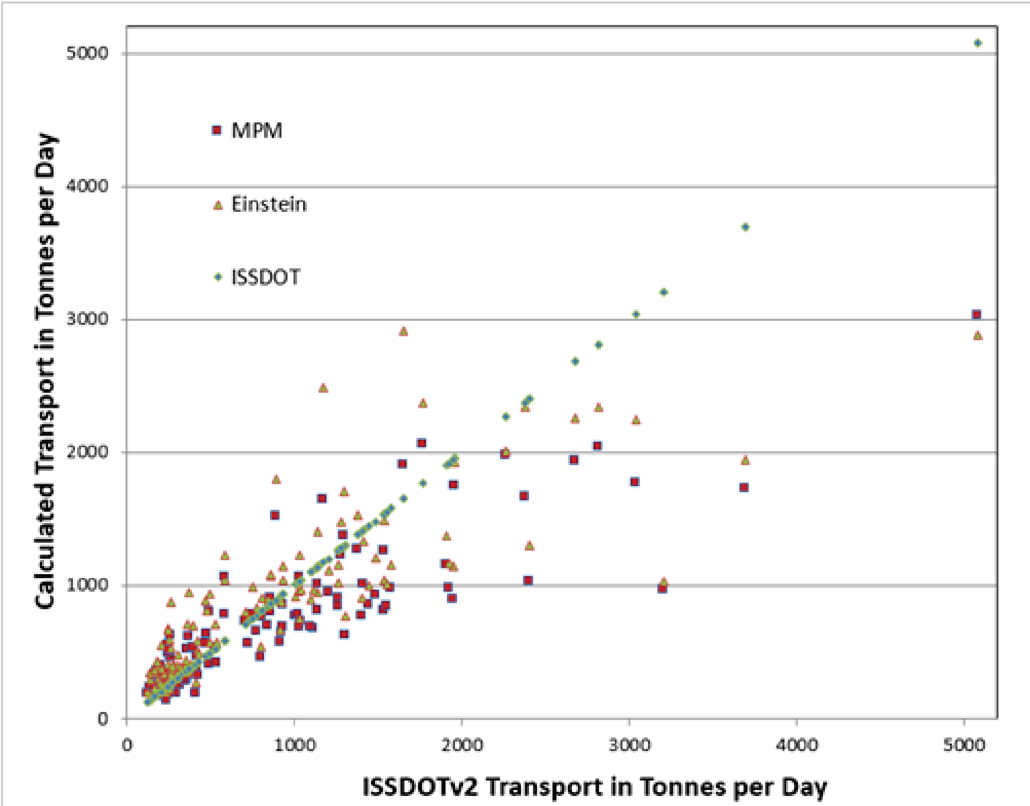

The question of sub-cross-section scale versus full-measured section is discussed next. No measured data (ISSDOTv2 values) are used in this discussion but only values computed by the transport functions on the two scales. This section compares the sum of bed load values computed for each sub-cross section to a single value computed for the full-measured section. The measured section is as shown in Figure 268.

Both the MPM and Einstein functions were compared in this way for all seven sites at the three different flow rates. The differences, calculated as a percentage of the full measured section value, are as follows: For the Einstein function, the percent differences range from -7% to 13% with an average difference of 1.65% and a root mean square error of 7%. For the MPM function, the percent differences range from -9.5% to 5.5% with an average difference of 0.25% and a root mean square error of 4%. The standard deviation of the percent differences is 6.74 and 4.01 for the Einstein and MPM functions, respectively.

Figure 271 shows a plot of the bed-load values computed at a sub-cross section scale vs. a single value computed from the full-measured section. As can be seen, the data closely follow the line of equality, except for the largest value from the Einstein function. This comparison of the measured-section value to the sum of individual swaths value shows that the two transport functions, which were developed using cross-section averaged data, can be used on smaller sub-scales.

Figure 271. Measured section values of bed load compared to sub-cross-section sums.

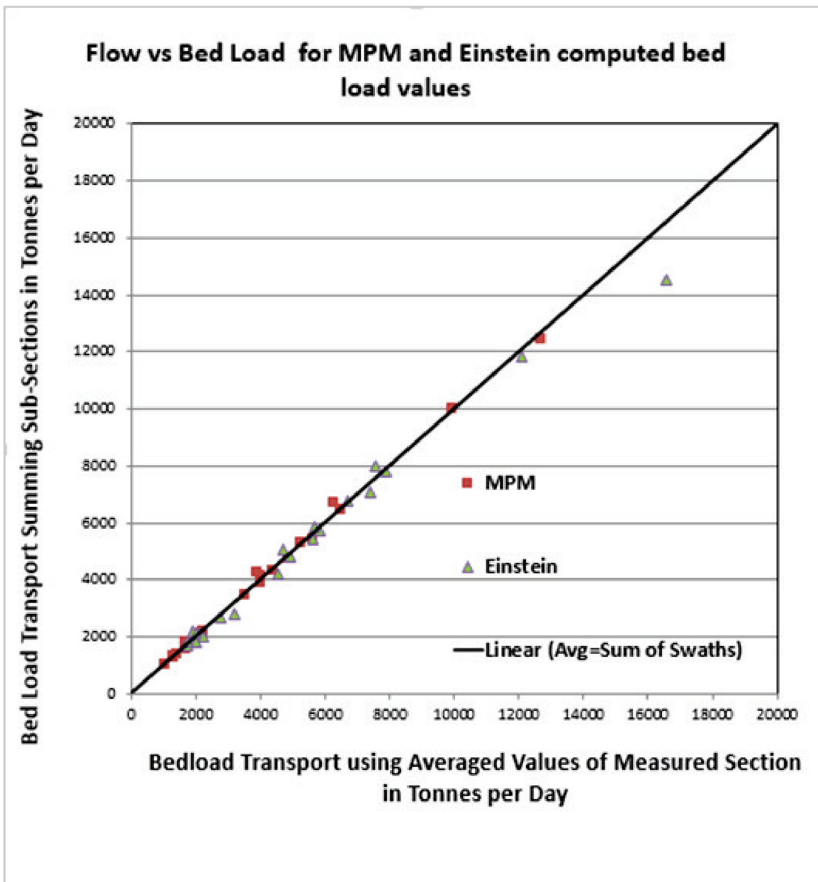

11.3 Future work

The data in this report cover an extensive range of a large sand bed river. They were obtained at flowrates varying from approximately 28,000 cfs to 130,000 cfs. Besides the analysis and compilation produced in this report, there are numerous other uses for this data. Future work should at least include some of the following actions and/or topics.

First, measurements at each site were obtained at only three flowrates. At some sites there were two relatively low flows and one high flow. At other sites a low, high, and medium flow were measured. Yet other sites had one low flow and two relatively high flows. In any case, when producing, for example, the bed-load rating curves as shown in this report, three data points (measurements) are a bare minimum. To have more confidence in using these curves, more data points would be necessary to fill in the gaps. Therefore, the first suggestion is that a similar effort be repeated with the stipulation that data only be collected at any site when the flowrate falls within a range for which data were not obtained in the first effort. This could be done for all sites, or if one site is more important than others, then only at that site. The important point would be to fill in the data gaps.

Even though the analytic emphasis was placed on the bed-load fraction and comparisons with bed load transport functions, the same could be done with total load transport functions. There is sufficient data in this report to accommodate such a study.

Included with such a study, one could also analyze transport rates for invividual grain classes.

At a given site, several different transport functions could be run either for total load or bed load and over a range of flows. The output from these different functions could be compared to the measured data. This pre-supposes that sufficient measured data were collected at that site to have some confidence in the rating curves. Then the function that provides predictions closest to the measured data could be selected as the function of choice for that site. Using such a procedure to select a transport function is important because different functions can, and often do, produce extremely variable results when using the same input data.

In addition to helping select an optimum transport function, the data in this report could possibly be used to make adjustments to coefficients in some functions where that might be appropriate to better calibrate the function with the specific site.

There is sufficient data in this report to verify 2D numerical sedimentation models in the vicinity in which the data were obtained. Once validated, these models can become very important and useful tools in evaluating present and future sedimentation patterns of a river when significant changes to it are planned.

With regards to geomorphological processes, this data set should find utility in analyzing how the relationships between features such as cross-section geometry, grain size distributions, and conveyance might change from upstream to downstream.

Finally, it was also noted when viewing cross-section plots of the color contours of velocity, that the higher velocities usually coincided with the highest amount of bed load transport. The lateral location in the cross section of these highest values is not always in the deepest water. This seems to be especially true in bends as opposed to straight reaches and/or crossings. Studying the cause of these differences and the effect this has on the deposition patterns could be very helpful in developing a predictive channel eveloution capability. Such a capability depends on being able to quantify the amount of bed load involved in building and moving bars, crossings, and other channel features. Because it is now feasible to quantify the temporal and spatial changes of bed load for specific locations, it should be possible to use this information to assist in developing and verifying channel evolution models.

References

Abraham, D., J. Shelley, T. McAlpin, and J. Adenihun. 2016. Verification of bedload transport formula at the sub-cross-section scale. In *Proceedings of the International Conference on Fluvial Hydraulics (River Flow 2016), St. Louis, USA, 11-14 July 2016*, 342–343. CRC Press/Balkema.

Abraham D., R. Kuhnle, and A. J. Odgaard. 2011. Validation of bed load transport measurements with time sequenced bathymetric data. *ASCE Journal of Hydraulic Engineering* 137(7):723–728.

Colby, B. R., and C. H. Hembree. 1955. Computations of total sediment discharge, Niobrara River, near Cody, Nebraska. U.S. Geological Survey Water Supply Paper 1357. Washington, D.C.

Entrix Incorporated. 2011. Missouri River commercial dredging final environmental impact statement. U.S. Army Corps of Engineers. Accessed December 19, 2013. http://www.nwk.usace.army.mil/Missions/RegulatoryBranch/MissouriRiverCommercialDredging.aspx.

Einstein, H. A. 1950. *The bed-load function for sediment transportation in open channel flows*. Soil Conservation Service Technical Bulletin No. 1026. https://naldc.nal.usda.gov/download/CAT86201017/PDF.

Galloway, J. M., D. L. Rus, and J. S. Alexander. 2013. *Characteristics of sediment transport at selected sites along the Missouri River during the high-flow conditions of 2011*. U.S. Geological Survey Scientific Investigations Report 2013–5006. Reston, VA: U.S. Geological Survey.

Heath, R. E., G. L. Brown, C. D. Little, T. C. Pratt, J. J. Ratcliff, D. D. Abraham, D. Perkey, N. B. Ganesh, K. Martin, and D. P. May. 2015. *Old River Control Complex sedimentation investigation*. ERDC/CHL TR-15-8. Vicksburg, MS: U.S. Army Engineer Research and Development Center.

Holmes, R. R., Jr. 1996. *Sediment transport in the lower Missouri and the central Mississippi Rivers, June 26 through September 14, 1993*. U.S. Geological Survey Circular 1120-I. Reston, VA: U.S. Geological Survey.

Jordan, P. R. 1965. *Fluvial sediment of the Mississippi River at St. Louis, Missouri*. U.S. Geological Survey Water-Supply Paper 1802. Reston, VA: U.S. Geological Survey.

Mahmood, K. 1981. *Missouri River bed-load evaluation through multi-channel sequential profiles*. U.S. Army Corps of Engineers, MRD Sediment Series No. 23. Washington, DC.

Meyer-Peter, E., and R. Muller. 1948. Formula for bedload transport. In *Proceedings of the 2nd Meeting of the IAHR*, Stockholm, 39–64.

Rus, D. L., J. M. Galloway, and J. S. Alexander. 2015. *Characteristics of sediment transport at selected sites along the Missouri River, 2011–12*. U.S. Geological Survey Scientific Investigations Report 2015–5127. Reston, VA: U.S. Geological Survey. http://dx.doi.org/10.3133/sir20155127.

WEST Consultants, Inc. 1999. *Missouri River levee unit L385 sediment analysis*. Bellevue, WA. Report submitted to the U.S. Army Corps of Engineers, Kansas City District. http://www.nwk.usace.army.mil/Portals/29/docs/regulatory/modredging/pubs/L385Analysis.pdf.

REPORT DOCUMENTATION PAGE

Form Approved
OMB No. 0704-0188

1. REPORT DATE
May 2017

2. REPORT TYPE
Final Report

3. DATES COVERED *(From - To)*

4. TITLE AND SUBTITLE
Sediment and Hydraulic Measurements with Computed Bed Load on the Missouri River, Sioux City to Hermann, 2014

5a. CONTRACT NUMBER

5b. GRANT NUMBER

5c. PROGRAM ELEMENT NUMBER

6. AUTHOR(S)
David Abraham , Marielys Ramos-Villanueva, Thad Pratt, Naveen Ganesh, David May, William Butler, Tate McAlpin, Keaton Jones, John Shelley, and Daniel Pridal

5d. PROJECT NUMBER

5e. TASK NUMBER

5f. WORK UNIT NUMBER
HC2022

7. PERFORMING ORGANIZATION NAME(S) AND ADDRESS(ES)
Coastal and Hydraulics Laboratory
U.S. Army Engineer Research and Development Center
3909 Halls Ferry Road
Vicksburg, MS 39180-6199

8. PERFORMING ORGANIZATION REPORT NUMBER
ERDC/CHL TR-17-8

9. SPONSORING/MONITORING AGENCY NAME(S) AND ADDRESS(ES) (see reverse)

10. SPONSOR/MONITOR'S ACRONYM(S)
NWK; NWO

11. SPONSOR/MONITOR'S REPORT NUMBER(S)

12. DISTRIBUTION/AVAILABILITY STATEMENT
Approved for public release; distribution is unlimited.

13. SUPPLEMENTARY NOTES

14. ABSTRACT
This work was performed to assist the U.S. Army Corps of Engineers, Omaha and Kansas City Districts, in quantifying sediment bed load and suspended load at several sites on the Missouri River for the purpose of defining sediment-discharge rating curves and for possible parameterization of bed-load transport equations. Seven sites were selected, and all sites were surveyed three times, separated by at least 4 weeks (or 20% flow difference) between surveys. Multi-beam, acoustic Doppler current profiler, suspended sediment, and bed material samples were collected for each site visit. As requested by the Districts, all units are in English units. In addition to quantifying all the intended data types listed above, bed-load transport values were computed for all sites and all trips using the ISSDOTv2 method and compared with the Meyer-Peter Mueller and Einstein bed-load transport functions. The study provides a complete sediment picture (bed load, suspended bed-material load, and wash load) over a 630-mile reach of a large sand bed river, with seven sites representing increasingly larger flows along the river length. The data set will be very useful for additional studies.

15. SUBJECT TERMS
Bed load, Missouri River, Sedimentation and deposition, Sediment transport, Suspended sediments

16. SECURITY CLASSIFICATION OF: a. REPORT	b. ABSTRACT	c. THIS PAGE	17. LIMITATION OF ABSTRACT	18. NUMBER OF PAGES	19a. NAME OF RESPONSIBLE PERSON
Unclassified	Unclassified	Unclassified	SAR	237	David Abraham
					19b. TELEPHONE NUMBER *(Include area code)* 601-634-2846

9. SPONSORING/MONITORING AGENCY NAME(S) AND ADDRESS(ES) (concluded)

U.S. Army Corps of Engineers, Kansas City District
601 E 12th St.
Kansas City, MO 64106

U.S. Army Corps of Engineers, Omaha District
1616 Capitol Ave., Ste. 9000
Omaha, NE 68102